Master Thesis

ASSESSING HEALTH-RELATED ECONOMIC BENEFITS FROM REDUCED PARTICULATE MATTER IN AIR USING BENMAP-CE

MAISHA KABIR

18MCE017P

Department of Civil Engineering

Chittagong University of Engineering and Technology (CUET)

Chattogram-4349

Bangladesh

2023

ASSESSING HEALTH RELATED ECONOMIC BENEFITS FROM REDUCED PARTICULATE MATTER IN AIR USING BENMAP-CE

By

Maisha Kabir

Student ID:18MCE017P

A Thesis Submitted to the Department of Civil Engineering, in partial fulfillment of the requirements for the degree of MASTER OF SCIENCE IN CIVIL ENGINEERING

Department of Civil Engineering

CHITTAGONG UNIVERSITY OF ENGINEERING AND TECHNOLOGY

December 2023

DEDICATION

To my beloved and truly amazing **Parents,**

and

To my **Husband**

List of Publications

Conference

- **M.Kabir**, SK Pal, "Analyzing the effects of PM_{10} exposure on health and economy, a case study of Chattogram City Corporation, "Proceedings of the Second International Conference on Advances in Civil Infrastructure and Construction Materials (CICM 2023); MIST, Dhaka, Bangladesh; 26-28 July 2023; pp. 1364-1374

APPROVAL STATEMENT

The thesis titled **Assessing Health Related Economic Benefits from Reduced Particulate Matter in Air using BenMAP-CE** Submitted by **Maisha Kabir,** Roll No: **18MCE017P**, Session: **2018-2019** has been accepted as satisfactory in partial fulfilment of the requirements for the degree of **MASTER OF SCIENCE IN CIVIL ENGINEERING** on **09 December 2023.**

BOARD OF EXAMINATION

1. **Dr. Sudip Kumar Pal** — Chairman (Supervisor)
   Professor
   Department of Civil Engineering, CUET

2. **Dr. Aysha Akter** — Member (Ex-Officio)
   Head and Professor
   Department of Civil Engineering, CUET

3. **Dr. Md. Reaz Akter Mullick** — Member (Internal)
   Professor
   Department of Civil Engineering, CUET

4. **Dr. Mst. Farzana Rahman Zuthi** — Member (Internal)
   Professor
   Department of Civil Engineering, CUET

5. **Dr. Muhammad Ashraf Ali** — Member (External)
   Professor
   Department of Civil Engineering, BUET

DECLARATION STATEMENT

I hereby declare that the work contained in this Thesis has not been previously submitted to meet requirements for an award at this or any other higher education institution. To the best of my knowledge and belief, the Thesis contains no material previously published or written by another person except where due reference is cited. Furthermore, the Thesis complies with PLAGIARISM and ACADEMIC INTEGRITY regulation of CUET.

Maisha Kabir

Date: 20-11-2023 18MCE017P

Department of Civil Engineering

Chittagong University of Engineering and Technology

(CUET)

DECLARATION BY THE SUPERVISOR(S)

This is to certify that **Maisha Kabir** has carried out this research work under my supervision, and that she has fulfilled the relevant Academic Ordinance of the Chittagong University of Engineering and Technology, so that she is qualified to submit the following Thesis in the application for the degree of MASTER of SCIENCE in Civil Engineering. Furthermore, the Thesis complies with the PLAGIARISM and ACADEMIC INTEGRITY regulation of CUET.

Dr. Sudip Kumar Pal

Professor

Department of Civil Engineering

Chittagong University of Engineering and Technology

ACKNOWLEDGMENT

First and foremost, the author conveys her profound gratitude to the almighty Allah.

The author would first want to use this opportunity to recognize the contributions of the associated individuals which helped to bring this research successfully to a conclusion.

The author would like to express sincere and heartfelt gratitude to **Dr. Sudip Kumar Pal,** Professor**,** Department of Civil Engineering, Chittagong University of Engineering and Technology (CUET) for his proper guidance, sincere supervision, and co-operation throughout this dissertation.

The author would like to thank **Dr. Aysha Akter**, Professor and Head, **Dr. Md. Reaz Akter Mullick**, Professor, Dr. **Mst. Farzana Rahman Zuthi**, Professor**,** Department of Civil Engineering, (CUET)**,** and **Dr. Muhammad Ashraf Ali,** Professor, Department of Civil Engineering, BUET for serving as a member of the Examination Board and also for their feedback and encouragement, as well as for being available, whenever I needed the guidance.

The author would also like to thank Directorate of Research and Extension (DRE), CUET for the financial assistance in conducting the study. I truly appreciate the constant support from the students of Port City International University for their constant support during the field work. Additionally, I appreciate the cooperation and support provided by Md. Anwarul Islam, Assistant Technical officer, and Md. Rabiul Hossain, Lab Attendant, during my activities at the Environmental Engineering Laboratory, CUET.

Finally, the author expresses a deep sense of gratitude and indebtedness to her teachers, colleagues, friends and family for their endless devotion, encouragement, and mental support throughout the tenure of the research wo

Abstract

The residents of Chattogram City Corporation (CCC) are grappling with serious health risks due to air pollution, especially during the dry period. The Institute for Health Metrics and Evaluation (IHME) has documented a significant number of premature deaths attributed to polluted air. While the government has implemented policies to curb air pollution, their impact often falls short due to a lack of comprehensive benefit modeling for decision-making. There is a lack of localized studies on air pollution and its health impacts, particularly in Chattogram, with gaps in understanding the correlation between air pollution, heavy metals, mortality, and economic burden, highlighting the urgent need for investigations using tools like BenMAP-CE to assess the efficacy of pollution reduction measures. This study bridges the gap by utilizing the BenMAP-CE tool to assess health and economic benefits resulting from airborne particulate matter reduction. The study centers around the development of BenMAP-CE, utilizing data on particulate matter (PM) in the air, population statistics, air pollution hazards as well as health hazards due to road dust, and economic data. PM data has been gathered from Landsat 8 and selected monitoring sites in the CCC area. Trace metals in road dust were identified using acid digestion and atomic absorption spectrophotometry.

The 24-hour average concentrations of PM_{10} and $PM_{2.5}$ in air during November and December, obtained from Landsat 8 and cross-referenced with CAMS data, ranged from 84 to 532 $\mu g/m^3$ and 70 to 339 $\mu g/m^3$, respectively, with averages of 181 to 246 $\mu g/m^3$ and 108 to 190 $\mu g/m^3$ over the study period. These concentrations were found to exceed BNAAQS and WHO 24-hour threshold values, indicating a hazardous situation linked to associated health risks. The study reveals a temporal trend of rising PM concentrations from 2017 to 2019, followed by a decrease in 2020, a peak in 2021, and a slight decline in 2022. Elevated concentrations of metals like Mn, Zn, Fe, Cr, Cu, and Ni were also identified, potentially exacerbating air-associated health issues. The BenMAP-CE tool demonstrates substantial health and economic benefits achievable through air quality improvement policies in CCC. The study estimates the prevention of 7185 to 11643 premature deaths, translating to an economic benefit ranging from 1.131 billion US dollars to 2.297 billion US dollars, contributing 0.45% to 0.82% to the country's GDP. Cardiovascular diseases accounted for more premature deaths than respiratory diseases, with the top 5 causes of death ranked as IHD>Stroke>COPD>LRI>LC. The age group 5 to 17 exhibited premature morbidity effects related to asthma and lower respiratory infections.

বিমূর্ত

চট্টগ্রাম সিটি কর্পোরেশনের (সিসিসি) বাসিন্দাগন বায়ু দূষণের কারণে, বিশেষ করে শুষ্ক সময়ে মারাত্মক স্বাস্থ্যঝুঁকির মুখোমুখি হন। ইসস্টিটিউট ফর হেলথ মেট্রিক্স অ্যান্ড ইভালুয়েশন (আইএইচএমই) দূষিত বায়ুর জন্য দায়ী উল্লেখযোগ্য সংখ্যক অকাল মৃত্যুর নথিভুক্ত করে থাকে। যদিও সরকার বায়ু দূষণ রোধে নীতিগুলি বাস্তবায়ন করছে, সিদ্ধান্ত গ্রহণের জন্য ব্যাপক সুবিধা মডেলিংয়ের ঘাটতি থাকার কারণে উল্লেখিত নীতিগুলির প্রভাব পরিবেশের উপর প্রায় কমই পড়ে। বায়ু দূষণ এবং এর ফলে স্বাস্থ্যের উপর প্রভাবের ক্ষেত্রে স্থানীয় গবেষণার অভাব রয়েছে, বিশেষ করে চট্টগ্রামে, বায়ু দূষণ, ভারী ধাতু, মৃত্যুহার এবং অর্থনৈতিক চাপের মধ্যে পারস্পরিক সম্পর্ক বুঝার মধ্যদিয়ে দিয়ে দূষণ কমানো ব্যবস্থার কার্যকারিতা মূল্যায়ন করতে বেনম্যাপ-সিই -এর মতো সরঞ্জামগুলি ব্যবহার করে তদন্তের জরুরি প্রয়োজন তুলে ধরে। বেনম্যাপ-সিই টুল ব্যবহারের মাধ্যমে এই অধ্যয়নটি বায়ুবাহিত কণা পদার্থ হ্রাসের ফলে উদ্ভদ স্বাস্থ্য এবং অর্থনৈতিক সুবিধাগুলি মূল্যায়নে ব্যবধান পূরণ করে। বাতাসে বস্তু কণাকার পদার্থ, জনসংখ্যার পরিসংখ্যান, বায়ুদূষনের পাশাপাশি রাস্তার ধূলোর কারণে স্বাস্থ্যের ঝুঁকি এবং অর্থনৈতিক ডাটা ব্যবহার করে বেনম্যাপ-সিই সম্প্রসারণের মাধ্যমে এই অধ্যয়নটি কেন্দ্রীভূত। ল্যান্ডস্যাট ৮ এবং (সিসিসি) এলাকায় নির্বাচিত মনিটরিং সাইট থেকে পিএম ডেটা সংগ্রহ করা হয়েছে। রাস্তার ধুলায় ট্রেস ধাতুগুলি অ্যাসিড হজম এবং পরমাণু এবসরপশন স্পেকট্রোফোটোমেট্রি ব্যবহার করে চিহ্নিত করা হয়েছে।

ল্যান্ডস্যাট ৮ থেকে প্রাপ্ত এবং ক্যাম্পস ডেটার সাথে ক্রস-রেফারেন্সে নভেম্বর এবং ডিসেম্বরে বাতাসে বস্তুকণা ১০ (পিএম ১০) এবং বস্তুকণা ২.৫ (পিএম ২.৫) -এর ২৪ ঘন্টার গড় ঘনত্ব যথাক্রমে ৮৪ থেকে ৫৩২ মাক্রোগ্রাম/ঘনমিটার এবং ৭০ থেকে ৩৩৯ মাক্রোগ্রাম/ঘনমিটার পর্যন্ত। অধ্যয়নের সময়কালে গড় ঘনত্ব ১৮১ থেকে ২৪৬ মাক্রোগ্রাম/ঘনমিটার এবং ১০৮ থেকে ১৯০ মাক্রোগ্রাম/ঘনমিটার। এই ঘনত্বগুলি বিন্যাক্স এবং ডাব্লিওএইচও ২৪-ঘন্টা থ্রেশহোল্ড মানকে অতিক্রম করেছে, যা সংশ্লিষ্ট স্বাস্থ্য ঝুঁকির সাথে যুক্ত একটি বিপজ্জনক পরিস্থিতি নির্দেশ করে। গবেষণাটি ২০১৭ থেকে ২০১৯ সাল পর্যন্ত বস্তুকণা ঘনত্ব বৃদ্ধির একটি সাময়িক প্রবণতা প্রকাশ করে, তারপরে ২০২০-এ হ্রাস, ২০২১-এ সর্বোচ্চ এবং ২০২২-এ সামান্য হ্রাস। এমএন, জেডএন, এফই, সিআর, সিইউ এবং এনআই ধাতুগুলির উচ্চতর ঘনত্ব শনাক্ত করা হয়েছিল যা সম্ভাব্য বায়ু সম্পর্কিত স্বাস্থ্য সমস্যা গুলিকে বাড়িয়ে তোলে। বেনম্যাপ-সিই টুল (সিসিসি)-তে বায়ু মানের উন্নতি নীতির মাধ্যমে অর্জনযোগ্য যথেষ্ট স্বাস্থ্য এবং অর্থনৈতিক সুবিধাগুলি প্রদর্শন করে। সমীক্ষায় আনুমানিক হিসাবে ৭১৮৫ থেকে ১১৬৪৩ অকাল মৃত্যু প্রতিরোধের হিসাব করা হয়েছে, অর্থনৈতিক সুবিধার জন্য তা ১.১৩১ বিলিয়ন মার্কিন ডলার থেকে ২.২৯৭ বিলিয়ন মার্কিন ডলারে (ইউএসডি, ২০২১) রূপান্তর করা হয়, যা দেশের জিডিপিতে ০.৪৫% থেকে ০.৮২% অবদান রাখে। শ্বাসযন্ত্রের রোগের তুলনায় কার্ডিওভাসকুলার রোগগুলি বেশি অকাল মৃত্যুর জন্য দায়ী, মৃত্যুর শীর্ষ ৫টি কারণ আইএইচডি>স্ট্রোক>সিওপিডি>এলআরআই>এলসি হিসাবে স্থান পেয়েছে। ৫ থেকে ১৭ বছর বয়সীরা হাঁপানি এবং নিম্ন শ্বাসযন্ত্রের সংক্রমণ সম্পর্কিত অকাল অসুস্থতার প্রভাব প্রদর্শন করেছে।

Table of Contents

List of Figures

Fig. No. **Figure Caption** **Page No.**

List of Tables

Table No. **Table Caption** **Page No.**

NOMENCLATURE

Acroynyms

AQI	Air Quality Index
BNAAQS	Bangladesh National Ambient Air Quality Standard
BenMAP-CE	Benefit Mapping and Analysis Program-Community Edition
CCC	Chattogram City Corporation
COI	Cost of illness
COPD	Chronic Obstructive Pulmonary Disease
CR	Concentration Response
Cr	Chromium
Cu	Copper
Fe	Iron
HIA	Health Impact Assessment
IHD	Ischemic Heart Disease
IHME	Institute of Health Metrics and Evaluation
LC	Lung Cancer
LRI	Lower Respiratory Infection
Mn	Manganese
MRAD	Minor Restricted Activity Days
NCD	Non-Communicable Diseases
Ni	Nickel
PM	Particulate Matter
USEPA	United States Environmental Protection Agency
WHO	World Health Organization
WLD	Work Loss Days
WTP	Willingness to pay
Zn	Zinc
5-COD	5-Causes of Death

Chapter 1. INTRODUCTION

1.1 Background

The delicate balance of life on the Earth depends critically on keeping clean air, which affects not just people but also animals, plants, water bodies, soil, and environment as a whole. Individuals breathe in more than 11,000 litres of air each day, according to health and wellness studies (Maria Trimarchi and Ann Meeker, 2001). However, this inhaled air, often known as ambient air, is found frequently contaminated with particulate matter or gases enriched by natural and anthropogenic inputs is presenting a potential hazard to the well-being of individuals and aquatic lives.

In 2022, a staggering 7 million people worldwide met premature deaths due to air pollution (*WHO*, 2022), as reported by the World Health Organization (WHO). People in the South Asian country would live 5.4 years longer if pollution levels met WHO guideline. Globally, ambient pollution contributes significantly to health burdens, attributing to 29% of lung cancer, 25% of ischemic heart disease, 24% of strokes, and 17% of respiratory infections (*IQAir*, 2019). Bangladesh, consistently ranking among the most polluted countries globally from 2018 to 2021 (*The World Bank*, 2023), faced severe consequences, with air pollution and identified as the second leading cause of mortality and illness in 2019 (*IQAir*, 2022). In EPIC report it is found that residents of its capital Dhaka reduce live expectancy by 7.7 years. As per, Institute for Health Metrics and Evaluation (IHME, 2019), indicated that an annual death toll of approximately 173,500 due to air pollution in the country during the year 2019. In Bangladesh, the percentage of deaths attributed to air pollution by cause is as follows: 49% Chronic Obstructive Pulmonary Disease (COPD), 22% diabetes,

24% ischemic heart disease (IHD), 37% lung cancer, and 35% stroke (State of Global Air, 2019). The impact of air pollution was prominent among the top five causes of early death, with 78,145 to 88,229 deaths in Bangladesh attributed to air pollution in the same year (The World Bank, 2022).

Among all pollutants, particulate matter emerges as the most harmful, creating the most dangerous health effects. Particulate matter's pervasive presence in the air is deeply intertwined with the health hazards that populations face. These tiny particles, often invisible to the naked eye, become a potent threat upon inhalation. Beyond respiratory problems, air pollution affects lung growth, elevates the risk of cardiovascular diseases, and contributes to lung cancer. Rapid infrastructure development economic expansion, industrialization, and vehicle emissions, identified as man-made contributors, to deteriorating air quality in metropolitan areas (Hien and Kor, 2022; Zhao et al., 2010), demand urgent action. A specific emphasis on reducing $PM_{2.5}$, a significant air pollutant constituting 30-50% of particulate matter, is crucial (Begum et al., 2013a). As a decade has passed with ongoing developments, the anticipation is that air pollution dynamics must adapt accordingly, necessitating more localized studies. Particulate matter, a serious public health hazard in Dhaka metropolis, primarily results from human activities (Rouf, 2011). Breathing air with airborne particulate matter has severe health impacts, contributing to various respiratory conditions, chronic diseases, and an increased risk of cardiovascular effects and early death (Abelsohn et al., 2002; Dockery et al., 1993; Pope III, 2002). Studies indicate statistical links between increasing levels of thoracic coarse particles PM_{10} and ultrafine particles $PM_{2.5}$ and an elevated risk of heart attacks (Dockery et al., 1993; Pope III, 2002).

Moreover, an often-overlooked aspect is the association of heavy metals with particulate matter. The chemical composition of atmospheric particulate matter is complex, encompassing various components such as metals, inorganic ions,

organic aerosols, and elemental carbon (Badaloni et al., 2017; Ogundele et al., 2017; Žero et al., 2017). Metals are released into the environment via several processes, including high-temperature incineration, the burning of fossil fuels and wood, industrial emissions, vehicle exhaust, tire and brake wear, road dust, the weathering of crustal materials, and natural events (M. Ahmed et al., 2016; Fomba et al., 2018). Upon inhalation, these varying-sized particles may become stuck in various areas of the respiratory system. Of particular concern are heavy metals like arsenic (As), cadmium (Cd), nickel (Ni), and lead (Pb). Even at low concentrations, these metals exhibit significant toxicity, posing a direct threat to respiratory health and other vital organs (P. Gao et al., 2018; and Z.-F. Gao et al., 2019). The interplay between particulate matter and heavy metals amplifies the potential health risks, demanding a nuanced approach to air quality management.

The global cost of health damage associated with exposure to air pollution is $8.1 trillion, equivalent to 6.1 percent of global GDP (World Bank, 2021). In 2019, Bangladesh suffered economic losses from air pollution, amounting to approximately 3.9% to 4.4% of its GDP (World Bank, 2023). In 2018, the cost of a premature death amounted to 14,000 million USD for 96,000 lives lost (State of Global Air, 2019). Apart from it, there are morbidity related costs such as work loss days, increased health care cost, lowered economic productivity, lost household income, and lastly school absenteeism. By successfully reducing air pollution, $54 trillion can be saved from the resulting health benefits (World Bank, 2023). The World Health Organization (WHO) underscores the importance of clean air for human health and wellbeing. Therefore, evaluating premature deaths and economic advantages associated with lowering airborne particulate matter levels in line with WHO criteria is important.

To evaluate the possible public health effects of changes in air quality, including premature deaths, diseases, and their associated economic costs, a variety of sophisticated techniques have been created (Anenberg et al., 2016a). For calculating the health and financial effects linked to variations in air quality conditions, notable software programs including AirQ+, BenMAP-CE, EBD, GMAPS, SIM-AIR, and IOMLIFET have been seen to be used (Anenberg et al., 2016a; Bayat, Planning, et al., 2019). In recent times, BenMAP-CE (Benefits Mapping and Analysis Program - Community Edition) stands out due to its flexibility and capable in estimating both human health aspects and at the same time transform economic costs from air control measures. BenMAP-CE is a robust and user-friendly health impact model that combines geographic information systems (GIS) capabilities, catering to both beginner and experienced users (Bayat, Planning, et al., 2019; D. Kim et al., 2019), established by the US Environmental Protection Agency (US EPA, 2022). As from the recent studies with this tool it has been seen that this program makes it easier to calculate the costs and health effects related to changes in air quality conditions (N. Fann et al., 2009; US EPA, 2022).

The surge in health impact assessment utilization, particularly through tools like BenMAP-CE, marks a pivotal advancement. Numerous research papers (Safari et al., 2022; (Aldegunde et al., 2023; Ding et al., 2019a; Voorhees et al., 2014a; Stewart et al., 2017; L. Chen, Shi, Gao, et al., 2017; Davidson et al., 2007; Hassan et al., 2021; Manojkumar and Srimuruganandam, 2021; Van Munster, 2018; Voorhees et al., 2014b) have successfully used modeling techniques to determine premature fatalities and economic gains while covering air quality in time and space to evaluate health consequences. In a noteworthy study conducted in the city of Qom, implementing a control scenario with a with a $PM_{2.5}$ decrease of 10 $\mu g/m^3$ emerged as a potentially transformative measure. The reported outcome

suggested that such an intervention could prevent approximately 4,694.5 premature deaths, accompanied by a corresponding economic benefit of approximately 855.91 million USD (Safari et al., 2022). Another study conducted in Cartagena de Indias, revealed that a reduction in $PM_{2.5}$ concentrations could lead to economic gains of up to US$100 million, specifically in the context of non-accidental fatalities (Aldegunde et al., 2023). The economic impact of altering $PM_{2.5}$ concentrations was further underscored in a study on the Southern California Air Basin (SoCAB), where it was determined that such alterations resulted in the avoidance of 750 mortalities among individuals aged 30-99 years, with a 95% confidence interval ranging from 508 to 990 (Stewart et al., 2017). Notably, studies done in China showed significant drops in hospital admissions, outpatient visits, and premature deaths that were attributed to improved air quality (Ding et al., 2019a; Voorhees et al., 2014a).

Beyond these factors, the unintentional inhalation of particulate matter from road dust introduces additional health risks due to the transport of heavy metals into the body (Gujre et al., 2021; Wiseman et al., 2021; Zhu et al., 2021). Vulnerable populations, such as the elderly and children with weakened immune systems, bear the brunt of prolonged exposure to metallic elements in urban environments. Assessing health concerns linked to metal exposure from road dust often relies on the US Environmental Protection Agency's method, covering direct ingestion, inhalation, and skin contact (Duong and Lee, 2011). Studies note high metal concentrations in road dust, with circumstances linking these concentrations to carcinogenic hazards (Men et al., 2018, 2021). Extensive investigations into road dust pollution and the levels of heavy metal concentrations in Dhaka, as well as analyses of heavy metal contamination dangers in cities like Chittagong City, emphasize the multifaceted nature of

health hazards associated with air pollution (F. Ahmed et al., 2007; Alamgir et al., 2015; Kabir et al., 2021a; Nargis et al., 2022; Newaz et al., 2021; Pal and Roy, 2021).

Within the above context, it is seen that widespread methods and diverse geographical areas, air pollution, and associated health hazard is documented. Several recent research has examined the health and economic advantages associated with air pollution using the BenMAP-CE formulation, establishing a thorough comprehension of its use in estimating the cost and health effects of air quality improvements as well as highlighting its robustness and user-friendly nature. The number of integrated studies related to air pollutants in particular with dust particles such as $PM_{2.5}$ and PM_{10}, a fraction of dust that is readily available to inhalable, digestible with foods from nearby road environments, and potential to be in touch with skin for different age groups, different geographic locations with dissimilar air pollution content stratification, are still underrated. Furthermore, the presence of trace metals that pose health risks in particulate air pollutants and their associations with health and economic benefits are not studied in depth and need investigation. In this argument, an improved air environment advocacy guided by the relevant laws, rules, and regulations by local and global authorities, the benefits acquired are still ambiguous and need more studies to explain the justification of control measures are in operation.

1.2 Problem Statement

Poor air quality is widely recognized for its profound health implications, particularly concerning respiratory and cardiovascular diseases. Particulate matter (PM) is a complex blend formed in the atmosphere through interactions of gaseous precursors, primarily originating from human activities. It comprises various chemical components, including sulfate, nitrate, ammonium, black carbon (BC), and organic carbon. Furthermore, high concentrations of heavy metals in the air can worsen disorders linked to the air, which raises serious

worries about the possible harmful consequences of air pollutants on human health. It's important to acknowledge that air quality is not a uniform global issue; instead, it varies regionally. Research highlights the varying health and economic benefits achievable in different regions, influenced by factors such as local pollution sources, climate conditions, population density, and the vulnerability of specific communities to air pollution.

The existing research landscape reveals gaps in understanding the localized impact of air pollution, particularly in areas like Chattogram, where evidence points to substantial annual deaths linked to airborne particulate matter. Despite being among the most affected regions, no dedicated studies have explored the specific correlation between air pollution and mortality in Chattogram. Additionally, the association of heavy metals with particulate matter, a complex blend released into the environment through various anthropogenic processes, poses a significant health risk that demands attention. The absence of research in this specific geographical area and the lack of comprehensive studies utilizing tools like BenMAP-CE to assess the efficacy of pollution reduction measures underscore the urgency for focused investigations. This research aims to bridge these gaps by providing a thorough background on air pollution's global and regional context and subsequently delving into the specific challenges faced by Chattogram. The study's primary objective is to employ BenMAP-CE comprehensively, evaluating the effectiveness of environmental policies, and assessing changes in premature deaths and incidents following air pollution reduction measures along with their economic impact.

1.3 Research Questions

Urban air pollution, particularly stemming from the road traffic sector, not only jeopardizes individual health but also poses significant challenges to the broader economy. As the air environment deteriorates, healthcare expenditures soar due

to the treatment of pollution-induced illnesses, putting immense strain on public health systems. Diminished workforce productivity, resulting from pollution-related health issues, introduces a drag on overall economic output. The costs of environmental cleanup and the financial burden on governments to implement air quality measures further compound economic challenges. Widening economic disparities affect vulnerable communities disproportionately. Additionally, the global economic competitiveness of urban areas is jeopardized, impacting tourism, investment, and business activities. Despite these palpable connections, the link between health and the economy in the context of urban air pollution remains a complex and unfolding narrative, necessitating more in-depth studies for a nuanced understanding and the development of comprehensive mitigation strategies. The research questions addressing the study are as follow:

- how the polluted air affects healthy living health and economic wise in urban setting
- whether the presence of trace metals in air exaggerate human health and incur additional cost in treatment
- whether or not a modeling tool BENMAP-CE can predict health and economic benefits from the improved air environment.

1.4 Objectives

The aim of this study is to evaluate health and economic benefits derived from the reduction of particulate pollutants in the air by analyzing their spatio-temporal variation and investigating associated health hazards from road dust. The specific objectives of this study are:

- to assess the spatio-temporal variation of particulate pollutants in air to understand pollution status and spatial variability.

- to investigate the human health hazard associated with the trace elements in air from the road dust.
- to model health and economic benefits from the reduction of particulate matter in air of Chattogram City Corporation considering the WHO guidelines and BNAAQS standard.

1.5 Scope

Typically, air pollution data relies on average values that encompass all seasons. Acknowledging that air quality tends to deteriorate during summer and winter due to reduced precipitation, it is important to note the contrasting impact of the rainy season, which often leads to improved air quality. Focusing solely on the winter period for assessment may inadvertently lead to an overestimation of compliance with WHO and other national air quality standards. Conversely, a comprehensive consideration of air quality throughout the entire year may offer a more accurate representation of the overall scenario. However, the presence of the rainy season could potentially result in an underestimation of the true pollution levels. To refine assessments and specifically gauge the crude estimate of maximum pollutants, the focus is placed on the winter period. Also, in the absence of a specific sampler, a representative sample of urban road dust is obtained by considering a fraction that is either suspended or deposited at a height of 6 meters.

- This study focuses on the 41 wards within Chattogram City Corporation, analyzing data from the months of November and December, which fall within the winter season, spanning from 2017 to 2022. It assesses air pollution, including particulate matter (PM) fractions and airborne heavy metals.
- The health impacts considered encompass all-cause mortality, cardiovascular diseases, respiratory diseases, and the Global Burden of

Disease (GBD) recognized top five causes of death: Ischemic Heart Disease (IHD), Chronic Obstructive Pulmonary Disease (COPD), Stroke, Lower Respiratory Infection (LRI), and Lung Cancer (LC), as well as Non-Communicable Diseases (NCD), for individuals aged 25-99. Additionally, the study evaluates morbidity outcomes such as hospital admissions due to respiratory and cardiovascular diseases, minor restricted activity days, and work loss days. For children, the study examines allergy rhinitis, and asthma.

- The study also incorporates the Value of Statistical Life (VSL) to assess the financial implications of premature death, drawing on estimates from organizations like the United States Environmental Protection Agency (US EPA), the World Bank and the Organization for Economic Co-operation and Development (OECD), regional studies. Costs of illness (COI) and people's willingness to pay (WTP) are employed to estimate expenses related to preventive morbidity, with healthcare service costs varying by health outcome.
- The BenMAP-CE model utilizes these parameters to estimate potential reductions in mortality and morbidity and the associated economic benefits.

1.6 Organization of the thesis

The dissertation is composed of five chapters and was structured in the subsequent sequence. **Chapter 1** the thesis serves as an introduction, presenting the study's background, problem statement, research questions, objectives, significance, and research area.

In Chapter 2, the focus shifts to an in-depth exploration of air pollution, covering Bangladesh's air quality and regulations, air pollution sources and its impact, airborne-heavy metal pollution and its health risks, a short introduction on

satellite imagery modeling approaches, and the introduction of the BenMAP-CE tool for health impact assessment. Global research on air pollution's health impact and financial benefits of pollution management is also reviewed here.

Chapter 3 outlines the methodologies used, summarizing historical air quality data collection from ground and satellite measurements, detailing the satellite data measurement process, explaining BenMAP's operational mechanics and data inputs, and discussing heavy metal data extraction, processing, and index generation. This chapter underscores the importance of these methods for achieving the study's objective. This chapter emphasizes the significance of these methodologies in achieving the study's objectives.

Chapter 4 presents the study's results comprehensively, describing spatial and temporal pollutant dispersion patterns across different age groups, emphasizing potential health and financial benefits from pollution reduction. Visual representations clarify the role of key factors like pollutant concentration, population distribution, incidence rates, and relative risk in the study's findings. The chapter concludes with a discussion, justifying the outcomes and comparing them to expectations, along with an evaluation of BenMAP's application in assessing health and financial consequences, including heavy metal contamination in dust, health risk, and correlation analysis.

Chapter 5 succinctly outlines the primary findings, study implications and following on a few scopes for future studies.

Chapter 2. LITERATURE REVIEW

2.1 General

Polluted air presents a substantial and invisible peril to human existence, as it is accountable for an estimated 7 million premature fatalities annually, with children accounting for approximately 600,000 of these deaths (*IQAir*, 2020). There exists a significant correlation between air pollution and a multitude of diseases, both in direct and indirect manners. In addition to health implications, the activity in question presents a substantial environmental hazard and also contributes to the phenomenon of global warming.

Bangladesh, specifically, encounters significant challenges pertaining to air quality, as evidenced by the highest level of air pollution in 2020 within its capital city, Dhaka, and other major cities Chattogram and Sylhet (*IQAir*, 2022). The nation exhibits the most severe air pollution globally, characterised by an average annual $PM_{2.5}$ concentration of 77.1 ($\mu g/m^3$) of air, surpassing the World Health Organization's recommended exposure level by a factor of seven. The region experiences a mortality rate of 13-22 percent due to air pollution, underscoring the pressing necessity for enhanced air quality monitoring and heightened societal consciousness regarding this issue.

Global research on air quality is experiencing significant expansion due to the increased accessibility of novel tools and data. Satellite-based sensors are currently employed for the purpose of atmospheric monitoring, facilitating the ability to track air quality in both spatial and temporal dimensions. Also, there is an increasing body of evidence indicating that the presence of heavy metals adsorbed onto particulate matter (PM) plays a pivotal role in the toxicity and detrimental health impacts associated with PM (Bollati et al., 2010). While

breathing, significant amounts of heavy metals are always inhaled, which can lead to both carcinogenic and non-carcinogenic health risks to the human body.

This chapter not only examines the matter of air pollution and its impacts but also delves into the concept of air quality modeling as a method of elucidating the condition of the air in a specific area. It also offers a comprehensive summary of assessments regarding the adverse health outcomes of air pollution. Additionally, the chapter looks into satellite imagery data to create a empirical equation to calculate air quality data from the prior year. This chapter discusses the effects of airborne heavy metals on human health, focusing on the effects of zinc, lead, iron, chromium, nickel and manganese in particular. Additionally, in this chapter, there are brief summaries of pertinent literature.

2.2 Air pollution sources and types

Before delving into the examination of air quality inside our designated study location, Chattogram City, it is imperative to furnish pertinent details regarding air pollution and the consequential impacts of airborne contaminant. The following articles examine the concept of air pollution and its effects.

2.2.1 Air pollution

The presence of substances, including gases, liquid droplets, or solid particles, in the atmosphere in concentrations above their typical atmospheric values is commonly referred to as air pollution. The aforementioned phenomenon can exert a discernible adverse impact on the well-being of individuals, as well as the well-being of other organisms, flora, and inanimate substances. The term "air pollution" has also been described as the introduction of harmful substances into the atmosphere, resulting in adverse health effects such as ocular and nasal irritation, throat discomfort, and respiratory difficulties (*US EPA*, 1994). Environmental pollution represents a significant ecological crisis that is currently

confronting our global community. Historically, the natural environment, consisting of the atmosphere, terrestrial surfaces, and aquatic systems, exhibited a state of purity, remaining unaltered, uncontaminated, and providing optimal conditions for the sustenance of various forms of life. Nevertheless, the present circumstances represent a stark contrast to the aforementioned scenario. In contemporary times, the environment has undergone a state of pollution, contamination, and undesirability, thereby presenting a substantial peril to the well-being of various life forms, encompassing the human species.

Governments across the globe establish defined thresholds for permissible levels of air pollutants, thereby delineating the demarcation line that distinguishes acceptable air quality from unacceptable conditions. Unadulterated air functions as a standard for evaluating the magnitude and trends of atmospheric contamination. Numerous regulations and regulatory procedures have been established to tackle the matter at hand, with governmental entities and organizations continually assessing the effects of increased amount of various gaseous and particulate pollutants in the Earth's atmospheric level. The severity and health concerns are contingent upon the severity of pollutants to which an individual is exposed, the time-period of such exposure, and the individual's susceptibility to these pollutants. The issue of air pollution is complex and affects people on a local, regional, national, and even international scale. In order to address the many origins and effects of air pollution and provide cleaner air for people and the environment, comprehensive policies and cooperative efforts at all levels of government are required.

Global

A serious problem that transcends territorial boundaries and has an impact on many aspects of our planet's life is global pollution. Significant environmental issues are impacted by air pollution on a worldwide scale, most notably the

depletion of stratospheric ozone brought on by CFC (chlorofluorocarbon) emissions. During the period spanning from 1985 to 1995, extensive research was conducted to establish a correlation between the depletion of stratospheric ozone and the subsequent increase in ultraviolet (UV) radiation levels, which in turn led to a rise in the incidence of skin cancer (Slanina, 2010). The emission of smog originating from industrial regions in China has a possibility of being transported to adjacent countries such as South Korea and Japan, thereby exerting a discernible influence on their atmospheric conditions and air quality (C.-H. Kim et al., 2021).

Currently, the problem of global air pollution is made worse by the rising quantities of numerous contaminants. Along with greenhouse gases, aerosols, and liquid water in the form of clouds, radioactive materials, which disturb the Earth's radioactive equilibrium, play important roles in changing the climate. These interrelated climatic effects have added a new dimension to air pollution, with complicated and wide-ranging effects on agriculture, water supplies, and vulnerable groups, exacerbating existing disparities and challenges.

Regional

Regional air pollution is the term used to describe environmental deterioration within a particular region or geographic area. Based on regional industries, population density, climate, and topography, pollution sources and effects can differ. The December 1952 incident in London, United Kingdom, stands out as a highly notorious case of regional air pollution. The city experienced a dense layer of smog due to the confluence of low temperatures and elevated levels of sulphur dioxide emissions stemming from coal combustion (*BBS*, 2002). The occurrence referred to as the Great Smog persisted over a span of multiple days, resulting in a significant number of premature fatalities and respiratory ailments. Due to emissions from industry, traffic, and power generation, the Pearl River Delta in

southern China, which is a highly urbanised and industrialised area, has endured significant air pollution (M. Hu et al., 2021). Poor air quality and frequent smog outbreaks are a result of a combination of regional emissions and the terrain of the area, which traps pollutants. For its enormous population, the PRD region has struggled to reduce air pollution and improve air quality.

Local

Local air contamination refers to the pollution of the atmosphere within a certain geographic region, typically encompassing both urban and rural areas. This type of pollution is often influenced by nearby sources of emissions. The issue of local air pollution in urban settings is considerably exacerbated by the existence of traffic congestion, which is also a significant source of pollutants like nitrogen oxides (NOx), particulate matter (PM), and volatile organic compounds (VOCs). A study conducted in Barcelona, Spain, which found a link between traffic-related pollution and a higher risk of asthma in children living close to major roadways (Petavratzi et al., 2005). Local industry can be a significant trace of air pollution because of the emissions of pollutants such particulate matter, nitrogen oxides, and sulphur dioxide (SO_2). The air quality in certain regions can be significantly affected by residential heating and cooking behaviors, especially during the winter season. A study conducted in rural China revealed that the utilization of solid fuels for cooking and heating purposes led to elevated levels of air pollution, both indoors and outdoors and that exerted a substantial impact on the health of the local population (Zhou et al., 2018).

2.2.2 Origins of atmospheric contaminants

Polluted air can arise from both natural and human-induced activities. The diagram presented in Fig. 2.1 illustrates the standard air pollution system commonly found in each region.

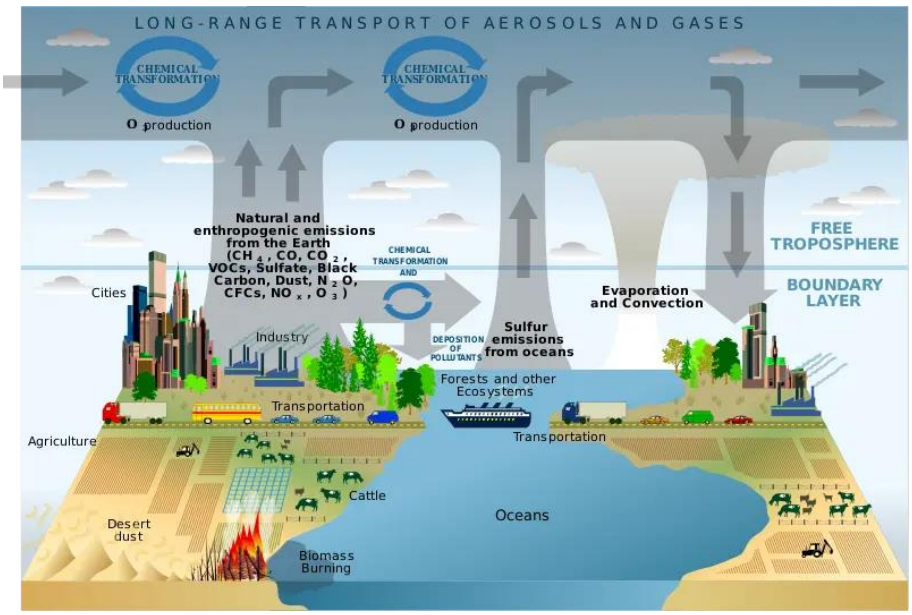

Fig. 2.1 Graphical representation of Air pollution sources adopted from (Air Pollution and Climate Change, 2002)

The provided diagram depicts the prevalent origins of air pollution, as well as the processes by which pollutants are transported and transformed within the atmosphere. Furthermore, it showcases the impact of these pollutants on various environmental resources. The presence of air pollution has a significant impact on various environmental components, including soil, water, natural resources, human health, and diverse materials. Fig. 2.1 shows the main causes of air pollution, how they move through the atmosphere and change, and how they affect different environmental resources. Water, soil, the environment, human health, and even various materials are all impacted by air pollution. Wildfires, eruptions of volcanic rock, wind erosion, pollen dispersion, organic molecule evaporation, and naturally occurring radioactivity are some examples of natural occurrences that contaminate the air. There isn't much natural pollution that occurs. However, the following human activities contribute to air pollution:

a) Emissions from Manufacturing and Industrial Activities: Carbon monoxide, organic pollutants, and toxins are released into the atmosphere in large quantities by industrial operations, waste incinerators, power

plants, and petroleum refineries. These pollutants affect the environment and people's health negatively and add to air pollution.

b) Fossil fuel combustion: This is a significant contributor to the emissions of both primary and secondary pollutants from transportation, including vehicles such as cars, trucks, trains, ships, and airplanes. Managing air pollution is difficult due to the extensive use of vehicles, which is both a significant contributor to pollution and an essential aspect of modern living.

c) Chemical application in household and agriculture: Chemicals are released into the air through various household activities such crop dusting, fumigation, the use of cleaning supplies, pesticides, and fertilizers, which add to air pollution.

d) Mining Activities: The emissions of carbon monoxide, sulfur dioxide, and nitrous oxide from mining operations and the associated truck traffic contribute to smog formation and health problems. Mercury particles, which can cause serious health issues if inhaled excessively, can also be released by gold miners.

e) Fallout from radioactive sources: When employed in industrial processes, radioactive sources can leak dangerous levels of sulfur dioxide as well as traces of heavy metals into the air, resulting in environmental damages such tree defoliation and undergrowth damage.

f) Chemical-based pesticides: Despite helping farmers safeguard their crops, chemical pesticide use has been linked to air pollution. If pesticide emissions get into the food chains of animals, birds, and marine life, they can cause harm.

g) Fertilizer dust or powder: Although fertilizers are useful for speeding up crop development, they can also contribute to air pollution when their dust builds up and releases ammonia and nitrogen oxide, which cause

acid rain and global warming. Methane, a strong greenhouse gas that traps heat in the atmosphere and contributes to the greenhouse effect, is another byproduct of this pollution.

2.2.3 Categories of Air Pollutant

On the basis of origin

Polluted air can be classified into two distinct groups based on their source: natural air pollutants and anthropogenic air contaminants.

Natural air pollutants originate from natural sources and undergo various environmental processes. These encompass emissions originating from: Volcanic Eruptions characterized by the release of gases and particles, including sulphuric dioxide and volcanic ash. Also, the presence of particulate matter originating from dust storms and aerosols derived from sea-salt, both transported by wind currents. Moreover, forest fires are natural disasters that result in the release of smoke, particulate matter, and various gases into the atmosphere. Lightning discharges generate nitrogen oxides (NO_x) and ozone (O_3). Furthermore, Soil outgassing refers to the natural emission of gases, such as methane (CH_4) and radon, from the soil.

Anthropogenic air pollutants originate from human activities and are mostly associated with industrial, transportation, and waste management operations. The pollutants consist of emissions that originate from stationary sources, including power plants, industrial sites, refineries, and incinerators. Examples of several air pollutants commonly found in the atmosphere are sulphur dioxide (SO_2), nitrogen oxides (NOx), volatile organic compounds (VOCs), and particulate matter (PM).

On the basis of sources

Polluted air can be classified into two main categories: primary pollutants and secondary pollutants, which are differentiated based on their respective sources (Masters, 2004a).

a) Primary pollutants: Primary Pollutants are substances that are released directly into the atmosphere from identifiable sources. As an illustration, carbon monoxide (CO) and sulphur dioxide (SO_2) are primary pollutants that are emitted directly from vehicle exhaust and industrial facilities, respectively.
b) Secondary pollutants: Secondary pollutants are formed through chemical interactions that occur in the atmosphere, involving primary pollutants and naturally occurring compounds. Such as, ground-level ozone (O_3) is considered a secondary pollutant that arises from the chemical reaction between nitrogen oxides (NOx) and volatile organic compounds (VOCs) emitted by vehicles and industrial activities, when exposed to sunlight within the atmosphere.

On the basis on state of matter

Air contaminants can exist in variety states of matter, including gas, liquid, and solid forms (Masters, 2004a). These diverse types of air contaminants exhibit varying traits and atmospheric behaviors and these types are discussed below:

a) Gaseous Pollutants

At normal temperatures and pressures, air contaminants known as "gaseous pollutants" exist as gases. They are well-mixed molecules or substances that may travel great distances in the air. Carbon monoxide (CO), sulphur dioxide (SO_2), nitrogen oxides (NOx), ozone (O_3), volatile organic compounds (VOCs), ammonia (NH_3), and hydrogen sulphide (H_2S) are a few examples of gaseous

pollutants. Secondary pollutants like ozone and particulate matter are formed as a result of chemical reactions in which gaseous pollutants can take part.

b) Particulate Pollutant (Aerosols):

Aerosols, usually referred to as particulate pollutants, are solid or liquid particles dispersed in the atmosphere. From big dust particles to tiny, microscopic aerosols, they range in size. Particulate pollutants can be emitted from both anthropogenic and natural origins, and their presence can give rise to a diverse range of adverse consequences for both human health and the environment. Particulate matter includes dust and soil particles, soot and black carbon, fly ash, pollen, sea salt aerosols and others. This particulate matter is divided into numerous subcategories with various size distributions:

i) Total suspended particulate matter (TSPM): TSPM is a metric used to quantify the concentration of airborne particles that have been collected by a high-volume bulk sample method on a filter substrate. This grouping encompasses particles of all sizes.

ii) PM_{10}: Particles with a size of less than 10 μm diameter are referred to as PM_{10}. Comparatively speaking, these particles are larger than $PM_{2.5}$ and $PM_{1.0}$.

iii) $PM_{2.5}$: Particles with a size of less than 2.5 μm diameter are referred to as $PM_{2.5}$. These are smaller, finer particles that can quickly enter the respiratory system at great depths.

iv) $PM_{1.0}$: Particles with a size of less than 1 μm diameter are referred to as $PM_{1.0}$. Even though they are smaller than $PM_{2.5}$, these particles can nevertheless be more dangerous to human health since they can enter the lower respiratory tract.

While particles having a diameter smaller than 2.5 μm are referred to as "fine particles," those between 10 μm and 2.5 μm are referred to as "coarse particles." The term "fine particle" also refers to ultrafine particles ($PM_{0.1}$), which are smaller than 0.1 μm. Ultrafine particles have garnered significant attention due to their minuscule dimensions and potential impact on human health and the environment.

On the basis of type of releases

Based on their emission characteristics, sources of air pollutants may be classified into three distinct groups (John H. Seinfeld, 1985).

a) Point Sources:
    i. Continuous Emissions: Power Plants - Power plants that utilise fossil fuels for the purpose of electricity generation emit a constant stream of carbon dioxide (CO_2), sulphur dioxide (SO_2), nitrogen oxides (NO_x), as well particulate matter into the Earth's atmosphere.
    ii. Puff Releases: In certain industrial operations, such as chemical manufacturing or metal smelting, there may occur intermittent releases of toxic gases, volatile organic compounds (VOCs), or hazardous air pollutants.
b) Line sources: Line sources are commonly observed in the form of motor vehicles, which traverse highways and roads. During the operation of automobiles, various pollutants such as carbon monoxide (CO), nitrogen oxides (NO_x), hydrocarbons (HC), and particulate matter (PM) are emitted.
c) Area sources: Wildfires have been identified as a substantial contributor to air pollution. When forest or grassland fires of significant magnitude transpire, they emit substantial quantities of smoke, particulate matter, as well as deleterious gases such as carbon monoxide and volatile organic compounds, which are detrimental to air quality. Also, large spills of volatile liquids, like

petrol or industrial chemicals, can result in local sources of air pollution when the liquids evaporate, releasing harmful vapors into the environment.

On the basis of chemical composition

The chemical compositions of air pollutants are diverse (Masters, 2004b). These entities can be categorized into:

i. Organic: Organic air pollutants encompass a variety of compounds, such as hydrocarbons, aldehydes, ketones, amines, and alcohols, among other examples.
ii. Inorganic: Inorganic air pollutants encompass a range of substances, including carbon compounds (such as carbon monoxide - CO and carbonates), nitrogen compounds (such as nitrogen oxides - NO_x and ammonia - NH_3), sulphur compounds (such as hydrogen sulphide - H_2S, sulphur dioxide - SO_2, sulphur trioxide - SO_3, and sulfuric acid - H_2SO_4), halogen compounds (such as hydrogen fluoride - HF and hydrogen chloride - HCl), as well as particulates such as fly ash and silica.

2.2.4 Criteria pollutants

Six air pollutants have been identified as significantly detrimental to human health among the various major air pollutants. The establishment of ambient air quality guidelines serves the purpose of regulating and limiting the levels of pollutants present in the atmosphere, considering their significant impact on human welfare. The six pollutants under consideration include Carbon Monoxide (CO), Lead (Pb), Nitrogen Dioxide (NO_2), Sulphur Dioxide (SO_2), Ozone (O_3), and Particulate Matter. The term "Criteria Pollutants" is commonly employed to denote these pollutants, as they serve as criteria utilized by regulatory bodies for the evaluation and control of air quality standards. The term "criteria" denotes that these pollutants adhere to established standards that

are derived from scientific criteria to safeguard public health and the environment.

The existence of air pollution can lead to adverse effects on both human health and the environment. A wide variety of air pollutants have been identified, which have been found to have established or prospective adverse effects on human health, plants, materials, and the environment. The pollutants primarily originate from the combustion processes associated with space heating, power generation, and motor vehicle traffic. Pollutants emitted from these sources have the potential to pose not only localized challenges but can also disperse over considerable distances. However, recent research has indicated that the primary negative consequence of polluted air and its impact on human health (USEPA, 2007). Therefore, the subsequent subsections primarily focus on the health effects of air pollutants.

Particulate matter

Particulate matter (PM) refers to a heterogeneous combination of liquid droplets and solid particles that are suspended in the atmosphere. The atmospheric composition encompasses several physical constituents, such as particulate matter, including dust, dirt, soot, smoke, and liquid droplets.

Different processes result in the generation of PM, with combustion producing very small particles and mechanical activities causing coarse particles to form through sedimentation. Smaller particles with lesser masses can float in the air for longer periods of time. These small particles are created from fundamental particles by techniques like condensation and coagulation. The generation process of fine and coarse particles in dust can be depicted as shown in Fig. 2.2.

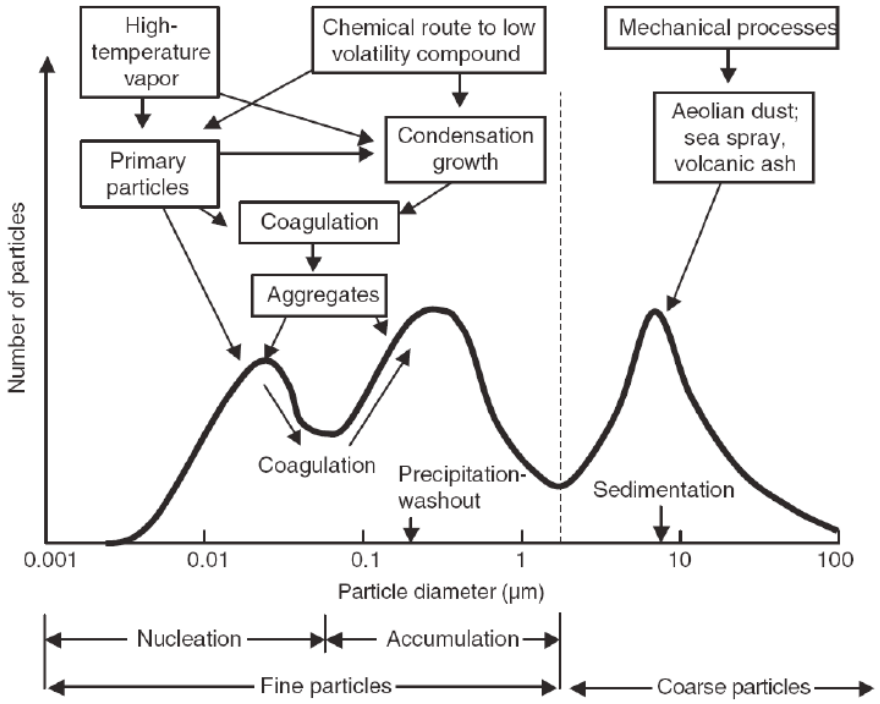

Fig. 2.2 Typical size distribution of the troposphere's dust, along with some of its origins and formation processes (Slezakova et al., 2012)

The utilization of the term "aerodynamic diameter" is prevalent in the scientific community to describe the size of particles. This term refers to the diameter of an imaginary sphere that possesses the same settling velocity. The aerodynamic diameter of the particles that are most relevant to health impacts ranges from 0.1 to 10 μm. Particles that are less than this range move randomly (Brownian Movement) and can coagulate to become larger than 0.1 μm in size. Particles bigger than 10 μm in size, however, relocate down more easily. In the Earth's atmosphere, 90% of all respirable PM are of natural origin, while just 10% are caused by humans (Pfeiffer, 2005) . The size of anthropogenic PM is often smaller compared to that of natural PM, with the smaller particles being more hazardous to human health.

Particulate matter (PM) poses health risks depending on both its chemical make-up and the exact areas of the respiratory system where it settles. PM can penetrate and lodge in different areas of the respiratory system when we breathe them in,

which can have a variety of negative health impacts (Fauser and Forsogsanlag Riso., 1999). The hairs and lining of the nose can capture large PM particles larger than 10 μm, preventing them from penetrating further into the respiratory system. These larger particles can be removed from the body through coughing and sneezing after being caught in the nose. Smaller particles, especially those between 2.5 μm and 10 μm, have the potential to enter the tracheobronchial system, which contains the lungs' airways. The muco-ciliary escalator is a defense mechanism used by the respiratory system in this situation. These particles are attracted to the mucus in the airways, and the cilia, which resemble microscopic hairs, help the mucus flow upward and towards the throat. Once in the throat, the mucus is either swallowed or spit out, thereby clearing the respiratory system. Even tiny particles, known as $PM_{2.5}$, can get deep inside the lungs' alveolar region, which is where gas exchange takes place. The absence of the muco-ciliary process in the alveolar region makes it more difficult to remove these microscopic particles from the lungs (*AIR CLEANERS FOR PARTICULATE CONTAMINANTS*, 2020). Radioactive materials or particulate matter that is insoluble, such as fibro genic dust (e.g., silica, asbestos, and coal dust), have the potential to get trapped inside the alveoli for extended periods of time, leading to the development of health problems. A number of harmful health impacts, including respiratory conditions, chronic bronchitis, bronchoconstriction (narrowing of the airways), lower lung functions, and higher death rates (Dockery and Pope III, 1994; Dockery et al., 1993; Laden et al., 2006; Pope and Dockery, 2006a, 2006b; Schwartz and Dockery, 1992b, 1992a) are associated with exposure to PM, particularly $PM_{2.5}$ and black carbon (BC). These health hazards are especially worrisome because $PM_{2.5}$ particles can have long-lasting effects on people's health because they can enter the respiratory system deeply.

Carbon monoxide

The incomplete burning of carbon-based fuels, such as petrol, diesel, natural gas, coal, and wood, results in the production of carbon monoxide (CO), a gas that lacks odor and color. Carbon monoxide (CO) can originate from a range of sources, such as automobiles, industrial activities, heating systems, and wildfires. The substance exhibits strong affinity for erythrocytes, hence diminishing the transportation of oxygen to bodily organs, resulting in a range of symptoms ranging from moderate cephalalgia to severe carbon monoxide intoxication. Prolonged exposure to some factors has detrimental effects on health, particularly among populations that are more susceptible. The implementation of carbon monoxide (CO) detectors, appropriate ventilation systems, regular equipment maintenance, and prompt medical intervention are essential components for the prevention of CO-related incidents and the promotion of safety(Goldsmith and Landaw, 1968; Mayr et al., 2005). Carbon monoxide (CO) is frequently referred to as "the silent killer" because of its imperceptible characteristics.

Oxides of sulphur (SO_x)

Oxides of sulphur, often known as SO_x, are colorless gaseous chemicals produced largely during the combustion of sulfur-containing fuels like coal and oil. They include sulphur dioxide (SO_2) and sulphur trioxide (SO_3). During combustion, sulphur is emitted as SO_2, with a negligible quantity of SO_3 as well. Free radical reactions involving OH- and SO_2 can further convert SO_2 to SO_3. When SO_2 is released, it can combine with water vapour to create sulfuric acid (H_2SO_4), which is the primary reason behind "acid rain." Sulphate aerosols, a large portion of the particulate matter in the air, are created when sulfuric acid molecules mix. These sulphate particles are frequently smaller than 2 μm, allowing them to enter the respiratory system deeply and cause harmful effects to health (Khalaf et al.,

2022a). Respiratory discomfort, reduced lung activities, and an exaggerated risk of cardiovascular disease and respiratory infections have all been linked to SO_2 exposure (Khalaf et al., 2022b; Rall, 1974). When SO_2 and particulate matter are present in a dusty environment, the protective cilia in the respiratory tract can become paralyzed, allowing hazardous particles to enter the respiratory tract and settle in the lungs. This combination has been linked to numerous health issues related to air pollution.

Oxides of nitrogen (NO_x)

The impact of nitrogen dioxide (NO_2) on human health is most notably manifested through respiratory problems. Short-term exposure to NO_2 can cause acute symptoms like coughing, wheezing, and difficulties in breathing. Long-term exposure, even at relatively low levels, has been linked to more chronic respiratory issues including asthma, bronchitis, and other forms of chronic obstructive pulmonary disease (COPD) (Hoffmann et al., 2022). Moreover, vulnerable populations such as children, the elderly, and individuals with pre-existing health conditions are at an even higher risk. Chronic exposure to NO_2 has also been implicated in reduced lung function growth in children and may exacerbate the severity of asthma attacks (Boningari and Smirniotis, 2016; Kampa and Castanas, 2008a).

Typically, the main source of NOx emissions comes from fuel. The bulk of NOx emissions take the form of NO, which at atmospheric quantities (1.0 ppm) has no known negative impact on health. However, oxidation can change NO into NO_2 and vice versa. When NO_2 and hydrocarbons interact with sunlight, photochemical smog, which is unhealthy, can result. Acid rain is also a result of the reaction between NO_2 and hydroxyl radicals in the atmosphere, which results in the production of nitric acid (HNO_3).

Lead (Pb)

Vehicles burning petrol with the antiknock additive tetraethyl lead $(C_2H_5)_4Pb$ are the main source of lead emissions. Inorganic particles are the main form of lead emission into the atmosphere. Although lead can also be consumed when it falls on food products, the primary method through which humans are exposed to airborne lead is by breathing. About half of the lead particles that are inhaled are absorbed into the circulation, leaving about one-third of them in the respiratory system (Fowler et al., 1993). Lead poisoning can have significant consequences, encompassing behavioral alterations characterized by anger, violence, and destructiveness, challenges in acquiring knowledge, convulsions, enduring and irreversible impairment of brain function, and even fatal outcomes (Assi et al., 2016; Ebrahimi et al., 2020). Children and expectant mothers are two of the groups that are most susceptible to the harmful effects of lead.

Photochemical smog and ozone

When nitrogen oxides (NOx), different hydrocarbons, and sunlight interact to create photochemical smog, a number of intricate chemical processes take place that result in a class of secondary pollutants called "photochemical oxidants." Ozone is the most prevalent component of photochemical smog, along with peroxy acetyl nitrite (PAN), peroxy benzoyl nitrite (PBN), formaldehyde, acrolein, and others. This kind of smog is frequently observed in heavily populated areas of big cities, where the weather is ideal for its development. Unfortunately, photochemical pollution can harm paint, rubber, and plastics in addition to being extremely detrimental to both plant and animal life. Human beings encounter a diverse range of health issues, one of which is ocular irritation. This particular condition is mostly attributed to the presence of formaldehyde, acrolein, and PAN. Individuals encounter a diverse range of

health issues, one of which is ocular irritation, predominantly triggered by formaldehyde, acrolein, and PAN (*Handbook of Air Pollution From Internal Combustion Engines*, 1998). Ozone (O_3), which shields us from damaging UV radiation in the upper atmosphere (stratosphere), is also hazardous at even low dose of concentrations in the troposphere, where it causes chest constriction, mucous membrane irritation, rubber breaking, and injury to flora. Ozone exposure has been related in recent research to human premature death, with higher ozone concentrations being associated with higher total mortality rates as well as cardiovascular and respiratory mortality rates (S.-Y. Kim et al., 2020). The National Research Council (*Climate Change and Food Security*, 2010) discovered in a recent study by the National Academy of Sciences that O_3 rises human premature mortality. According to the study, for every 10 ppb of ozone, total mortality increases by 0.82%.

2.3 Traces of heavy metal in air

Particulate matter ($PM_{2.5}$), comprising particles with a diameter of 2.5 micrometers or smaller, represents a substantial type of air pollution. The issue of $PM_{2.5}$ is of particular concern owing to its diminutive size and elevated surface area to mass ratio. This attribute renders it a proficient transporter of biologically accessible transition metals or metalloids. The human body can readily absorb these metals or metalloids through different pathways, including ingestion, dermal contact absorption, and inhalation (Abd Elnabi et al., 2023; Jan et al., 2015; Witkowska et al., 2021). Heavy metals possess the capacity to inflict harm and interfere with the optimal operation of diverse organs within the human body, encompassing the brain, kidneys, lungs, liver, and blood. The toxicity of the substance can result in both acute and chronic effects. Extended exposure to heavy metals can lead to degenerative alterations in muscles and nerves, akin to health disorders such as Parkinson's disease, multiple sclerosis, muscular

dystrophy, and Alzheimer's disease (Jaishankar et al., 2014a). In addition, prolonged and consistent exposure to specific heavy metals has the potential to elevate the likelihood of developing cancer.

Repetitive and extended exposure to these metallic elements or their compounds has the potential to inflict damage upon nucleic acids, disturb the endocrine system, and affect the reproductive system, thereby potentially resulting in the development of cancer (Jaishankar et al., 2014). According to a study conducted in 2010, the global mortality rate due to diseases associated with air pollution was reported to be over 200,000 individuals (*Healthy People 2030*, 2020). Furthermore, it is worth noting that in October 2013, the International Agency for Research on Cancer (IARC), which is the specialized cancer agency of the World Health Organization (WHO), officially designated outdoor pollutants as a 1st Group human carcinogen (*American Cancer Society*, 2022). Due to their potential to have a substantial impact on public health, particulate matters have attracted heightened attention from the scientific community.

The present research findings play a critical role in enhancing our understanding of the dispersion patterns of heavy metals in the atmosphere, thereby facilitating comprehensive pollution management strategies and ensuring compliance with air quality regulations. Moreover, the data serves the purpose of identifying sources of pollution, formulating effective control strategies, enhancing public awareness, and aiding policymakers in assessing the health hazards linked to exposure to heavy metals. This study conducted a comprehensive assessment of heavy metal concentrations throughout the city of Chattogram for the most recent year. Subsequently, evaluations were performed to determine the potential carcinogenic and non-carcinogenic risks associated with these concentrations.

2.3.1 Heavy metal in air and their sources

The presence of traces of heavy metals in the atmosphere constitutes a form of air pollution that can exert detrimental impacts on both human well-being and the natural surroundings. Various heavy metals, including lead, mercury, cadmium, arsenic, and chromium, can be emitted into the atmosphere through both natural and anthropogenic means. Table 2.1 provides a concise compilation of prevalent pollutants and their origins within the road traffic setting.

The atmosphere can be enriched with heavy metals through various natural processes, such as volcanic eruptions, wildfires, and dust storms. During these events, particulate matter carrying heavy metals is emitted into the air. Nevertheless, it is anthropogenic activities that serve as the principal sources of heavy metal air pollution. Various anthropogenic activities, including industrial processes such as mining, smelting, and metal processing, as well as the combustion of fossil fuels from vehicles and power plants, waste incineration, and specific manufacturing processes, result in the substantial emission of heavy metals into the atmosphere. Upon being released into the atmosphere, this particulate matter containing heavy metals has the potential to remain suspended in the air for varying durations, contingent upon factors such as their size and prevailing atmospheric conditions.

Particles have the capacity to undergo long-range transportation and subsequently deposit onto the Earth's surface through either dry or wet deposition mechanisms. This process can result in the contamination of various environmental compartments, including soil, water bodies, and vegetation. The concentration and composition of heavy metals are contingent upon the specific rock type and environmental factors that exert influence on weathering mechanisms.

Table 2.1. Common pollutants typically observed in runoff from roads and highways, adapted from (Sarkar, 2002) and (Pal, 2012)

Pollutants	Sources
Lead (Pb)	Leaded gasoline from auto exhaust, tire wear, lubricating oil and grease, bearing wear and atmospheric fallout
Zinc (Zn)	Tyre wear, motor oil and grease
Iron (Fe)	Auto body rust, steel highway structures such as bridges and guardrails and moving engine parts
Copper (Cu)	Metal plating, bearing and brushing wear, moving engine parts, brake lining wear, fungicides and insecticides
Cadmium (Cd)	Battery manufacturing, metal soldering or welding is the most prominent, anti-corrosive metal plating, tire wear and insecticide application etc.
Chromium (Cr)	Construction industry is via cement, Metal plating, stainless steel welding, moving parts and brake lining wear
Nickel (Ni)	Diesel fuel and gasoline, lubricating oil, metal plating, bushing wear, brake lining wear and asphalt paving
Manganese (Mn)	Moving engine parts

2.3.2 Contamination Factor of Airborne Road Dust Particles

The Contamination Factor (CF) is indeed a critical metric in assessing the potential health risks associated with heavy metal contamination. Generally, a higher CF value indicates a higher concentration of a specific heavy metal in the sample compared to the control or background level. This increased level of contamination factor of heavy metals might subsequently pose greater health risks to humans and other living organisms (Kamran et al., 2013; Ametepey et al., 2018; Masindi and Muedi, 2018).

Several studies (Herngren et al., 2005; Suryawanshi et al., 2016a) have provided evidence indicating that existence of heavy metal in air is contaminated because of human activities and the land use in its vicinity. Suspended metals in air, which are derived from various sources such as vehicle traffic, pavements, and industrial activities. The aforementioned pollutants are recognized for their ability to endure in the environment and cause extensive consequences, resulting in detrimental effects on resilient species, the disappearance of vulnerable

invertebrates, and potential risks to human well-being (Jadaa and Mohammed, 2023; Tchounwou et al., 2012a). In this study, to evaluate the level of contamination of individual metals found in road dust, the methodology proposed by (Hakanson, 1980) has been utilized. This approach facilitates the correlation between the levels of concentrations of heavy metals, and their associated contamination levels.

The health impact also varies on different factors such as the route of exposure (ingestion, inhalation, dermal contact), the vulnerability of the population (e.g., children, pregnant women), and the presence of other contaminants. Therefore, while a high CF is often an alarming sign necessitating immediate intervention, a comprehensive risk assessment is essential for determining the true health risks involved. In summary, the Contamination Factor can serve as a preliminary index for gauging the health risks associated with heavy metal pollution, but it's one part of a multi-faceted risk assessment process.

2.3.3 Human health risk linked with airborne dust particles

This section of the human health risk assessment delves into the correlation between the specified heavy metals in air and a range of health outcomes, encompassing both cancerous and non-cancerous diseases. Activation of pulmonary inflammatory processes, lung damage and cardiac diseases can arise from inhaling airborne pollutants, including oxidant gases like ozone, nitrogen dioxide, or particulate air pollution (Briffa et al., 2020a; Yuan et al., 2016). This exposure may also lead to increased oxidative stress and disruption of barrier mechanisms due to heavy metal exposure, subsequently impairing DNA repair (Azeh Engwa et al., 2019; Balali-Mood et al., 2021; Mitra et al., 2022; Pyatha et al., 2022). The consequences include inflammation and tissue destruction in the lungs, presenting as obstructive lung disease. Toxic metals (such as As, Cd, Pb, and Hg) as well as certain essential metals like (Co, Cu, Cr, Ni, and Se) function

as metalloid estrogens and could enhance the susceptibility to cardiovascular disease (CVD) through their ability to disrupt endocrine processes (Choe et al., 2003). Literature Review shows that imbalanced levels of Zn, Cu, Cr and Ni are associated with increasing CVD risk (Kampa and Castanas, 2008b; A. Yang et al., 2020). Moreover, Cu is as essential heavy metal but still excessive of it causes cellular damage (Tchounwou et al., 2012b).

The carcinogenic risks associated with exposure to arsenic, chrome, and nickel, particularly in certain chemical forms, have been firmly established through epidemiological and experimental studies (Cone, 1987; Fishbein et al., 1981; *IARC Monographs on the Evaluation of Carcinogenic Risks to Humans*, 1996). Also, Metals associated with health disease like asthma, often based on case reports, encompass nickel (Block and Yeung, 1982; *IARC Monographs on the Evaluation of Carcinogenic Risks to Humans*, 1996; MALO et al., 1982; NOVEY et al., 1983), and chromium (MOLLER et al., 1986). Effects such as tachycardia, elevated blood pressure, and anemia attributed to the inhibitory impact on hematopoiesis have been noted as outcomes of heavy metal pollution, particularly involving mercury, nickel, and arsenic (Y.-C. Huang and Ghio, 2006).

Additionally, epidemiological investigations have associated dioxin exposure with heightened mortality due to ischemic heart disease, and animal studies have demonstrated that heavy metals can elevate triglyceride levels as observed in mice (Dalton et al., 2001). Also, commonly encountered symptoms including irritation of the nose and throat, subsequent bronchoconstriction, and breathlessness, particularly among individuals with asthma, tend to manifest following heightened exposure to sulfur dioxide (Balmes, Fine and Sheppard, 198), nitrogen oxides (Kagawa, 1985), and specific heavy metals such as arsenic, nickel, or vanadium. Furthermore, the development of ulcers constitutes a significant issue among individuals exposed to chromium, with ulcers often

persisting for extended durations of several months, accompanied by notably sluggish healing rates.

Moreover, when humans come into contact with chromium compounds at elevated concentrations, the presence of these compounds can result in a reduction in erythrocyte glutathione reductase activity, thereby diminishing the capacity to convert methemoglobin to hemoglobin. Furthermore, exposure to chromate compounds is associated with the induction of DNA damage, which can lead to the formation of DNA adducts, aberrations in chromosomes, sister chromatid exchanges, and modifications to DNA (Matsumoto et al., 2006; O'Brien et al., 2001).

Iron reactions help in the respiratory process of most aerobic organisms. If not properly protected, it can act as a catalyst in reactions that form radicals and destroy biomolecules, cells, tissues, and the entire organism. Children are very receptive to iron toxicity as they are in contact with lots of iron-containing products. Iron toxicity, i.e., ferrous toxicosis, occurs in four stages (Bhasin et al., 2002; Ryan and Aust, 1992).

However, the respiratory system does not always constitute the sole or primary target for the toxicity of metal compounds, even when their entry into the body occurs through inhalation. Exposure pathways can also include ingestion and skin contact, prompting the need for health risk assessments. Consequently, chronic inhalation of substances like lead, mercury, or manganese might result in systemic effects, such as neurological harm, without causing substantial respiratory damage. In contrast, certain metals like cadmium or nickel can induce alterations in both lung and kidney functions, potentially influenced by the route of exposure. Hence, it is crucial to recognize the possibility of extra-pulmonary manifestations in the context of metal toxicology.

The Health Risk Assessment (HRA) model is employed to quantify the impact of contaminants on human health. The procedure consists of four parts, namely risk characterization, hazard identification, exposure assessment, and dose-response evaluation. In order to assess the influence of trace elements on human health, it is important to collate data from previous studies to ascertain possible risks. The evaluation of exposure primarily centers on the process by which heavy metals are transferred from their origin to the site of exposure and then received by the receptor.

As significant environmental pollutants, heavy metals are notorious for their toxicity, persistence, and incapacity to dissolve. Heavy metals can enter the body primarily by inhalation, dust ingestion, and skin contact. Children are particularly susceptible to this because of their proneness to hand-to-mouth transmission and other exposures, which can result in considerable absorption of contaminated dust. Dose-response analysis looks at the connection between exposure to heavy metals and the consequences for human health. To quantify the danger that people may encounter, all the facts from the above processes are merged in the final step of risk categorization.

2.4 Air pollution scenario in Bangladesh

The main contributors to air pollution in Bangladesh encompass a range of factors, namely the expanding population, emissions originating from vehicles and industries, the utilization of fossil fuels for cooking and power production, and inadequate waste management practices. The concentration of substantial industrial operations in prominent urban centers including as Dhaka, Gazipur, Chittagong, Khulna, Narayanganj, and other divisional towns has led to the degradation of air quality, therefore presenting significant health hazards to the populace.

Out of the regions, Narayanganj exhibits a notable distinction as the most polluted area in relation to the concentration of particulate matter (Biswas, 2019). In addition to Narayanganj, high levels of particle matter are also seen in Dhaka, Gazipur and Chattogram. In contrast, Sylhet exhibits the lowest concentration of particulate matter (PM). The major causes of particulate matter in the city of Dhaka are emissions from brick kilns and vehicles (Begum et al., 2013b; Biswas, 2019). In Dhaka, air pollution from automobile emissions has remained steady despite a recent rise in traffic. The stability observed can be attributed to the implementation of laws such as the prohibition of two-stroke engine-powered three-wheelers and the imposition of limitations on the mobility of diesel engine-equipped trucks. The implementation of these measures has led to a substantial reduction in the adverse impacts of traffic-related air pollution inside the urban area. (Mahmood et al., 2019).

The concentration of particulate matter (PM) in Dhaka, Chittagong, Gazipur, Sylhet and Narayanganj from 2014 to 2017 was examined in a study by (Mahmood et al., 2019) . The results showed that both $PM_{2.5}$ and PM_{10} concentrations in these cities were higher above the 24-hour average Bangladesh National Ambient Air Quality Standards (BNAAQS). This shows that the amounts of particulate matter above the regulatory authorities' permissible limits, potentially creating health concerns for the local people. Similar findings were found in a different study by (Masum and Pal, 2020) that covered eight cities in Bangladesh. In most instances, the study found that $PM_{2.5}$ was the crucial pollutant for the Air Quality Index (AQI), underscoring the importance of this particle in assessing the quality of the air. In Rajshahi and Barisal, the AQI indicated a declining trend, whereas it increased in Narayanganj, Dhaka, and Chittagong.

Compared to metropolitan locations, rural areas were found to have lower levels of pollution because of things like lower population density, restricted industrialization, and less traffic. Nevertheless, it was found that these regions' agriculture and animal farms, which produce dust, smoke, and methane (CH_4), are major sources of air pollution. These results underline the complexity of Bangladesh's sources of air pollution and the regional variations in air quality.

Emissions from cooking activities can have an impact on indoor air quality in rural Bangladesh. When compared to cleaner fuels like LPG, which are frequently used in rural households, biomass fuels cause PM levels to be greater (Begum et al., 2010). Various businesses, such as pulp, sugar mills, tanneries, paper mills, textile factories, pharmaceutical enterprises, oil refineries, compound producers, composting facilities, and chemical manufacturers, make substantial contributions to air pollution inside industrial zones. Furthermore, the transportation of fine particles across large distances, in conjunction with local sources, plays a significant role in exacerbating air pollution in Bangladesh. Due to its geographical location, the nation is susceptible to transboundary pollution originating from neighboring countries including as India, Pakistan, and Nepal (Begum et al., 2011; Dihan et al., 2023; Ommi et al., 2017). The functioning of numerous brick kilns in their entirety, coupled with the substantial transboundary movement of particulate matter throughout the winter season, leads to the occurrence of elevated concentrations of PM at certain intervals. The multifaceted challenges pertaining to air quality in Bangladesh arise from a variety of pollution sources.

In fact, research that have been published in the scientific literature have given evidence connecting Bangladesh's high levels of air pollution to a higher mortality risk from respiratory and cardiovascular illnesses (CVD). According to research by (Massey et al., 2013), the country's greater air pollution exposures are

linked to a higher incidence of cardiovascular disease (CVD) and respiratory conditions, which could result in an increase in mortality rates for these conditions. High blood pressure is identified as the primary risk factor for mortality in Bangladesh, followed by smoking and outdoor air pollution (Health Effect Institute, 2019). Based on findings from a comprehensive worldwide status of the air assessment, it was observed that Bangladesh encountered a total of 122,400 annual deaths in the year 2015, which were directly associated with the adverse effects of exposure to $PM_{2.5}$ (Health Effects Institute, 2017). Over the course of the past twenty years, there has been a notable rise in mortality rates associated with air pollution, with estimates indicating a significant increase of 52% specifically in the context of Bangladesh show in Fig. 2.3.

The rise in mortality rates can be attributed to various factors, including increased exposure to harmful elements, population expansion, inadequate access to accurate diagnosis, and limited availability of effective treatment options.

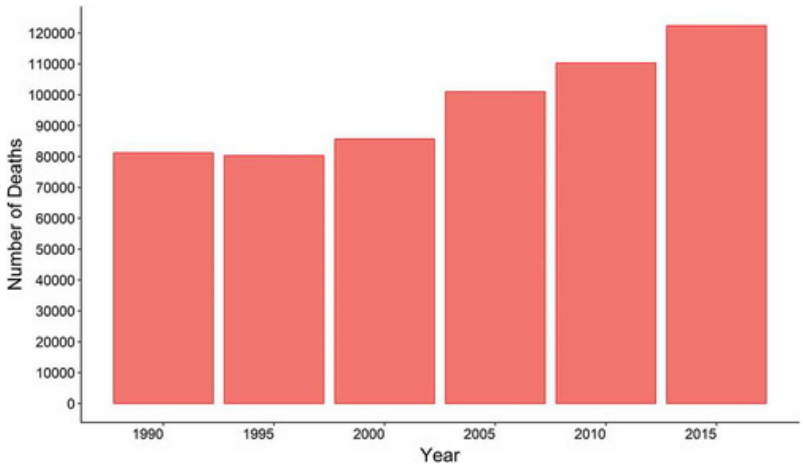

Fig. 2.3 Number of mortalities linked to exposure to $PM_{2.5}$ (Health Effect Institute, 2019)

A recent study conducted in Dhaka reported a total of 9051 premature deaths in 2016 that were attributed to exposure to $PM_{2.5}$. The study provided a 95% confidence interval for this estimate, ranging from 4596 to 12,025. The study

found that there were a total of 4435 premature deaths (95% CI: 1721–5304) attributed to ischemic heart disease (IHD), also premature deaths of 2669 (95% CI: (1850–4135) attributed to stroke, 500 deaths (95% CI: 204–649), attributed to lung cancer (LC), 1246 deaths (95% CI: 684–1689) attributed to chronic obstructive pulmonary disease (COPD), and 201 premature deaths (95% CI: 137–248) attributed to acute lower respiratory infection (ALRI) (Maji, Arora, et al., 2018).

In 1997, the nation of Bangladesh introduced ambient air quality guidelines as a component of the Bangladesh Environmental Conservation Rules (BECR), 1997. This measure represented a key milestone in the efforts to tackle air pollution concerns. Over the course of its development, the nation has endeavored to tackle the issue of air pollution, frequently seeking counsel and assistance from international organization's such as Asian Development Bank (ADB), United Nations Environment Program (UNEP) and the World Bank (WB). These organizations have been involved in the development of strategies and initiatives with the objective of mitigating and managing air pollution in Bangladesh. The Department of Environment (DoE), which serves as the governmental body assigned with the task of safeguarding the environment in Bangladesh, has been actively engaged in the formulation of an 'Air Pollution Reduction Policy for Bangladesh. The alignment of this program with the ideals articulated in the Malé Declaration on Control and Prevention of Air Pollution (DoE, 2012) signifies the nation's commitment to addressing air pollution concerns and safeguarding the environment for the welfare of its residents.

2.5 Air pollution assessment in Chattogram City, Bangladesh

The largest port in Bangladesh is in Chattogram, which is situated at latitude 22.22°N and longitude 91.47°E. Chattogram sees heavy traffic, especially in the core city area. The city's primary road system stretches northward to the industrial zones and southward to the port area. These highways experience

heavy traffic flow and are frequently encumbered by all-day traffic jams. Notably, vehicles carrying goods between the port and the industrial regions make up a sizable portion of this traffic. There are significant emissions of black diesel smoke due to the region's difficult topography, stop-and-start nature of congested traffic, and the age and weight of most trucks.

The main source of air pollution in Chattogram City is thought to be motorized transportation. They are thought to be the biggest contributors to total pollution levels. Though green landscape around Chattogram city and monsoon heavy rainfall helps to reduce the intensity of air pollution, a significant change in land uses and human intervention aggravate the degradation of air quality (Rouf et al.,2012). Over the course of six years, the average yearly concentration of $PM_{2.5}$ and PM_{10} in Chattogram City was 5–6 times and 3 times, respectively, higher than the Bangladesh National Ambient Air Quality Standard (BNAAQS) (A. K. Majumder et al., 2020). Decrease in human activity during the COVID-19 shutdown resulted in a 26% improvement in the air quality index value compared to the previous dry season conducted in a study of Chattogram City (Masum and Pal, 2020).

Only a small amount of research has been done on Chattogram's air quality. The data that is currently available, however, indicates that Chattogram's air quality is comparable to that of Bangladesh's metropolis, Dhaka, which is notorious for its severe air pollution. According to a recent World Bank report, air pollution causes millions of episodes of disease and 10,800 premature deaths annually in Dhaka. Research on the city of Chittagong's air quality has been done by the Norwegian Institute of Air Research (NILU), which has improved knowledge of the area's air pollution levels and associated health effects. More detailed examinations and study are needed to better pinpoint and address the problems

with Chittagong's air quality and to develop workable solutions to protect the public's health.

2.6 Satellite image analysis for air quality detection

Satellite datasets are employed for the purpose of air quality monitoring owing to their exceptional capacity to provide comprehensive worldwide coverage and data that is either real-time or nearly real-time. This enables the continuous assessment of atmospheric contaminants across vast regions. These datasets serve as a valuable addition to the existing ground-based monitoring networks, enabling the concurrent measurement of many pollutants like NO_2, SO_2, CO, O_3, and aerosols. Among the most widely utilized are the Landsat series, dating back to 1972, offering multispectral imagery indispensable for land cover classification and environmental assessments. Launched in February 2013 by NASA and the United States Geological Survey (USGS), Landsat 8 is a satellite in the Landsat program (*USGS*, 2021). It is a member of a group of satellites that have been taking pictures of the Earth's surface for many years. With the help of its operational land imager (OLI) and thermal infrared sensor (TIRS), Landsat 8 can take detailed images of the Earth. With only a little amount of image swath overlap, the Landsat 8 satellite can cover the entire planet in a systematic manner because of its polar sun-synchronous orbit. It can take pictures in the visible, near-infrared, short-wave infrared, and thermal infrared ranges of the electromagnetic spectrum (*Computers in Earth and Environmental Sciences*, 2022). These spectral bands offer important details on the type of flora present, water bodies, and other environmental characteristics. The enhanced spatial resolution of Landsat 8 over its predecessors is one of its distinguishing qualities. The visible, near infrared, and shortwave infrared bands have a resolution of 30 meters, and the thermal infrared bands have a resolution of 100 meters

(*GISGEOGRAPHY*, 2023). This improved resolution makes it possible to track changes to the Earth's surface throughout time in greater detail and accuracy.

2.7 Air quality guidelines and air quality index

Standards for air quality are implemented to establish the uppermost allowable thresholds for air pollutants within specific timeframes. Table 2.2 presents the air quality standards established in Bangladesh, in conjunction with the standards set forth by the United States Environment Protection Agency (USEPA) and the World Health Organization (WHO).

Table 2.2. Standards adopted from different organization for air pollutants

Pollutant	Averaging Period	National Ambient Air Quality Standards for Bangladesh μg/m^3 (2005)	WHO Guideline Values μg/m^3 (2021)	US EPA Standards μg/m^3 (2000)
SO_2	Annual	80	-	78
	24-hr	365	40	
Pb	Annual	0.5	0.5	365
NO_X	Annual	100	10	53*
	24-hr	-	25	100
CO	24-hr	-	4*	-
$PM_{2.5}$	Annual	15	05	15
	24-hr	65	15	35
PM_{10}	Annual	50	15	-
	24-hr	150	45	150

N.B.: CO is in mg/m^3; 53 is for 1-hr averaging period

Upon comparison, it is evident that the local standards presented in the table bear resemblance to the standards established by the USEPA. Various standards are established for different pollutants, with consideration given to their average exposure duration, as this factor significantly influences the health risks associated with them. Also, the table illustrates that the WHO Guideline Values are stricter than the NAAQS and USEPA Standards. The primary purpose of regulatory bodies is to create appropriate standards for each pollutant in order

to safeguard public health and alleviate the adverse effects of air pollution on the populace.

The Air Quality Index (AQI) is used to track daily air quality in any region, providing data on levels of air pollution and related health hazards for individuals. The Department of Environment (DoE) established national ambient air quality standards for these pollutants. The Air Quality Index (AQI) standards applicable to Bangladesh are presented below in Table in 2.3.

The air quality index (AQI) in Bangladesh is based on five criterion pollutants: ozone (O_3), carbon monoxide (CO), sulphur dioxide (SO_2), and particulate matter (PM_{10} and $PM_{2.5}$). The pollutants mentioned are regulated by national ambient air quality laws implemented by the Department of Environment (DoE). These regulations are responsible for establishing the parameters for the nation's Air Quality Index (AQI). The Air Quality Index (AQI) provides an indication of the potential health risks associated with exposure to various pollutants for humans during a certain timeframe, ranging from hours to days.

Table 2.3. Air Quality Index for Bangladesh (DoE, 2019)

Air Quality Index (AQI) range	Category	Color	Cautionary Statement
0-50	Good	Green	Little potential to affect public health
51-100	Moderate	Yellow Green	Unusually sensitive individuals
101-150	Caution	Yellow	Identifiable groups at risk
150-200	Unhealthy	Orange	General Public at risk; sensitive groups at greater risk
201-300	Very Unhealthy	Red	General Public at grester risk; sensitive groups at greateest risk

The AQI measures air quality on a scale from 0 to 300, with a number of 0-50 indicating good air quality with no major risks and 300 denoting a dangerously high amount of pollution. According to the Department of Environment (DoE),

an air quality index (AQI) value of 100 is generally regarded as adequate. A higher AQI may be tolerated by people with stronger immunity and health.

2.8 Existing Air Pollution Reduction Policy Measures in Bangladesh

The air quality in metropolitan regions of Bangladesh is gradually decreasing. The citizens must prioritize the establishment of a cleaner and more sustainable environment considering the increasing health, economic, and environmental problems linked to inadequate air quality. To mitigate air pollution, it is imperative for the government to enact comprehensive policies that can successfully tackle these issues.

Over time, the Government of Bangladesh (GoB) has conducted several programs to improve the air quality in cities in Bangladesh. In July 1999, the Government of Brazil (GoB) took action to remove lead from gasoline in order to reduce the harmful emissions caused by this contaminant. During the early 2000s, the presence of 2-stroke wheeled baby taxis significantly contributed to the formation of a dense layer of black smoke, particulate matter (PM), and hydrocarbons that covered the skies of Dhaka city and other major urban centers. In 2003, the government implemented a prohibition on 2-stroke baby taxis in Dhaka city and gradually eliminated them which led to a 41% decrease in $PM_{2.5}$ concentration (DoE and World Bank, 2019). In addition, the promotion of Compressed Natural Gas (CNG) as a vehicle fuel aims to significantly reduce emissions from burning petroleum and achieve lower levels of greenhouse gas emissions. In 2005, Bangladesh updated its vehicle emission requirements to include EURO-II for new and light cars, and EURO-I for on-road and heavy trucks (Hossain et al., 2021). Furthermore, the government took a significant step by issuing a High Court order in 2019 to close down existing illegal brick kilns and prohibit the establishment of brick kilns in commercial, residential, and environmentally sensitive areas around Dhaka city. Also, the government has

decided to transition using concrete blocks instead of bricks in all upcoming government projects by 2025, aiming to minimize brick production, a major source of air pollution in the country. At the start of 2020, a series of nine instructions were issued which included requirements such as transporting waste and construction materials in vehicles that are covered, making sure that construction materials at sites under construction are properly covered, city corporations spraying water on roads, and stopping the operation of vehicles that are considered unsuitable (Dhaka Tribune, 2023). Additionally, efforts are being made to explore and adopt more environmentally friendly technologies for brick production to mitigate emissions from brickfields (Hossain et al., 2021).

Furthermore, the government is actively encouraging the adoption of environmentally friendly technology like solar panels by providing incentives such as tax exemptions and decreased import charges (Hossain et al., 2021). The air pollution reduction strategy in Bangladesh highlights several capacity constraints in pollution control, such as inadequate resources for monitoring, laboratories, inventory compilation, health effect evaluations, and stove certification. Pollution reduction techniques in Bangladesh rely on qualitative multi-criteria evaluation due to the limitations of quantitative benefit-cost modeling (Sharma et al., 2019). The World Bank has been actively assisting the Bangladesh government by giving both technical and financial aid in the development of legislation, implementation of CASE project and plans to minimize air pollution. In 2019, the government presented a preliminary version of the Clean Air Act to effectively regulate the overall air quality in Bangladesh. Despite the submission of the draft, the legislation has not been implemented. Furthermore, the government of Bangladesh and the German International Cooperation (GIZ) work together to develop energy-efficient technologies that lower the consumption of fossil fuels, indoor air pollution, and greenhouse gas emissions (GIZ, 2021). Concern over the social cost of air pollution is becoming

more prevalent among economists and politicians, highlighting the necessity for stricter measures to get cleaner air in cities.

2.9 Particulate matter's effect on human health

Human health is directly impacted by air pollution, especially when it reaches high levels and causes fatalities or serious respiratory disorders. Worldwide, several urban areas have linked air pollution to early deaths. Epidemiological research may be classified into two primary categories: time-series studies, which examine the impacts of short-term exposure to particulate matter (PM), and cohort studies, which evaluate the consequences of prolonged, chronic exposure to PM.

Exposure to air pollution for long-term can hasten the aging of lung tissue, exacerbate cardiovascular diseases, and contribute to chronic obstructive pulmonary disease, which can lead to early death. Acute exposure, also known as short-term exposure to abrupt jumps in pollution levels, can be particularly dangerous to people with a history of cardiopulmonary disorders or those who are more sensitive, and can even result in premature death. Air pollution can lead to a number of health problems in addition to raising the death rate in communities, increasing the total morbidity effect on human health. Some of the prominent health-related morbidity implications include adult chronic bronchitis, child acute bronchitis, hospital admissions for respiratory and cardiac conditions, asthma attacks, visits to the emergency room, minor restricted activity days, and respiratory symptom days (Guttikunda, 2012).

2.9.1 Health Effects Related to Mortality

The selection of $PM_{2.5}$ and PM_{10} for the quantitative assessment of health effects is grounded in their widespread use as exposure metrics in epidemiological studies worldwide. In the last twenty years, numerous epidemiological studies conducted on five continents have consistently emphasized the correlation

between mortality and morbidity and different durations of exposure to pollutant concentrations, such as particulate matter (PM). These durations include 24 hours, or long-term exposure lasting more than a year. The expected effects on mortality are expected to be predominantly evident among elderly adults with pre-existing cardiovascular and respiratory ailments, as well as among babies. Air pollution's influence on human mortality encompasses diverse health outcomes. For example, there is evidence linking prolonged subjection of individuals to $PM_{2.5}$ with increased numbers of cardiovascular mortality and lung cancer in adults. Furthermore, there is a correlation between exposure to particulate matter (PM) and death from any cause, regardless of age.

Short term exposure-associated mortality

In the early stages of studying short-term fluctuations in air pollution's health impacts, researchers initially focused on severe pollution episodes, tracking death counts over time. By the early 1990s, daily time series studies emerged, moving away from extreme events and examining daily mortality changes linked to more typical, moderate air pollution fluctuations. A review on mortality related to short term exposure is provided in Table. 2.4.

A novel method called the case-crossover study design was introduced by (Maclure, 1991) and adopted by (Pope III, 2002). In contrast to traditional methods of time series analysis, this particular technique focuses on aligning the exposure event with control periods at the time of death. This alignment allows for the inclusion and examination of other factors, such as day of the week, seasonal fluctuations, and long-term trends. This approach also allows for assessing individual-level factors.

It's worth noting that short-term exposure over a day or a few days are unlikely to raise mortality increases in air pollution. Studies have found modest effects; for example, a 10 $\mu g/m^3$ increase in $PM_{2.5}$ might lead to around a 1% rise in

mortality (Pope and Dockery, 2006a). In recent years, there has been a notable change in study focus towards comprehending the intricate connections between daily fluctuations in air pollution and their significant implications for human health.

Table 2.4. A concise overview of various studies related to short-term mortality rates, as summarized by (Pope and Dockery, 2006a)

Study	Primary Sources	Exposure Increment	Percent Increases in Relative Risk of Mortality (95% CI)		
			All Cause	Cardiopulmonary	Lung Cancer
Harvard Six Cities, original	Dockery et al. 1993[26]	10 μg/m³ $PM_{2.5}$	13 (4.2, 23)	18 (6.0, 32)	18 (−11, 57)
Harvard Six Cities, HEI reanalysis	Krewski et al. 2000[177]	10 μg/m³ $PM_{2.5}$	14 (5.4, 23)	19 (6.5, 33)	21 (−8.4, 60)
Harvard Six Cities, extended analysis	Laden et al. 2006[184]	10 μg/m³ $PM_{2.5}$	16 (7, 26)	28 (13, 44)[a]	27 (−4, 69)
ACS, original	Pope et al. 1995[27]	10 μg/m³ $PM_{2.5}$	6.6 (3.5, 9.8)	12 (6.7,17)	1.2 (−8.7, 12)
ACS, HEI reanalysis	Krewski et al. 2000[177]	10 μg/m³ $PM_{2.5}$	7.0 (3.9, 10)	12 (7.4, 17)	0.8 (−8.7, 11)
ACS, extended analysis	Pope et al. 2002[179]	10 μg/m³ $PM_{2.5}$	6.2 (1.6, 11)	9.3 (3.3, 16)	13.5 (4.4, 23)
	Pope et al. 2004[180]			12 (8, 15)[a]	
ACS adjusted using various education weighting schemes	Dockery et al. 1993[26]	10 μg/m³ $PM_{2.5}$	8–11	12–14	3–24
	Pope et al. 2002[179]				
	Krewski et al. 2000[177]				
ACS intrametro Los Angeles	Jerrett et al. 2005[181]	10 μg/m³ $PM_{2.5}$	17 (5, 30)	12 (−3, 30)	44 (−2, 211)
Postneonatal infant mortality, U.S.	Woodruff et al. 1997[185]	20 μg/m³ PM_{10}	8.0 (4, 14)	–	–
Postneonatal infant mortality, CA	Woodruff et al. 2006[186]	10 μg/m³ $PM_{2.5}$	7.0 (−7, 24)	113 (12, 305)[c]	–
AHSMOG[b]	Abbey et al. 1999[187]	20 μg/m³ PM_{10}	2.1 (−4.5, 9.2)	0.6 (−7.8, 10)	81 (14, 186)
AHSMOG, males only	McDonnell et al. 2000[188]	10 μg/m³ $PM_{2.5}$	8.5 (−2.3, 21)	23 (−3, 55)	39 (−21, 150)
AHSMOG, females only	Chen et al. 2005[189]	10 μg/m³ $PM_{2.5}$	–	42 (6, 90)[a]	–
Women's Health Initiative	Miller et al. 2004[190]	10 μg/m³ $PM_{2.5}$	–	32 (1, 73)[a]	
VA, preliminary	Lipfert et al. 2000, 2003[190,192]	10 μg/m³ $PM_{2.5}$	0.3 (NS)[d]	–	–
VA, extended	Lipfert et al. 2006[193]	10 μg/m³ $PM_{2.5}$	15 (5, 26)[e]	–	–
11 CA counties, elderly	Enstrom 2005[194]	10 μg/m³ $PM_{2.5}$	1 (−0.6, 2.6)	–	–
Netherlands	Hoek et al. 2002[195]	10 μg/m³ BS	17 (−24, 78)	34 (−32, 164)	–
Netherlands	Hoek et al. 2002[195]	Near major road	41 (−6, 112)	95 (9, 251)	–
Hamilton, Ontario, Canada	Finkelstein et al. 2004[197]	Near major road	18 (2, 38)	–	–
French PAARC	Filleul et al. 2005[198]	10 μg/m³ BS	7 (3, 10)[f]	5 (−2,12)[f]	3 (−8,15)[f]
Cystic fibrosis	Goss et al. 2004[200]	10 μg/m³ $PM_{2.5}$	32 (−9, 93)	–	–

[a]Cardiovascular only; [b]Pooled estimates for males and females; pollution associations were observed primarily in males and not females; [c]Respiratory only; [d]Reported to be nonsignificant by author; overall, effect estimates to various measure of particulate air pollution were highly unstable and not robust to selection of model and time windows; [e]Estimates from the single pollutant model and for 1989–1996 follow-up; effect estimates are much smaller and statistically insignificant in an analysis restricted to counties with nitrogen dioxide data and for the 1997–2001 follow-up; furthermore, county-level traffic density is a strong predictor of survival and stronger than $PM_{2.5}$ when included with $PM_{2.5}$ in joint regressions; [f]Estimates when six monitors that were heavily influenced by local traffic sources were excluded; when data from all 24 monitors in all areas were used, no statistically significant associations between mortality and pollution were observed.

It's worth noting that short-term exposure over a day or a few days are unlikely to raise mortality increases in air pollution. Studies have found modest effects; for example, a 10 μg/m³ increase in $PM_{2.5}$ might lead to around a 1% rise in mortality (Pope and Dockery, 2006a). In recent years, there has been a notable change in study focus towards comprehending the intricate connections between daily fluctuations in air pollution and their significant implications for human health.

Mortality resulted from prolonged exposure

Studies examining daily time series consistently observe immediate impacts of exposure to particulate matter (PM), although provide inadequate understanding of the long-term consequences or the contribution of pollution to chronic illnesses (McMichael et al., 1999). Cross-sectional studies examining population-based mortality rates were largely dismissed due to concerns about controlling for individual risk factors like smoking (Pope and Dockery, 2006a).

Table 2.5. Correlation between long-term particulate exposure and the percentage increase in relative risk of mortality, along with the corresponding 95% confidence intervals (CI). Source: (Pope and Dockery, 2006a)

Study	Primary Sources	Exposure Increment	Percent Increases in Relative Risk of Mortality (95% CI)		
			All Cause	Cardiopulmonary	Lung Cancer
Harvard Six Cities, original	Dockery et al. 1993[26]	10 μg/m³ $PM_{2.5}$	13 (4.2, 23)	18 (6.0, 32)	18 (−11, 57)
Harvard Six Cities, HEI reanalysis	Krewski et al. 2000[177]	10 μg/m³ $PM_{2.5}$	14 (5.4, 23)	19 (6.5, 33)	21 (−8.4, 60)
Harvard Six Cities, extended analysis	Laden et al. 2006[184]	10 μg/m³ $PM_{2.5}$	16 (7, 26)	28 (13, 44)[a]	27 (−4, 69)
ACS, original	Pope et al. 1995[27]	10 μg/m³ $PM_{2.5}$	6.6 (3.5, 9.8)	12 (6.7,17)	1.2 (−8.7, 12)
ACS, HEI reanalysis	Krewski et al. 2000[177]	10 μg/m³ $PM_{2.5}$	7.0 (3.9, 10)	12 (7.4, 17)	0.8 (−8.7, 11)
ACS, extended analysis	Pope et al. 2002[179] Pope et al. 2004[180]	10 μg/m³ $PM_{2.5}$	6.2 (1.6, 11)	9.3 (3.3, 16) 12 (8, 15)[a]	13.5 (4.4, 23)
ACS adjusted using various education weighting schemes	Dockery et al. 1993[26] Pope et al. 2002[179] Krewski et al. 2000[177]	10 μg/m³ $PM_{2.5}$	8–11	12–14	3–24
ACS intrametro Los Angeles	Jerrett et al. 2005[181]	10 μg/m³ $PM_{2.5}$	17 (5, 30)	12 (−3, 30)	44 (−2, 211)
Postneonatal infant mortality, U.S.	Woodruff et al. 1997[185]	20 μg/m³ PM_{10}	8.0 (4, 14)	–	–
Postneonatal infant mortality, CA	Woodruff et al. 2006[186]	10 μg/m³ $PM_{2.5}$	7.0 (−7, 24)	113 (12, 305)[c]	–
AHSMOG[b]	Abbey et al. 1999[187]	20 μg/m³ PM_{10}	2.1 (−4.5, 9.2)	0.6 (−7.8, 10)	81 (14, 186)
AHSMOG, males only	McDonnell et al. 2000[188]	10 μg/m³ $PM_{2.5}$	8.5 (−2.3, 21)	23 (−3, 55)	39 (−21, 150)
AHSMOG, females only	Chen et al. 2005[189]	10 μg/m³ $PM_{2.5}$	–	42 (6, 90)[a]	–
Women's Health Initiative	Miller et al. 2004[190]	10 μg/m³ $PM_{2.5}$	–	32 (1, 73)[a]	
VA, preliminary	Lipfert et al. 2000, 2003[190,192]	10 μg/m³ $PM_{2.5}$	0.3 (NS)[d]	–	–
VA, extended	Lipfert et al. 2006[193]	10 μg/m³ $PM_{2.5}$	15 (5, 26)[e]	–	–
11 CA counties, elderly	Enstrom 2005[194]	10 μg/m³ $PM_{2.5}$	1 (−0.6, 2.6)	–	–
Netherlands	Hoek et al. 2002[195]	10 μg/m³ BS	17 (−24, 78)	34 (−32, 164)	–
Netherlands	Hoek et al. 2002[195]	Near major road	41 (−6, 112)	95 (9, 251)	–
Hamilton, Ontario, Canada	Finkelstein et al. 2004[197]	Near major road	18 (2, 38)	–	–
French PAARC	Filleul et al. 2005[198]	10 μg/m³ BS	7 (3, 10)[f]	5 (−2,12)[f]	3 (−8,15)[f]
Cystic fibrosis	Goss et al. 2004[200]	10 μg/m³ $PM_{2.5}$	32 (−9, 93)	–	–

[a]Cardiovascular only; [b]Pooled estimates for males and females; pollution associations were observed primarily in males and not females; [c]Respiratory only; [d]Reported to be nonsignificant by author; overall, effect estimates to various measure of particulate air pollution were highly unstable and not robust to selection of model and time windows; [e]Estimates from the single pollutant model and for 1989–1996 follow-up; effect estimates are much smaller and statistically insignificant in an analysis restricted to counties with nitrogen dioxide data and for the 1997–2001 follow-up; furthermore, county-level traffic density is a strong predictor of survival and stronger than $PM_{2.5}$ when included with $PM_{2.5}$ in joint regressions; [f]Estimates when six monitors that were heavily influenced by local traffic sources were excluded; when data from all 24 monitors in all areas were used, no statistically significant associations between mortality and pollution were observed.

Recent focus has shifted to resource-intensive prospective cohort studies, such as the Harvard Six Cities and American Cancer Society (ACS) studies, which consistently estimate effects on all-cause and cardiopulmonary mortality. The Harvard study had higher estimates, partly due to the ACS cohort having a higher proportion of well-educated individuals and differences in geographic

area size (Brunekreef and Sunyer, 2003). A wide range of data of mortality related to long term exposure is provided in Table 2.5.

Incorporating local pollution sources in conjunction with community-wide background concentrations has the potential to increase relative risk estimates twofold. This indicates that relying exclusively on metropolitan-wide averages to assess the impacts of particulate matter (PM) on mortality may result in an underestimation of the actual health consequences. For infant mortality findings, exposure timeframes differ from those of adults, warranting further exploration of age-specific susceptibility and causes of death (Woodruff et al., 2006).

2.9.2 Health Effects Related to Morbidity

Numerous epidemiological investigations have identified correlations between distinct particulate matter (PM) measurements and a multitude of morbidity outcomes. These include but are not limited to asthma attacks, chronic bronchitis, respiratory hospital admissions, decreased lung function, minor restricted daytime activities, respiratory symptoms, lower respiratory illness and school absenteeism. A relatively small number of these studies have been conducted outside of North America and Europe, while the majority have been conducted in cities across these two continents. However, there is greater uncertainty when extrapolating these morbidity findings to developing countries. This is due to the fact that calculating the impact requires both a baseline incidence rate (the frequency of health outcomes in the absence of PM exposure) and a concentration-response function (the link between PM levels and health outcomes). It can be difficult to apply these estimations precisely to developing nations because there may not be enough data from those nations. However, there is now a growing amount of evidence from other rapidly emerging economies that allows for some tweaks and adjustments when applying the estimates to these places. Despite the unknowns, regional evidence offers

important insights into the possible health effects of PM in various regions of the world.

2.10 Economic Valuation Methods of Mortality and Morbidity Effects

The health effects of air pollution are evaluated through the implementation of diverse methodologies. The most straightforward method is the Value of Statistical Life (VSL) technique, which assigns the same value to each life lost irrespective of remaining life expectancy. However, the mortality hazards associated with this method may be inflated.

Loss of Life Expectancy (LLE) is a more popular methodology in Europe. Based on changes in pollutant levels and concentration-response curves, it modifies age-specific mortality risks (Bayat, Ashrafi, et al., 2019). The costs of long-term exposure to health are estimated using the average LLE, which is calculated by summing the number of surviving years across a variety of exposure cases and multiplying by the Value of a Life Year (VOLY).

The human capital approach calculates the deferred value of productivity loss (labour earnings) in order to determine the societal cost of illness or early mortality (Conte et al., 2002). As it doesn't take into consideration the varying subjective values that people place on life, it is regarded as a lower-bound estimate. The Cost of Illness (COI) technique is another one that's employed; it takes medical costs as well as indirect costs like treatment costs and missed pay due to illness into account (Torres, 2004).

2.11 Health risk assessment tools

Health Risk Assessment (HRA) is a systematic analytical approach utilized to evaluate and predict potential health risks arising from exposure to various pollutants or toxins. Often used interchangeably with Health Impact Assessment (HIA), HRA focuses on assessing the hazards posed by atmospheric

contaminants to the general population. Conversely, HIA analyzes the impact of policy interventions or regulatory improvements on public health outcomes resulting from changes in air pollutant levels.

The World Health Organization (WHO, 1999) defines Health Impact Assessments (HIAs) as a set of procedures and methodologies to assess the potential effects of policies, programs, or projects on population health. HIAs incorporate epidemiological study results and data on environmental and health outcomes to assist policymakers in developing health-protective policies (Quigley and Taylor, 2004). The HIA process involves screening, scoping, risk analysis assessment, reporting, and tracking implementation effects.

The Air Pollution Health Risk Assessment (AP-HRA) process begins by identifying the policy question and planning the assessment. It then involves selecting an appropriate tool for HRA, implementing the chosen tool, and integrating the assessment outcomes into HIA for policymakers to make informed decisions. The integration of data from HRA into HIA is crucial for addressing policy inquiries and arriving at well-informed decisions.

For AP-HRA, there are several computer-based tools available, and the majority of these tools use similar methodologies based on concentration-response (CR) functions obtained from epidemiological research (Anenberg et al., 2016b). The results of Health Impact Assessments (HIA) can be visualized using basic methods or software like Epi-Info or ESRI's Arc-GIS, giving a clear depiction of the health effects brought on by exposure to air pollution. During a summoned expert meeting organized by the World Health Organization (WHO), the primary objective was to analyze the methodologies and instruments utilized for evaluating the health risks linked to air pollution at various geographical levels, including local, national, and worldwide scales. The meeting entailed a comprehensive discussion on twelve distinct instruments sourced from diverse

regions worldwide, all of which were specifically designed for the objectives (Anenberg et al., 2016b).

Examples of commonly used AP-HRA tools:

- AirQ+ is a software tool that has been developed by the World Health Organisation (WHO). This study assesses the health consequences associated with the exposure to atmospheric contaminants, encompassing premature mortality as well as the occurrence of respiratory and cardiovascular ailments. The tool incorporates various factors such as pollutant concentration, population data, and health effect estimate in order to evaluate the impact of air pollution on disease burden.
- The Benefits Mapping and Analysis Programme (BenMAP): BenMAP is a software application that has been upgraded by the United States Environmental Protection Agency (USEPA). BenMAP is a commonly employed tool in the field of Regulatory Impact Analysis, utilised for the purpose of quantifying the health impacts linked to alterations in air pollution. This tool enables users to assess the potential health-related advantages and quantify them in monetary terms by considering the avoidance of healthcare expenses.
- AERMOD and CALPUFF: AERMOD and CALPUFF are two widely employed atmospheric dispersion models utilised for the evaluation of air pollutant dispersion patterns and their subsequent influence on air quality. These models facilitate the simulation of pollutant transport and transformation within a designated geographical region, thereby aiding in the comprehension of pollution's spatial dispersion and its potential ramifications on public health.
- AirSENCE: It is a mobile application that serves the purpose of evaluating the current state of air quality in real-time, as well as identifying any associated

health hazards. The system utilises sensors to quantify atmospheric contaminants and offers users insights regarding prevailing air quality levels and the corresponding health hazards.

- SimAir: SimAir is a software application that is widely used for air quality modeling and the evaluation of health concerns in metropolitan settings. The software application emulates air quality data and offers health risk assessments for various pollutants.
- IRAP-hp: The Integrated Relative Risk Model for Human Populations (IRAP-hp) is a computational tool utilised for the assessment of health risks linked to the exposure of human populations to air pollutants. The assessment considers several risk variables and health outcomes, hence enabling the evaluation of impacts on different demographic cohorts.

2.12 BenMAP-CE and related research

In this study, the Benefits Mapping and Analysis Programme Community Edition (BenMAP-CE) was used. In Regulatory Impact Analysis, BenMAP-CE is used to predict the health effects related to changes in air pollution exposure. These estimates are frequently presented as Attributable Risk (AR) estimates (US EPA, 2018, 2015). BenMAP-CE users can calculate the health effects of population exposure to air pollution through a process known as a health impact assessment. It quantifies the relationships between air pollution levels and health outcomes, including premature mortality, respiratory diseases, and cardiovascular diseases. These relationships are centered on concentration-response functions based upon epidemiological studies.

In addition to considering how changes in air pollution levels would affect people's health, BenMAP-CE can also evaluate the financial costs and gains connected with those changes. Users are able to capitalise on the health advantages of better air quality in terms of reduced healthcare expenses and

enhanced productivity. Analysing data in a spatial manner is made possible by the tool's Geographic Information System (GIS) capabilities, which it contains. By identifying susceptible populations, this feature aids in comprehending the spatial distribution of health concerns. BenMAP-CE aids in the assessment of different air quality management scenarios and policy actions. Users are able to model the potential negative consequences on economic growth and public health of various regulatory, legislative, and emission-reduction plans. To provide context-specific health risk assessments, users of the software can combine local air quality data with demographic data and exposure data.

Health benefits often included in Health Impact Assessments (HIA) include several indicators such as mortality rates, prevalence of chronic diseases, rates of hospitalizations, emergency department visits, occurrences of acute illnesses not requiring hospitalization, exacerbations and recurring episodes of illnesses, work and school absenteeism, and minor restricted activity days (MRADs). The BenMAP program provides accessible unit values for several health endpoints. These unit values are essential for figuring out the expenditures involved or for valuing the health advantages. The United States Environmental Protection Agency (USEPA, 2015) guidelines from literature review served as the foundation for this material (Fann et al. 2008). These unit values allow HIAs to more thoroughly evaluate the economic impact of health gains brought on by changes in air pollution levels.

2.12.1 Research in the international context

Extensive study has been undertaken to ascertain the diverse impacts of particulate air pollution on human health at a worldwide scale (L. Chen, Shi, Gao, et al., 2017; Davidson et al., 2007; Hassan et al., 2021; Manojkumar and Srimuruganandam, 2021; Van Munster, 2018; Voorhees et al., 2014b). The literature reveals that BenMAP-CE has been widely employed in the United

States, and its usage has expanded to many other countries in the last decade. BenMAP-CE has been used outside of the US in nations like China, India, Pakistan, Malaysia, Korea, South Africa, Rome, Spain, and Tehran, among others. Achieving the PM_{10} 24-hour mean National Standard limit and the 24-hour mean WHO standards in Cape Town would lead to a decline in pollutant levels and, as a result, a reduction in the excess risk of mortality in the city, according to the study's findings in South Africa (Keen and Altieri, 2016). BenMAP-CE has been used to estimate future decreases in $PM_{2.5}$ levels over the contiguous United States (CONUS) under the RCP 4.5 scenario and RCP 8.5 climate scenarios, and this has had a positive impact on both health and the economy. For RCP 4.5, the estimated reduction in $PM_{2.5}$ resulted in about 63,000 fewer all-cause deaths, about 5,300 fewer admissions to cardiovascular hospitals, with economic benefits of about 560 billion USD for all-cause mortality, 240 million USD for cardiovascular hospital admissions, 450 million USD for respiratory hospital admissions, and similarly for RCP 8.5, the anticipated reduction in $PM_{2.5}$ levels resulted in even greater benefits, including an estimated 83,000 avoided all-cause deaths, 7,000 fewer cardiovascular hospital admissions, with an economic benefits of $740 billion USD for all-cause mortality, and 320 million USD for cardiovascular hospital admissions (P. Yang et al., 2019). Brazilian cities that were analyzed in 2017 may have avoided anywhere from 2,378 to 6,282 deaths from all causes by adopting the WHO's $PM_{2.5}$ air quality criteria. This demonstrates the necessity of enforcing $PM_{2.5}$ regulations across the country and upgrading air quality monitoring, which will significantly enhance public health. The highest ambient $PM_{2.5}$ and ozone concentrations are found in states like Colorado, Pennsylvania, Texas, and West Virginia, which has a substantial influence on health. The reduction of $PM_{2.5}$ precursor emissions from this industry yields advantages ranging from $6,300 to $320,000 per ton, depending on the specific pollutant species (Fann et al., 2021). There are 300 premature deaths prevented

annually by limiting exposure to $PM_{2.5}$, with a 95% confidence interval ranging from 60 to 580 as indicated in another study (Abel et al., 2018). With a 95% confidence interval ranging from $0.13 billion to $9.3 billion, the economic impact of these averted premature deaths is estimated to be $2.8 billion. In Qom, there were found to be 4694.5 premature deaths in scenario I, where the reduction in $PM_{2.5}$ is to 2.4 $\mu g/m^3$. The number of attributable premature deaths fell to 2475.94 in scenario II with a reduction to 10 $\mu g/m^3$. For scenario I and scenario II, the associated costs of these early deaths were estimated to be 855.91 million USD and 451.40 million USD, respectively (Ho et al., 2023). Multiple studies suggest that the use of this tool is becoming more widespread as an efficient method for evaluating the health effects of air pollution and assisting in the development of policy choices in various geographical areas.

The decline in air quality inside the Indian subcontinent and its surrounding nations has garnered significant international interest. Bangladesh, China, India, and Pakistan demonstrate considerable eminence in the realm of global air pollution, since they collectively comprise 49 out of the 50 cities exhibiting the greatest levels of pollution on a global scale (*IQAir*, 2020). Consequently, there has been a notable increase in research endeavors aimed at examining the levels of particulate matter (PM) and its corresponding health effects within this geographical area. In the context of India, an assessment of health benefits was conducted using the BenMAP-CE tool, which took into account the achievement of air quality standards set by the World Health Organisation (WHO) and other relevant entities. The research findings indicated that a significant number of states observed a substantial increase in health benefits associated with a decrease in all-cause mortality (Manojkumar and Srimuruganandam, 2021). A study conducted in China utilizing the environmental benefits mapping and analysis programme (BenMAP) demonstrated a decline in $PM_{2.5}$ concentrations

by 14.53 percent throughout the period spanning from 2016 to 2018. The observed decline in premature mortality during the autumn season, with a range of cases spanning from 7,214 to 81,681, might be attributed to several factors, such as lung cancer, respiratory ailments, and cardiovascular disorders. Notably, there exists a significant correlation between this drop and the aforementioned health issues (G. Luo et al., 2020). Furthermore, past research in China has mostly concentrated on short-term health effects. For instance, there were 87,280 preventable fatalities attributable to emergency department visits, cardiovascular illnesses, and respiratory diseases if the 24-hour mean $PM_{2.5}$ levels were reduced to a standard (75 $\mu g/m^3$) (L. Chen and Bai, 2017), 3,800 preventable deaths in China were estimated after adopting the reduction scenario as per WHO guideline (Meng et al., 2019), while in another study it was calculated that long-term exposure to $PM_{2.5}$ in Shanghai reduced daily all-cause mortality occurrences by 6 to 26 and annual cases by 39 to 1,400 (Voorhees et al., 2014a). Another study in China adopted WHO IT-1 standards for controlling $PM_{2.5}$ concentrations and these simulations predicted that mortality benefits could reach 24.0% (C. Song et al., 2017). In a study, there are 2,024,290 cases of preventable mortality in Pakistan for a population of 73 million people due to lung cancer and ischemic heart disease (Hassan et al., 2021). Additionally, the overall cost of this fatality is $1 billion USD in Pakistan. Therefore, the BenMAP-CE model has been employed in these countries to assess and estimate the health benefits related to air pollution mitigation measures.

2.12.2 Related studies in Bangladesh

Air pollution in Dhaka city has been linked to 3,580 premature deaths annually, 10 million days of activity restriction, and 87 million days of respiratory symptoms (ADB and CAI Asia, 2006). The economic impact of these health issues could be between $60 million and $270 million, or 1.7% and 7.5% of the gross

domestic product of Bangladesh. The total economic estimate due to air pollution would be significantly higher if we took into account additional problems such as traffic jams, global warming, material contamination, and aesthetic degradation (S. Xie et al., 2003). A study, assessed the health advantages brought about using compressed natural gas (CNG) as fuel in the city of Dhaka where . it was discovered that the introduction of CNG alone averted 5,200 premature deaths in 2007, resulting in annual investments of US$ 0.99 billion (about 1.4% of the overall GDP) (Wadud and Khan, 2013). To the best of our knowledge, no study has yet used the BenMAP-CE model to assess the health implications of changing ambient $PM_{2.5}$ and PM_{10} levels, despite substantial research on air quality and its detrimental effects in many cities throughout Bangladesh. Furthermore, it is clear from the literature analysis that different regional factors have an impact on air quality, making it a regional phenomenon. By analyzing the spatial and temporal changes of $PM_{2.5}$ and PM_{10} concentrations in the ambient air and their effects on urban dwellers' health, this study seeks to close these information gaps. Additionally, it aims to measure how these variances affect people's health.

2.13 Summary

Recent research findings have highlighted the critical role of particulate matter (PM) in elevating premature mortality rates. PM is a complex mixture formed in the atmosphere through the interaction of gaseous precursors, largely originating from human activities. It encompasses a range of chemical components, such as sulfate, nitrate, ammonium, black carbon (BC), and organic carbon. Additionally, the existence of traces of heavy metals in the air, particularly when exceeding safe levels, can exacerbate air-related diseases. Certainly, the potential adverse effects of air pollutants on human health represent a significant and urgent concern.

The review of existing literature indicates substantial benefits linked to the application of air pollution health risk assessment tools. One particularly noteworthy tool in this regard is BenMAP-CE, developed (USEPA). BenMAP-CE stands out due to its advanced features, widespread adoption in various countries, and its flexibility that allows users to define their inputs. This tool is recognized for its effectiveness in conducting health impact assessments related to air pollution, underlining its value in the field of environmental and public health research. Furthermore, it's important to note that air quality is not a uniform global issue; instead, it is a localized concern. Research indicates that the potential health advantages and economic gains that can be achieved differ significantly from one region to another. This variability is influenced by a range of factors, including regional sources of pollution, local climatic conditions, population density, and the susceptibility of specific communities to air pollution.

Unfortunately, Chattogram a major city of Bangladesh is one of the most affected cities by particulate matter in air and there is clear evidence from the IMHE report as well as that every year there is around 173500 deaths in Bangladesh (IHME, 2019). Furthermore, it is important to highlight that there has been a lack of study conducted in a particular geographic region to investigate the association between air pollution and mortality. Furthermore, it is important to acknowledge that heavy metals often become associated with particulate matter that originates from anthropogenic sources, such as vehicular traffic on paved roadways. According to the literature review provided in the preceding section 2.3.4, it has been observed that exceeding the specified limits for heavy metal concentrations might result in adverse impacts on human health and exacerbate the diseases associated with air pollution.

Subsequently, after BenMAP-CE came into picture various countries around the world have adopted this tool to illustrate the shifts in premature deaths and

incidents following the implementation of air pollution reduction measures. As, air pollution is a localized issue, and different countries have different air pollution status and hence to fulfill these gaps this more specific studies utilized BenMAP-CE for evaluating alterations in health outcomes and conducting health risk assessments related to heavy metals in dust in local/regional scale are deemed necessary.

Chapter 3. METHODOLOGY

3.1 Introduction

The primary objective of this research endeavor is to assess the impact of air pollution on the overall welfare of the populace. The techniques employed to attain the study objectives are explained in this chapter. At the core of this investigation lies the implementation of the BenMAP-CE health impact assessment methodology. The geographical focus of this study is the Chattogram City Corporation, a pivotal financial center within Bangladesh. The initial step involved the development of an empirical model with the aim of predicting pollutant concentrations. This model, once developed, serves as an input for the BenMAP-CE framework.

Following this, an analysis of the population was undertaken to understand varying levels of pollutant exposure across different age groups. The following sections provide a comprehensive overview of the approaches utilized for evaluating the health effects associated with air pollution. Additionally, an elaboration is provided on the process of assigning value to diverse health endpoints, thus enabling the estimation of the financial consequences of the observed outcomes. Furthermore, the exploration conducted by this study extends into the intricate interplay between airborne heavy metals and the assessment, highlighting the complex relationship between the two.

Description of study area

Chittagong is the port city of Bangladesh and serves as a metropolitan district within Bangladesh. It holds the distinction of being the country's second-largest city and is in the southeastern region. Positioned along the estuaries of the Karnaphuli River, Chittagong is surrounded by hilly terrain and faces the Bay of

Bengal to the west. The city's geographical coordinates are approximately 22°20'06" N latitude and 91°49'57" E longitude. The location map of the study area is provided in Fig. 3.1. The total area of the Chittagong metropolis encompasses approximately 5,282.92 square kilometers, with the urban area covering around 2,054.90 square kilometers and the metro area spanning approximately 2,510 square kilometers.

Chattogram has a tropical monsoon climate with hot, rainy summers and cool, dry winters. In the winter, temperatures range from 12° to 17°, while the monsoon season sees a range of 29° to 35°. The city experiences yearly precipitation ranging from 2159 mm to 3048 mm, with sporadic peaks up to 3810 mm, with the majority falling between May and September, during the monsoon season (Hossain et al., 2020). There are 211 mahallas and 41 wards in the Chattogram City Corporation Area (CCC), each with a different level of population density. The wards are the smallest administrative units of the city. With a total of 558,037 dwellings, the area has an average population density of 16,677 per square kilometer (Bangladesh. Parisaṃkhyāna Byuro. Statistics and Informatics Division, 2011).

Chattogram, located in Bangladesh, serves as a significant center for education, healthcare, business, and functions as a prominent port city. The main aim of this study is to evaluate the effects of air pollution on the health of the general population. It has witnessed significant demographic shifts due to a substantial influx of people from surrounding districts, resulting in a daily surge of vehicles and heavy traffic congestion.

The city's strategic location as a primary port and industrial center has attracted significant international investment, particularly in sectors such as textile manufacturing, shipbreaking, and oil refining. Remarkably, Chattogram accounts for over 40% of Bangladesh's industrial production, 80% of its foreign

trade, and 50% of the nation's total income, contributing significantly to the country's overall economic development (Robiul Hussain et al., 2016).

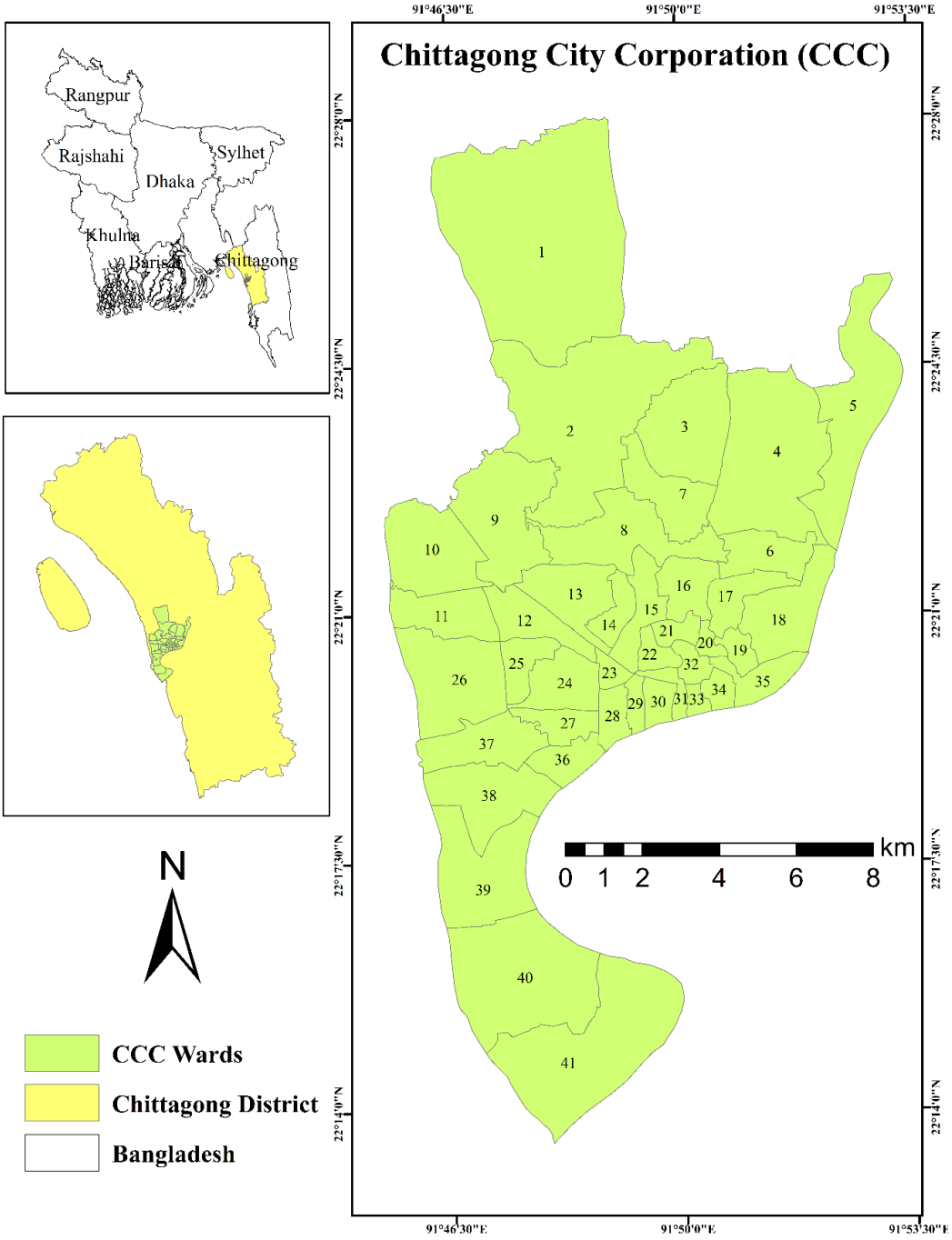

Fig. 3.1 Study Area of CCC with 41 wards

The 41 wards of Chattogram City Corporation delineate the administrative divisions within the city. Each ward represents a specific geographical area, encompassing neighborhoods, residential zones, commercial districts, and other urban spaces. The designation of each ward along with their number is provided in Table 3.1.

Table 3.1. Designation of each ward

Ward No	Ward Name	Ward No	Ward Name	Ward No	Ward Name	Ward No	Ward Name
W-1	South Pahartali	W-12	Saraipara	W-23	North Pathhantuli	W-34	Patharghata
W-2	Jalalabad	W-13	Pahartali	W-24	North Agrabad	W-35	Boxirhat
W-3	Panchlaish	W-14	Lalkhan Bazar	W-25	Rampur	W-36	Gosaildanga
W-4	Chandgaon	W-15	Bagmaniram	W-26	North Halishahar	W-37	North Middle Halishahar
W-5	Mohra	W-16	Chawkbazar	W-27	South Agrabad	W-38	South Middle Halishahar
W-6	East Sholashahar	W-17	West Bakolia	W-28	Pathantuli	W-39	South Halishahar
W-7	West Sholashahar	W-18	East Bakolia	W-29	West Madarbari	W-40	North Patenga
W-8	Sholokbahar	W-19	South Bakolia	W-30	East Madarbari	W-41	South Patenga
W-9	North Pahartali	W-20	Dewan Bazar	W-31	Alkaran		
W-10	North Kattali	W-21	Jamal Khan	W-32	Anderkilla		
W-11	South Kattali	W-22	Enayet Bazar	W-33	Firinghee Bazar		

However, this rapid industrialization has also led to a surge in air pollution levels. Increasing concentrations of pollutants like $PM_{2.5}$, PM_{10}, SO_2, and NOx are primarily attributed to industrial activities, power generation, and transportation. The concentration of particulate matter has surpassed the annual (BNAAQS) due to the implementation of an unplanned development plan

(Khatun Syed Yusuf Saadat Kashfia Ashraf, 2023) . The consequences of this air pollution are severe, contributing significantly to respiratory illnesses and premature mortality in Bangladesh. Additionally, urban areas have seen a rise in vehicular emissions, further exacerbating the pollution issue. Recognizing the immediacy of this challenge, this study seeks to determine the reduction in premature deaths associated with the decrease in particulate matter level.

3.2 Particulate matter monitoring and sampling sites

In this study, particulate matter concentrations are being assessed at 56 sampling locations across Chattogram City, encompassing all 41 wards. To ensure the study's objectives are achieved and the safety of both the crew and road users is ensured, careful selection of each location has been undertaken.

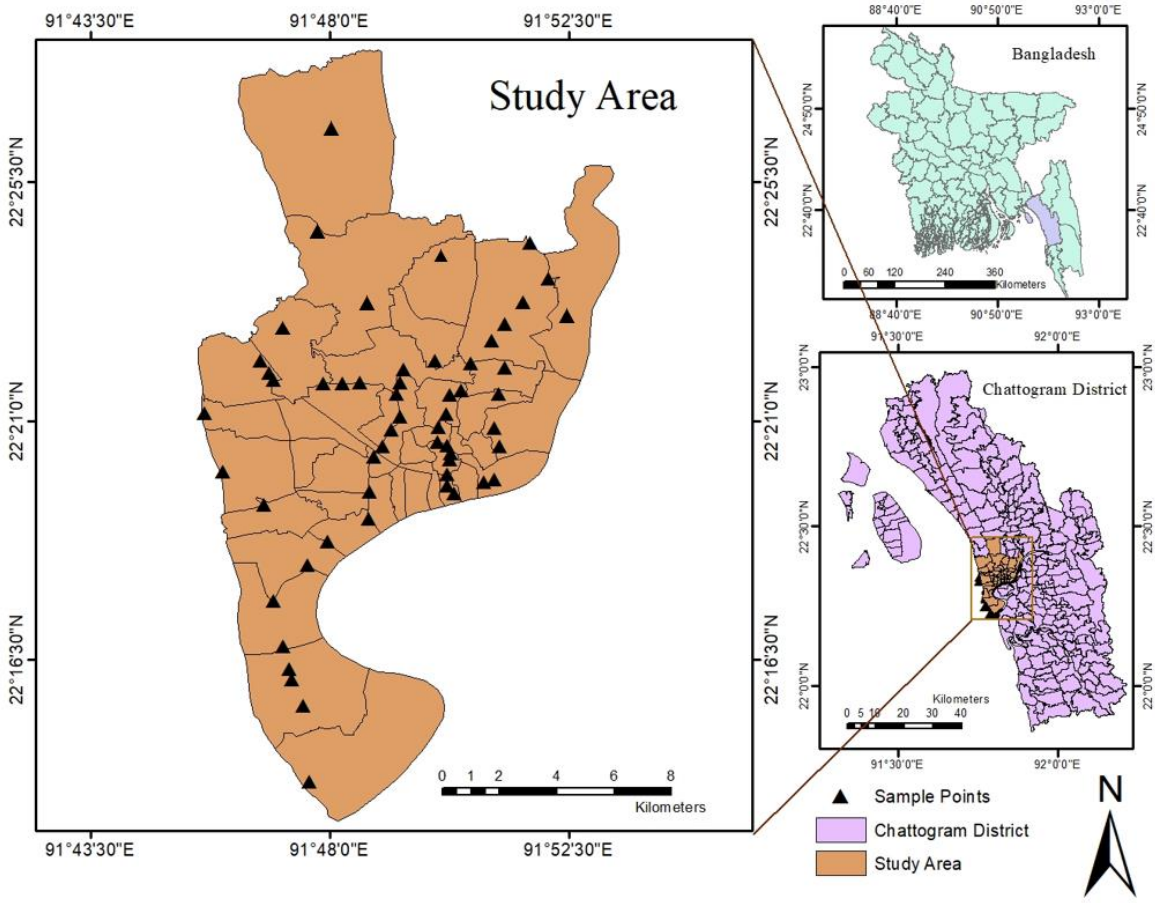

Fig. 3.2 Sampling points of Particulate Matter Concentrations in the study area (CCC)

Data collection took place in the month of November-December when there is no or less precipitation and when air pollution tends to be more severe. At each sampling location, $PM_{2.5}$ levels have been continuously monitored over a 24-hour duration to determine the average concentration. This sampling has been done for both the years 2021 and 2022. For the measurement of particulate matter concentrations, the "Temtop Air Quality Monitor Professional $PM_{2.5}$, PM_{10}, Formaldehyde (LKC1000S+)" particle detector has been utilized. The device utilizes advanced sensor technology to capture real-time data on these air pollutants. These sensors can detect and quantify particulate matter concentrations in the air by analyzing the scattering of light caused by particles passing through the sensor chamber. The device likely provides continuous monitoring and displays real-time readings on its interface and recognized for its compact and lightweight design, it offers a high-resolution measurement capability of 0.1 $\mu g/m^3$, covering a measurement range of 0 to 999 $\mu g/m^3$. Also, noteworthy feature is the instrument's auto-calibration capability and quick response time, facilitating the provision of consistent and dependable data on $PM_{2.5}$ and PM_{10} concentrations within a brief duration of 3-4 minutes. The detector machine is placed in a representative location, ensuring stability and avoiding extreme temperatures or vibrations. For optimal sampling, the device is installed at a height of approximately 1 to 3 meters above the ground, taking into consideration the pollutant being measured. Specific calibration guidelines are followed, as outlined in the product manual, to maintain accuracy. The monitor's interface is utilized for real-time data readings. And the computation of 24-hour average values for air quality metrics is achieved through the summation of individual data points, which represent pollutant concentrations during each hourly interval. This cumulative sum is subsequently divided by the total number of hours within the 24-hour period. The Fig. of the device used is given in the annex Fig. A.1.

(a) (b)

(c) (d)

Fig. 3.3 The photographs showing some of the sampling sites taken during the air quality monitoring period at a) Agrabad, b) Halishahar, c) GEC junction,d) 2 NO. gate Junction

Wards 38-41, situated in the lower southwestern direction, and Ward 2 in the northwestern area, are closely located near industrial zones. These wards experience heightened pollution levels due to emissions from industrial processes, chemical factories, and industrial waste. The population density in these regions, driven by their role as working zones, exacerbates the pollution

burden. Additionally, Wards 24 and 27, located within the central southwestern Agrabad area, function as the city's principal central business district. The dynamic commercial activities and heavy traffic congestion in this area contribute to increased waste generation and air pollution, leading to localized pollution concerns. The locations of some of the sampling sites are provided in Fig. 3.3.Another aspect is that a segment of Ward 1 serves as a transportation hub linking various destinations. Wards 11 and 24-26, currently undergoing extensive construction activities, are prone to encountering dust and noise pollution stemming from construction sites. Wards 4-6 and Wards 1, 3, 7, 8, 15, and 16, positioned in the southeastern sector, primarily consist of residential zones. However, these wards also encompass educational, commercial, and roadway areas.

Inadequate infrastructure in these regions may contribute to increased levels of air pollution. In contrast, Wards 9-12, predominantly featuring residential and commercial zones, exhibit comparatively lower pollution levels. Ward 8, along with Wards 13 and 14, forms a significant roadway hosting various commercial establishments. Additionally, Wards 17, 18, 19, and 35, currently undergoing extensive construction and grappling with poor infrastructure, may experience dust pollution. Moreover, Wards 28-30 and 36-37, positioned adjacently in the southeast, are primarily characterized by residential land use. Overall, the distribution of pollution within different wards of the city results from a combination of industrial activities, commercial centers, traffic congestion, construction endeavors, and varying levels of infrastructure.

3.3 Trace elements of road dust sampling and analysis

3.3.1 Heavy metal

Trace of elements in road dust particularly heavy metal was primarily aimed to obtain relevant insights for subsequent health impact analysis. In the absence of

a designated sampler, a representative sample of urban road dust is obtained by selectively considering a fraction that is either suspended or settled at a height of 6 meters. This strategic sampling method takes into account the dynamic nature of road dust, capturing particulate matter at a height that reflects potential human exposure. By focusing on suspended or deposited particles at this specific elevation, the sampling approach aims to ensure a more accurate depiction of air quality, especially in urban environments where road dust significantly contributes to particulate pollution. In this study, samples were collected from locations featuring industries, commercial zones, or significant roadways.

A total of 19 road dust samples were gathered from primary roadways within the Chittagong City Corporation network. The sampling sites station are depicted in Fig. A.2. The sites were chosen through a meticulous evaluation of the objectives of the field investigations, as well as the well-being of the workers engaged in the sample procedure and the general public using the roads. The prioritization of efficient and timely collection and transportation of samples from the field to the laboratory was also emphasized. The collection of road sediment samples took place during the winter months of November and December 2021, which coincided with a period of low precipitation. The selection of this specific time frame was made with the intention of reducing potential fluctuations in the environment and guaranteeing a consistent approach to data collection.

Field sampling

Prior research has sampled dust particles resuspended from the roadside environment using a variety of techniques, each having advantages and downsides. Two often used methods include road dust collection using a portable vacuum cleaner with a view scope (Deletic and Orr, 2005; Goonetilleke et al., 2009; Grottker, 1987) and dry street sweeping using a brush and dustpan.

Fine particulate matter containing heavy metals has been sampled from various sources, including roadside areas, trees, objects, and elevated structures. This sampling process is vital for assessing the presence and distribution of heavy metal pollutants in the air. Pictures of taking samples from two of the sites are given in Fig. 3.4.

(a) (b)

Fig. 3.3 The photographs showing sample collection from roadside trees/infrastructures at a) Agrabad and b) 2 NO. gate

Sample preparation for laboratory analysis

The following steps were taken to analyse the amount of heavy metals in the dust from roads:

- **Sieving and Drying**: Stones, pebbles, and biological waste were taken out using a large sieve, followed by drying. Sand and sediment samples were taken, and they were air dried. After that, they were put in acid-washed containers and kept for 24 hours in a 105 °C oven. It took longer for samples that weren't completely dried to reach a consistent weight. Using a pestle and mortar that had been acid-washed, the dry sediment samples were completely crushed before being put through a ASTM sieve size No. 200. Using a high precision analytical balance, 5 gm of the finely crushed samples were obtained. The remaining portion of the material was kept for further use.

A total pictorial representation of the total stated procedures is shown in Fig. 3.5.

Samples after Sieving and Drying

Acid digestion process

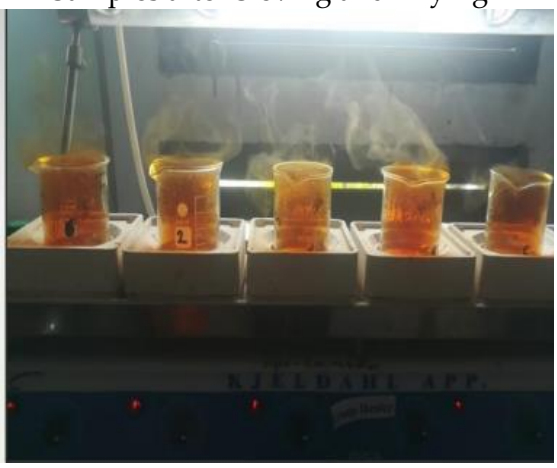

Heating of the mix

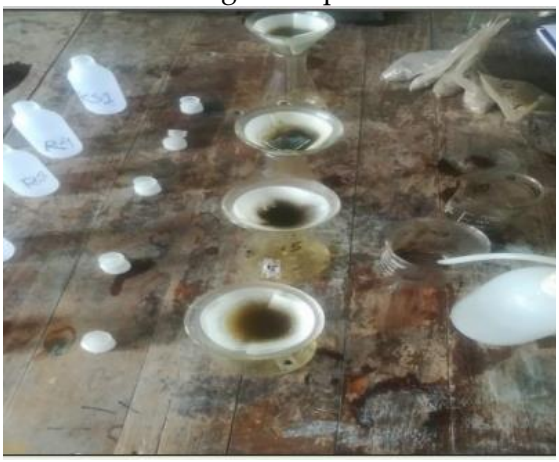

Filtration of the sample after heating and cooling

Fig. 3.4 Sample preparation for heavy metals in air borne particles at Environmental Engineering Laboratory, CUET

- **Acid Digestion**: 80 ml of acid (a combination of 70% nitric acid and HCl in a ratio of 3:1) was added after the 5 g samples were placed to an acid-washed Teflon beaker.
- **Heating of the mix:** A watch glass was placed over the beaker. An electric hot plate was utilized for heating due to its capability to regulate temperature effectively and distribute it uniformly. Subsequently, the samples were allowed to sit for a duration of two hours until no further formation of brown fumes occurred, while maintaining a controlled temperature range of 90 ℃-100 ℃ to ensure complete digestion (Parker 1972)

- **Filtration**: The samples were mixed for 5 minutes after reaching room temperature before being run through a glass funnel with Whatman filter paper (42 NO.). Deionized water was then used to dilute the resultant solutions to a final volume of 50 ml.

Analysis of heavy metals

The filtrate was kept for further examination in a volumetric flask. The contents of Mn, Cu, Ni, Cr, Zn and Fe in the acid-digested samples were determined using a Hanna Multimeter Photometer (Model: HI83326), and the results were expressed in parts per million (ppm). For each component, the results were presented as a dry weight basis. To account for any potential background interference, a blank solution (Mn, Cu, Ni, Cr, Zn and Fe) was run under the same analytical conditions as the sample solution.

The mass of the dried sediment and the determined metal concentration from a 50 ml sample examined by Flame Atomic Absorption Spectrometry (FAAS) were used to calculate the heavy metal content in sediment as shown in Eq 3.1.

$$\text{Metal concentration in mg/kg(dry weight)} = D \times E/F \quad (3.1)$$

where, D is the metal concentration reading obtained from the FAAS in mg/L, E is the sample volume in ml, F is the weight of sediment mass used for acid digestion in grams.

3.3.2 Analytical protocol

Hanna Multiparameter Photometer

The Hanna Multiparameter Photometer HI83300 is a compact and versatile meter with two operational modes: Photometer and Probe. In Photometer mode, it allows for the immediate measurement of a cuvette using its integrated optical system. On the other hand, in Probe mode, continuous measurement is facilitated by connecting a Hanna digital electrode to the 3.5 mm port. So, this study utilized

the photometer mode as it offers advantages such as sensitivity, speed, and the ability to analyze multiple samples quickly. Hence certain factors like dropper usage, powder packet usage, preparation of cuvette and time should be taken into account while using the photometer method. This adaptable photometer can measure a variety of parameters with high accuracy, making it a practical and economical choice for water analysis. It may also detect dissolved oxygen (DO), total dissolved solids (TDS), conductivity, ammonia, nitrate, phosphate, and a number of heavy metals, among other characteristics.

- **Principles**

The principles of photometry and colorimetry are used in the operation of the Hanna Multiparameter Photometer. It uses a light source to shine light through the sample solution and depending on the concentration of the analyte being measured, the sample absorbs wavelengths of light. When reacting with the target analyte, the photometer uses reagents to induce color changes in the sample, resulting in colored compounds that absorb light at particular wavelengths.

To ensure accurate readings, the instrument is calibrated using standard solutions with known analyte concentrations. This creates a linear connection between light absorbance and analyte concentration. The photometer uses a light detector to determine how much light is passing through the sample, and then processes the electrical impulses to provide concentration results that can be displayed or used in other analyses.

- **Accuracy and Detection Limit**

The multiparameter photometer is set up for elemental analysis by pressing the auto-zero switch. The cuvette must be installed in the instrument holder in order

to analyse a particular element. The accuracy and detection limit of studied metal of Hanna Multiparameter is provided in Table 3.2 and the instrument image is given in annex Fig. A.12. Each method has separate accuracy assessment and detection limit. Then, each sample is run three times for a total of four seconds. The sample might need to be diluted if the concentration of the element in it exceeds the measurement range of the photometer.

Table 3.2. Accuracy and Detection Limit of Studied Metal

Limits	Cu (mg/L)	Fe (mg/L)	Cr (µg/L)	Zn (mg/L)	Mn (mg/L)	Ni (g/L)
Accuracy	±0.02 mg/L±4% of reading	±0.04 mg/L±2% of reading	±10 µg/L ±4% of reading	±0.03 mg/L±3% of reading	±0.2 mg/L±3% of reading	±0.07 g/L±4% of reading
Detection range	5.00	5.00	300	3.00	20.0	7.00

To determine the actual concentration of the studied sample, the dilution factor of the sample is taken into consideration by multiplying the measured value by the dilution factor.

3.3.3 Pollution assessment of heavy metal

Given that this study exclusively centers on human health risk assessment, the assessment of airborne dust pollution was performed through the utilization of the Contamination Factor (C_f) and Degree of Contamination (C_{deg}).

Determination of Degree of Contamination

The evaluation of metal contamination in road dust was conducted using the methodology outlined in the study by (Pal, 2012). The framework consisting of four categories, namely Contamination Factor (C_f) and Degree of Contamination (C_{deg}), to assess the degrees of metal contamination was adopted from a study (Hakanson, 1980). The calculation of the Degree of Contamination (C_{deg}) involves the aggregation of contamination variables pertaining to each element that has

been examined in the road dust samples. The contamination factor C_f can be defined as following Eq. 3.2.

$$C_f = \frac{C_i}{C_n} \quad (3.2)$$

Where, C_i is the mean concentration of metal and C_n is the concentration of a reference value for individual metal. In this study, the C_n is the standard preindustrial reference values from Hakanson, 1980. This reference value is also used in other studies conducted in Bangladesh (Al-Razee, 2021; Banu et al., 2013; Hossain et al., 2019; M. A. Islam et al., 2020; Md. S. Islam et al., 2015). All these reference values are provided in Table 3.3.

Table 3.3. Background values of studied heavy metal

C_n	Mn	Cu	Ni	Cr	Zn	Fe
mg/kg	252	57.4	85.525	68.9	52.74	19240

The degree of contamination by the six heavy metals in road dust from the study areas was determined as following Eq. 3.3 (Hakanson, 1980):

$$C_{deg} = \sum C_f \quad (3.3)$$

The classification that has been modified to suit the particular heavy metals examined in this investigation has been displayed in Table 3.4

Table 3.4. Categories of contamination factor and contamination degree

Class	C_f value	Category	C_{deg} value	Category
Class1	$C_f < 1$	Low contamination	$C_{deg} < 6$	Low degree of contamination
Class 2	$1 \leq C_f < 3$	Moderate contamination	$6 \leq C_{deg} < 12$	Moderate degree of contamination
Class 3	$3 \leq C_f < 6$	Considerable contamination	$12 \leq C_{deg} < 24$	Considerable degree of contamination
Class 4	$6 \leq C_f$	High contamination	$24 \leq C_{deg}$	Very high degree of contamination

The classification of degrees of contamination in this study was initially established according to the recommendation of Hakanson (1980), which encompassed eight contaminants. Nevertheless, the examination conducted in this research was centered on six specific heavy metals. Consequently, the categorization of contamination levels was modified and aligned with the methodology proposed by (Suryawanshi et al., 2016b)

3.3.4 Risk assessment for human health

The study aimed to evaluate both non-carcinogenic and carcinogenic risks associated with human exposure to air borne dust in urban residential areas. The research examined whether trace elements produced in air particulate can be considered potentially harmful to human health. These elements can enter the body through three pathways: (i) direct ingestion of particles from surfaces ($CDI_{ingestion}$), (ii) inhalation of particles released from dust through the mouth and nose ($CDI_{inhalation}$), and (iii) absorption of hazardous elements on the skin from particles (CDI_{dermal}) (X.-S. Luo et al., 2015).

To assess non-carcinogenic risk, Eq. 3.4-3.9 were employed, while Eq. 3.10-3.13 based on (USEPA, 1989; 'USEPA', 1997; USDOE, 2011) were used to evaluate carcinogenic risk. Both adults and children were considered in calculating the potential hazard exposures.

- **For non-cancerous dose**

$$CDI_{ing} = C_{soil} * IngR * EF * ED * CF/(BW * AT) \quad (3.4)$$

$$CDI_{dermal} = (C_{soil} * SA * AF_{soil} * ABS_d * ED * CF)/(BW * AT) \quad (3.5)$$

$$CDI_{inh} = C_{soil} * InhR * EF * ED * CF/(PEF * BW * AT) \quad (3.6)$$

$$HQ = CDI/R_fD \tag{3.7}$$

$$HI = \sum HQ = HQ_{ing} + HQ_{dermal} + HQ_{inh} \tag{3.8}$$

$$HQ = \frac{CDI_{ing}}{R_fD_{ing}} + \frac{CDI_{dermal}}{R_fD_{dermal}} + \frac{CDI_{inh}}{R_fD_{inh}} \tag{3.9}$$

Lifetime carcinogenic risk indicated the additional likelihood of an individual developing cancer over their lifetime due to cumulative exposure to possible carcinogens. Detailed explanations of symbols and constant values can be found in the Table A.1.

- **For cancerous dose**

$$CDI_{dermal} = (C_{soil} * SA * AF_{soil} * ABS_d * ED * CF * CF_{ing} * ABS_{GI})/(BW * AT) \tag{3.10}$$

$$CDI_{ing} = C_{soil} * IngR * EF * ED * CF * CF_{ing}/(BW * AT) \tag{3.11}$$

$$CDI_{inh} = C_{soil} * InhR * EF * ED * CF * IUR * 10^3/(PEF * BW * AT) \tag{3.12}$$

$$Total\ Risk = \sum_{i=1}^{n} Risk \tag{3.13}$$

The study proceeded by calculating the chronic daily intake (CDI) for each metal or metalloid and exposure pathway ($CDI_{ingestion}$, CDI_{dermal}, and $CDI_{inhalation}$). These values were then divided by the corresponding reference dose to determine the hazard quotient (HQ), which reflects the non-carcinogenic risk for systemic toxicity Eq 3.8. For elements like Chromium (Cr) and Nickel (Ni), the increased lifetime cancer risk was measured by multiplying the dose with relevant slope factors given in Table A.2-A.3.

Although there can be synergistic interactions among certain metals (X.-S. Luo et al., 2015; X. Xu et al., 2013) it was assumed that all metal hazards were additive. Consequently, the cumulative non-carcinogenic risk was evaluated using the

hazard index (HI, Eq. 3.8), while the total cancer risk was calculated using Eq. 3.13.

Dermal absorption reference toxicity values were obtained using the Risk Assessment Information System (RAIS) (USDOE, 2011). These values were derived from oral reference doses by considering gastrointestinal absorption factors. The reference dose (R_fD in $mgkg^{-1}day^{-1}$) represents the estimated highest acceptable risk to the population from daily exposures, with considerations for sensitive groups like children. There are two R_fD values: one for ingestion and another calculated as R_fD ($mgkg^{-1}day^{-1}$) multiplied by the gastrointestinal absorption factor (ABS_{GI}) for dermal contact.

Health impacts were evaluated based on comparisons between CDI and R_fD as well as HQ values. When CDI is less than R_fD and HQ is 1 or less, no adverse health impacts are anticipated. Conversely, when CDI exceeds R_fD and HQ exceeds 1, adverse health impacts are likely to occur ('USEPA' 1989; US EPA, 2001).

Carcinogenic risks were classified as follows: risks less than 10^{-6} are considered insignificant (a 1 in 1,000,000 chance of individuals developing cancer), risks between 10^{-6} and 10^{-4} are generally acceptable depending on exposure conditions (Y. Hu et al., 2012; Kabir et al., 2021b), and risks exceeding 10^{-4} are deemed unacceptable by most international regulatory agencies ('USEPA', 1989). The value 10^{-6} is also the target risk for carcinogens as per a study (Epa and Factors Program, 2011).

3.3.5 Correlation analysis

Correlation analysis is a dynamic method utilized to elucidate the relationship between two distinct parameters. Pearson's correlation coefficient, a fundamental measure, is calculated by dividing the average covariance of both variables by

the outcome of their standard deviations. This coefficient assumes values between -1 and 1, representing different degrees of correlation. A value of +1 signifies a perfect positive linear relationship, indicating that as one variable (X) increases, the other variable (Y) increases in a proportional manner. Conversely, a value of -1 indicates a perfect negative linear relationship, where an increase in X results in a decrease in Y. A correlation coefficient of 0 suggests no linear correlation between the variables.

3.4 Health impact assessment using BenMAP-CE

In this study BenMAP-CE health impact assessment model has been used to estimate the number of premature deaths associated with reduction of $PM_{2.5}$ and PM_{10} levels in Chattogram City Corporation region. This section describes the framework and model assumptions, the study's model domain, the input data requirements for BenMAP-CE, and the execution procedure for the model.

3.4.1 BenMAP-CE

BenMAP-CE model involves analyzing the effects of air pollution on the environment, particularly focusing on human health impacts. The repercussions on individual human health may materialize in the scenario of an elevated mortality rate or a multitude of morbidities. To quantify these health effects, epidemiological concentration-response (CR) functions are utilized in conjunction with the population at risk and the concentration changes of various policy alternatives. Afterwards, the monetary costs associated with prevented incidents or the willingness to pay to have them avoided are applied to the valuation of each health case. Air pollutants have the potential to induce a wide range of health complications. Based on a review of the literature, epidemiological studies have been undertaken to ascertain the functions of CR for a variety of health endpoints. In order to calculate the overall impact, the

health parameters of each detrimental pollutant are incorporated into the model and their monetary values are summed.

This study utilizes typical urban concentrations of PM_{10} and $PM_{2.5}$ as markers of air pollution in order to assess the health impacts. This study employs a comprehensive strategy to monitor air pollution exposure in an urban setting by splitting the whole city into grids and analyzing pollution sources in segmented regions, rather than just focusing on bigger metropolitan sources. This facilitates a more intricate comprehension of pollution "hot spots" that might potentially have an influence on particular demographic groups without substantially influencing the general metropolitan average.

3.4.2 Model assumptions

The primary assumptions taken into account in this analysis are listed here.

- Most often, data on pollution exposure are gathered from monitoring stations located in centralized areas. Although they may not adequately reflect individual exposure levels, statistics on pollution exposure are frequently collected from monitoring stations that are situated in centralized locations.
- For incidence rate, this study relies on the national incidence rate as there is insufficient data on local incidence rate.
- The health impact function used in this study is based on epidemiological research adopted from literatures. To identify any potential overlaps in environmental circumstances and demographic characteristics, the researchers try to use studies from nations that are geographically adjacent to the study site. They also take into account international epidemiological studies that could provide pertinent information about the negative consequences of exposure to air pollution on health.

- For the economic assessment, this study considers World Bank-assessed Willingness-To-Pay (WTP) values specific to Bangladesh. Additionally, in cases where such data is unavailable, this study incorporates Cost of Illness (COI) or WTP values from other relevant literatures.

3.5 Data sources of the model

A framework of the data requirements of BenMAP-CE model for assessing the health-related economic benefits as well as how the inputs are preprocessed for the software is shown in Fig. 3.5.

3.5.1 Chattogram City Corporation shapefile

The shapefile for Chattogram City Corporation (CCC) containing the recently restructured 41 wards, the first step of Fig. 3.5 was procured from Geodash, as illustrated in Fig. 3.1. The acquired CCC shapefile underwent two distinct modifications using ArcGIS software. Originally, the file contained data with a finer level of detail, featuring multiple polygons for each ward division. This acts as the main layer file. Following this, attribute tables were generated to consolidate the relevant rows and columns associated with the air quality grid representation. To ensure congruity with incidence data, ArcGIS was utilized to dissolve the polygons at the ward division level, resulting in a more unified representation. This acts as the boundary layer.

Details regarding the spatial grid that was utilized for the analysis, including the location of each grid cell. In shapefiles, the presence of integer fields denoted as "Column" or "Col" and "Row" is mandated. These fields are required to possess a unique combination of values for every form encompassed within the shapefile. Analogous to the Column and Row field values observed in Regular Grid Definitions, these column and row values are deemed indispensable for the seamless integration of the Shapefile Grid Definition with other data sources.

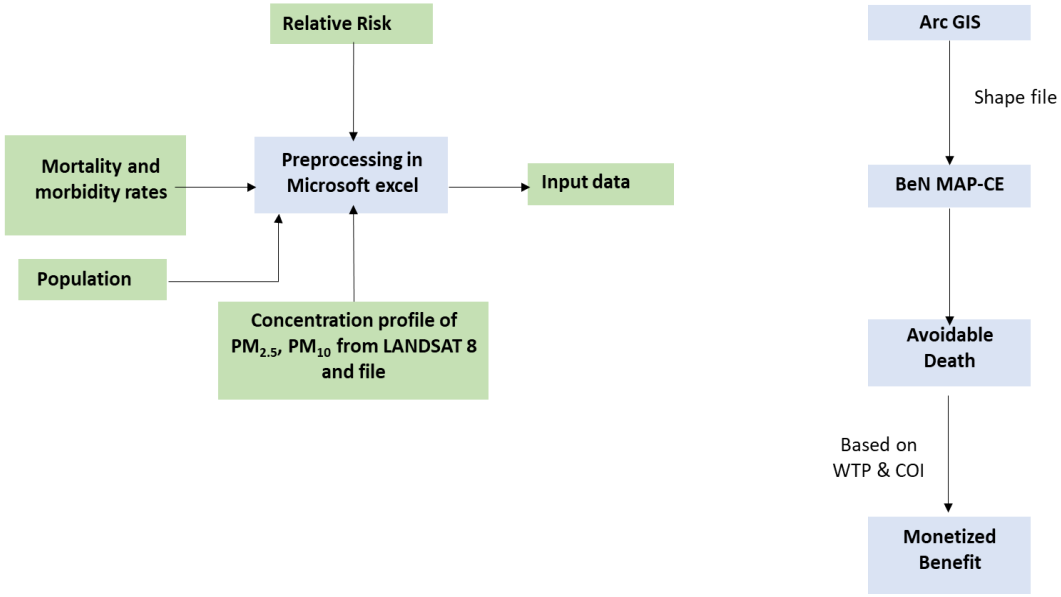

Fig. 3.5 Framework for the BenMAP-CE model

3.5.2 Pollutant data as model input

The estimation of alterations in population exposure to air pollutants is of utmost importance in conducting health impact analyses, as it facilitates the establishment of a link between anticipated changes in air pollution and their potential implications for public health. Comparing two separate air pollution levels at various time intervals is necessary to estimate changes in ambient pollutant concentration. The initial existing air pollution levels are referred to as the baseline level or scenario, while the subsequent levels are typically determined after a change, such as a regulatory intervention. Air quality monitoring data of a place, air quality modeling data, or a mix of both can be used to gauge exposure to air pollution at these two time points. BenMAP uses four primary categories to estimate exposure for Health Impact Assessment (HIA): model direct technique, monitor direct technique, model and monitor relative technique, and model rollback technique (USEPA, 2015)

The assessment of Particulate Matter (PM_{10} and $PM_{2.5}$) in Chattogram was the primary concern of our investigation. The CAMS-7 monitoring station, strategically placed close to CDA residential area, with coordinates of latitude 22.3° N and longitude 91.81°E, collect data on these pollutants but this data was not sufficient to cover up the full Chattogram City Corporation Region. As a result, this study collected data from various stations by a portable machine. Nevertheless, despite the monitoring station's accessibility, to have accuracy and to visualize the temporal trend, this study developed an empirical model to estimate the pollutant concentration.

Monitored data from sites

In this study, particulate matter concentrations at 56 sampling locations were monitored across Chattogram City, covering all 41 wards. To ensure the study's objectives were met and the safety of the crew and road users, each location was carefully selected. For measuring $PM_{2.5}$ concentrations, the study used the "Temtop Air Quality Monitor Professional $PM_{2.5}$, PM_{10} Formaldehyde (LKC1000S+)" particle detector. This device is compact, lightweight, and offers a high-resolution of 0.1 $\mu g/m^3$, with a measurement range of 0-999 $\mu g/m^3$. To account for $PM_{2.5}$ fluctuations and create concentration maps, the study strategically chose sampling locations based on a grid pattern.

The Temtop Air Quality Monitor Professional $PM_{2.5}$, PM_{10} Formaldehyde (LKC1000S+) was the chosen particle detector for this study due to its accuracy and reliability. The instrument features auto-calibration capability and responds quickly, providing steady and trustworthy data on $PM_{2.5}$ and PM_{10} concentrations in just 3-4 minutes. Its effectiveness in gathering real-time data at the 56 sample sites across Chattogram City makes it an invaluable tool for our air quality analyses. Data collection took place during the dry season (winter) when air

pollution tends to be more severe. The study continuously monitored $PM_{2.5}$ levels at each sampling location for 24 hours to determine the average concentration.

Modeled data

Acquisition of data

Field measured air quality data was collected from various monitoring points for the dry period in the years 2021, and 2022 following the procedures outlined in section 3.4.2. Concurrently, remote sensing data for the same time was extracted from the USGS Earth Explorer website (earthexplorer.usgs.gov). This combined dataset is valuable for studying and analyzing air quality trends and variations over the specified years and months, using both ground-based monitoring and remote sensing information.

Data preprocessing

The process of radiometric correction in Landsat 8 (L8) data entails radiance or reflectance values being created from Digital Number (DN) values. Two calibration rates are used in this technique. The first rate uses sensor calibration data to convert the DN values the sensor has recorded into at-sensor radiance. The at-sensor radiances are then converted to surface of the earth radiance values using the second rate. A precise formula for applying this radiometric correction is provided in the Landsat 8 Data User's Handbook, producing precise radiance or reflectance values that can be further studied and interpreted.

- **TOA radiance conversion**

The detectors of remote sensing satellites exhibit a linear response to the incoming radiance, regardless of whether it originates from the Earth's surface or internal calibration sources. The resulting output is discretized into 16-bit values, commonly known as Digital Numbers (DN), which serve as a representation of

the varying levels of brightness. These values are converted to the reflectance for Landsat 8 OLI and TIRS data is determined using the following Eq. 3.14

$$p\lambda = \frac{(M_p + Q_{cal}) * A_p}{\cos(\theta_{sz})} \quad (3.14)$$

Where, $p\lambda$ = TOA planetary reflectance M_p = Band-specific multiplicative rescaling factor from the metadata A_p = Band-specific additive rescaling factor from the metadata Q_{cal} = Quantized and calibrated standard product pixel values (DN) θ_{sz} = Local solar zenith angle

- **Atmospheric Adjustment**

  The subsequent procedure following the calculation of Top of Atmosphere (TOA) Reflectance entails the acquisition of Atmospheric Reflectance. The TOA Reflectance is a composite outcome that arises from the combined effects of both atmospheric reflectance and surface reflectance. The acquisition of Surface Reflectance can be achieved directly through the utilization of the Landsat 8 Surface Reflectance data product, which is provided by the National Aeronautics and Space Administration (NASA). Through the utilization of this data product, it becomes possible to isolate and differentiate the distinct contribution of atmospheric reflectance from the overall top-of-atmosphere (TOA) reflectance. This facilitates a more precise and accurate comprehension of the reflectance characteristics of the Earth's surface in Landsat 8 imagery. Here, Eq 3.15 provides a way of calculating the atmospheric adjustment.

  $$Atmospheric\ Reflectance = TOA\ Reflectance - Surface\ Reflectance \quad (3.15)$$

- **Preprocessing of Images**

  Image pre-processing encompasses a set of crucial techniques that are performed prior to the extraction of precise features and information from a downloaded raster image.

- **Sub-setting of the image**
- The process of image sub setting is employed in order to extract the designated study area, Chattogram city, from the obtained remote sensing image. The "Extract by mask" tool in ArcMap was employed to isolate the Chattogram region from the satellite image, facilitating a precise and targeted examination of the designated study area.
- **GPS location linking and identification**

  After the subsetting process, the images are prepared for subsequent processing. The subsequent procedure entails establishing a connection between the GPS coordinates of various air quality monitoring stations and overlaying them onto the images in order to accurately determine their respective positions on the site map. The GPS coordinates for the monitoring stations were obtained from Google Earth and subsequently connected to the subsets of satellite images using ArcMap.
- **Obtaining the values from GPS locations**

  The "extract multi values to points" function in ArcMap's spatial analyst toolbox is used to extract the DN values (pixel values) after connecting the GPS positions of the air quality monitoring sites to the subsetted images. At the corresponding monitoring sites, these numbers represent atmospheric reflectance. The association between the DN values for each of the eight bands in the satellite image and the criterion pollutant monitoring data is then determined using correlation.

- **Multiple linear regression analysis**

  The study involved linking atmospheric reflectance to indicators of air quality. The associations between several air quality measures and the bands of Landsat 8 OLI and TIRS that were found to be most correlated were then

examined using multiple linear regression models. Different air quality indices and top spectral factors each underwent a distinct regression modeling process. The two sets of variables were then gradually added together by ranking them up until the R square values stabilized. Regression equations were created for the purpose of predicting air quality metrics using the coefficients derived from the chosen variables. With a 95 percent level of confidence, the multiple correlation coefficients (R^2), standard error of the mean Y estimate (SE (Y)), and probability (P) were used to assess the statistical significance of the regression models. Using the regression techniques, air quality maps for each of the dependent variables (air quality parameters) were created. The suggested algorithms were also tested with ground truth data and atmospheric reflectance information obtained from Landsat OLI and TIRS satellite pictures recorded on December 22, 2021.

- **Regression model verification**

Before forecasting trends in air quality, the model obtained needs to be validated to evaluate its accuracy and precision. The "root mean square error" methodology is used to validate this information given in Eq 3.16.

$$RMSE = \sqrt{\frac{1}{N}\sum_{i=1}^{n}(M_i - O_i)^2} \tag{3.16}$$

Using the "extract multi values to points" capabilities in ArcMap's spatial analyst toolkit, emissions of all criterion pollutants from various monitoring stations are retrieved from the maps produced by the regression model. These numbers show the projected trends in air quality for December 2022. In MS Excel, the projected and observed values are compared to determine how much the predicted values deviate from the actual air quality monitoring data. The root mean square error is then calculated.

Computation of air pollutants in BenMAP-CE

In order to monitor and model direct data pertaining to baseline air pollutant levels, BenMAP employs the method of inverse distance weighting to calculate the average amount of air pollution exposure inside each grid cell, based on the data obtained from neighboring monitoring stations. The Voronoi Neighbor Average (VNA) technique operates on the idea that the impact of neighboring monitors should be more pronounced compared to that of distant sites. The weights (w_i) are assigned based on an inverse relationship with the distance (d_i) between the goal point and each monitor. The interpolant may be defined as a computed value that is obtained by taking a weighted average of the values of the sample points. The interpolant is a weighted average of the sample point values. The weight (w_i) is calculated using Eq. 3.17.

$$w_i = \frac{\frac{1}{d_i}}{\sum_i^N \frac{1}{d_i}} \tag{3.17}$$

where N represents the number of sample points and d represents the separation between the target point and each of the monitors. Also, the VNA approach has a number of benefits, one of which is the ability to create spatial links clearly and consistently between disconnected places using monitor data. When scaling is used, it can be used for both spatial and temporal interpolations. Furthermore, the "Voronoi" cells' size and form can change to accommodate the population's and the monitors' varying spatial distributions. For control scenarios, BenMAP's Monitor Rollback function can be used to change the available monitor data by either raising it or decreasing it by a specific amount.

3.5.3 Population dataset

The official census bureau is a trustworthy and helpful resource for getting population data. Population statistics at different local levels, including county,

census tract, and zip-code levels, are provided through census data. The Bangladesh Bureau of Statistics, however, has not been changed to reflect the new ward division in the case of Chattogram. As a result, the study utilizes the population dataset from WorldPop (*WorldPop*, 2023) which offers a different and practical source of population statistics. WorldPop offers global population datasets that are created using a combination of geographic modeling methods, demographic information, and satellite imagery.

Processing of data

The zones (districts, municipalities, or wards) or administrative entities for which the population-related statistics are generated need to be identified in order to process raster data that has been extracted from the world population. The Worldpop population data is then superimposed with the defined zone boundaries. Following data overlay, several summary statistics are computed using zonal statistical analysis in GIS software (such as ArcGIS or QGIS). The total population, average population density, maximum and minimum populations, and the standard deviation of the population within each zone are statistics that are frequently utilized. WorldPop provides population data in age bins (e.g., 0-5 years, 6-10 years, 11-15 years, etc.). Regardless of the initial age bin classifications, population data from smaller geographic units can be combined with data from bigger ones using zonal statistical analysis in Arc GIS.

Forecasting data

Hence, the population for the year 2022 was estimated by geometrical increase method. Geometrical Increase Method is used as it is widely used for population projection and the population growth is also showing geometrical trend. So, in this article the population of 2022 is projected by this method. The following expression Eq. 3.18 is used for forecasting.

$$P_t = P_o\ (1 + i)^t \quad (3.18)$$

Where, P_t= Population at some time in the future, P_o= base population, i= annual rate increase, and t= period of time in years. The health impact was estimated considering all the population at risk. Here, the population's growth rate has been taken as 1.1%, which is determined by averaging the population changes over the last 5 years.

3.5.4 Health endpoints and population age group

For the purpose of analysis, the population was divided into two distinct age groups: (a) 25-99 and (b) 5-17 years.

In Scenario I, the focus was on age groups ranging from 25 to 99, all of whom were exposed to air pollution. Health outcomes considered encompassed all causes of death, cardiovascular diseases, and respiratory disorders. The emphasis of the study was also on morbidity, particularly unnecessary hospital admissions due to cardiovascular and respiratory conditions. The age group 25 to 99 was selected due to their heightened susceptibility to air pollution, attributed to increased outdoor activities and use of public transportation. The health endpoints mentioned above were assessed for both particulate matter types.

As highlighted in the previous subsection 2.2.5.1, $PM_{2.5}$ is recognized as more hazardous than PM_{10}. and hence, this study also takes into consideration other health endpoints, including the Global Burden of Disease (GBD) 5-Cause of Death (COD) and Non-Communicable Diseases (NCD) with Lower Respiratory Infections (LRI), as well as Minor Restricted Activity Days (MRAD) and Work Loss Days (WLD), all of which are associated with $PM_{2.5}$ within this age scenario. Furthermore, given that there is a stronger global association between $PM_{2.5}$ and the incidence of 5-COD and NCD+LRI, for this reason the study adopts the Global Exposure-Mortality Model (GEMM) and the Log Linear (LL) model for

estimating the potential health benefits associated with mitigating $PM_{2.5}$ pollution. This approach allows for a more comprehensive and accurate assessment of the health impacts and potential improvements related to $PM_{2.5}$ reduction efforts.

Scenario II revolved around school-age children aged 5 to 17, a group more susceptible to conditions like lower respiratory infections and asthma, which could lead to school absenteeism. The specific disorders in question were associated with the primary health outcomes under consideration for this particular age group. The incidence dataset presented in section 3.5.5 indicates that these disorders have a higher incidence rate in this age group compared to the adult population, making them important focal points for health analysis within this specific demographic.

3.5.5 Incidence and mortality dataset

The term "Incidence dataset" describes the overall number of new harmful health effects that develop over time in a certain geographic area. Incidence rate provides insights into the risk of developing a specific condition. The mortality rate represents the number of deaths within a population during a specified period. It's a measure of how deadly a specific disease or condition is within that population. The rates indicated above are employed in tandem with concentration-response functions to estimate the health impacts associated with changes in air pollution levels. The provided data offers insights into the incidence and mortality rates of specific health outcomes within a particular population. The data for this study was obtained from the Institute for Health Metrics and Evaluation (IHME, 2023). Different health endpoints have different incidence or prevalence rates, and these are provided in Table 3.5.

Table 3.5. Incidence and Mortality Rates adopted from IHME (Rate per 100,000)

Health Outcomes	Year		
	2017	2018	2019
All Cause	835.86	845.75	855.82
Cardiovascular Disease	367.60	372.91	377.61
Respiratory Disease	122.83	140.83	141.21
Ischemic Heart Disease (IHD)	146.10	149.78	153.07
Chronic Obstructive Pulmonary Disease	80.88	81.25	82.66
Stroke	184.25	184.63	184.82
Lung Cancer (LC)	10.98	11.33	11.66
Lower Respiratory Infections (LRI)	24.82	25.78	26.70
Non-Communicable Diseases (NCD)	687.91	700.30	711.55
Hospital Admission, Respiratory	1166.79	1198.40	1239.08
Hospital Admission, Cardiovascular	996.21	1012.22	1031.27
Minor Restricted Activity Day (MRAD)		0.02137*	
Work Loss Days (WLD)		0.00678*	
Asthma (5-17 years)	172.44	172.08	173.19
LRI (5-17 year)	7320.45	7332.16	7341.06

N.B: MRAD adopted from (Global Ostro and Rothschild, 1989) and WLD adopted from (Global Adams et al, 1999)

However, the Institute for Health Metrics and Evaluation (IHME) has provided updates to their data up until the year 2019. For the period 2020-2022, the data from 2019 was utilized, following a similar approach employed in other scholarly investigations (Bayat, Planning, et al., 2019; Manojkumar and Srimuruganandam, 2021). Due to a lack of sufficient local data on the incidence of minor restricted activity days and work loss days, this study has chosen to

utilize globally available data as presented in Table 3.5. The sources of these health endpoints are provided below the table. In the context of health impact assessments and epidemiological studies, it's common to use mortality rates to assess the impact on mortality (death) and incidence rates to evaluate the impact on morbidity (non-fatal health outcomes). Hence this study assesses the overall premature death and incidences using the data provided in Table 3.5.

3.5.6 Concentration response function

A health impact function oversees figuring out how many more unfavorable health impacts there are due to changing how exposed you are to air pollution. The size of the affected population with characteristics (age, race, and ethnicity), the incidence rate of the adverse health effect, and an effect coefficient known as Beta (ß), which is derived from epidemiological studies, are among the inputs to this function. A specific adverse health impact's percentage change per unit of pollution is shown by the symbol ß (beta). These equations are developed from concentration-response (C-R) functions, which calculate the correlation between the concentration of an air pollutant and the risk of negative health effects. The relationship between a one-unit changes in air pollution (x) and a one-unit change in the incidence or prevalence of a health outcome (y) is described by CR functions, which are commonly referred to as effect estimates or health impact functions. The odds ratios (OR) or relative risk ratios (RR) utilised to depict these functions are derived from epidemiological research that has been published. The odds ratio (OR) or relative risk (RR) is utilised to assess the probability or potential of a shift in the health status of a population in response to a specific alteration in pollutant levels. The predominant reporting formats utilised in academic literature for epidemiological research concerning $PM_{2.5}$ encompass linear regression, Poisson regression, logistic regression, and conditional logistic regression. In addition to this, the GEMM (Global Exposure Mortality Model)

model has the potential to be integrated into BenMAP-CE. The log linear model and GEMM model were utilised in this work.

Log-Linear

A representative log-linear form health impact assessment is given in Eq. 3.19. This is the most widely used form in BenMAP-CE.

$$\Delta y = y_0(1 - e^{\beta * \Delta PM}) \quad (3.19)$$

where, Δy = health benefits, y_o = baseline incidence rate, β = concentration-response coefficient,ΔX = difference in $PM_{2.5}$ or PM_{10} concentration, Pop = population, RR = relative risk

The concentration response coefficient can be intended from the relative risk (RR) obtained from epidemiological studies using the Eq. 3.20 where ΔPM denotes the variation in pollutant concentration that was utilized to determine the relative risk in the epidemiological study.

$$\beta = \frac{\ln (RR)}{\Delta PM}; \quad (3.20)$$

- **Mortality effects**

The selection of health endpoints was guided by several considerations, including literature references (World Bank, 2006), alignment with the International Classification of Diseases (ICD-10) code system, incorporation of outcomes supported by exposure-response studies, and reliance on available statistical data encompassing mortality and morbidity incidence rates. Accordingly, the chosen health endpoints encompass a spectrum of impacts, including all-cause mortality, mortality linked to cardiovascular and respiratory conditions, mortality arising from 5-COD (Five Causes of Death) and NCD (Non-Communicable Diseases), as well as morbidity instances such as hospital

admissions due to respiratory and cardiovascular diseases, occurrences of minor restricted activity days, instances of work loss days, and the prevalence of asthma and LRI. The harmonization of HIFs or CRFs within the same health endpoint was achieved through a fixed-effects pooling approach.

The selection of Health Impact Function (HIF) functions and their associated parameters holds utmost significance when utilizing the BenMAP model to estimate the effects of pollutant exposure on a population's health. This is particularly relevant considering that many of these functions and parameters have been formulated based on data from the United States, Europe, and China.

However, these regions possess distinctive population features such as density, mortality rates, life-quality indices, etc. Additionally, their air quality characteristics in terms of particulate matter concentration and composition, as well as meteorological conditions, differ notably from those observed in our study area. For the selection of functions, first research was conducted for countries within Asian Continent and then outside it as that local and regional search was missing. The following things were taken into consideration (a) length of exposure to $PM_{2.5}$ concentration prioritizing the long-term effects (b) in accordance with the age group evaluated in the epidemiological studies (c) population exposed. Due to the absence of the function the study adopted the function given in Table 3.6.

The GEMM NCD + LRI (Non-Communicable Disease + Lower Respiratory Infection) was employed to represent the GEMM measurements pertaining to nonaccidental fatalities (J. Xu et al., 2021). Due to the absence of an exposure-response relationship for Non-Communicable Diseases (NCDs) within the LL (log-linear) model, this study chooses to utilize the Non-Accidental health endpoint in conjunction with the LL model to account for variations. BenMAP offers the capacity to pool CR functions from many studies utilizing meta-

analysis techniques such as pooling, which combines beta estimates from various research works while taking study variations into account.

Table 3.6. Concentration Response Coefficient for mortality effects

Health Endpoints	Pollutant	Coefficient β	References
All Cause	$PM_{2.5}$	0.0036 (0.0011-0.0061)	(Kan et al., 2007)
	$PM_{2.5}$	0.0040 (0.0019-0.0062)	(Peng et al., 2009a)
	PM_{10}	0.0035 (0.0018-0.0052)	(B. Chen et al., 2004)
	PM_{10}	0.0032 (0.0028-0.0035)	(Shang et al., 2013)
Respiratory	$PM_{2.5}$	0.0095 (0.0016, 0.0173)	(Kan et al., 2007)
	$PM_{2.5}$	0.0143 (0.0085, 0.0201)	(Peng et al., 2009b)
	PM_{10}	0.0056 (0.0031, 0.0081)	(B. Chen et al., 2004)
	PM_{10}	0.0043 (0.0037-0.0049)	(Shang et al., 2013)
Cardiovascular	$PM_{2.5}$	0.0041 (0.0001,0.0082)	(Kan et al., 2007)
	$PM_{2.5}$	0.0053 (0.0015, 0.0090)	(Peng et al., 2009a)
	PM_{10}	0.0044 (0.0023, 0.0064)	(B. Chen et al., 2004)
	PM_{10}	0.0032 (0.0028-0.0035)	(Shang et al., 2013)
IHD	$PM_{2.5}$	0.009531(0.0079, 0.011162,)	(Cesaroni et al., 2013)
COPD	$PM_{2.5}$	0.0113 (0.0095,0.0122)	(Yin et al., 2017)
Stroke	$PM_{2.5}$	0.0131 (0.0122-0.0148)	(Yin et al., 2017)
Lung Cancer	$PM_{2.5}$	0.004879 (0.007056, 0.002702)	(Cesaroni et al., 2013)
LRI	$PM_{2.5}$	0.0062 (0.00027, 0.0096)	(Cai et al., 2019)
Non-Accidental	$PM_{2.5}$	0.013976 (0.0146, 0.0133)	(F. Lu et al., 2015)

According to the USEPA (US EPA, 2018; USEPA, 2015), BenMAP offers a variety of pooling choices, including addition method, subtraction method, user-assigned weights, random-effect model, and fixed-effect model. Several of the aforementioned health outcomes are derived from a collection of individual epidemiological studies. These studies are consolidated through a process known as "pooling," adhering to the recommended BenMAP configuration as elucidated earlier. In a parallel manner, findings from economic studies are also amalgamated for certain outcomes. For instance, a composite outcome such as

respiratory-related hospital visits involved assigning a 50% weighting to results obtained from. The procedure for aggregating evidence from multiple studies adhered to the established approaches of the U.S. EPA, as described earlier**.**Each research within the existing body of literature provides risk estimates based on individual distributions. Random effects pooling is employed to account for the variability in individual risk estimations, hence enabling the provision of a single mean risk estimate.

Global Exposure Mortality Model

A statistical model called the Global Exposure Mortality Model (GEMM) calculates the relationship between exposure to fine particulate matter ($PM_{2.5}$) and mortality. A group of scholars from the University of Oxford under the direction of Richard Burnett created the model (Burnett et al., 2018a). The GEMM estimates the shape of the link between $PM_{2.5}$ exposure and mortality using data from 41 cohort studies from 16 different countries. The following variables are taken into account by the model: the amount of $PM_{2.5}$ in the air, the amount of time exposed, the person's age and sex, and the presence of underlying medical disorders.

The GEMM 5-COD (5-Causes of death) model was utilized to evaluate the additional deaths linked to $PM_{2.5}$ exposure for five major diseases among adults aged 25 and older. To allow comparison with the previous results obtained from the LL (log linear) model, Burnett et al. (2018) developed distinct GEMMs for each of the five primary causes of death: ischemic heart disease (IHD), stroke, chronic obstructive pulmonary disease (COPD), lung cancer, and lower respiratory infections (LRIs). These separate models are denoted as GEMM 5-COD. To deal with the intricacies of the analysis, adult subgroups (ages > 25 years) were used in both the GEMM and LL (Log Linear) models to calculate

excess deaths. Uncertainty ranges were expressed using 95% confidence intervals (95% CIs), as adopted from (Burnett et al., 2018a).

The global exposure mortality model (GEMM) investigates the relationship between mortality rates in different age groups and annual mean ambient $PM_{2.5}$ concentrations expressed as z [$\mu g/m^3$]. Eq. 3.21 represents the hazard ratio function used to express the association (Nasari et al., 2016).

$$GEMM(z) = exp\left\{\frac{\theta \ln\left(\frac{z}{\alpha}+1\right)}{1+\exp\left(-\frac{z-\mu}{\vartheta}\right)}\right\} \quad (3.21)$$

The shape of the response function is specifically determined by non-communicable diseases (NCD) and lower respiratory infections (LRI), as well as the five distinct causes of death listed in the study by (Burnett et al. 2018). These parameters are all included in the GEMM model. These characteristics, which are critical for calculating the number of $PM_{2.5}$-related deaths, are included in Table 3.7.

Table 3.7. Concentration Response Coefficient by GEMM model for 5-COD and NCD

Endpoints	θ	St. Err θ	μ	A	N
NCD+LRI	0.143	0.01807	15.5	1.6	36.8
IHD	0.2969	0.01787	12	1.9	40.2
Stroke	0.272	0.07697	16.7	6.2	23.7
COPD	0.251	0.06762	2.5	6.5	32
LC	0.2942	0.06147	9.3	6.2	29.8
LRI	0.4468	0.11735	5.7	6.4	8.4

Also, the Global exposure mortality model uses the following Eq. 3.22 to determine the number of fatalities (Y) that can be directly linked to air pollution at locations.

$$\Delta y = \left(\frac{1 - GEMM(z_0)}{GEMM_z}\right) * Y_o * Pop \quad (3.22)$$

where the concentrations of ambient air pollution are, respectively, z and z_0; The age-specific base mortality is Y_0; where Pop denotes the population by age exposed to air pollution.

- **Morbidity effects**

Morbidity consequences are to health issues or illnesses that do not result in mortality, yet can engender substantial health complications or on fatal health outcomes, diminished quality of life, and economic burdens. The relationship between PM pollution and hospital utilization, specifically hospital admissions primarily for cardiovascular disease (CVD) and respiratory disease (RD), has been examined in these studies. Additionally, the impact on work loss days and minor restricted activity days has been taken into account for individuals aged 25 years and older. The data are represented in Table 3.8.

Table 3.8. Concentration Response Coefficient for Morbidity Effects

Health Endpoints	Pollutant	Coefficient β	References
Hospital Admissions, Cardiovascular	$PM_{2.5}$	0. 0068(0.0043-0.0093)	(Hong and LaBresh, 2006)
	PM_{10}	0.0066 (0.00336-0.0095)	(Peng et al., 2009a)
Hospital Admissions, Respiratory	$PM_{2.5}$	0.0161 (0.0087 0.02350	(Shang et al., 2013)
	PM10	0.0124 (0.0086,0.0162)	(B. Chen et al., 2004)
Work Loss Days	$PM_{2.5}$, PM_{10}	0.0046 (0.00496,0.00424)	(Ostro and Rothschild, 1989)
Minor Restricted Activity Days	$PM_{2.5}$, PM_{10}	0.00741(0.00811,0.00671)	(Ostro and Rothschild, 1989)
Asthma	$PM_{2.5}$	0.04367 (0.04455, 0.04279)	(Tetreault et al 2016)
LRI	$PM_{2.5}$	0.02546 (0.03507,0.01583)	(Parker et al 2009)

For the age group of 5-17, the scope narrows down to two specific health conditions: asthma and lower respiratory infections (LRI). These conditions prevent these individuals from attending school, and due to their stronger resistance, the incidence rate for other health outcomes is nearly negligible for this age group.

3.5.7 Valuation function

BenMAP-CE uses either willingness to pay (WTP)-based valuation functions or cost of illness (COI)-based valuation functions to estimate the monetized benefits for morbidity endpoints. The willingness to pay (WTP) measures how much people are prepared to pay in exchange for a lower risk of getting sick or dying. A condition's observable direct and indirect costs are used by COI to determine the value of a health effect. Due to the inclusion of the value of reduced pain and sufferings of individual, a WTP-based estimate is anticipated to be more precise than a COI-based estimate. COI estimates are occasionally used as a stand-in for WTP estimates because they are occasionally difficult to obtain.

BenMAP-CE typically uses the value of statistical life (VSL) to assess monetized benefits for mortality endpoints. VSL is a WTP-based estimate that was developed from a substantial body of observed or elicited estimates of the monetary value that a person would be ready to trade for marginally lower death risks. It is crucial to remember that VSL does not represent the worth of the life of any one specific person. Instead, it symbolizes the typical value society accords a statistical existence. As a result, the VSL may not always be equivalent to the sum of money that a person would be ready to spend in order to prevent their own demise.

- **Mortality effects**

The commonly used approach to measure the economic advantages of this policy is through the application of the Value of Statistical Life (VSL) concept. The pooled health outcomes were then evaluated in BenMAP-CE by multiplying the assigned economic value by the respective quantity of each outcome by Eq. 3.23.

$$Health\ Benefits = Death\ Avoided * VSL \tag{3.23}$$

The concept of Value of Statistical Life (VSL) is discussed by (Wadud and Khan, 2013) as the monetary value that is allocated by individuals to mitigate mortality risks or to tolerate their escalation. The idea of Value of Statistical Life (VSL) pertains to the marginal rate of substitution that exists between an individual's wealth and their risk of mortality (Hammit, 2008). Ongoing discussions continue to exist, particularly in poor countries, questioning the legitimacy of the Value of Statistical Life (VSL) concept. However, it has garnered acknowledgment as a credible methodology within the field of economics (Viscusi 2004) and is extensively utilized for policy evaluation. As a result, the determination of health benefits stems from the assigned value of the Value of Statistical Life (VSL).

The incorporation of the Value of Statistical Life (VSL) in policy assessments, as demonstrated by the approach employed by the United States Environmental Protection Agency (USEPA) in its latest Regulatory Impact Analyses (USEPA 2005, 2007), is predicated on assuming equal value for every life saved, regardless of the remaining life expectancy of the affected individuals. One noteworthy advantage of this model lies in its inherent simplicity, which is further complemented by the abundance of available value of statistical life (VSL) estimates. However, a significant drawback of this approach is its tendency to frequently result in an overestimation of benefits, particularly when assessing potential health hazards associated with prolonged exposure.

Although the Value of Statistical Life (VSL) has been the subject of extensive research, developing nations like Bangladesh have had very few studies conducted on it, which has caused considerable variances in the estimated values (Wadud and Khan, 2013). The Organization for Co-operation and Development (OECD) countries' VSL data (VSL_{OECD}) is used as a starting point in many of the studies. The most recent estimate, the VSL for OECD nations is $3.83 million (at purchasing power parity (PPP) 2011) (Narain and Sall, 2016). The Value of

Statistical Life (VSL), derived from an analysis of 26 value-of-life studies, has an average VSL value of $8.7 million in 2015 U.S. dollars (USEPA, 2010). In comparison to (Friedrich and Droste-Franke, 2005) in Europe, (DEFRA, 2008) employes an implied valuation of 1.1 million (2002 GBP) and GBP 1 million (2000 €). The estimated VSL values in India likewise exhibit significant variation, with some studies estimating values between Rs. 1 million (Bhattacharya et al., 2007) and Rs. 56 million (SHANMUGAM, 2001), and others reporting values between Rs. 14.5 million and Rs. 35 million (Simon et al., 1999).

The observed discrepancies can be attributed to the utilisation of diverse valuation methodologies. Nevertheless, while using the identical research approach and considering the concept of purchasing power parity (PPP), a study ascertain that China exhibits a readiness to spend around US$ 1 million to mitigate health hazards, a figure that is comparable to affluent nations (Krupnick et al., 2006). This information can be used as a starting point for modifications to create a VSL that is suitable for each country's economic situation. In the absence of national research, the "benefit-transfer" approach, as put forth by (Narain and Sall, 2016), can be utilized to adapt the unit health costs from external studies to a local context. This scaling of the Value of Statistical Life (VSL) adjustment accounts for variations in income levels. The Eq. 3.24 is given below:

$$VSL_{Target} = VSL_{Base} * \left(\frac{GDP_{Target}}{GDP_{Base}}\right)^{Elasticity} \quad (3.24)$$

Where, VSL_{Target} and GDP_{Target} is the value which needs to be determined for a country and VSL_{Base} and GDP_{Base} is the reference value which is used for estimation and elasticity usually depends on the socio economic condition of the country.

In 2013, a contingent valuation study was conducted in the two major cities of Bangladesh, Dhaka and Chittagong, aiming to ascertain people's willingness to pay (WTP) for reducing the risk of death attributed to air pollution revealing the

mean Value of Statistical Life (VSL) varied in purchasing power parity (PPP) terms from 17,480 to 22,463 USD and the GDP per capita for the same year ranged from 9.78 to 12.57 times this value (A. Majumder et al., 2015).

Given its focus on urban centers, substantial disparities in economic conditions, and lower values in comparison to other published estimates for Bangladesh and international benchmarks like the OECD and US EPA, the VSL estimated in this study might indeed represent a conservative lower limit. An assessment of Bangladesh's Value of Statistical Life (VSL) was conducted where a value of US$ 40,000 (1997 US$), encompassing a range extending from US$ 30,000 to US$ 0.7 million was proposed, yet the status of PPP-adjustment for this valuation remains indeterminate (Miller, 2000). However, the status of PPP-adjustment for this value remains unclear. Another research estimated the VSL for Bangladesh within the range of US$ 1,783 to US$ 2,922, signifying a significant reduction compared to Miller's estimation (Mahmud, 2009). A VSL value has also been provided by World Bank which is US$ 28251 (2002) for Bangladesh (World Bank, 2006).

To consider the impact of rising real income over time on Willingness to Pay (WTP) values, specific valuation functions are modified through a process known as income growth adjustment. Users of BenMAP-CE are afforded the flexibility to select various values to adjust the sensitivity of WTP regarding these income fluctuations, enabling a more precise evaluation of the effects of income growth on valuation outcomes. Although there are costs involved in reducing air pollution, the advantages typically surpass the expenses. The cost-benefit analysis conducted for Bangladesh estimated a benefit-to-cost ratio of 3.67 in 2030, considering the impact on morbidity, as per the guidelines set by the WHO Interim Target 1 (World Bank, 2022a). These findings demonstrate that the

benefits of mitigating air pollution, such as lower healthcare costs and reduced work absences, greatly outweigh the corresponding expenses for Bangladesh.

The study employed the VSL value for Bangladesh, amounting to $142,709 USD in 2015 international dollars, which is the most recent study "Valuing Mortality Risk Reductions in Global Benefit-Cost Analysis", (Robinson et al., 2019) and this estimate originated from international research utilizing the benefit transfer approach, a method commonly employed for assessing individuals' willingness to pay for risk reduction.

- **Morbidity effect**

The technique for evaluating health effect costs, such as willingness-to-pay (WTP) or Cost of Illness (COI), as considered by the World Bank in 2006, along with other literature and web sources, is utilized to assess the monetary values of morbidity effects. The precise values for various health consequences are provided in Table 3.9. The table also provides the data of US EPA and China to portray the variation between the values. The World Bank data, initially established for the United States in 1990 using the Willingness to Pay (WTP) methodology, has been customized for the context of this research to correspond with the reference period spanning from 2017 to 2022. The specific data for Bangladesh underwent a process that involved initial adjustments to the values to account for changes over time by aligning them with base years. Subsequently, the data underwent further estimations and adjustments for both Purchasing Power Parity (PPP) and Gross National Income (GNI).

When conducting the valuation based on other literature that uses the COI (Cost of Illness) method, the Eq. 3.25 by (D. Huang et al., 2012) is applied to calculate the total value.

$$COI_j = COH_j + DGDP * T_j \tag{3.25}$$

Where, COI_j is the average medical treatment cost for a disease j for each case, DGDP is the GDP per capita, T_j is the average labor time lost due to disease j for each case and COI_j is the average cost of illness of disease j for each case.

Table 3.9. Unit costs for health endpoint (Morbidity)

Health Endpoint	Unit Value (USD)	Source	Method
Hospital Admission, Respiratory	8343 (4.82 mean length of stay) + (medical charge cost $10696)	US EPA values	COI
	611 ($ 2023)	Bangladesh	COI
	2454 (2010 CNY) (Including length of stay and medical cost)	China	COI
	73.68 ($2002)	World Bank	WTP
Hospital Admission, Cardiovascular	16918 (5.05 mean length of stay) + (medical charge cost 16045)	US EPA values	COI
	5006 (2010 CNY) (Including length of stay and medical cost)	China	COI
	2149 ($ 2023)	Bangladesh	
Asthma	1.10	World Bank	WTP
	219	US EPA values	COI
LRI (child)	600 (1-year medical cost)	US EPA values	COI
	0.87	World Bank	WTP
Minor Restricted Activity Days	0.92	World Bank	WTP
Work Loss Days	0.92	World Bank	WTP

Source: World Bank (South, 2006); (US EPA, 2011) ; Bangladesh (National Heart Foundation of Bangladesh, 2023); China (Zhang et al., 2018)

BenMAP-CE uses inflation datasets or discount rates to modify valuation estimates for health benefits to take price changes over time into account. The adjustments of values were carried out using a discount rate of 3%, following the recommendation by the US EPA (Environmental Protection Agency), especially when dealing with data from recent years and provided in Table 3.10.

Table 3.10. Estimated Economic Parameter for the study year 2017-2022

Health effects	2017	2018	2019	2020	2021	2022
	Bangladesh WTP (US$)					
Mortality	157408	167968	177244	187376	197651	213064
Hospital Admission, Respiratory	120.2	147.38	161.8	168.21	192.24	208.26
Hospital Admission, Cardiovascular	317	388	427	443	507	550
Asthma	4.73	5.8	6.3	6.6	7.57	8.19
LRI	4	5.1	5.4	6.8	7.2	8.1
Minor Restricted Activity Days	3.97	4.87	5.36	6.57	6.36	6.89
Work Loss Days	3.97	4.87	5.36	6.57	6.36	6.89

For projections into future years, the values were subsequently inflated accordingly. Detailed values for the years 2017-2022, incorporating both inflation rates and, if necessary, discount rates, are presented below. In cases where the unit cost of Hospital Admission due to Cardiovascular conditions was unavailable, this study employed a predictive approach based on the cost of illness. The breakdown of costs is provided in Table A.4. and A.5. for reference.

3.6 BenMAP-CE model setup

In order to ensure the reproducibility of the data, a number of processing steps were undertaken to conform to the necessary formats for interoperability with the BenMAP program. In the BenMAP-CE software, the emissions data for each year, regardless of whether it was obtained from monitoring or modelling, was considered as an individual project, all of which had a shared configuration. The configuration included definitions of grids, data on population, pollution, and other pertinent datasets.

In the BenMAP-CE software, shapefiles were employed to demarcate the spatial boundaries within which the program will assign air quality data, evaluate health effects, and aggregate results. In the BenMAP-CE software, it was imperative that each grid definition possesses a unique and non-repetitive

column and row index. The shapefile was then projected to WGS1984. The "Create Crosswalk" function was employed to calculate the degree of spatial intersection across distinct scales, facilitating the construction of a correlation between one shapefile and another. This calculation enables the smooth transition and computation across multiple shapefiles, hence offering important insights across diverse geographic resolutions. The completion of this stage required a significant amount of time; however, it was important to ensure the accuracy of the study. Furthermore, it was advisable to identify the shapefile as the default administrative layer and allocate it a priority value of "1" in the "Drawing Priority" field for the purpose of this study. This guarantees that the layer was prioritized and appropriately depicted in the analysis. In contrast, the boundary layer was commonly designated a priority level of "2," primarily employed for the inclusion of mortality and morbidity rates, as well as valuation data. It was imperative to emphasize that the border shapefile does not conform to a grid format. On the other hand, the priority 1 shapefile consists of 41 rows and 1 column. Within this framework, the 41 rows symbolize the internal cells or grid cells, which correspond to the 41 wards of CCC. Conversely, the solitary column functions as the external layer or barrier.

The air quality data obtained from the model was associated with the shapefile by aligning the corresponding rows and columns. The respective Pollutant Metrics for both pollutants were described as D24HourMean, which represents the 24-hour mean concentration. The exclusion of seasonal measures in this analysis was done for the sake of simplicity. However, it is worth noting that they can be readily integrated into future analyses if deemed necessary.

Population data was obtained from Worldpop data, which was specifically created for the study region and its accompanying grid. The Population Datasets category includes a dataset of population at the ward level, stratified by age,

obtained from WorldPop. This dataset has been processed and converted into an Excel file format (.xlsx). The provided Excel file contained data for columns, namely Race, Ethnicity, Gender, Age Range, Column, Row, and Value as like provided in Fig. 3.6. These columns have been structured in accordance with the prescribed format to ensure compatibility with BenMAP-CE. Further details pertaining to the meanings of these columns can be accessed in the BenMAP-CE handbook published by the U.S. Environmental Protection Agency in 2017. The column labelled "Column" functions to demarcate the boundary, whilst the column labelled "Row" denotes the population count of each ward. Below is a sample of the dataset that has been provided.

The dataset on Incidence/Prevalence Rates comprises age-stratified data, which involves categorizing the baseline mortality into distinct age groups, as illustrated in Table 3.6. The dataset was obtained by importing data from an Excel file (.xlsx). It includes data fields such as Endpoint, Type, Race, Ethnicity, Gender, Start Age, End Age, Row, Column, and Value. These columns adhere to the specifications outlined by BenMAP-CE, as stated by the U.S. Environmental Protection Agency in 2017. The "Column" was spatially correlated with the boundary shapefile, as the nature of this dataset does not lend itself to a grid-based representation. The values within the dataset were derived by estimation methods utilizing the national death rate specific to each respective age group.

Column	Row	Year	Ethnicity	Race	Gender	AgeRange	Population
1	1	2022	All	All	Both	25TO99	50893
1	2	2022	All	All	Both	25TO99	172539
1	3	2022	All	All	Both	25TO99	77805
1	4	2022	All	All	Both	25TO99	132936
1	5	2022	All	All	Both	25TO99	34368
1	6	2022	All	All	Both	25TO99	32573
1	7	2022	All	All	Both	25TO99	82377
1	8	2022	All	All	Both	25TO99	125176

Fig. 3.6 Preprocessing of population file in BenMAP-CE (adopted from model file)

In this study, the Health Impact Functions were chosen from a diverse range of sources, encompassing the default EPA Standard Health as well as epidemiological studies that are specifically relevant to the Asian subcontinent. The selection process also involved the utilization of the Global Exposure Mortality Model (GEMM) dataset. The health impact functions that were selected were clearly described and successfully incorporated into the study, as demonstrated in Table 3.6.-3.8. The economic valuation functions employed in this study, used to assess the economic worth of reducing mortality risk, were derived from World Bank and other literatures related to valuation research. These studies employed methods like willingness to pay (WTP) and Cost of illness (COI) approaches. To ensure consistency, the amount was kept in the US dollar. In cases where multiple cost estimates existed across different years within a single study, the most recent estimate was chosen. To account for inflation, cost estimates from different years were adjusted using Consumer Price Index (CPI) figures, with the currency year set as 2017.

3.7 BenMAP-CE model pathway

The analysis within BenMAP was conducted through a series of steps outlined as follows:

- Pollutant Identification: Defining the pollutants PM_{10} and $PM_{2.5}$.
- Loading Air Quality Data: Establishing Baseline and Control scenarios.
    - Baseline Scenario: Utilizing $PM_{2.5}$ and PM_{10} data for the study period of 2017-2022.
    - Control Scenario: Applying the WHO standard for air quality.
- Population Data Incorporation.
- Execution of Health Impact Assessment: The BenMAP software employed a Monte Carlo simulation to estimate the number of deaths attributed to changes in fine particle ($PM_{2.5}$) concentrations across different scenarios. This

process involved generating a distribution of Monte Carlo estimates for each grid cell, wherein probability distributions for concentration-response (C–R) coefficients were utilized for various health outcomes. Random values were drawn from these distributions to calculate incidence rates, which represent the rate of health outcomes related to $PM_{2.5}$ exposure. This procedure was repeated 5000 times to create a distribution of estimated incidence rates for each grid cell, capturing uncertainty. For each cell, key values were extracted from this distribution: the median for a central estimate, the 2.5th percentile for a conservative lower boundary, and the 97.5th percentile for an upper boundary of uncertainty. Regional estimates of deaths linked to reduced $PM_{2.5}$ concentrations were obtained by aggregating these cell-level estimates, providing an encompassing assessment of the health impact across the studied region.

- Execution of Valuation: BenMAP-CE estimates the economic benefits under projected scenarios for the avoided mortalities and morbidities using the WTP or COI values.
- Exporting Results

  Lastly, it's worth noting that BenMAP-CE offers the capability to visualize each Health Impact Function and Valuation Function. Following their export from BenMAP-CE, the shapefiles are then imported into ArcGIS, facilitating the generation of the resulting visual representations. Furthermore, the data tables are exported as well. These data tables encompass demographic information relevant to the population falling within the designated age range of the function. Within these tables, point estimates for incidence or valuation are provided, alongside statistical measures like the mean and standard deviation. This approach establishes a standardized denominator, permitting comparisons of outcomes across distinct functions. To sum up, a

comprehensive audit trail report is available for the model, offering an intricate record of all inputs and choices made during the modeling process.

3.8 Concluding Remarks

Regrettably, the current state of air quality monitoring in Chattogram is characterized by limitations and insufficiencies stemming from a range of challenges, including the availability of historical data, geographical coverage, and the scope of parameters being monitored. Additionally, there is a notable absence of established national regulations governing the control and management of particulate matter in air specifically $PM_{2.5}$ and PM_{10}. While Chattogram has two monitoring stations located in Khulshi near the TV station and Agrabad, concerns have arisen regarding the reliability of air quality reports provided by the TV station's Continuous Air Monitoring System (CAMS). To address these concerns, this study has developed an empirical model to predict PM_{10} and $PM_{2.5}$ data for the entire Chattogram City Corporation area from 2017 to 2022. Additionally, it examines the concentrations of various heavy metals such as iron (Fe), chromium (Cr), copper (Cu), nickel (Ni), zinc (Zn), and manganese (Mn), as well as relevant indicators, to assess potential health risks associated with these pollutants. A road map of the study is provided in Fig. 3.7. Furthermore, this research evaluates the overall reduction in premature mortality linked to the reduction of $PM_{2.5}$ and PM_{10} levels using the incidence and prevalence rates for each specific diseases from IHME within the Chattogram City Corporation Area using the BenMAP-CE tool. The study incorporates economic data specific to Bangladesh, as well as data from the Organization for Economic Co-operation and Development (OECD) and relevant literature, to quantify the substantial financial consequences of air pollution on public health. The projected benefits of pollution reduction for each research year are expressed

in monetary terms, providing a practical assessment of the economic value associated with improving air quality and the resulting benefits for public health.

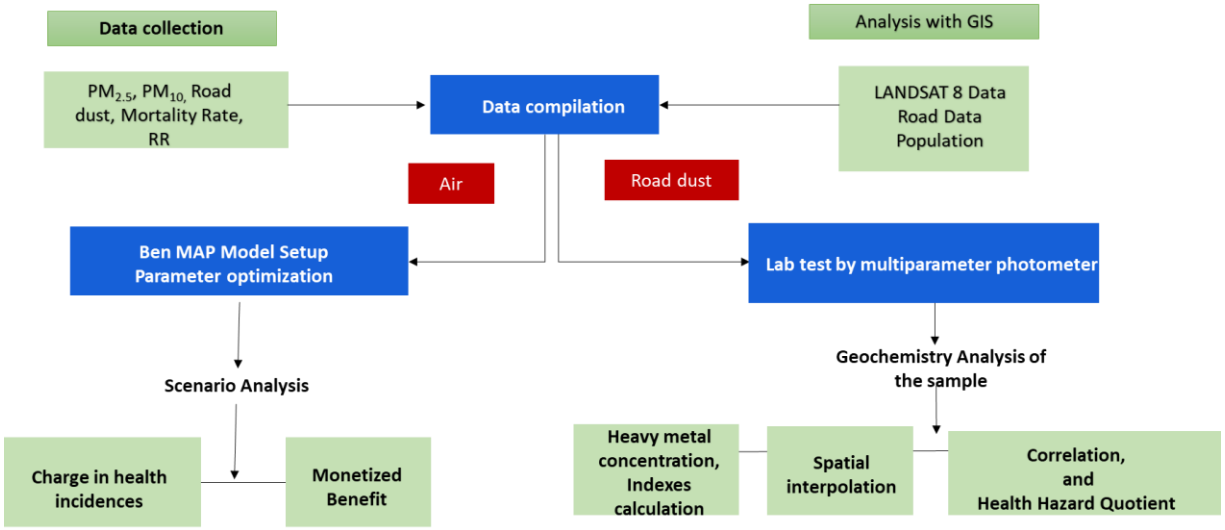

Fig. 3.7 Road map of the study

The findings of this study hold significant potential for guiding the development of effective strategies to enhance air quality monitoring, improve air quality (particularly concerning $PM_{2.5}$ and PM_{10}), and ultimately enhance the overall well-being of the population.

Chapter 4. RESULTS and DISCUSSIONS

4.1 Introduction

The presentation, analysis, and interpretation of findings from diverse data sources and how they relate to one another are covered in detail in this chapter. The present study initiated the research procedure by conducting an analysis of field particulate matter (PM) concentrations data and Landsat data in several locations within Chattogram City Corporation (CCC). The first things to identify correlations between Landsat band values and particulate matter (PM) levels at designated monitoring sites in order to establish feasibility of prediction models. The model with the highest level of precision was determined by conducting an extensive review process, which included evaluating these models by testing them with data from a different year but within the same geographical region. This model demonstrates the regional distribution and temporal variability of PM concentrations inside the CCC metropolis. Moreover, the chapter extensively examines the existence of six heavy metals traces inside the dust, providing comprehensive information on their degrees of contamination, accomplishing health risk evaluations, and performing correlation analyses with the particulate matter. The study utilized the BenMAP-CE model to assesses the health consequences associated with particulate matter, encompassing both the enduring impacts on mortality and morbidity. The text culminates in an economic evaluation of various policy ideas and their potential effects. The findings aid in assessing the impact of air pollution on human health and overall welfare.

4.2 Air quality assessment

4.2.1 Development of the empirical model and accuracy assessment

The outcomes of the formulated regression models are elucidated in annex Table A.6, revealing the predictive efficacy of diverse regression models in estimating variations in air pollutants with respect to geographical locations. It is noteworthy that the first model, which combines bands 1, 2, and 4, showed the best match for predicting $PM_{2.5}$ concentrations. This model demonstrated a strong linear connection between predicted and observed $PM_{2.5}$ values, with an R-squared (R^2) value of 0.654. This finding suggests that the proposed model has the potential to account for approximately 65.4% of the observed fluctuations in $PM_{2.5}$ concentrations. The model's individual variables also showed notable p-values, highlighting their close relationship to $PM_{2.5}$ concentrations. The second model, which combines bands 1, 2, and 3, on the other hand, showed the best fit for predicting PM_{10} concentrations, with an R^2 value of 0.516. The atmospheric reflectance data were taken from Landsat OLI and TIRS satellite photos captured in December 2022, together with associated ground truth data, to validate the model. Furthermore, five years' worth of air particulate concentrations were produced using the established regression algorithms. In contrast to other places, concentrations around industrial and urban areas typically showed greater values. These results highlight the regression models' effectiveness in identifying spatial trends of air quality over time.

By incorporating atmospheric reflectance data collected from Landsat imagery, the multivariate regression models described by Eq. A.1 and A.2 provided in annex, this study able to forecast ground-level concentrations of $PM_{2.5}$ and PM_{10}.

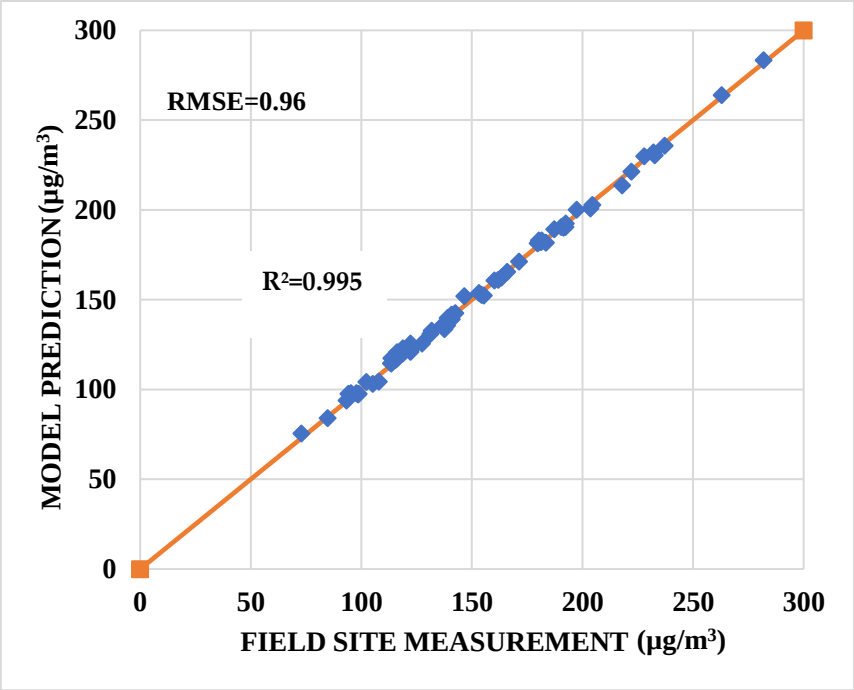

Fig. 4.1 Predicted versus field measured $PM_{2.5}$ concentration data over different sampling sites

The model was initially developed using Landsat 8 satellite imagery having a resolution of about 30 meters, comprised of daily 24-hour average data of Chattogram City Corporation Area from November to December 2021. Subsequently, its performance was assessed using ground data with different dataset of Landsat 8 imagery for the period of November to December in 2022. Fig. 4.1 and 4.2 show the relationship between computed $PM_{2.5}$ and PM_{10} 24h-average values determined from satellite-derived estimates and the observed measured quantities in CCC area.

Furthermore, the root mean square error (RMSE) values were calculated in order to measure the forecasts' level of accuracy. The RMSE for $PM_{2.5}$ was calculated to be 0.96, and the RMSE for PM_{10} to be 0.892. These RMSE values demonstrate that the model performed well in estimating both $PM_{2.5}$ and PM_{10} concentrations, indicating that its predictions were generally accurate. The root mean square

error (RMSE), which can be used to evaluate models, is regarded as good when it is within the range of 0.75 RMSE to 1 (D. N. Moriasi et al., 2007) .

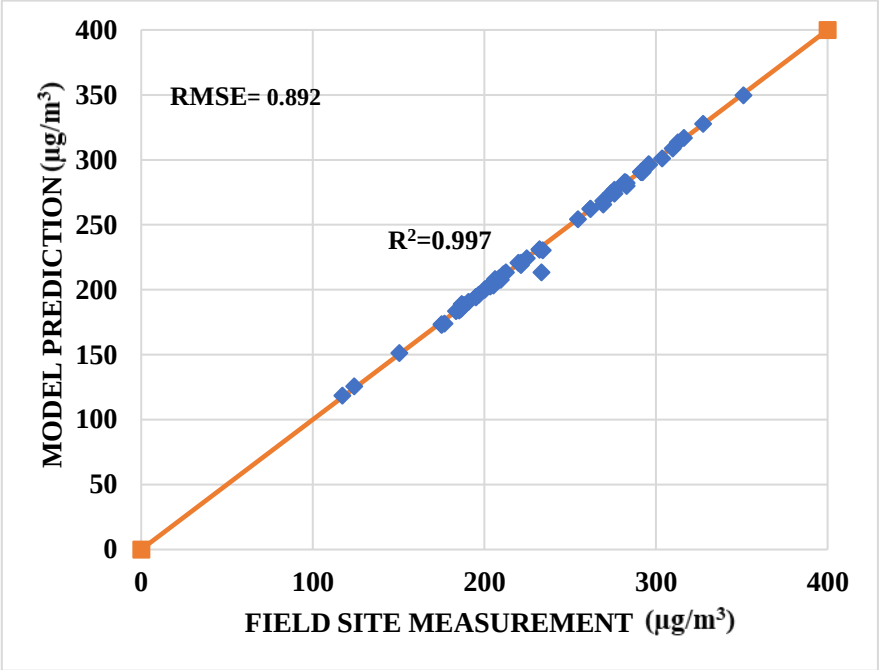

Fig. 4.2 Predicted versus field measured PM_{10} concentration data over different sampling sites

In comparison to the previous studies in China and India this study showed a satisfactory agreement though the geographic locations are different. Furthermore, RMSE and R^2 both values for $PM_{2.5}$ in this study are reported as 0.96 and 0.995 that are greater than China where a linear mixed effects model with a RMSE of 7.82 µg/m³ and R^2=0.80 has been developed that predict $PM_{2.5}$ concentrations in Fuzhou, China satisfactorily (L. Yang, 2020). As well as a statistical measure of R^2=0.9335 and RMSE =20.97 µg/m³ were obtained from the successful estimation of $PM_{2.5}$ concentrations over Delhi, India, using Landsat 8 OLI images considering the meteorological parameters constant (Mishra et al., 2021). The observed variations in these results can be attributed to the differences in geographical factors, land use patterns, meteorological conditions, and the local road traffic environment between the study areas. These factors can significantly influence the dispersion and concentration of air pollutants, thereby

affecting the accuracy of predictive models. Despite these variations, the current study's higher RMSE and R^2 values suggest a strong performance of the developed model in predicting $PM_{2.5}$ concentrations in the specific context of Chattogram City.

Similar patterns and observations are also found for PM_{10}. In this case R^2 and RMSE values are found 0.9997 and 0.892 respectively that are comparable with the studies conducted in Spain and Ecuador (Alvarez-Mendoza et al., 2019). In the Ecuadorian study, a selected model achieved an RMSE of 6.22 and R^2 of 0.68, allowing for the generation of PM_{10} concentration maps from publicly available remote sensing data. Similarly, the model selected in Spain had an R^2 and RMSE of about 0.94 and 0.2529 respectively (Fernández-Pacheco et al., 2018). These data are comparable with the study and the differences are obvious due to the geographical variations.

In conclusion, it has been shown that multivariate regression models using atmospheric reflectance data from Landsat have the ability to estimate ground-level $PM_{2.5}$ and PM_{10} concentrations. The model's successful application to satellite imagery from various years, together with the approach's efficacy and the relatively low RMSE values, confirms the accuracy of the forecast.

4.2.2 Spatio-temporal variation of $PM_{2.5}$ and PM_{10} concentration

Temporal variation

The descriptive statistics of $PM_{2.5}$ and PM_{10} concentrations obtained from the Landsat 8 Imagery for the years 2017-2022 are illustrated in Fig. 4.3 and 4.4 respectively. The maximum and minimum data are also aligned with the data of CAMS-6 and CAMS-7 *(DoE*, 2019). Both $PM_{2.5}$ and PM_{10} exhibit similar trends, with the year 2021 recording the highest maximum PM concentration. Notably, the PM concentrations for the consecutive five-year period from 2017 to 2022

surpass the limits set by both the Bangladesh National Ambient Air Quality Standards (BNAAQS) and the World Health Organization (WHO). Also, the distributions of the PM concentration datasets across these five years exhibit variations, displaying non-linear trends and skewed distributions.

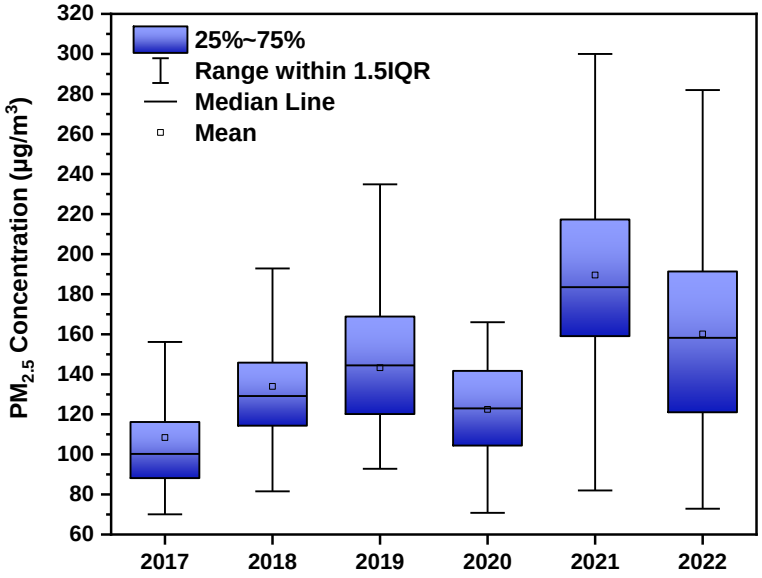

Fig. 4.3 Box plot showing temporal trends along with basic statistics of $PM_{2.5}$ from 2017-2022

The PM concentrations are found as high as 5 to 13 times for $PM_{2.5}$ and 3.5 to 10 times for PM_{10} in comparison to BNAAQS 24-hour threshold values (65 µg/m³ for $PM_{2.5}$ and 150 µg/m³ for PM_{10}) and WHO (25 µg/m³ for PM $_{2.5}$ and 50 µg/m³ for PM_{10} respectively indicating dusty situation that is linked to associated health hazard. The results found in this study was like a study focused on Chittagong City, where the maximum concentration was 254.9 µg/m³ in December and the lowest concentration, 57 µg/m³, in July of 2008 (Rouf et al., 2012a). Also, the peak values found for $PM_{2.5}$ and PM_{10} were 321 µg/m³ and 474 µg/m³, respectively during January 2013 conducted by a survey in Chittagong City which is consistent with our study as well (Hossen et al., 2018). In 2020, the model predicted a highest value of 175 µg/m³ and 300 µg/m³ of $PM_{2.5}$ and PM_{10}, respectively, in this study which seemed to have a good agreement with the

study carried out in Chittagong City during the covid lockdown period where the value of $PM_{2.5}$ and PM_{10} are found to decrease significantly and show a peak value of 177.95 μg/m³ and 289 μg/m³, respectively, in Chittagong City (Masum and Pal, 2020).

In Fig. 4.3 and 4.4 respectively, between 2017 and 2022, the average PM_{10} concentrations were 181, 188, 218, 192, 314, and 246 μg/m³, while the average $PM_{2.5}$ concentrations were 108, 134, 143, 123, 190, and 160 μg/m³, respectively. With the greatest PM_{10} concentrations, ranging from 123 μg/m³ to 463 μg/m³, and $PM_{2.5}$ concentrations, ranging from 82 μg/m³ to 339 μg/m³; the year 2021 stands out highest among these years. In the study carried out in Chittagong City in 2018, the PM_{10} and $PM_{2.5}$ concentrations exhibited a peak value of 210 μg/m³ and 280 μg/m³ in January and the lowest value was recorded in July (Hoque et al., 2022a). The value observed during the dry period is comparable with this study.

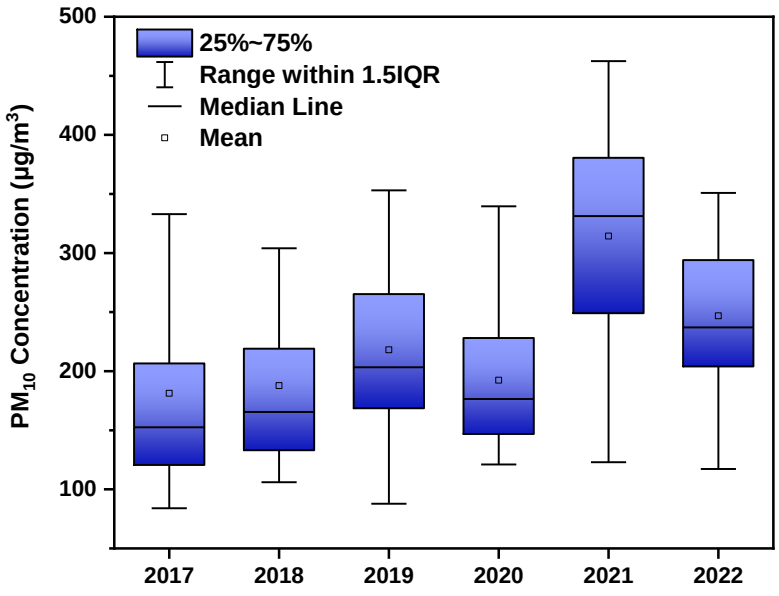

Fig. 4.4 Box plot showing temporal trends along with basic statistics of PM_{10} from 2017-2022

The temporal trend in Fig. 4.3 and 4.4 revealed an increase in the concentration of both $PM_{2.5}$ and PM_{10} from 2017 to 2019, followed by a slight decrease in 2020.

There showed a noticeable peak in 2021, after which the concentrations experience another moderate decline in 2022. The rise in particulate matter levels can be attributed to a combination of factors, primarily the prolonged absence of precipitation during this period, ongoing road construction and excavation activities, and pollution from numerous moderate and large industries, as well as emissions from unfit vehicles and the burning of garbage (Rouf et al., 2012a). The year 2020 stood out as distinct from the other five years due to the widespread shutdowns and disruptions caused by the COVID-19 pandemic. However, it is crucial to emphasize that despite the decline observed in 2020, it remains noteworthy that the monitoring sites exceeded the 24-hour average and annual mean thresholds for PM concentration. The enhancement in air quality in 2022 was evident throughout Bangladesh, and this positive trend was facilitated by favorable weather conditions and a growing public awareness about the importance of embracing environmentally friendly practices such as reducing deforestations, improvement in the waste collection methods and expanding the use of public transportation system ('Dhaka Tribune', 2023).

Spatial variation of PM along the sampling sites

The monitoring sites consistently displayed poor air quality about PM concentration, as depicted in Fig. 4.5 and 4.6. The collected data from these monitoring sites, during November-December month of the year 2021-2022, revealed elevated PM values attributed to anthropogenic degradation of air quality. An interesting observation was the impact of COVID-19 restrictions, which led to reduced pollution levels in the year 2020 due to decreased activities. As depicted in Fig. 4.5, the monitoring sites primarily located at the intersections of different types of vehicles, such as 2NO. Gate, A.K.Khan, Agrabad, Bohoddarhat, Chawkbazar, Dewanhat, GEC Circle, Hatazhari Bus Station, Holy Crisent, Jamal khan, Jamuna Square, Kalamia Bazar, Laldighi Mosque, Lalkhan

Bazar, Shah Amanot Bridge Circle, Shersha Bus Stop, Wasa Circle, and Wirless, junctions recorded levels of $PM_{2.5}$ and PM_{10} ranging from 105 μg/m^3 to 232 μg/m^3 in the year 2022.These levels are approximately 8 to 12 times higher than the 24-hour average recommended by the World Health Organization. The field survey carried out in GEC Circle, Chattogram exhibited the highest concentration of particulate matter, measuring at 398 μg/m^3 (Hossen et al., 2018).

Additionally, elevated levels of particulate matter were consistently observed in densely populated areas of Chittagong City, such as Sholashar and GEC Cirlce, 2NO. Gate junction. Since these areas lack industrial activity, the primary source of pollution is likely to be vehicular traffic, which can contribute to elevated pollution levels.

The spatial trend, akin to the temporal pattern, displayed an upward trajectory from 2017 to 2019, followed by a decrease in 2020. Subsequently, it exhibited an increase, culminating in its peak in 2021, with a slight decline in 2022.Nonetheless, specific sites, including junctions of Jamuna Square, Rubi Gate, and Steelmill Khalpar, deviated from this trend, showing higher levels of air pollutants. In 2022, compared to 2021, PM_{10} levels were notably elevated at Jamuna Square, Rubi Gate, and Steelmill Khalpar, while $PM_{2.5}$ concentrations were higher at junctions of 2NO. Gate, A.K.Khan, Agrabad, Bohoddarhat, Dewanhat, and GEC Circle. However, despite the reduction in 2020 it is noteworthy that, the 24-hour average and annual mean limits for PM concentration were exceeded than WHO and BNAAQS threshold values at all monitoring sites.

In Fig. 4.5, the industrial locations, namely CEPZ, Katghar, Salt Gola Crossing, Steel Mill Khalphar, Technical Circle, and Textile, had a consistent temporal pattern, with the exception of CEPZ, which recorded the highest value of 237 μg/m^3 in 2022. Also, it is noteworthy to mention that recreational destinations

such as Foyslake trend, seeing a peak in the year 2022. Conversely, Patenga Sea beach site adhered to the anticipated pattern. The rise in population might result in heightened automotive traffic, construction, and other human activities that have an impact on air quality.

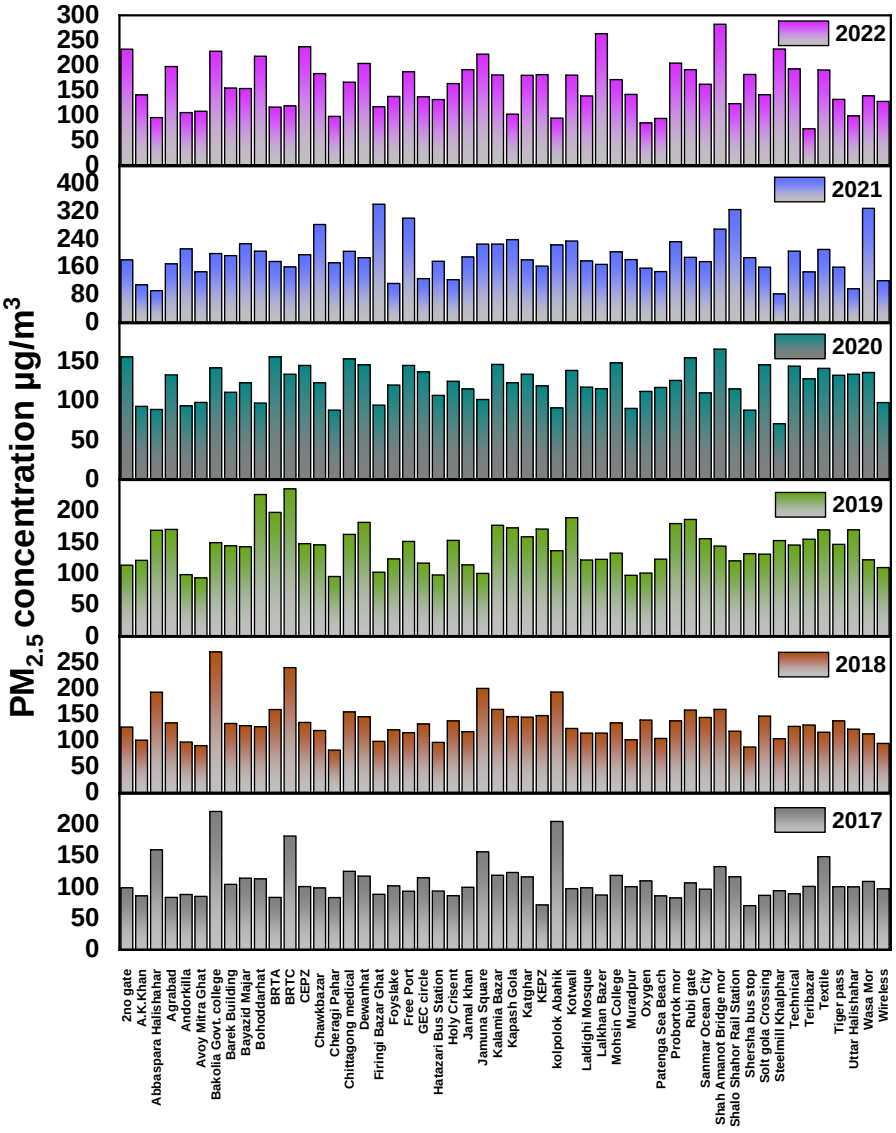

Fig. 4.5 $PM_{2.5}$ concentration of each site from 2017-2022

Based on the analysis of Fig. 4.5 and 4.6, it can be observed that Kolpolok Abashik, among the residential intersections of Uttar Halishahar, Muradpur, Lalkhan Bazar, and Kotowali, exhibited the highest level of pollution. Also, it has

been observed that sites such as Uttar Halishahar have exhibited an increasing trend in air quality throughout the years 2021 and 2022, as compared to the previous four years and these might be due to the ongoing development projects and constructional activities.

The chronological pattern seen in commercial sites, namely Agrabad, Andarkilla, Bayzid, Cheragi Pahar, Holy Crescent, Laldighi Mosque, Probortok Circle, and Wireless, is consistent through the six years as depicted in Fig. 4.5 and 4.6. Fig. 4.6 illustrates the Chittagong Medical College Site, which deviates from the overall trend by exhibiting a peak value in the year 2022. The values obtained in this study exhibit similarities to those reported in previous studies like the highest alarming concentration of PM_{10} was reported as 545 $\mu g/m^3$ in January 2007 (Rouf et al., 2012b) and also have similar ranges of value with another study conducted in CCC (Hoque et al., 2022b).

The areas exhibiting the highest PM levels remained relatively consistent over the years, with a notable exception in 2020 and also observed in other study (Masum and Pal, 2020). The spatial heterogeneity in air quality might be ascribed to the presence of diverse developmental endeavors as well meteorological phenomena in particular geographical areas. Unplanned development projects and haphazard infrastructure construction often result in heightened pollution concentrations. These activities have an impact on air quality, both in terms of space and time. The observation of the localized influence of development projects on air quality is a widely recognized phenomenon, highlighting the significance of including environmental considerations into urban planning and infrastructure development.

Also, the critical pollutant is $PM_{2.5}$ for which the average AQI values varies from 230 to 364 for the time frame 2017 to 2022 which indicates very unhealthy to

hazardous, and the severity group is elderly people and child with respiratory and heart diseases. Moreover, the pollutant PM_{10} have index greater than 100.

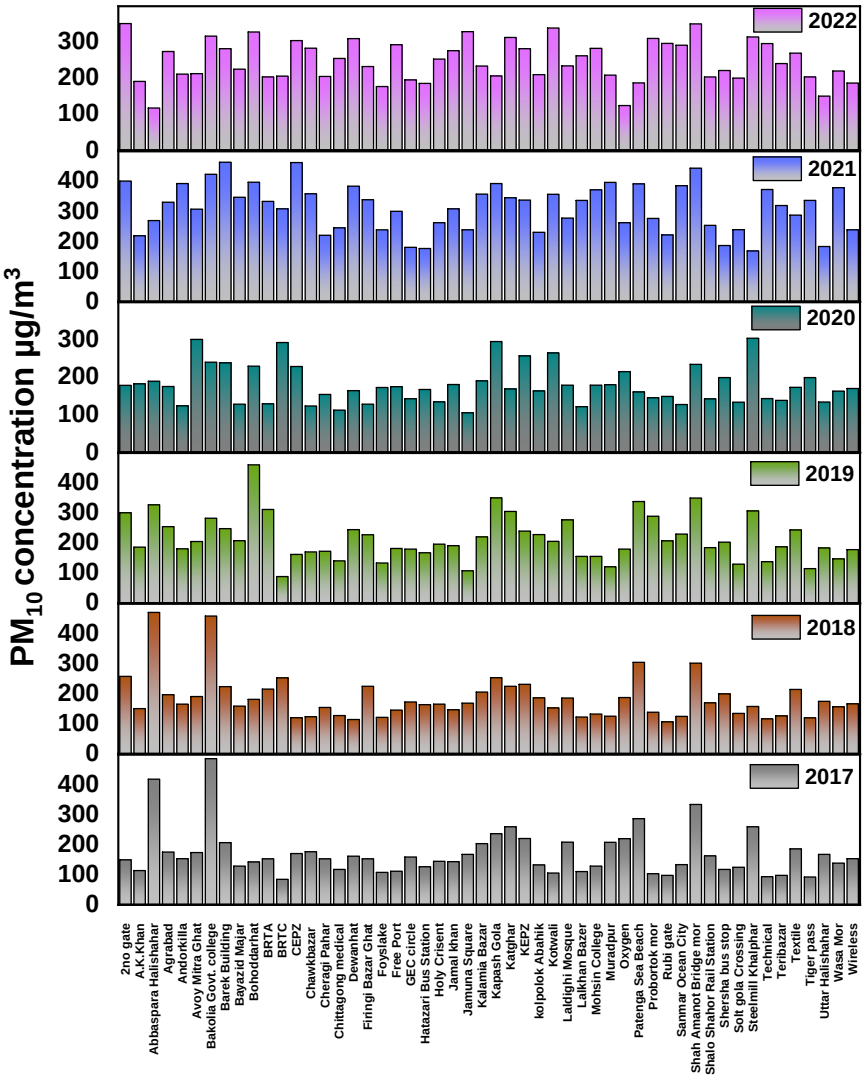

Fig. 4.6 PM_{10} concentration of each site from 2017-2022

The study's results offer valuable insights into the frequency of daily air pollution, particularly in areas with heavy truck and lorry traffic, which is primarily linked to the transportation of goods from the seaport to different regions across the country. The existence of traffic congestion and the difficult hilly terrain have a notable impact on the movement of passenger vehicles,

especially a substantial fleet of autorickshaws powered by three-stroke engines (Rouf et al., 2012b). This situation leads to a disorderly situation on the road network. The overall air quality in Chattogram is adversely affected by emissions from many businesses, including the steel, cement, and brick sectors, as well as kilns (Rouf et al., 2012b). These emissions contribute to the pollution levels in the immediate vicinity. Moreover, the conventional technique of manually sweeping roadways contributes to the release of even finer particulate matter into the sky. In periods of arid climatic conditions, unregulated urban development and maintenance activities have the potential to substantially contribute to particulate matter levels within the city. It is noteworthy to observe that during the period of the COVID-19 shutdown, there was a reversal in the prevailing circumstances, characterized by reduced traffic and business closures. Consequently, this led to a significant decrease in air pollutants resulting from lower anthropogenic inputs. The current period of lockdown serves as a poignant reminder for policymakers to consider the sometimes-neglected trade-off between tangible advantages for air quality and ongoing development objectives.

4.3 Traces of heavy metal in road dust on the selected sites

The presence of traces of heavy metal in the road dust depicted in Fig. 4.7, often in the form of suspended fractionated particles, considered in this study as captured particulate matter, which is easily inhaled, can be ingested through food from the vicinity of road environments, and has the potential to come into contact with the skin, remains inadequately recognized. This applies to individuals of various age groups and in different geographic locations with varying stratifications of air pollution content. Furthermore, it is important to note that there is a dearth of extensive scholarly investigation about the potential health risks linked to trace metals found in particulate matter air pollution. As a result, it is imperative to do further research in order to gain a more

comprehensive understanding of this topic, as elucidated in the subsequent section. Fig. 4.7 presents a box plot that visually represents the spectrum of heavy metal concentrations (expressed in mg/kg) found in airborne dust samples collected throughout the CCC region.

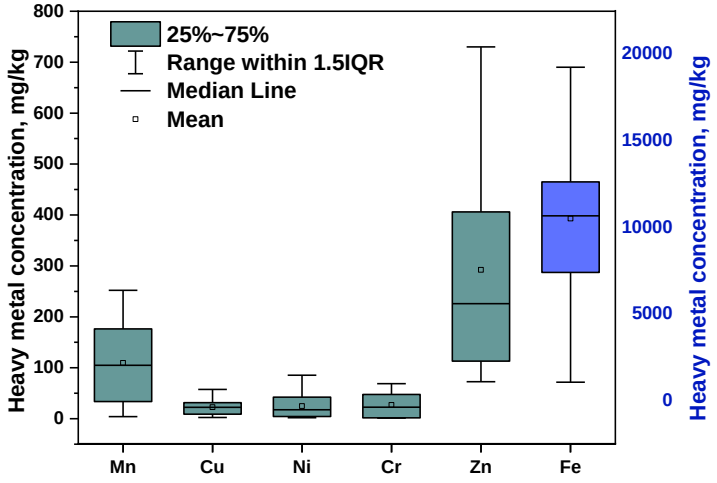

Fig. 4.7 Box Plot of heavy metal concentrations in air particulates

N.B. (Left Y axis represent Heavy Metal Concentration (mg/kg) for Mn, Cu, Ni, Cr, Zn and Right Y axis represent Heavy Metal Concentration (mg/kg) for Fe)

The heavy metals analyzed include manganese (Mn), copper (Cu), nickel (Ni), chromium (Cr), zinc (Zn), and iron (Fe). The concentrations of the heavy metals in the samples show varied degrees of dispersion and central tendency.

In particular, Ni has the lowest minimum value (1.14 mg/kg) and Fe has the highest maximum value (19,240 mg/kg), showing a wide range of values. Similar to this, the Fig. 4.7 shows that Mn, Zn, and Fe have a wider range of data than other metals. The mean concentration of Mn, Cu, Ni. Cr, Zn, and Fe are 109.53, 22.7, 24.8, 27.08, 292 and 10506 mg/kg. Ni have the lowest minimum value of 1.14 mg/kg whereas Fe has the highest maximum value of 19240 mg/kg.

From the literature review, the shale value of Mn, Cu, Ni, Cr, Zn, Fe is 850, 45, 68, 90, 160 and 47200 mg/kg respectively (TUREKIAN and WEDEPOHL, 1961). The

background value of Mn, Cu, Ni, Cr, Zn, and Fe 555, 8, 32, 61, 53, and 20696 mg/kg respectively adopted from a study (Halim et al., 2005). The investigation reveals that, while the average amounts of heavy metals typically remain below their corresponding shale values, some locations display heightened concentrations of metals like manganese (Mn), zinc (Zn), nickel (Ni), and copper (Cu). This observation implies the probable presence of pollutants in road dust, which may be linked to industrial operations and the release of emissions from vehicles. When comparing the concentrations of heavy metals in CCC with those in other countries such as Saudi Arabia, Ghana, Iran, and Malaysia, it becomes evident that some heavy metal pollution levels in CCC are higher, potentially due to local sources of pollution (Faiz et al., 2012; Han et al., 2017; Idris et al., 2020; Ite et al., 2014; Kamani et al., 2017; Ma et al., 2016; Proshad et al., 2023).

The spatial variability of these heavy metal concentrations is depicted in the Fig. 4.8. The spatial distribution of heavy metals, including Mn, Zn, Ni, Fe, Cr, and Cu, serves as an indicator of possible contamination in road dust. This contamination can be attributed to several sources such as industrial activity, market activities, unsanitary living conditions, inadequate waste disposal practices, and emissions from vehicles. The analysis of their concentrations indicated that their levels were seen to be elevated in locations such as EPZ and Bayzid (W-2 and W-41 and W-40), which are renowned for their industrial operations, as well as in commercial zones like Halishahar (W-39). Additionally, W-2 region boasts a comprehensive transportation infrastructure that effectively links the city with other destinations. Moreover, it serves as a hub for numerous markets.

Furthermore, it was observed that there were increased concentrations of chromium (Cr), copper (Cu), manganese (Mn), and nickel (Ni) in multiple locations, particularly in areas such as North Kattali (W-10) that are known for

their high traffic volume and unregulated construction practices. The presence of Cu, Ni, Cr and Mn can be seen more in Jalalabad, and North Middle Halishahar (W-2, and W-37). These findings highlight the widespread distribution of these heavy metals, emphasizing their presence in regions with significant vehicular movement and ongoing construction, which are contributing factors to their accumulation. And the concentration of Zn and Fe was higher where there are more industrial, vehicle repairing and commercial hubs.

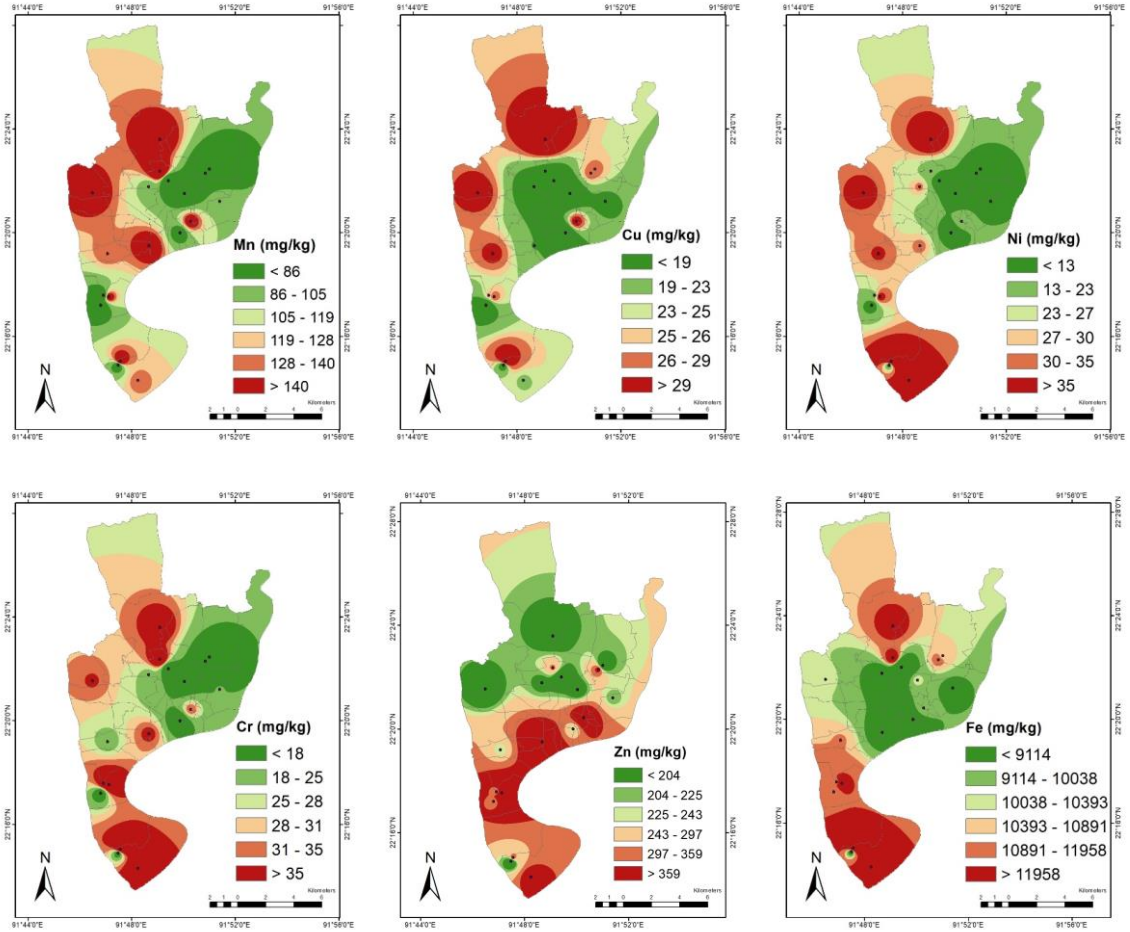

Fig. 4.8 Spatial patterns of concentration of studied metals in road dust in CCC area

Past studies show that the presence of heavy metals Mn, Ni have been associated with vehicle exhaust emissions, whereas, Cu, Fe and Cr may be caused by brake wear (Winther, 2010; Garg et al., 2000; Li et al., 2023). These results are consistent

with previous studies showing that local pollution sources, industrial activity, land use, and traffic emissions all affect heavy metal concentrations (Kader Newaz et al., 2020).

Heavy metals demonstrate a propensity to collect in regions defined by heightened pollution levels, particularly in industrial or commercial sectors. Furthermore, the Chattogram City Corporation (CCC) is faced with the issue of pollution due to the proliferation of a significant number of automobile repair shops and refueling stations. The area faces challenges related to pollution resulting from a combination of residential, manufacturing, and commercial operations, which collectively contribute to the worsening of environmental issues.

4.3.1 Contaminator factor and Degree of contamination

As detailed in section 2.3.2, the elevated levels of contamination factor associated with heavy metals of road dust may consequently present higher health risks to both humans and other living organisms (Ametepey et al., 2018; Kamran et al., 2013; Masindi and Muedi, 2018). This section of the results provides an overview of the contamination factor and the extent of contamination for the six specific heavy metals that were studied.

The contamination factor and degree of contamination for the 19 sites are illustrated in Fig. 4.9 and 4.10. The accompanying violin plot provides insight into the distribution of contamination for each metal. Concerning Mn, all sites exhibited contamination levels below a threshold, indicating low contamination. For Cu, three sites categorized as educational and recreational displayed contamination levels below 1, while others showed moderate contamination, except for EPZ, Halishahar, and Sagorika, which indicated moderate contamination. With respect to Ni, apart from VIP, Bayzid, and Port Road, all other sites displayed low contamination, while these three sites represented

moderate contamination. In the case of Cr, all sites depicted low contamination levels except for Port Link Road.

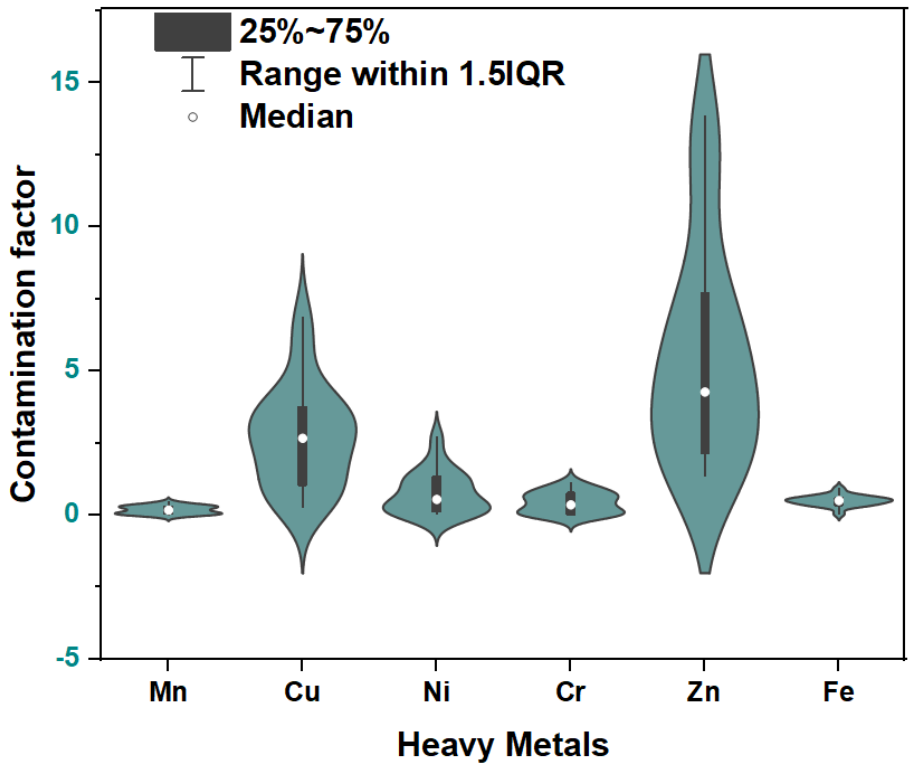

Fig. 4.9 Violin plot of distribution of contamination factor of heavy metals in road dust

Notably, Zn showed very high and considerable contamination levels for most sites. Locations like Shaloshahar, Port Road, Bay Shopping, Chadgaon, VIP, and Agraabad indicated high contamination, whereas others displayed considerable contamination. Lastly, Fe contamination level was very low across all sites.

The spatial variety of contamination levels is illustrated in Fig. 4.11 using an ArcGIS map. The contamination levels of the locations exhibit variability, whereas EPZ, Agarabad, VIP, Chadgaon, Bayzid, and Port Road demonstrate the highest values, which range from 12 to 24. In contrast, the remaining sites have pollution levels ranging from 6 to 12, suggesting a moderate degree of contamination.

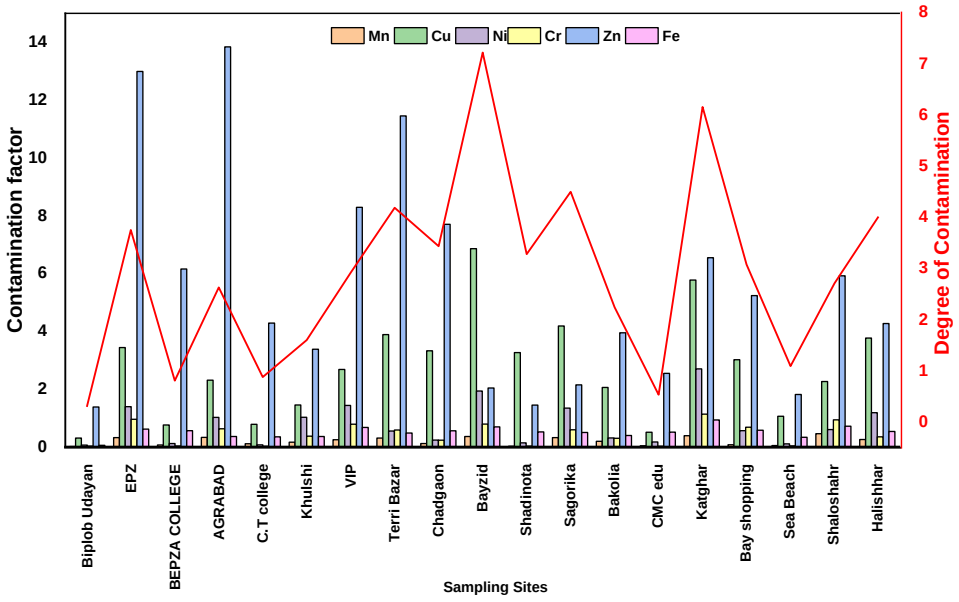

Fig. 4.10 Contamination factor and contamination degree of each sampling sites

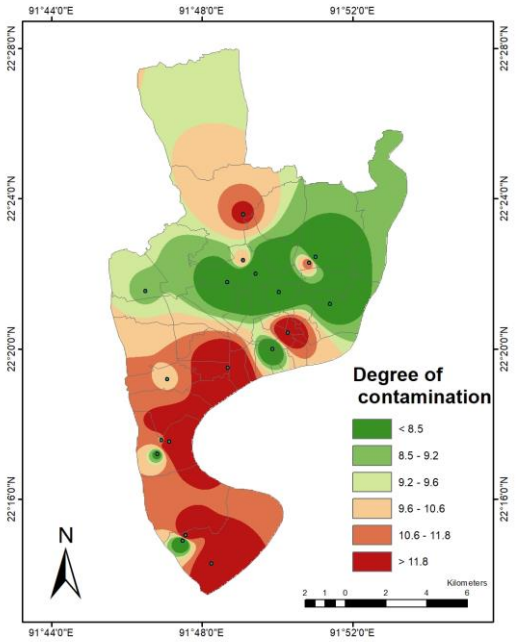

Fig. 4.11 GIS map representing spatial variability of Degree of Contamination.

The analysis of contamination levels indicated that each site fell within the range of 6 to 12 and 12 to 24, indicating a moderate to high degree of contamination at

these locations. The potential health hazards associated with these factors can be identified by a comprehensive health risk assessment.

Although these metals themselves do not directly pose any risk to health, the contamination levels of these metals may amplify the health risks associated with particulate matter. The findings indicate a significant presence of heavy metals in the airborne dust.

4.3.2 Correlation analysis

The correlations between different metals contained in road dust with particulate matter were examined using Pearson's correlation coefficient, as shown in Fig. 4.12. Pearson's correlation matrix was employed to identify the key characteristics that influence the movement and dispersion of metal contaminants within road dust. Analyzing metal interactions can also unveil the sources and pathways of metals in the (B. Song et al., 2018; Trujillo-González et al., 2016). To assess the correlations between the studied metals, Pearson's correlation coefficient (r) was calculated. Correlation coefficients ranging from 0.9 to 1 and 0.5 to 0.9 were classified as strongly and moderately correlated, respectively (Sojobi, 2016).

The relationships among the studied metals can provide valuable insights into the origins and pathways of these metals (Soltani et al., 2015). This investigation revealed several positive correlations between the studied metals, including Mn-Cu (0.65), Mn-Ni (0.73), Mn-Cr (0.86), Mn-Fe (0.58), Cu-Ni (0.78), Cu-Cr (0.68), Cu-Fe (0.67), Ni-Cr (0.82), Ni-Fe (0.66), and Cr-Fe (0.7). Also, a positive correlation was observed between PM_{10} and heavy metals except Fe. Certain notable positive relationships could be elucidated by the notion that enhancing specific road dust characteristics results in increased metal adsorption within the road dust, which, in turn, signifies shared pollution sources (Ramírez et al., 2020). The observed significant positive correlations among Mn, Cr, Ni, Fe, and Cu suggest that these

metals share common contamination sources primarily linked to industrial and traffic-related activities (X. Lu et al., 2009; Miguel et al., 1997; Rajaram et al., 2014).

Zn showed low to moderate associations, ranging from 0.15 to 0.47, with Cu, Fe, Ni, Cr, and Mn. Additionally, a negative correlation of about 0.019 $PM_{2.5}$-Cr, 0.0056 $PM_{2.5}$-Ni, 0.075 $PM_{2.5}$-Fe and 0.16 $PM_{2.5}$-Mn and a weak positive relationship between $PM_{2.5}$ and other heavy metals. However, a moderate relationship was found between $PM_{2.5}$ and PM_{10}.

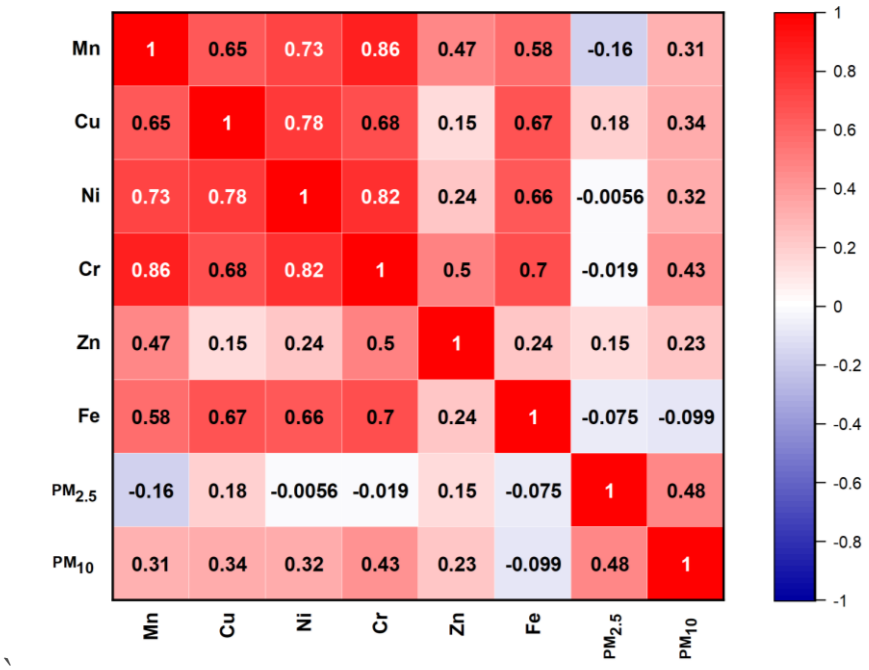

Fig. 4.12 Correlation plot among the studied trace metals in air

The observed negative association between $PM_{2.5}$ and heavy metals may be attributed to disparities in sources, atmospheric chemical reactions, deposition and removal methods, and fluctuations in the concentration of metals within $PM_{2.5}$. Nevertheless, it is imperative to acknowledge that this link in isolation does not offer a thorough evaluation of the related health hazards. The method of health risk assessment is of utmost importance as it evaluates the potential health hazards presented by these metallic substances. Undoubtedly, even in

cases where a robust association is lacking, the mere existence of minuscule quantities of heavy metals in the atmosphere has the potential to elicit health hazards, particularly when assessed in relation to the dosage or concentration of particulate matter.

The health hazards linked to the inhalation of airborne heavy metals are influenced by multiple factors, such as the specific types of metals, their toxicity levels, the duration and intensity of exposure, and the overall amount of particulate matter encountered. The strength of the association alone does not exclusively determine the related health concerns. Hence, it is imperative to carry out complete health risk assessments that consider all pertinent variables in order to achieve a comprehensive comprehension of the potential health risks linked to particulate matter and heavy metals present in the surroundings. Undoubtedly, even in cases where a robust association is lacking, the mere existence of minute quantities of heavy metals in the atmosphere has the potential to elicit health hazards, particularly when evaluated within the framework of particulate matter dosage or concentration.

4.4 Health risk assessment for exposure to heavy metal

The potential health implications for persons residing in close vicinity are severe due to the existence of traces of heavy metals in particulate matter. Consequently, the existence of dust contaminated with heavy metals gives rise to apprehension among the inhabitants in the area. It is noteworthy to mention that the concentrations of the heavy metals under investigation, namely Zn, Fe, Cr, Mn, Cu, and Ni, in the collected dust samples surpassed the background values (Halim et al., 2005). This finding implies a heightened susceptibility to health-related complications among persons who have been exposed to heightened concentrations of heavy metals.

4.4.1 Non-Cancerous risk assessment

The potential adverse effects of heavy metal contamination in the atmosphere can significantly increase the risks associated with both carcinogenic and non-carcinogenic health outcomes.(Peled, 2011). Heavy metals like Fe, Cr, Ni, Cu, Mn, and Zn, even at low levels of exposure, can exhibit high toxicity (Nirmalkar et al., 2021). Urban areas with significant vehicular traffic have reported associations between metals such as Cu, Ni, and Fe with the onset of respiratory and cardiovascular diseases (Kastury et al., 2018; Moryani et al., 2020). Despite Cr and Mn being considered essential elements, high concentrations of exposure to these metals can also lead to toxic effects in humans (Zheng et al., 2016).

Table 4.1. Non-Carcinogenic health risks for adult

Group	Adult					
	Mn	Cu	Ni	Cr	Zn	Fe
Ingestion $*10^{-3}$	6.52	1.56	3.40	24.7	2.67	41
Inhalation$*10^{-3}$	1.54		0.00192	0.00191	0.00196	30
Dermal$*10^{-3}$	0.0015	0.00104	0.00251	0.00247	0.00266	82
HI	0.008	0.0015	0.003	0.02	0.002	0.15
Σ HI			0.19			

The hazard quotients (HQ) estimated for dust samples from various sites via ingestion, cutaneous contact, and inhalation are shown in Table 4.1.and 4.2. The pattern of HQ values shows that ingestion was the main way that people were exposed to these heavy metals in humans: $HQ_{ingestion} > HQ_{dermal} > HQ_{inhalation}$. Notably, HQ values for kids were higher than for adults, which is consistent with findings from other study (Chonokhuu et al., 2019; Gbadamosi et al., 2018; Rastegari Mehr et al., 2017).

According to the assessment of the impact of various metals to non-carcinogenic risk (HQ) presented in Table 4.1 and 4.2, for both adults and children, Fe > Cr > Mn > Ni> Zn > Cu. Individual metal concentrations in the air, however, did not

provide a threat to the environment's health (Kacholi and Sahu, 2018). Except for Fe in case of child as depicted in Table 4.2, the Hazard Index (HI) values were typically below the safe threshold (HI <1). This shows that both children's and adults' heavy metal in dust samples did not include unusually high levels of non-carcinogenic hazards caused by these heavy metals.

Table 4.2. Non-Carcinogenic health risks for child

Group	Child					
Metals	Mn	Cu	Ni	Cr	Zn	Fe
Ingestion $*10^{-3}$	15	3.63	7.94	24.7	6.23	95
Inhalation$*10^{-3}$	0.0274		0.000341	0.0338	0.000348	58
Dermal$*10^{-3}$	0.000009	6.78	0.0165	16.2	0.00266	53
HI	0.0180	0.0037	0.0081	0.0412	0.00623	5.52185
Σ HI	5.59					

For Fe, cumulative HI values for child exceeded 1 for all three pathways, indicating a possible risk to human health. It's important to note that iron isn't regarded as having direct chemical toxicity in terms of harm to the environment. However, the geochemistry of other potentially harmful metals and the physical risk of depositing flocculent materials are also cited as reasons for its influence. Individuals are exposed to many heavy metals at once, making it more feasible to use integrated HI values to determine the true impact (Wahab et al., 2020). The elevated concentration of iron (Fe) is the primary factor contributing to the HI score beyond 1. As a result, children in the research area are more likely to experience non-cancerous consequences than adults are, especially in light of kids' propensity for hand-to-mouth behaviours (US EPA and Factors Program, 2011). This emphasises the possibility of chronic illnesses such headaches, nausea, and appetite loss among the inhabitants of the CCC region (Fonseca-Nunes et al., 2014; Wahab et al., 2020).

4.4.2 Cancerous risk assessment

The assessment of the impact of various metals to carcinogenic risk presented in Table 4.3, for both adults and children. The evaluation of carcinogenic risks (CR) related to nickel (Ni) encompassed many exposure paths, including ingestion, inhalation, and skin contact, whereas for chromium (Cr), only the ingestion route was considered presented in Table 4.3. Notable is the finding that the danger of cutaneous exposure to dust is 100 times lower than the risks of ingesting and inhalation (Grzetic and Ghariani, 2008). In order to calculate health risk, slope variables and soil exposures were used in the assessment as suggested in various studies elsewhere (Alfaro et al., 2015; Gbadamosi et al., 2018; Johnbull et al., 2018).

Table 4.3. Carcinogenic health risks for adult and child

Age Group	Adult		Child	
Metal	Cr	Ni	Cr	Ni
Ingestion	1.87E-15	8.58E-16	8.29E-16	3.80E-16
Inhalation		3.02E-11		4.95E-10
Dermal		6.25E-12		1.56E-12
Total Risk	1.87E-15	3.65E-11	8.29E-16	4.97E-10
Σ HI		5.3E-10		

According to Table 4.3 findings, Ni had considerably lower CR_{dermal} values in both adults and children, suggesting a lower overall carcinogenic risk (Baltas et al., 2020). The cancer risk (CR) values associated with the ingestion, inhalation, and cutaneous exposure routes, as well as the overall integrated CR value encompassing all carcinogenic metals, were found to be lower than the threshold of recognized risk tolerance ranging from 10^{-6} to 10^{-4} for both child and adult populations. It should be noted that metals including Fe, Mn, Cu, and Zn that are not considered human carcinogens were not included in CR analyses (Gbadamosi et al., 2018; Grzetic and Ghariani, 2008; Johnbull et al., 2018).

The research outcomes pertaining to potential carcinogenic hazards posed by heavy metal exposure in CCC region dust samples indicate that the related risks are negligible for both adult and child populations. While these metals might not present a significant direct health risk, even minimal exposure to them can be detrimental to human health, as previously discussed. Therefore, these metals, although not posing an immediate health risk based solely on their dosage, can still contribute to various health issues when in association with particulate matter. The assessment of premature cases of other health outcomes is conducted using the BenMAP-CE tool.

4.5 Health impact assessment using BenMAP-CE

4.5.1 Population exposure to $PM_{2.5}$ and PM_{10}

Temporal variation

Fig. 4.13 visually depicts the temporal distribution of population exposure to annual mean concentrations of $PM_{2.5}$ and PM_{10} from 2017 to 2022.

The data used in this analysis was obtained from population raster statistics provided by WorldPop. In the health impact assessment, two distinct age groups (25-99 and 5-17) were taken into account to assess various health outcomes. It's important to note that the age range of 5-17 demonstrated a lower proportion compared to the 25-99 age groups.

The year 2022 witnessed the recorded highest population density for the age group 25-99. The observed pattern in population exposure percentages to $PM_{2.5}$ and PM_{10} concentrations exhibits a consistent increase that can be likened to a geometric progression. Notably, in the year 2020, there was a decrease in exposure fractions among individuals aged 5-17. However, this trend was subsequently reversed in the following years, resulting in a future increase.

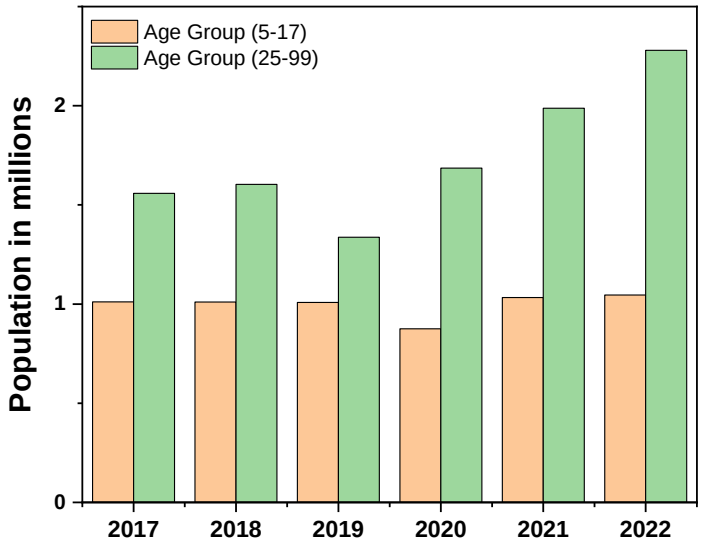

Fig. 4.13 Population distribution for age groups (5-17) and (25-99) over the study year

Spatial variability

The study employed the BenMAP-CE software to assess the correlation between the geographical distribution of the population and the extent of exposure across the 41 wards of CCC area. The objective was to ascertain whether the ward characterized by the largest population also had the highest degree of exposure. Furthermore, an assessment has been made to understand whether there was an upward trend in population growth inside the ward for exposure to air pollution.

It is anticipated that wards exhibiting a consistent upward trend in population growth will also demonstrate a corresponding increase in exposure levels. This alignment is expected because as the population grows, there is likely to be an influx of residents, leading to an increase in population exposure to air pollution. This observation aligns with findings from the literature review, further supporting the notion that population growth can influence exposure to environmental factors, including pollution (Ji et al., 2019).

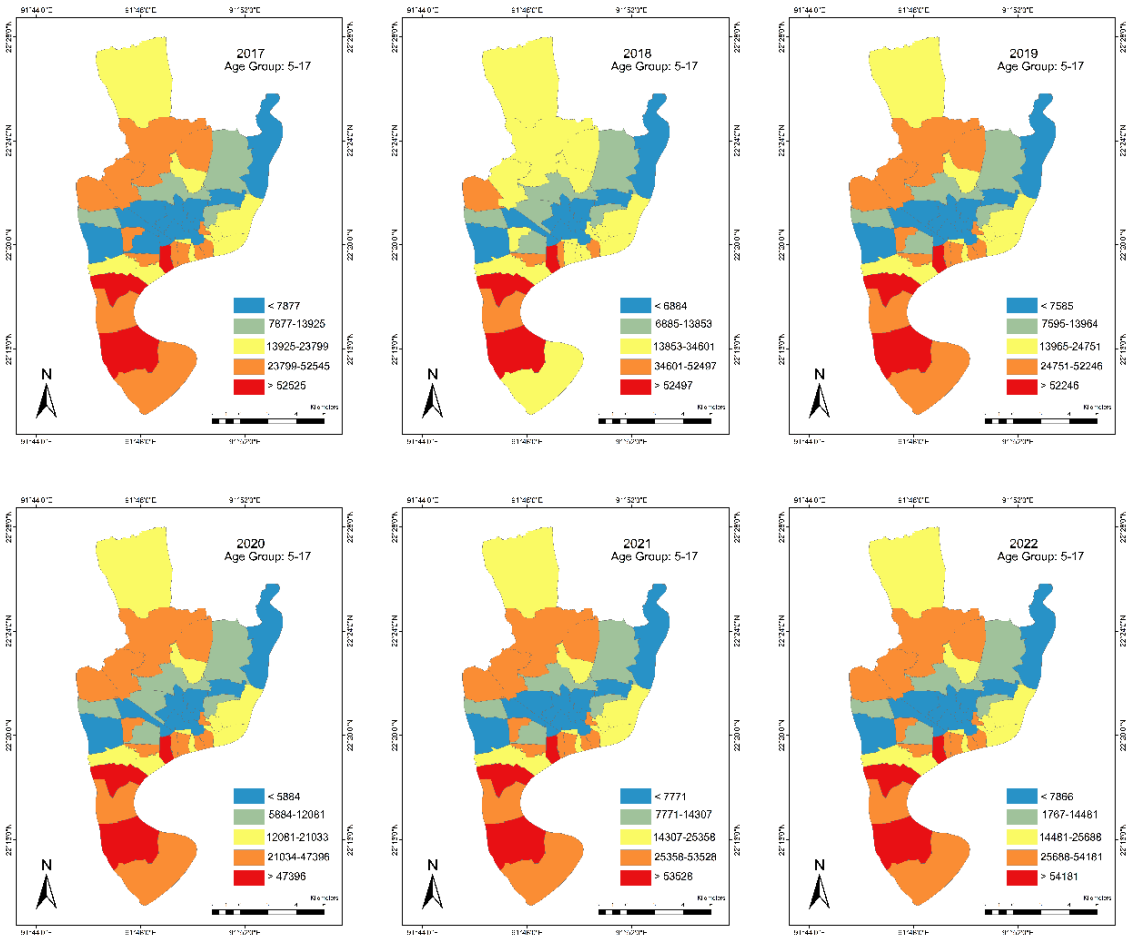

Fig. 4.14 Spatial variation of age group (5-17) for the consecutive 6 years

While there may be a few exceptional cases, a comprehensive examination of the spatial distribution of data at the ward level under the jurisdiction of the Chattogram City Corporation reveals a consistent exponential growth pattern in the majority of wards over a period of time. Ward No. 19, 22, 24, 27, 28, 30, 31, 35, 36, 38-41 in Fig. 4.14 particularly show an increased tendency from 2017 to 2019, with a little departure seen between 2019 and 2021, followed by another rise in 2022, when the age range of 25-99 is taken into account. The cumulative temporal picture was not changed by this departure, which is important.

It is worth noting that the age group between 5 and 17, as depicted in Fig. 4.14, did not exhibit the increased trend for the year 2020 as observed in preceding

years. In contrast, it was observed that all wards had diminished values in the year 2020, resulting in a reduced cumulative value compared to previous years.

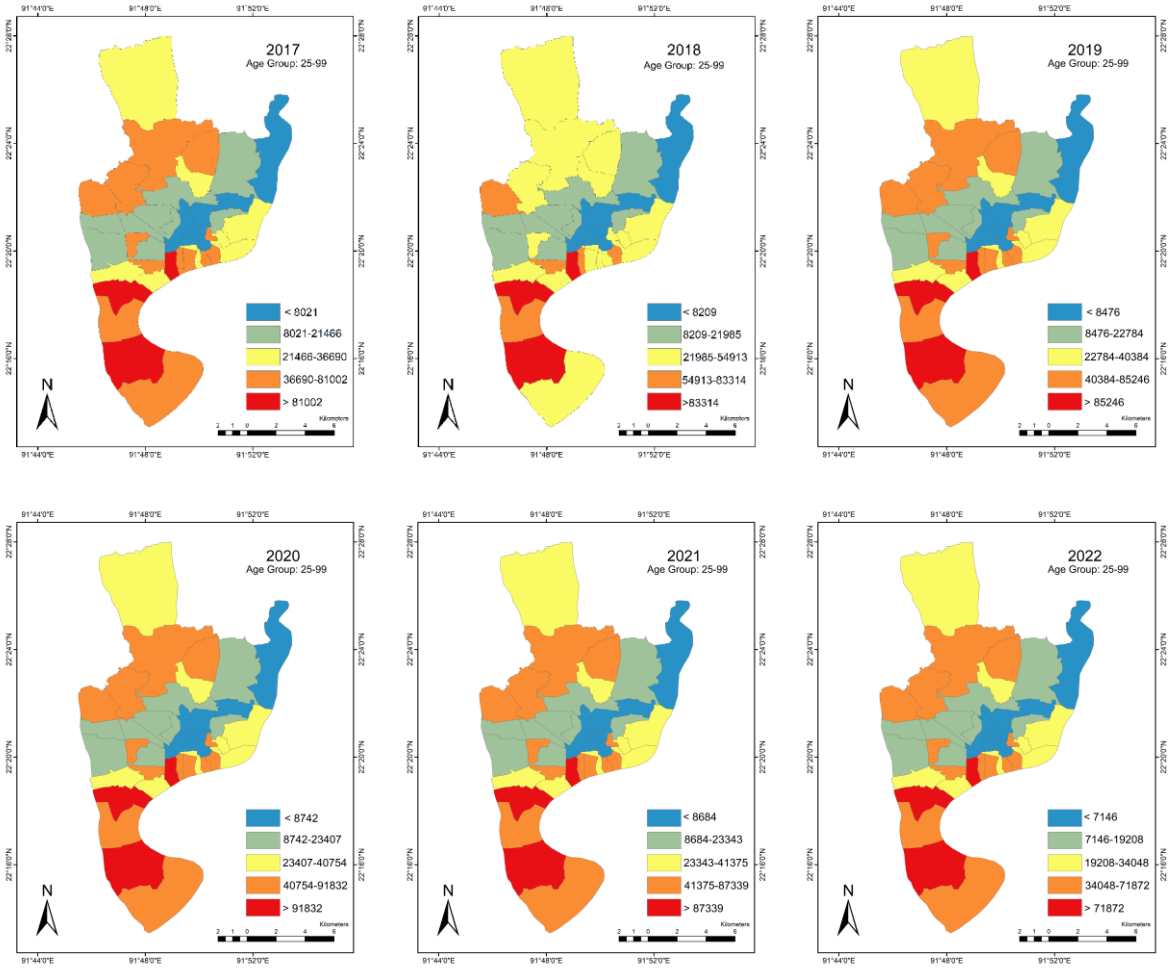

Fig. 4.15 Spatial variation of age group (25-99) for the consecutive 6 years

Figures 4.13 and 4.14 depict GIS maps illustrating the population density of the age ranges 25-99 and 5-17 by zone. Except for 2018, the others CCC maps showing the age range of 5 to 17 had consistent patterns in all wards. In contrast to previous years, the population ratio is unusually low in Wards No. 2, 3, and 9 in the year 2018. This finding holds true across both the distinct age groups, suggesting that in 2018, there was a deviation in the spatial distribution pattern, especially for the wards specified.

4.5.2 Simulated pollutant exposure level

The concentration maps for $PM_{2.5}$ and PM_{10} obtained by VNA method in BenMAP-CE are illustrated in Fig. 4.16 and 4.17, respectively.

These maps were generated using the Voronoi Neighbour Averaging (VNA) interpolation method, which was recommended in a prior study that the VNA method outperformed the Inverse Distance Weighting (IDW) and Ordinary Kriging (OK) methods, as assessed by (L. Chen, Shi, Li, Bai, et al., 2017) in their investigation conducted in China. Another study used the VNA method to obtain more precise results in Guangzhou, China (Ding et al., 2019b).

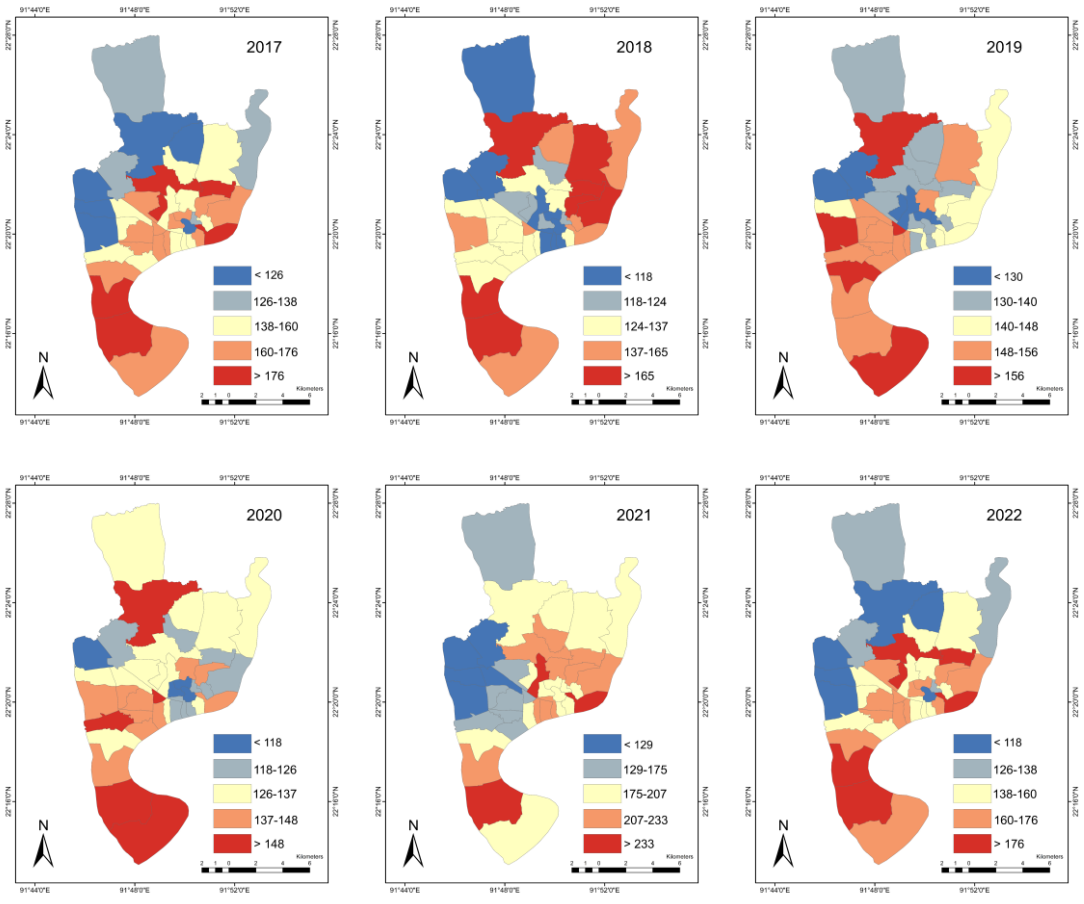

Fig. 4.16 Baseline $PM_{2.5}$ concentration level in CCC area (2017-2022)

The maps presented in Fig. 4.5 and 4.6 serve as the input data for the baseline exposure scenario within the BenMAP-CE software. These maps capture both regional and temporal variations spanning the period from 2017 to 2022. The exposure levels were calculated by combining model-generated data with observed measurements, and VNA interpolation was utilized to create gridded data that accurately represents air quality across the study area.

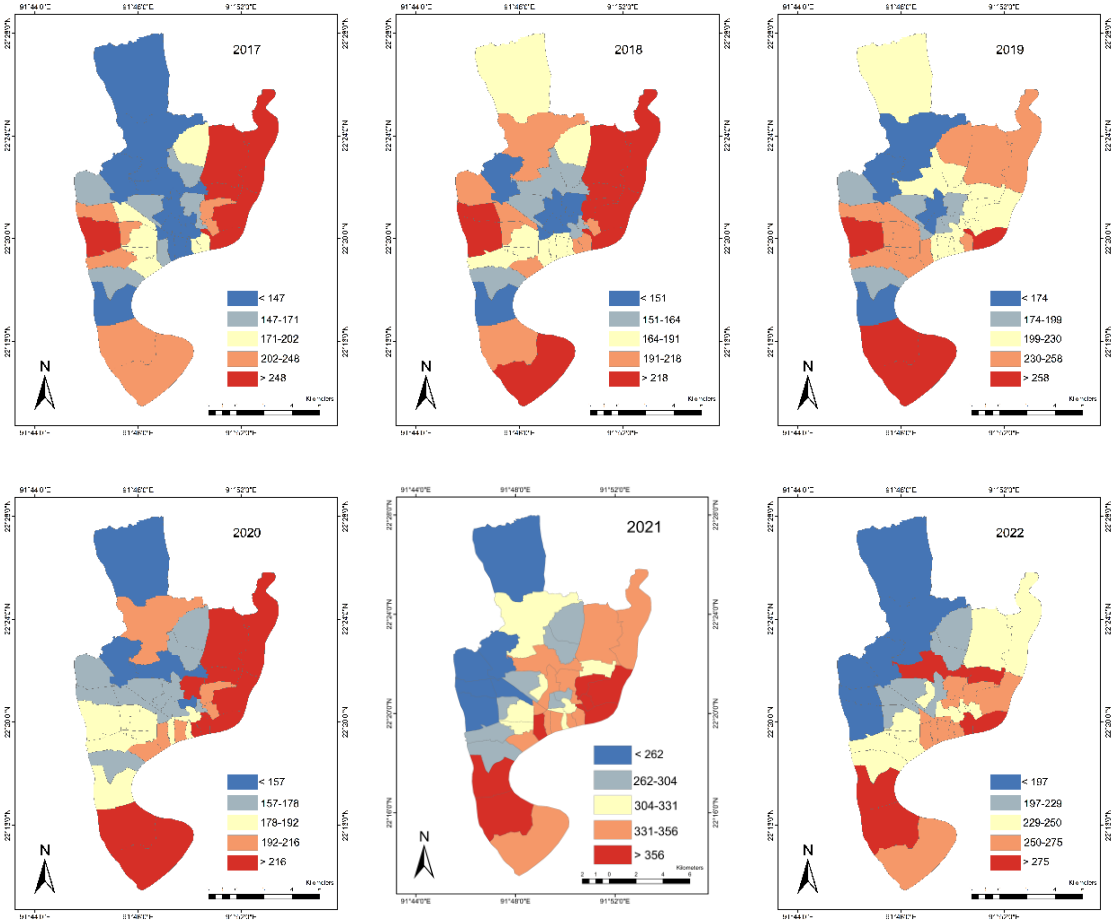

Fig. 4.17 Baseline PM_{10} concentration level in CCC area (2017-2022)

For $PM_{2.5}$ and PM_{10} control map scenarios was created by considering a hypothetical reduction of 10 μg/m^3 and 20 μg/m^3 respectively. This reduction was considered on the basis of WHO annual threshold values where comparison is

done using the 24-hour average monitored or modelled data to WHO annual value as also suggested in other studies (D. Kim et al., 2019; Maji, Ye, et al., 2018; Manojkumar and Srimuruganandam, 2021). Furthermore, the WHO reduction scenario is primarily considered because it is more stringent than the BNAAQS threshold value. However, in section 4.7, a comparison between WHO and BNAAQS simulations for the all-cause health endpoint is provided. This analysis helps quantify the potential health benefits associated with the improvement in air quality achieved by the reduction of $PM_{2.5}$ and PM_{10} levels.

After conducting a simulation of pollutant exposure and analysing the spatial distribution of the population, the BenMAP-CE software ultimately evaluates the premature health consequences of various health endpoints due to the decrease in particulate matter. The present evaluation integrates multiple variables, encompassing incidence and mortality rates and concentration response functions, in order to offer a thorough comprehension of the potential health advantages that may arise from the mitigation of particulate matter pollution.

4.5.3 Premature mortalities and morbidities attributable to pollutant and economic valuation

A thorough evaluation of the health effect assessment, which stems from the reduction in particulate matter, is presented in the subsequent section. The study primarily emphasizes the mortality rates linked to significant diseases connected with both $PM_{2.5}$ and PM_{10}. Following this, a comprehensive examination is undertaken to assess the Global Burden of Disease (GBD) associated with the five leading causes of death and Non-Communicable Diseases (NCD) in addition to Lower Respiratory Infections (LRI). Furthermore, morbidity cases are taken into account for both age cohorts. It is noteworthy to mention that mortality endpoints are not taken into consideration for the child group owing to their very low incidence rate and minimal exposure to ambient particulate matter. In

conclusion, the study culminates by conducting an analysis of fatalities that are ascribed to the exposure to particulate matter.

Temporal variation of avoided premature mortalities attributable to $PM_{2.5}$ and PM_{10} against WHO guideline for (age group 25-99)

Fig. 4.18 illustrates the premature mortality linked to all-cause, cardiovascular, and respiratory diseases among individuals aged 25-99. The focus of the Fig. 4.18 is the association between this mortality and the presence of $PM_{2.5}$. Using a long-term health impact function, it was estimated that by reducing the concentration of $PM_{2.5}$ by 10 $\mu g/m^3$, the cumulative avoided deaths for all causes were as follows: 5238 (95% CI: 3619-9091), 6618 (95% CI: 4682-10779), 7329 (95% CI: 5973-11716), 7050 (95% CI: 5210-11427), 8849 (95% CI: 6614-13357), and 8204 (95% CI: 6017-12796) for the years 2071 to 2022, respectively.

The year 2021 witnessed the attainment of the highest recorded value, which reached 8849, because to heightened ambient concentrations and population density. The long-term health impact function has determined that the estimated range of prevented impacts on cardiovascular mortality due to exposure to $PM_{2.5}$ concentrations is between 2462 and 4058 instances. Similarly, the equivalent range for avoided respiratory deaths falls within 1065 to 1769 cases. Significantly, the reduction in mortality rates attributed to cardiovascular and respiratory diseases accounted for around 49% to 63% and 18% to 19% of premature deaths across all causes, respectively.

In comparison to a study conducted in Brazil the maximum premature value due to all cause mortalities were 7097 cases, findings of which is consistent to this study (Andreao et al., 2018). The averted mortality rates in Tianjin, China, totalled 85,000 instances for all causes (with a 95% confidence interval of 17,000 to 150,000), with an associated monetary value of 42 million yuan annually (L. Chen, Shi, Li, Gao, et al., 2017) for age group 25-99 and these research also

showed a 67% decrease in cardiovascular mortality cases and a 9% decrease in respiratory mortality, and this ratio is consistent with this study as well.

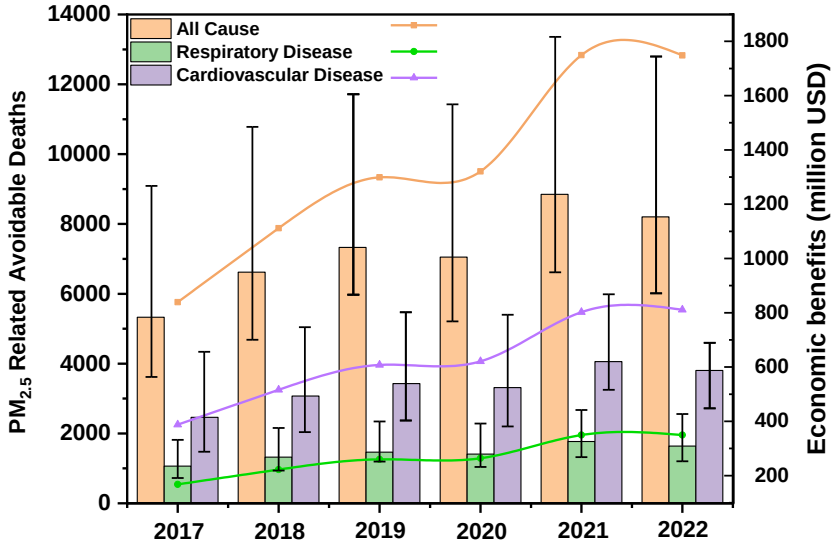

Fig. 4.18 Premature mortality attributable to $PM_{2.5}$ and economic benefits in six consecutive years

N.B. (Box Plot represents $PM_{2.5}$ related premature deaths-Left Y axis and Line Graph represents Economic Benefits in million USD-Right Y axis)

Notably, the analysis in China was done with a concentration of 75 μg/m^3, whereas the average concentration of the studied region was 188.6 μg/m^3, leading to somewhat higher preventable health ratios in the present scenario of the study. Similarly, averted cases of cardiovascular death from 1924 to 2911, respiratory mortality from 167 to 343 cases per year, and all-cause mortality ranging from 3175 to 5697 cases per year are noted in the Beijing-Tianjin-Hebei (BTH) region (L. Chen, Shi, Li, Gao, et al., 2017) . The observed pattern of the order of impacts—first mortality from all causes, then mortality from cardiovascular and respiratory disease—was consistent with the result of this study. However, the variability in results due to the absence of all local variables necessary for model output, healthcare system, air pollution control measures, LULC systems, legal infrastructure in relation to air pollution management.

The application of the Willingness to Pay (WTP) metric, as described in the study (Robinson et al., 2019) can be utilized to assess the economic consequences associated with premature fatalities across different causes of death, namely the average, lower bound (2.5th percentile), and upper bound (97.5th percentile) of mortalities. The economic influence because of cardiovascular disease was nearly three times as high as that from respiratory disease. This pattern was also seen in a case study done in China, where the economic impact of all-cause mortality was about 29632 million CNY, with cardiovascular advantages outpacing respiratory benefits by a ratio of three (L. Chen, Shi, Li, Gao, et al., 2017). In Fig. 4.18, the economic estimation is depicted in relation to the point estimate number of preventable deaths. The analysis of the study indicated that due to $PM_{2.5}$ that in 2017, a total of 5328 premature deaths would incur a cost of approximately 838 million USD, while 7329 preventable deaths would result in an estimated cost of around 1748 million USD. In a similar vein, the allocation of identical willingness-to-pay (WTP) values to respiratory and cardiovascular ailments results in respective costs of 350 million USD and 811 million USD and these costs are associated with the prevention of 1640 and 3806 fatalities in association with $PM_{2.5}$, respectively, in the year 2022. In Tehran, the total cost due to $PM_{2.5}$ related all-cause mortality cost about US $1504 million, and this is closer to the study's estimation (Bayat, Planning, et al., 2019).

For, Fig. 4.19 the highest mean value of 3964 (95% CI: 1980-4665) and lowest mean of 2861 (95%CI: 946-3858) of all cause premature premature death were obtained after rolling back to WHO standard to 20 $\mu g/m^3$ during the year 2017 and 2021 respectively. In every given scenario, the distribution of preventable fatalities constantly indicates substantial health consequences taking place within the CCC area.

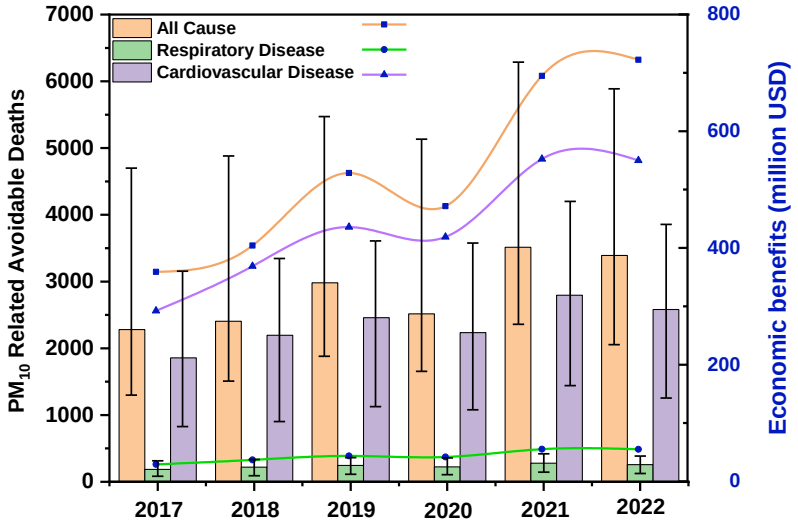

Fig. 4.19 Premature Mortality attributable to PM_{10} in 6 consecutive years

N.B. (Box Plot represents PM_{10} related premature deaths-Left Y axis and Line Graph represents Economic Benefits in million USD-Right Y axis)

The premature point impacts on respiratory and cardiovascular mortality expected to range from 185 to 279 and from 2861 to 3964 cases each year respectively. The cumulative count of preventable fatalities demonstrated an upward trajectory until the year 2019, through a reduction in 2020 because of enhanced atmospheric conditions during the COVID-19 era, and thereafter reached its zenith in 2021 followed by a marginal decrease in 2022 in both Fig. 4.18 and 4.19.

Based on a mean PM_{10} value of 79 g/m^3, a reduction in Shanghai's PM_{10} concentration were linked to a reduction in instances of 300 to 800 per year (Voorhees et al., 2014b). Notably, the mean PM_{10} concentration in this study was greater (314.3 g/m^3) which led to such a variation. According to the statistics, there were 262 cases of respiratory death, 1393 cases of all-cause mortality, and 517 cases of cardiovascular mortality in Seoul, South Korea after the hypothetical reduction in PM_{10} (D. Kim et al., 2019). So, the ratio of the order of premature mortalities of all cause, cardiovascular and respiratory is aligned with this study.

In the Fig. 4.19 it can be depicted that the economic benefits obtained by the hypothetically reducing the concentration of PM_{10} on all cause, cardiovascular and respiratory mortality were ranging from 982 to 1695, 292 to 549, and 14.4 to 80.5 million USD. Furthermore, the costs associated with health consequences in China showed significant inequalities, with respiratory disease in association to exposure to PM_{10} costing 110 million yuan and cardiovascular disease costing 800 million yuan, a nearly sevenfold difference (L. Chen, Shi, Li, Bai, et al., 2017). Based on willingness to pay, the Values of Statistical Life (VSL) in the case of Shanghai ranged from 84,000 to 2,100,000 yuan (Voorhees et al., 2014b). Also, a study in short term health impact in China were estimated to be 15.83 billion based on WTP and the values for cardiovascular deaths were more than respiratory and this scenario is depicted in this study as well.

Comprehensive economic assessments for the 2.5th and 97.5th percentiles of each year are presented in the Table A.7. The cost scenarios can vary significantly based on the socio-economic conditions and willingness to pay in different countries. A strong correlation exists between premature deaths and economic costs – as the number of premature deaths increases, the economic benefit on a country also rises. These conditions are closely tied to the air quality data of a given region.

Both the Fig. 4.18 and 4.19 demonstrate an initial increasing trajectory in economic benefits, primarily attributed to elevated rates of preventable deaths. However, there is a subsequent fall in 2020, followed by a slight decrease in 2022 relative to 2021 for the case all causes mortality only. Furthermore, the studied heavy metals were found not to pose non-cancerous health risks, as detailed in section 4.4.1. However, it's important to note that their significant presence in terms of dosage could potentially exacerbate health hazards related to particulate matter exposure, as supported by the literature review presented in section 2.3.3.

Spatial variation of avoided premature mortalities attributable to $PM_{2.5}$ and PM_{10} against WHO guideline for (age group 25-99)

The count of deaths attributed to pollutant exposure, understanding the potential contribution of different air pollutants to all-cause mortalities across various wards holds significant importance. The specific ward-wise contribution to all-cause mortality is illustrated in Fig. 4.20 and 4.21 respectively.

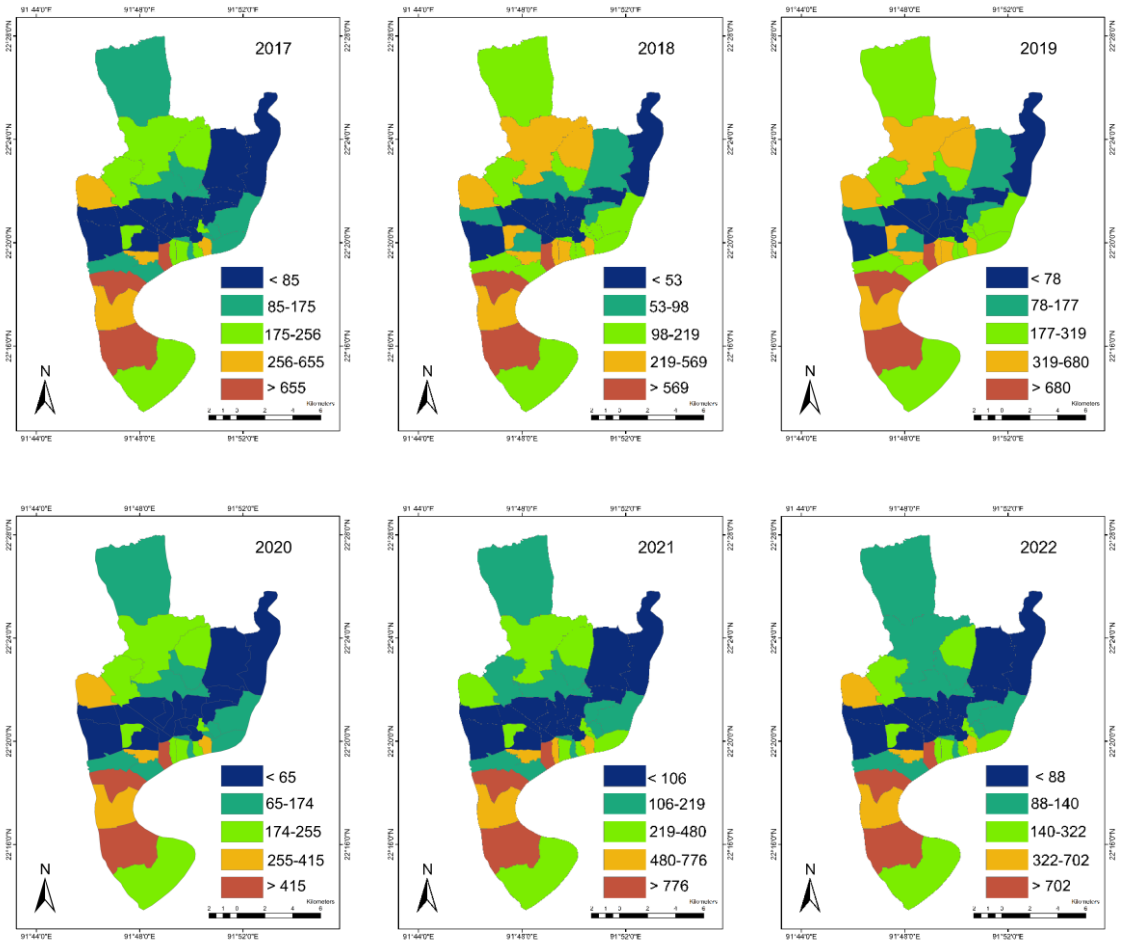

Fig. 4.20 Spatial distribution of the premature mortalities due to all cause in CCC for exposure to $PM_{2.5}$

A study using BenMAP-CE model stated that the large number of concentrated premature mortalities are concentrated in the region with large $PM_{2.5}$ delta concentration (G. Luo et al., 2020). This is quite visible in this study where North

Patenga (W-40) has the highest premature incidences in all the scenarios. Also, high population density plays an important role in resulting higher incidences (Ding et al., 2016).

The wards South Patenga (W-41), South Middle Halishahar (W-38), and Pathantuli (W-28) continuously exhibit the most significant association between $PM_{2.5}$ levels and mortality from all causes for a continuous period of six years. And the middle portion of the study area including Pahartali (W-13), Mohra (W-5), Sholokbahar (W-8), Northa Halishahar (W-26), South Kattali (W-11), and Saraipara (W-12) demonstrate the least premature death due to $PM_{2.5}$. Significantly, there is a discernible similarity in the patterns observed throughout the years 2017 and 2018, as well as in the years 2020 and 2021.

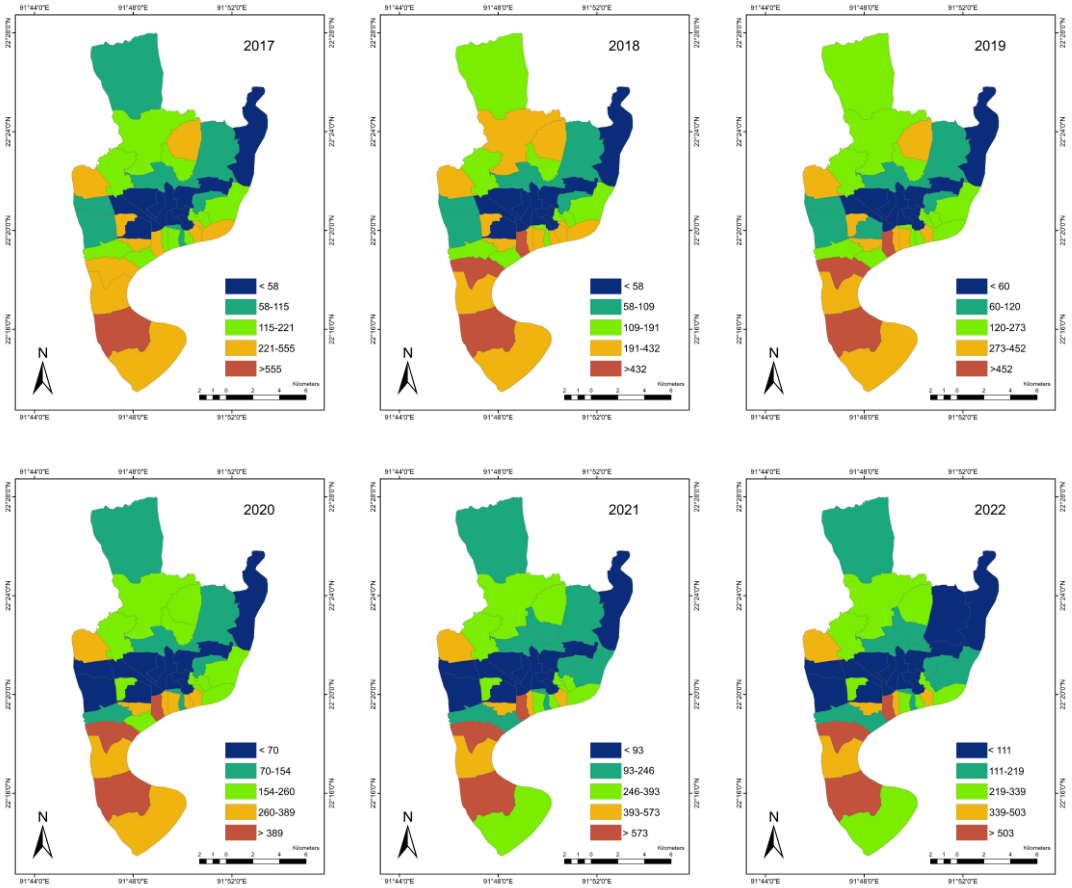

Fig. 4.21 Spatial distribution of the premature mortalities due to all cause in CCC for exposure to PM_{10}

A discrepancy is evident in the graphical representations of 2019 and 2022 as seen in Fig. 4.21, wherein Jalalabad (W-2) and Panchlaish (W-3) exhibit a notable shift from being the second biggest contributors to overall mortalities in 2019 to experiencing the second lowest number of preventable deaths in 2022. Moreover, in the recent timeframe spanning from 2021 to 2022, there has been a significant rise in premature fatalities observed inside Sholokbahar (W-8) and North Pahartali (W-9). The data from the past three years consistently demonstrated a recurring trend in preventable fatalities associated with PM_{10}. However, the years 2017, 2018, and 2019 exhibit distinct patterns while maintaining consistency in terms of the regions with the highest and lowest numbers of preventable deaths, which can be compared to the impact of $PM_{2.5}$. These patterns are a result of high levels of pollution and population density. Notably, compared to earlier years in Fig. 4.21, South Pahartali (W-1) causes more all-cause fatalities in the years 2018 and 2019. South Kattali (W-11), North Halishahar (W-26), and North Middle Halishahar (W-37) appear to have had better air quality over the recent three years (2020-2022). Moreover, W-2, W-3, and W-9 hold the second highest contribution to all-cause mortality in 2018, with W-3 taking on this role in 2017 and 2019—an exception from 2020 to 2022. The enhancement of air quality in certain regions can be attributed to the adoption of environmentally friendly practices and the completion of ongoing development projects, which are often sources of pollution.

The geographical pattern of premature mortalities due to cardiovascular and respiratory diseases closely resembles the distribution of all-cause premature mortalities as presented in Fig. A.4 -A.6.

Temporal pattern of premature premature deaths using GEMM and LL models (age group 25-99) for 5-COD (5-Causes of Death) and NCD+LRI (Non-Communicable Diseases + Lower Respiratory Infections)

Furthermore, apart from the commonly studied health outcomes such as all-cause, cardiovascular, and respiratory mortalities and morbidities, this research also took into account premature deaths attributed to the widely acknowledged 5-Causes of Death (5-COD). These specific causes are highly susceptible to the influence of $PM_{2.5}$ exposure and are associated with a substantial number of incidences.

The study involves the utilization of two distinct models, the LL (log-linear) model and the GEMM model (global exposure mortality model), to gauge the relative risk linked to exposure to $PM_{2.5}$ and its consequences on early deaths. The primary focus is on premature fatalities attributed to $PM_{2.5}$, divided into two categories: 5-COD, which encompasses fatalities from ischemic heart disease, stroke, lung cancer, chronic obstructive pulmonary disease, and lower respiratory infections, and NCD+LRI, which stands for non-communicable diseases and lower respiratory infections.

Due to disparities in the relative risk estimation methods employed by the LL and GEMM models, there are variations in the calculated relative risk values. Consequently, this leads to divergent outcomes in the results of the health impact assessment. As the LL model lacks a defined relative risk value for NCD+LRI, the relative risk value for non-accidental outcomes is utilised for comparative purposes as done in other literature reviews (Andreo et al., 2018; Bayat, Ashrafi, et al., 2019; Liu et al., 2021). This facilitates a comparative analysis of the two models with regards to the relative likelihood of non-accidental fatalities.

The study's outcomes, which highlight $PM_{2.5}$-related premature fatalities for both 5-COD and NCD+LRI, are visually depicted in Fig. 4.22. In every case NCD+LRI

is higher than 5-COD as it contains most of the health endpoints. The discrepancies in projected health outcomes arising from $PM_{2.5}$ exposure under different estimation methodologies in the LL and GEMM models are highlighted by Fig. 4.22 (a) and (b). In comparison to all-cause mortality provided in Fig. A.3 to the ratio of 5-COD in Fig. 4.26 (a) is (0.30-0.36) for LL model and (0.44-0.47) for GEMM model. For non-accidental in Fig. 4.22 (b) the ratio ranges from 0.43-0.53 for LL and from 0.71 -0.83 for GEMM model. And this ratio of this study is comparable with the results of other studies 122%, 82%, 63% and 54% respectively done in Tehran, China, and Southern China (Bayat, Ashrafi, et al., 2019; Liu et al., 2021; Maji, 2020; Wu et al., 2021).

Certainly, much like other health-related outcomes, the year 2021 saw a significant peak in total mortality, as indicated in Fig. 4.22, encompassing both 5-COD and (NCD+LRI) cases. Specifically, the log-linear model indicated a range of 3500 (95% CI: 2551-4123) for 5-COD cases and 5098 (95% CI: 3986-6004) for nonaccidental cases. On the other hand, the GEMM model yielded higher ranges, with 5-COD contributing to 4931 cases (95% CI: 3680-5463) and (NCD+LRI) cases reaching 8402 (95% CI: 7398-9263). The lowest $PM_{2.5}$ mortality in 2017 was 5938 (95% CI: 5289-6842) and 3790 (95% CI: 2919-4525), respectively, according to the GEMM (NCD+LRI) and LL (non-accidental) models. For the year 2017, the ranges for the GEMM (5-COD) and 5-COD utilizing LL models were 3433 (95% CI: 2362-3951) and 2598 (95% CI: 1846-3135), respectively. Again, the ratio of GEMM-5 COD to GEMM (NCD+LRI) is 0.86-0.90 whereas the ratio of LL 5-COD to LL (non-accidental death) is 0.68-0.75.

The GEMM model typically produces better estimates compared to the LL model since it incorporates data from other cohort studies, whereas LL mainly uses data from Chinese cohorts. (Wu et al., 2021) research. The relative risk function's

variability is revealed to be a significant source of ambiguity in calculating $PM_{2.5}$-related mortality (Burnett et al., 2018b).

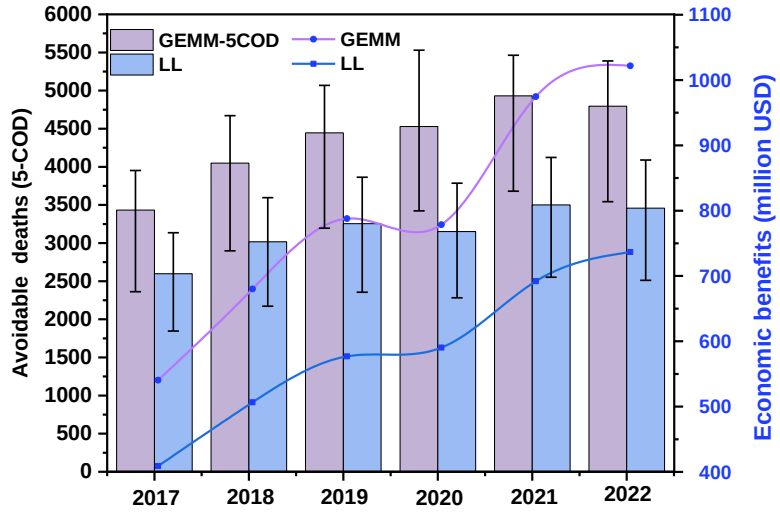

(a)

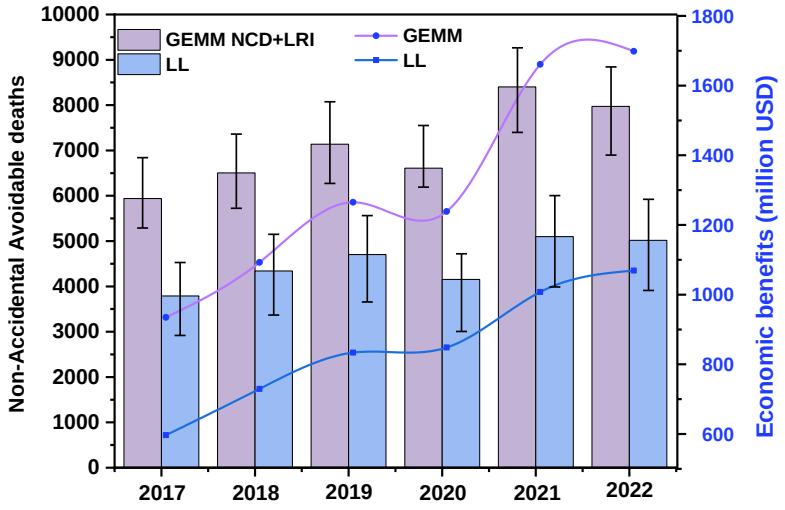

(b)

Fig. 4.22 (a) Premature deaths and economic benefits due to 5-COD, (b) Premature deaths and economic benefits due to NCD+LRI

N.B. (Box Plot represents PM_{10} related premature deaths-Left Y axis and Line Graph represents Economic Benefits in million USD-Right Y axis)

Other situations, including the investigation of 74 Chinese cities, 338 Chinese cities, Tehran, and a multiple exposure study in China, exhibit a comparable trend to the present study. These cases consistently demonstrate the prevalence of the GEMM model in yielding greater estimations compared to the LL model (Fang et al., 2016; Maji et al., 2018; Wu et al., 2021; Bayat et al. 2019).

The WTP values established by Hammitt and Robinson in 2011 were used in the study's economic valuation approach to quantify the costs related to preventing premature deaths (Hammitt and Robinson, 2011). Notably, the premature mortality in Fig. 4.22 obtained from the GEMM model were greater than those obtained from the LL model, showing a similar trend in financial advantages. The economic costs showed an escalating pattern until 2019, then decreased in 2020 before reaching their highest point in 2022, following tendencies seen for other health outcomes previously evaluated. Despite 2021 having the most preventable cases, the economic expenses were still higher in 2022 because of inflation and small variations from the year 2021 in premature cases. The study analysis, by the GEMM model, showed that the economic gains for 2022 totalled 1020 million USD for 4795 instances of 5-COD and 1700 million USD for 7971 cases of NCD+LRI. Similar results were obtained by using the LL model, which resulted in health benefits of 737 million USD for 3457 instances of 5-COD and 1070 million USD for non-accidental cases in 2022. The other economic estimates and are provided in Table A.8 and A.9.The economic value is aligned with the economic valuation in Tehran worth 2509 million USD for 5-COD and1000 million USD for IHD and lung cancer in Pakistan (Bayat, Ashrafi, et al., 2019; Hassan et al., 2021).

Furthermore, the inhalation of heavy metals in the atmosphere has been found to elicit the manifestations of Ischemic Heart Disease (IHD), Lower Respiratory Infections (LRI), Chronic Obstructive Pulmonary Disease (COPD), and Stroke, as

outlined in section 2.3.4 (Choe et al., 2003; Dalton et al., 2001; Kampa and Castanas, 2008a). Therefore, while these heavy metals may not individually pose significant health risks, their interaction with particulate matter can substantially increase the overall health risk (Guo et al., 2021; Tan et al., 2016). Consequently, this could lead to an increase in premature mortalities and exert additional pressure on GDP.

Furthermore, an exhaustive examination of the findings is provided in the Fig. 4.23, which includes a thorough breakdown of the mortality associated with $PM_{2.5}$ categorised by both the specific model and the individual disease.

This comprehensive analysis provides a more elaborate and precise examination of the mortality outcomes related to exposure to $PM_{2.5}$, specifically focusing on the five causes of death (5-COD) and non-communicable diseases with lower respiratory infections (NCD+LRI).

Over the course of the six consecutive years, consistent trends were observed in the results concerning health endpoints in Fig. 4.23.

Specifically, for the year 2021, the GEMM 5-COD model revealed the following contributions of various diseases to $PM_{2.5}$-induced mortality: (IHD) accounted for approximately 39% of the total, stroke accounted for 29%, (COPD) constituted around 18%, (LC) contributed about 3%, and (LRI) made up roughly 9% of the total mortalities. Notably, the ratio of GEMM-5COD to GEMM-NCD+LRI was calculated as 0.62, suggesting that a significant portion of diseases attributed to $PM_{2.5}$ falls outside the scope of the defined 5-COD classification.

The observed discrepancies in outcomes between the two models can be attributed to several factors inherent in the complex process of assessing health implications arising from exposure to $PM_{2.5}$. Notable among these are variations in hazard ratios utilized by each model for specific health conditions, differences

in the chemical composition of $PM_{2.5}$ across diverse sources and regions, the heterogeneous nature of particulate matter characterized by distinct sizes and compositions, the divergence in emission sources leading to diverse $PM_{2.5}$ constituents, and the intricate interplay of multiple pollutants in the atmosphere.

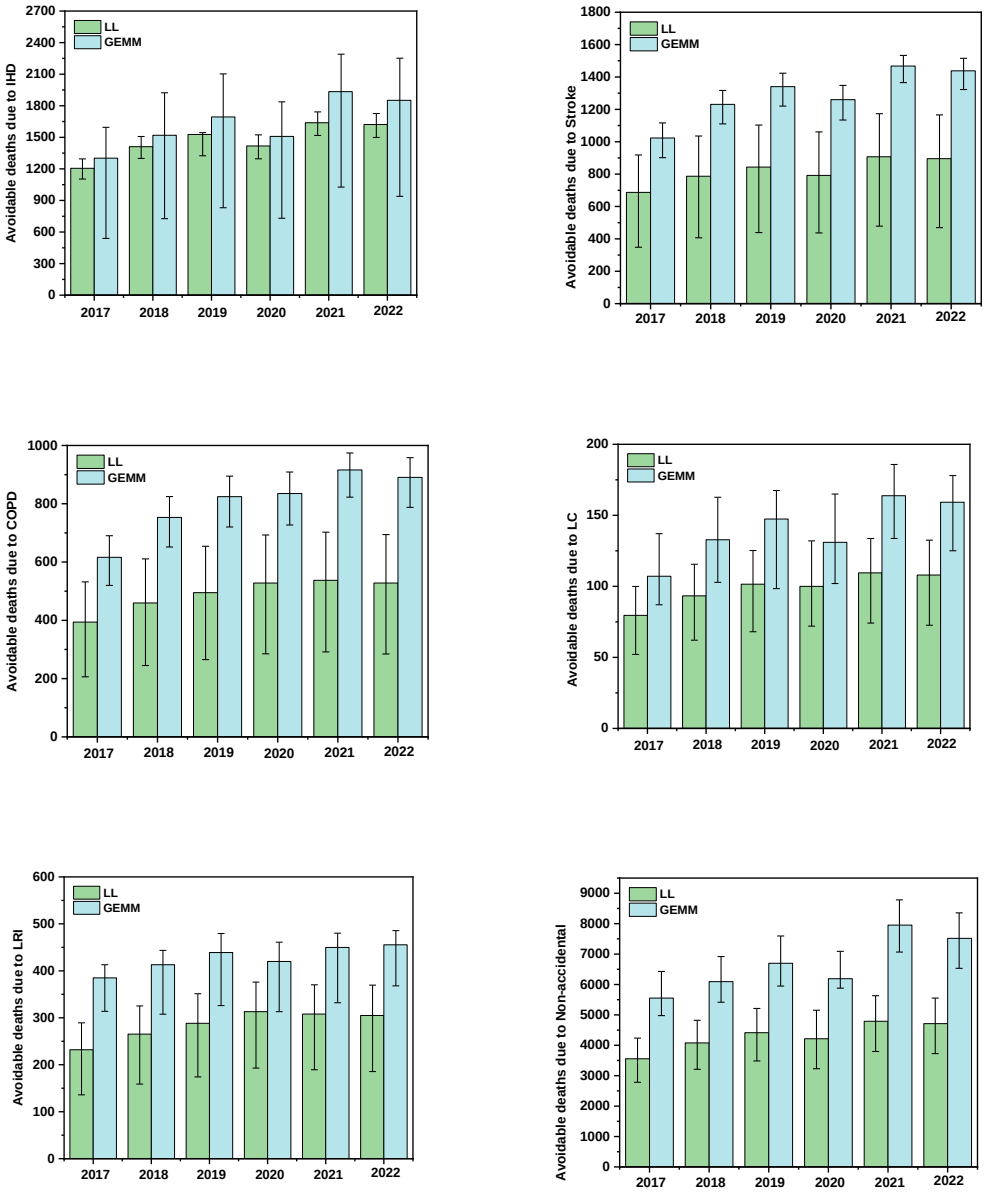

Fig. 4.23 Model Specific and cause specific mortality attributable to $PM_{2.5}$ in CCC area

The intricate and interconnected elements mentioned above collectively play a role in the nuanced and diverse results obtained from the two models, highlighting the complexities involved in conducting a full evaluation of the health effects associated with exposure to $PM_{2.5}$.

Spatial pattern of premature premature deaths using the LL and GEMM model (age group 25-99) for 5-Causes of death

The spatial pattern due to 5-COD using both LL model and GEMM model is shown in Fig. 4.24 and 4.25. Pollutant concentrations and population density were the main determinants of death burden, and this scenario is visible in the study of (Maji, Arora, et al., 2018; Wang et al., 2021; Wu et al., 2021).

For instance, regions with greater levels of pollution in Fig. 4.24 and 4.25, wards like North Patenga (W-40), South Middle Halishahar (W-38), North Halishahar (W-26), and North Kattali (W-1) showed higher rates of preventable incidences. But even when population estimates aren't taken into account, Wards like Panchlaish (W-3), East Bakalia (W-18), South Bakalia (W-19) and Dewan Bazar (W-20), which have lower population density, showed medium preventable occurrences because of baseline mortality rates. Similar to this, wards like Rampur (W-25) reported medium preventable incidents due to excessive pollution levels, although not having a significant population density. Each characteristic thus played a role in the diversity in preventable incidents.

In both GEMM and LL model, IHD was the highest cause of premature mortality in all wards. South Pahartali (W-1), Jalalabad (W-2), Panchlaish (W-3), North Pahartali (W-9), Rampur (W-25), South Agrabad (W-27) and West Madarbari (W-29), East Madarbari (W-30) and Alkaran (W-31) also contribute more than 50 % of the mortality burden in Fig. 4.24 and 4.25. Both the models showed same spatial pattern but a variation in the proportion of disease specific causes.

Overall, the results depict that the highest premature mortalities were in the region of high pollution or population density.

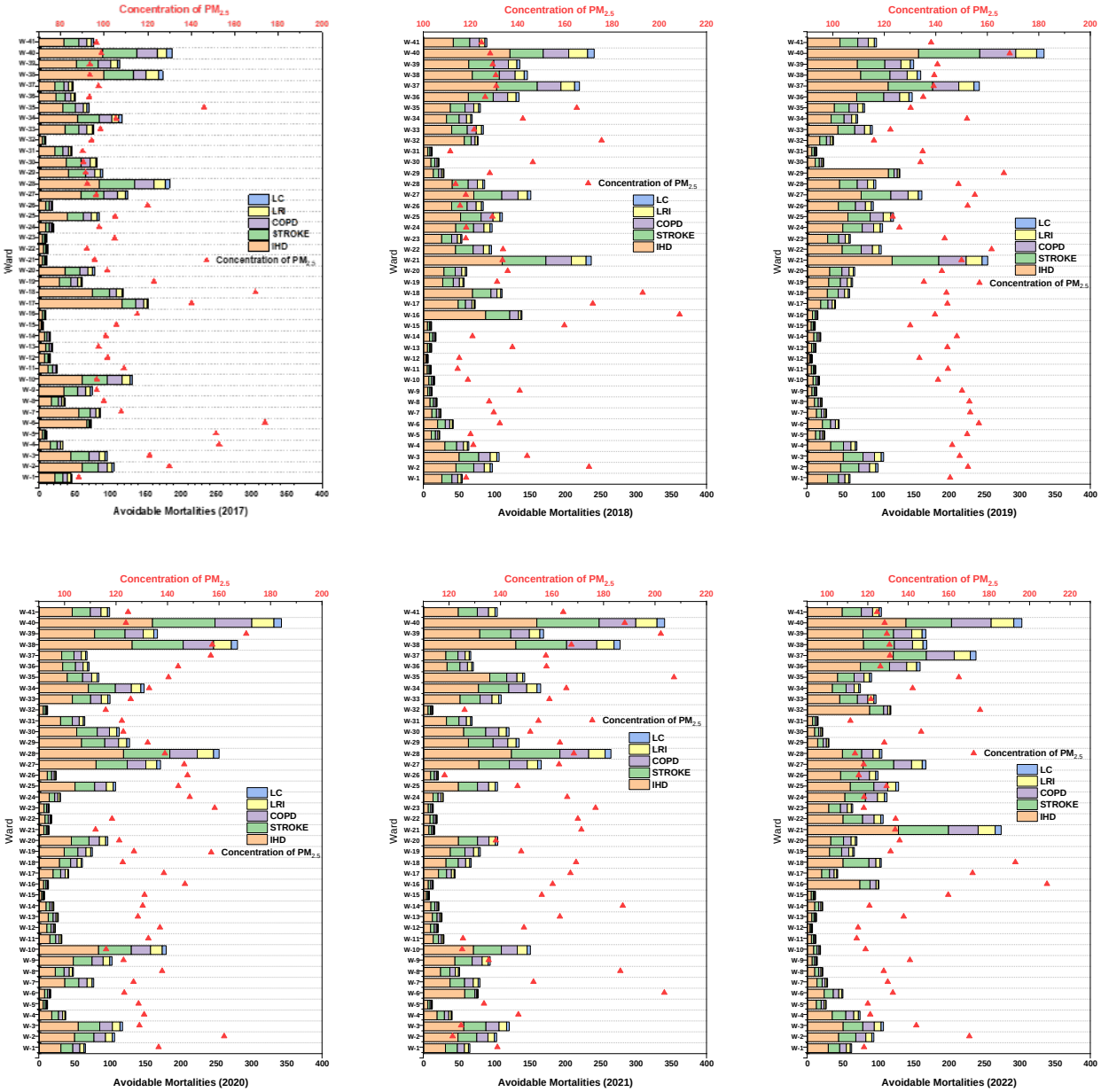

Fig. 4.24 Spatial distribution of 5-COD using LL model

N.B. (Top X axis represents $PM_{2.5}$ Concentration and Bottom X axis represents Premature Mortalities)

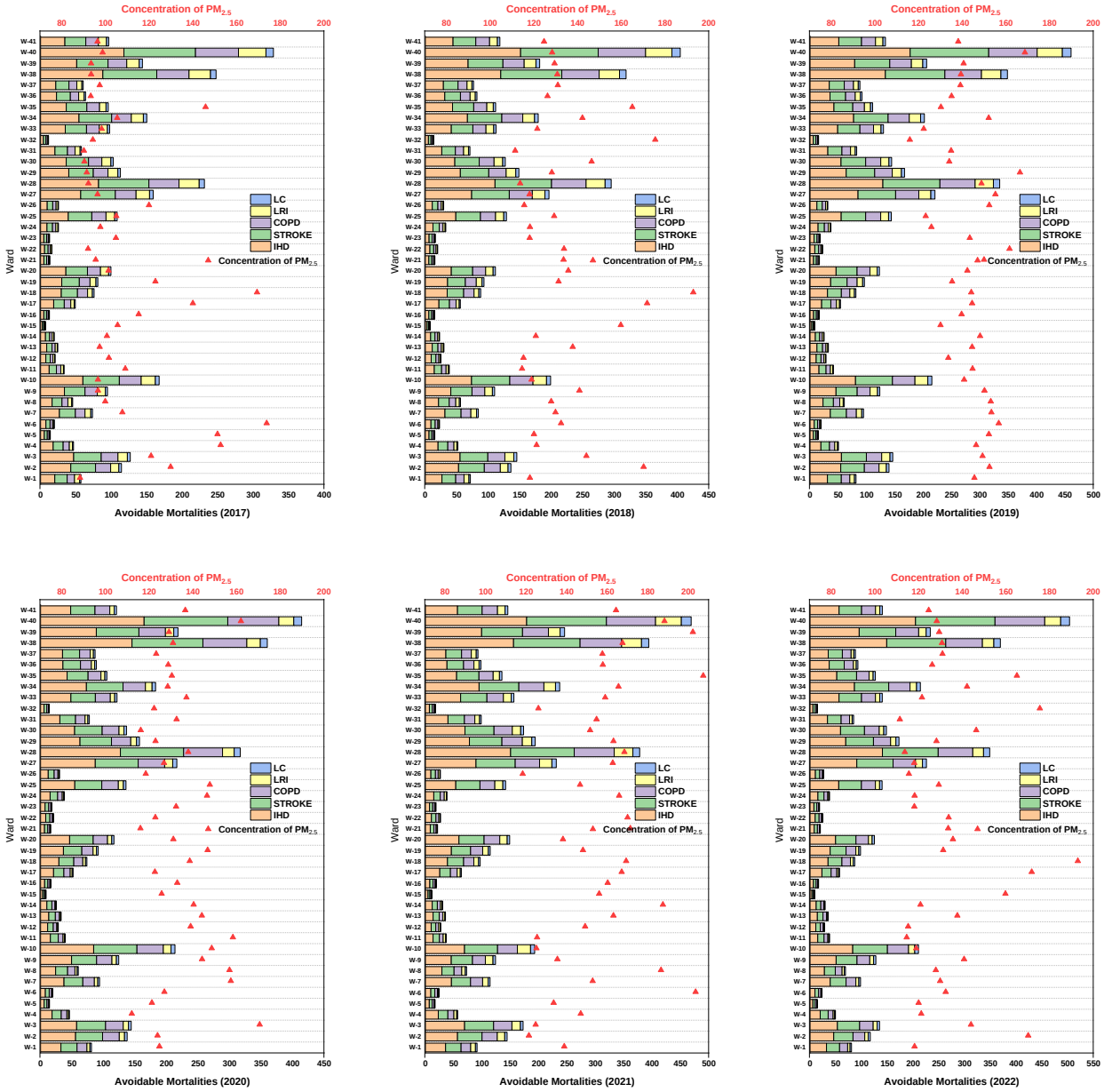

Fig. 4.25 Spatial distribution of 5-COD using GEMM model

N.B. (Top X axis represents $PM_{2.5}$ Concentration and Bottom X axis represents Premature Mortalities)

Apart from it the mortality rates also had an impact on the estimates. These spatial trends align with similar studies conducted in India, China, and Tehran, where areas with elevated pollutant levels and higher exposed populations

corresponded to maximum health benefits in terms of mortality reduction (Bayat, Planning, et al., 2019; Manojkumar and Srimuruganandam, 2021; Nasari et al., 2016; Wu et al., 2021).

The GEMM-NCD+LRI also shows similar spatial patterns as GEMM-COD with a slight variation and keeping the highest and lowest consistent with the previous studies. This is due to the variation in relative risk and also same thing hold good for Non-Accidental Deaths by LL-model given in Fig. A.7 and A.8.

Temporal variation of premature hospital admission attributable to $PM_{2.5}$ and PM_{10} (age group 25-99)

In addition to analyzing mortalities, this study also examined hospital admissions associated with sources of particulate matter concentration for the age group 25-99 as shown in Fig. 4.26 and 4.27. The number of hospital admissions for individuals in this age group was substantial, and there was clear evidence of people being admitted to hospitals for cardiac and respiratory diseases attributable to particulate matter (Amsalu et al., 2019; Gurung et al., 2017; Niu et al., 2021; Rahman et al., 2022; Sherris et al., 2021; Tian et al., 2019) . Furthermore, the presence of heavy metals in particulate matter contributed to an increase in the number of new hospital admissions (Briffa et al., 2020b; Tan et al., 2016) .

Over the course of six years, the range of $PM_{2.5}$-related hospital admissions because of cardiac outcomes in Fig. 4.26 were 933 (95% CI: 301-1610), 1234 (95% CI: 367-2117), 1419 (95% CI: 408-2427), 1346 (95% CI: 312-2308), 1826 (95% CI: 500-3097), and 1631 (95% CI: 425-2780). Also, Between the years 2017 and 2022, a range of 736 to 1476 instances of respiratory hospital admissions associated with $PM_{2.5}$ were recorded.

For the same period in Fig. 4.26, PM_{10}-related premature hospital admissions for cardiac and respiratory disorders ranged from 820 to 1595 and 661 to 1195 cases, respectively. The fluctuations in premature instances exhibit a similar trend to that observed in mortality rates across all causes.

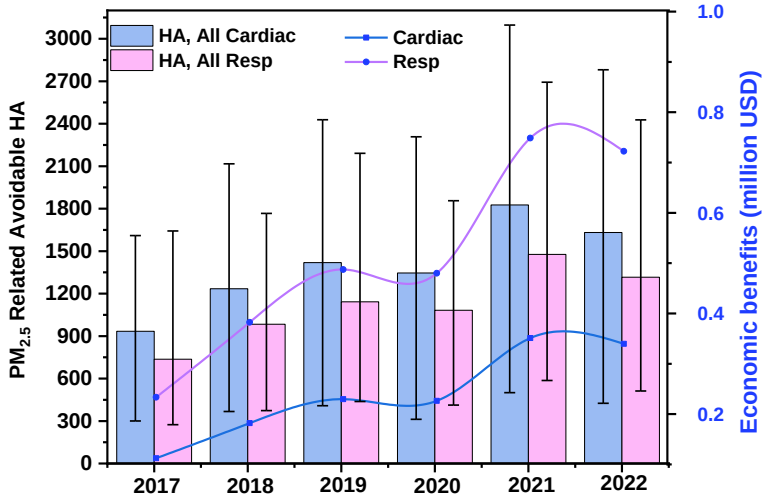

Fig. 4.26 Hospital Admissions attributable to $PM_{2.5}$ pollutant

N.B. (Box Plot represents $PM_{2.5}$ related premature incidences-Left Y axis and Line Graph represents Economic Benefits in million USD-Right Y axis)

Particularly, the proportion of $PM_{2.5}$ and PM_{10} contributed between 17% to 20% and 14% to 18% respectively of cardiac hospitalizations to all cause heath endpoint. Similarly, proportion of $PM_{2.5}$ and PM_{10} that contributed is 13% to 16% and 12% to 14%, respectively, to all causes of respiratory hospital admissions. For cardiac outcomes this study relies on COI method whereas for Respiratory admission this study based on WTP. Economic valuations for respiratory illnesses using the World Bank's health effect cost values through WTP range from 0.23 million to 0.75 million USD for $PM_{2.5}$ and 0.2 million to 0.55 million USD for PM_{10}. In order to estimate the health effects value for each year for Cardiac Outcomes, the economic value for Bangladesh, which came to 2146 USD for the recent based on multiple web sources and contemporary research, was

adjusted to the base year using the inflation factor. As a result, the financial burden associated with cardiac-related hospital admissions ranged from 0.098 to 0.3 million USD for PM_{10} and from 0.21 million to 0.62 million USD for $PM_{2.5}$.

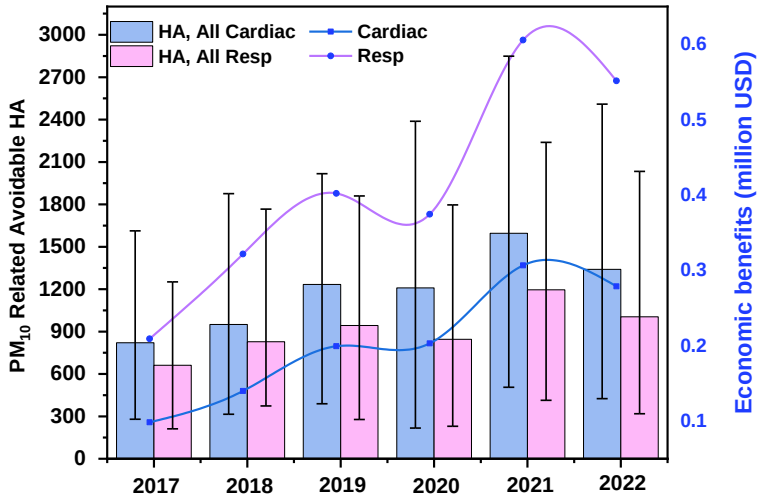

Fig. 4.27 Hospital Admissions attributable to PM_{10} pollutant

N.B. (Box Plot represents PM_{10} related premature incidences-Left Y axis and Line Graph represents Economic Benefits in million USD-Right Y axis)

A total of 565 and 575 hospital admissions for cardiovascular and respiratory conditions due to the exposure to $PM_{2.5}$, respectively, costing 3.2 and 1.8 million yuan (CNY), were recorded during the Asian Games in Guangzhou (Ding et al., 2016) where the premature cases number closer to this study. Like this, the Cost of Illness (COI) technique revealed that due to exposure to PM_{10}, Shanghai saw 5400 to 7900 unnecessary hospital admission cases each year, costing 20 to 30 million yuan (Voorhees et al., 2014b). There are variations in the economic cost as the healthcare condition is different in different parts of the world, so the cost varies accordingly. It's important to note that there aren't much research examining the connection between particulate matter and hospital admissions. The economic values related to the mean premature morbidities are shown Fig. 4.26 and 4.27 and the 2.5 and 97.5 percentile are given in the Table A.10. and A.11.

Spatial variation of premature hospital admission attributable to $PM_{2.5}$ and PM_{10} (age group 25-99)

While retaining consistent maximum and lowest morbidities, the spatial distribution over the course of six consecutive years demonstrates diverse scenarios in various time frames, similar to premature cases in all-cause fatalities. $PM_{2.5}$ related hospital admissions due to cardiac and respiratory outcome are shown in Fig. 4.28 and 4.29. Notably, there are differences between the GIS maps in $PM_{2.5}$ related hospital admissions of cardiac and respiratory outcomes. Divergent maps originate from differences in relative risk values and incidences, despite the age group and pollutant concentration parameters remaining constant. Similar findings for PM_{10} are described in the Fig. A.9 and A.10.

The study's results suggest that the observed differences in the maps can be mostly related to fluctuations in incidence rates and relative risk values, while holding population size and pollutant concentration constant. Moreover, an analysis of hospital admissions pertaining to two distinct outcomes highlights slight disparities. In the year 2019, a decrease in premature cases was observed in South Pahartali (W-1) pertaining to respiratory outcomes, however an increase was observed in premature cases for cardiac outcomes. Otherwise, the map showed the same trend for both the outcome for the other years.

In the period spanning from 2017 to 2022, the cities falling within the high-value range (146–483 cases) for hospital admissions linked to cardiac outcomes in Fig. 4.28 from $PM_{2.5}$ pollution in CCC area were situated in zones South Middle Halishahar (W-38), South Halishahar (W-39), and North Patenga W-40. On the other hand, the low-value area (10–32 cases) was distributed across the middle part of the study area, encompassing zones Chandgaon (W-4), Mohra (W-5), North Kattali (W-10), South Kattali (W-11), Pahartali (W-13), Lalkhan Bazar (W-14), Bagmaniram (W-15), North Pathantuli (W-23), and Enayet Bazar (W-22).

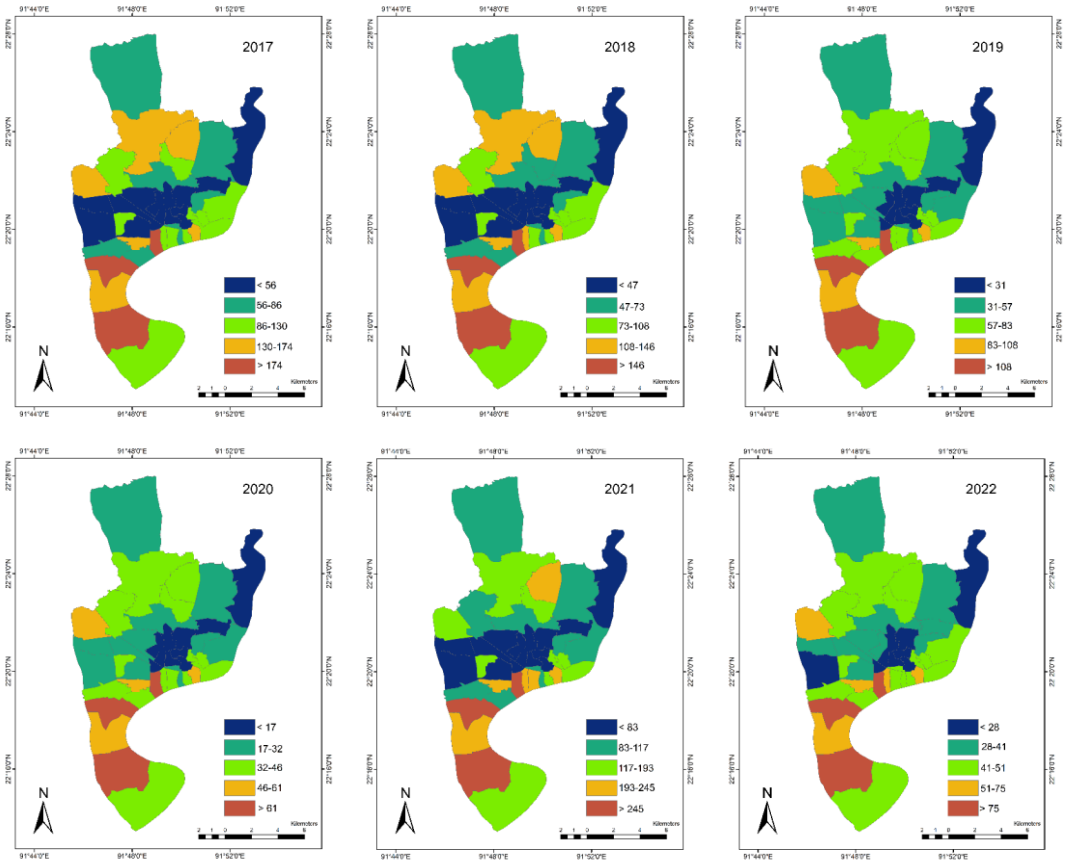

Fig. 4.28 Hospital admissions of premature cardiac outcome attributable to $PM_{2.5}$

Moreover, in Fig. 4.29 there was an observed rise in the number of urban areas that encountered a prevalence of respiratory premature morbidities linked to $PM_{2.5}$ pollution beyond the threshold of 153 instances during the period spanning from 2017 to 2022, except for a significant decline in 2020. The majority of these cases were primarily located in the North Patenga W-40 area and its surrounding districts, along with North Kattali W-10. During the period of 2017, the number of cities where the incidence of respiratory premature morbidities caused by $PM_{2.5}$ pollution remained below 10 instances.

Specifically, the number of such cities rose from 12 to 16 in 2022. Nevertheless, the number of cases had a significant decline in 2020, with only 9 reported instances, predominantly concentrated in the northeastern region of CCC.

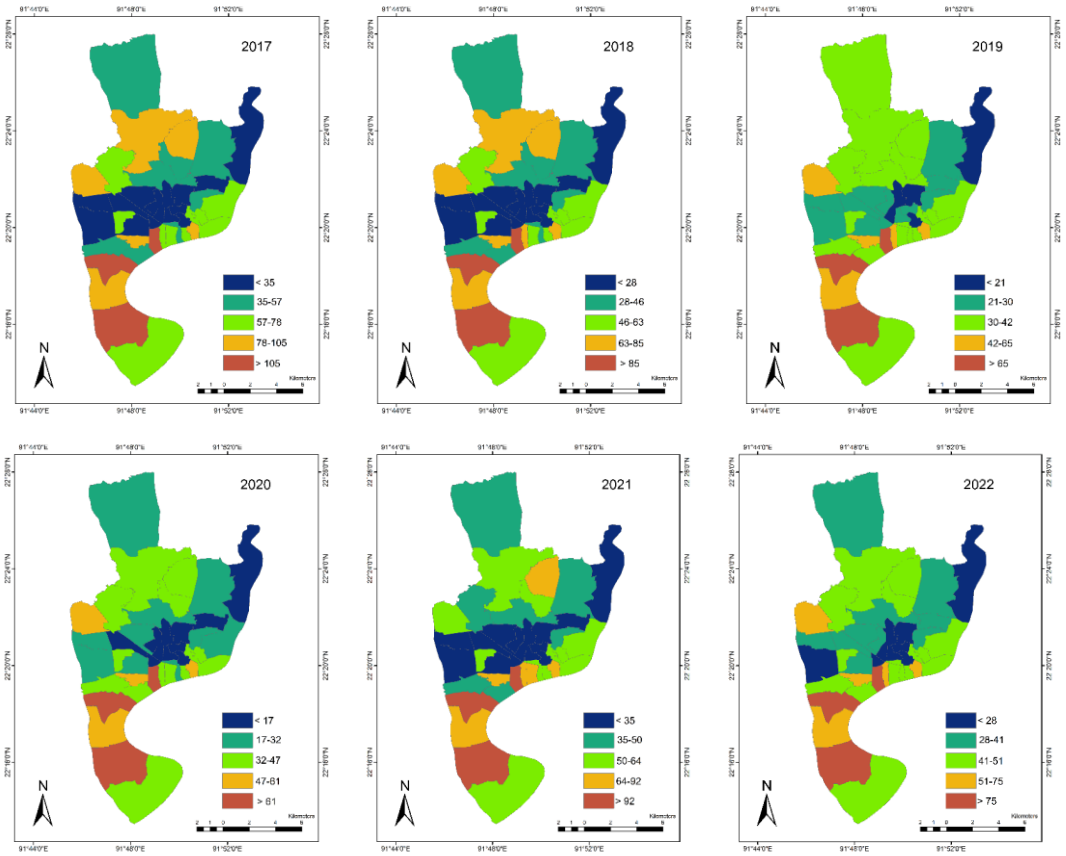

Fig. 4.29 Hospital admissions of premature respiratory outcome attributable to $PM_{2.5}$

The study findings indicated that the central section of the study area had the lowest percentage of preventable cases for both cardiac and respiratory illnesses, which aligns with the observed patterns in overall mortality rates. The observed regional patterns in health effect and benefit outcomes for each health condition are consistent with the findings of the study conducted by (L. Chen et al., 2010; Ding et al., 2016, 2019c). Hence, it can be deduced that alterations in relative risk (RR) values have a substantial impact on both respiratory and cardiac outcomes.

Temporal pattern of premature incidences of minor restricted activity days and work loss days

Minor restricted activity days are days when people are only mildly affected by air pollution in terms of their health, causing only minor annoyance, irritation, or respiratory symptoms that don't require hospitalization. Work loss days are the

number of days that people miss from working because of health problems brought on by exposure to air pollution, which has an effect on both their productivity and the economy. This exposure negatively impacts their productivity and thus affects the whole economy.

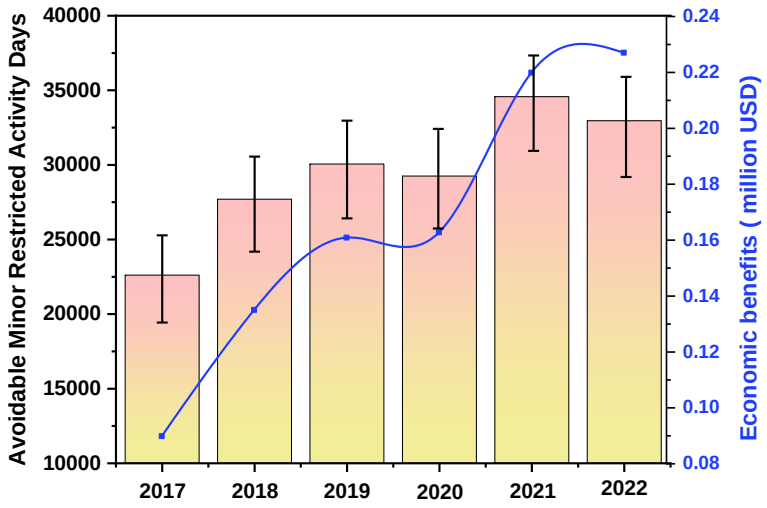

Fig. 4.30 Premature incidences due to Minor Restricted Activity Days

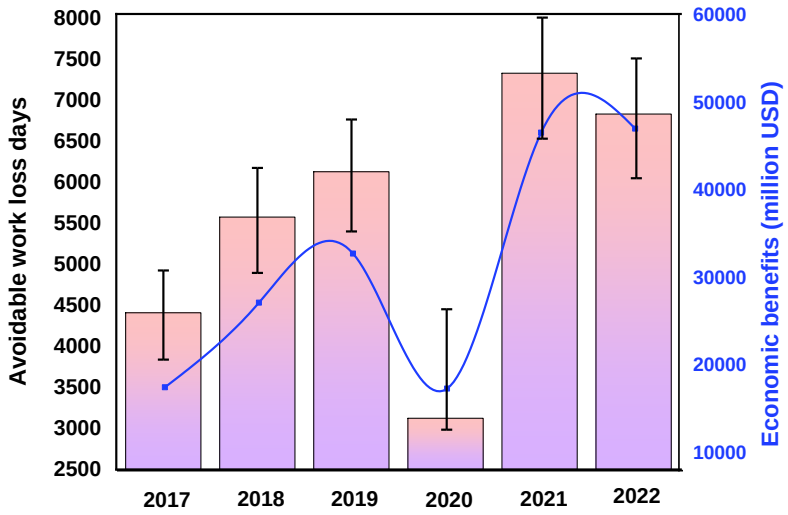

Fig. 4.31 Premature incidences due to Work Loss Days

N.B. (For Fig. 4.30 and 4.31 Box Plot represents $PM_{2.5}$ related premature incidences-Left Y axis and Line Graph represents Economic Benefits in million USD-Right Y axis)

The literature study revealed a robust correlation between $PM_{2.5}$ and these occurrences (Cowie, 2012; N. Li et al., 2022; Mccubbin, 2009, 2011; Y. Xie et al.,

2019). Moreover, it has been shown that the occurrence of specific illnesses is heightened by the intrusion of heavy metals in dust (X. Chen et al., 2022; Guo et al., 2021; Tan et al., 2016).

The number of premature incidents has been increasing steadily over the years, with COVID-19 having a significant impact in 2020. The maximum number of work loss days (7327) and minor restricted activity days (34573) result from reducing $PM_{2.5}$, translating into economic gains of 47066 and 227066 USD respectively achieved in the year 2022. Moreover, the year 2020 demonstrates the lowest combined health and economic advantages, with 3,123 of work loss days cases averted, corresponding to 17,397 USD in cost savings, and 29,247 fewer minor restricted activity days marked by preventable health issues, valued at 162,759 USD in Fig. 4.30 and 4.31. This trend mirrors the pattern observed in other health outcomes.

When compared to earlier studies, there was a substantial decline of 922,020 instances of minor restricted activity days upon reducing ozone levels (Hubbell et al., 2005). Moreover, the mitigated health impact assessment encompassed 57,000 cases related to WLD, and 340,000 cases of MRAD attributed to exposure to $PM_{2.5}$ (Neumann et al., 2021). Well, the variation in population and pollutant concentration caused a variation in the result and the economic estimation of 2.5 and 97.5 percentile are provided in Table A.12 and A.13.

Spatial Pattern of premature incidences of minor restricted activity days and work loss days

Fig. 4.32 and 4.33 shows the regional distribution of premature incidents associated with restricted activity days and work loss days.

Over time, the spatial distribution has remained essentially stable. In Fig. 4.32 North Kattali (W-10) showed greater preventable incidents in the years 2021 and

2022, which can be related to a higher population and pollutant concentration in that area. South Patenga (W-41) consistently showed less preventable incidents throughout the study period, except for 2017.

Also like the other health outcomes, North Patenga (W-40) has the highest premature incidences in these two-health endpoint as well. Many garment factories and industries, which are major sources of air pollution, are concentrated in this area. Any reduction in the current pollution levels is directly linked to a decrease in the number of premature incidents. Additionally, being a commercial hub, the higher influx of population in this area further contributes to a greater number of premature incidents. Also, during the covid period 2020, the scenario remained the same for W-1 with less premature cases only.

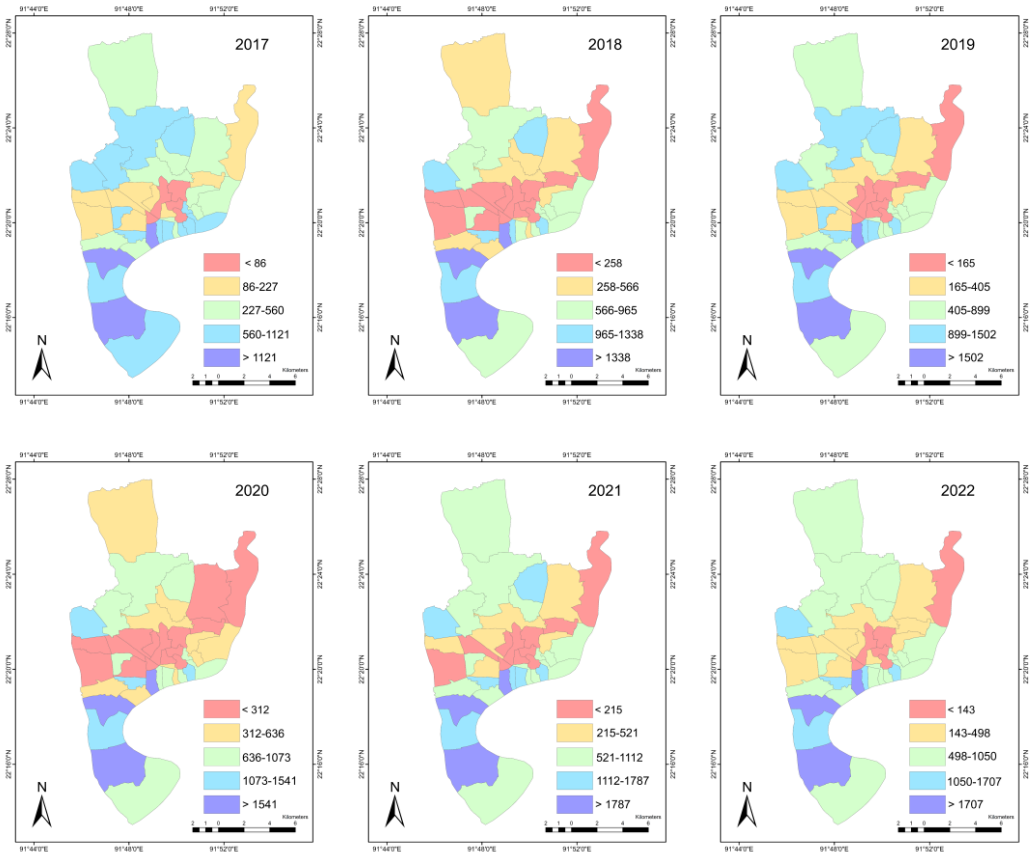

Fig. 4.32 Spatial pattern of premature incidences due to minor restricted activity days

Also, the two outcomes have differences in their spatial variation which could be visibly observed in South Pahartali (W-1) and South Patenga (W-41) as shown in Fig. 4.32 and 4.33. These wards have lesser premature incidences for WLD outcomes in Fig. 4.33. The highest and lowest premature zones remain constant like MRAD, but some variations can be observed such as South Kattali (W-11) and North Halishahar (W-26) have least premature incidences in WLD. The spatial pattern of premature incidents due to WLD and MRAD have variances according to relative risk and incidence rate. But the spatial pattern almost remains constant as the population exposed, pollutant concentration, and likewise the incidence rate was constant.

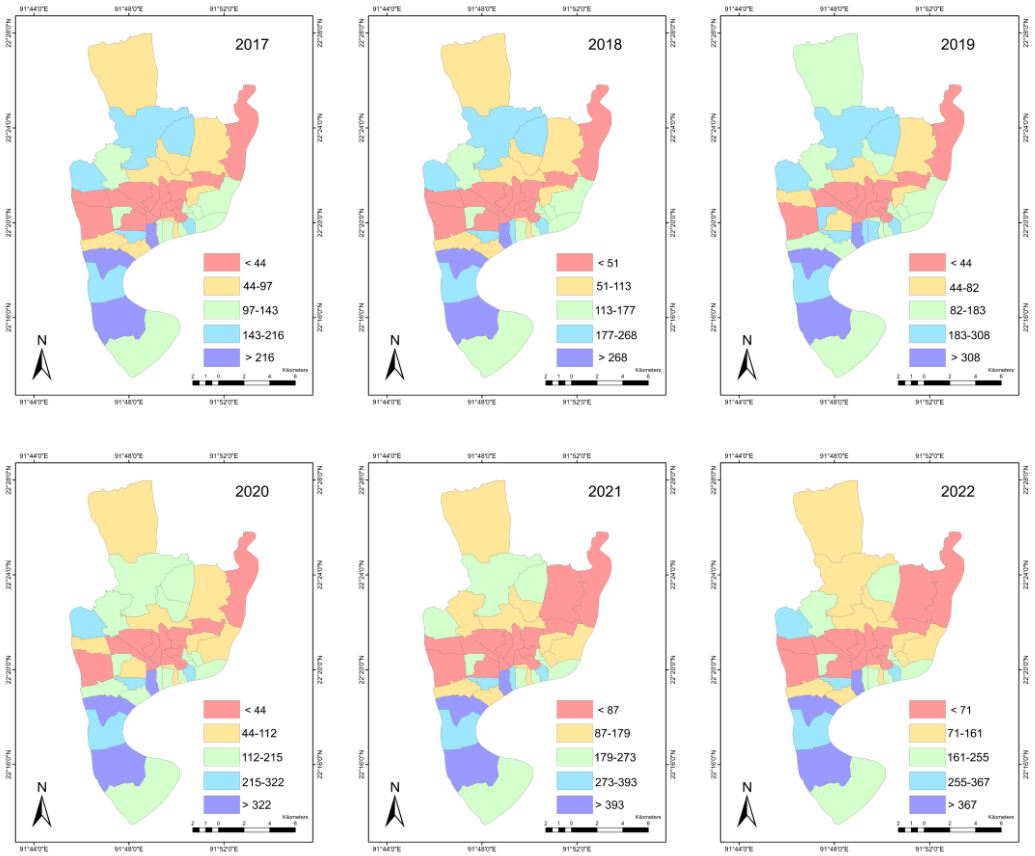

Fig. 4.33 Spatial pattern of premature incidences due to Work Loss Days

Temporal pattern of premature incidences of asthma and lower respiratory infections (age group 5-17)

Exposure to $PM_{2.5}$ is associated with a high incidence of asthma and lower respiratory infections in children aged 5 to 17 years old, according to the literature (Nishikawa et al., 2021; Roy et al., 2023; Tian et al., 2019), which are being evaluated as discrete medical concerns in this study. Each of these conditions presents with unique symptom profiles, encompassing features like hay fever-like symptoms, chest constriction, ongoing coughing, nasal congestion, and various other respiratory challenges, including chest sensations and breathing difficulties.

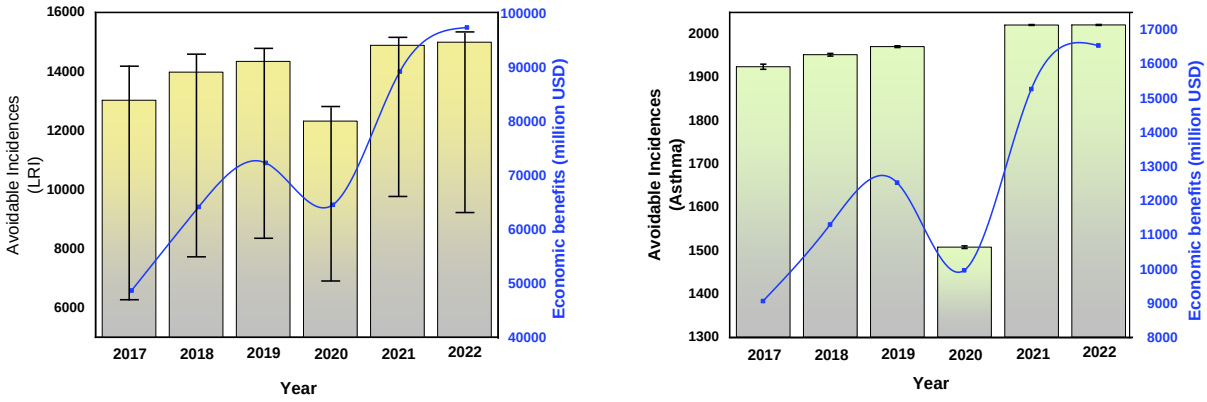

(a) (b)

Fig. 4.34 Premature incidences due to (a) asthma and (b) lower respiratory infections

N.B. (Box Plot represents $PM_{2.5}$ related premature incidences-Left Y axis and Line Graph represents Economic Benefits in million USD-Right Y axis)

Thoroughly analyzing these separate categories emphasizes the potential impact on children's ability to participate in school and partake in their typical routines, as it could potentially lead to absenteeism and hinder their involvement in school-related endeavors.

When compared to the mean data, the health incidence of asthma shows consistent patterns between the 2.5th and 97.5th percentiles. Furthermore, the preventable incidents for 2021 and 2022 are extremely comparable to one another. The top preventable asthma cases were 2020, and the peak for LRI was 14992 cases in the year 2022 showed in Fig. 4.34. The economic cost associated with asthma occurrences ranges from 9075 USD to 16552 USD using the World Bank assigned economic values. Similarly, it is anticipated that from 2017 to 2022, the economic burden of LRI (lower respiratory infections) will be between 48851 USD and 97449 USD. A large variation can be seen in the cumulative number, and this is mainly due to the incidence rate. Compared to a prior study conducted in the United States, a decrease in $PM_{2.5}$ levels relating to asthma exacerbations resulted in approximately 71,00 preventable incidents, along with 23,000 premature cases of lower respiratory infections (LRIs) (Neumann et al., 2021) . A variation could be found in the number with this study as there is differences in population and air quality scenarios. The economic estimates of 2.5 and 9.75 percentiles are provided in Table A.12 and A.13.

Spatial pattern of premature incidences of asthma and lower respiratory infections (age group (5-17)

There exist variations in the spatial distributions of the two health outcomes presented in Fig. 4.35 and 4.36. This is due to the relative risk and incidence rate as the other two parameters are kept constant.

The most premature incidents for both the outcomes occur in North Patenga (W-40). In Fig. 4.35 and 4.36 there are visibly some differences in some wards, such as Jalalabad (W-2) and Panchlaish (W-3), which had fewer preventable incidents in 2018 because of lower population density. North Halishahar (W-26), North Kattali (W-10), and South Middle Halishahar (W-38) also vary from the norm in

2020. Nevertheless, over the years under consideration, the geographic variance of asthma has remained largely constant.

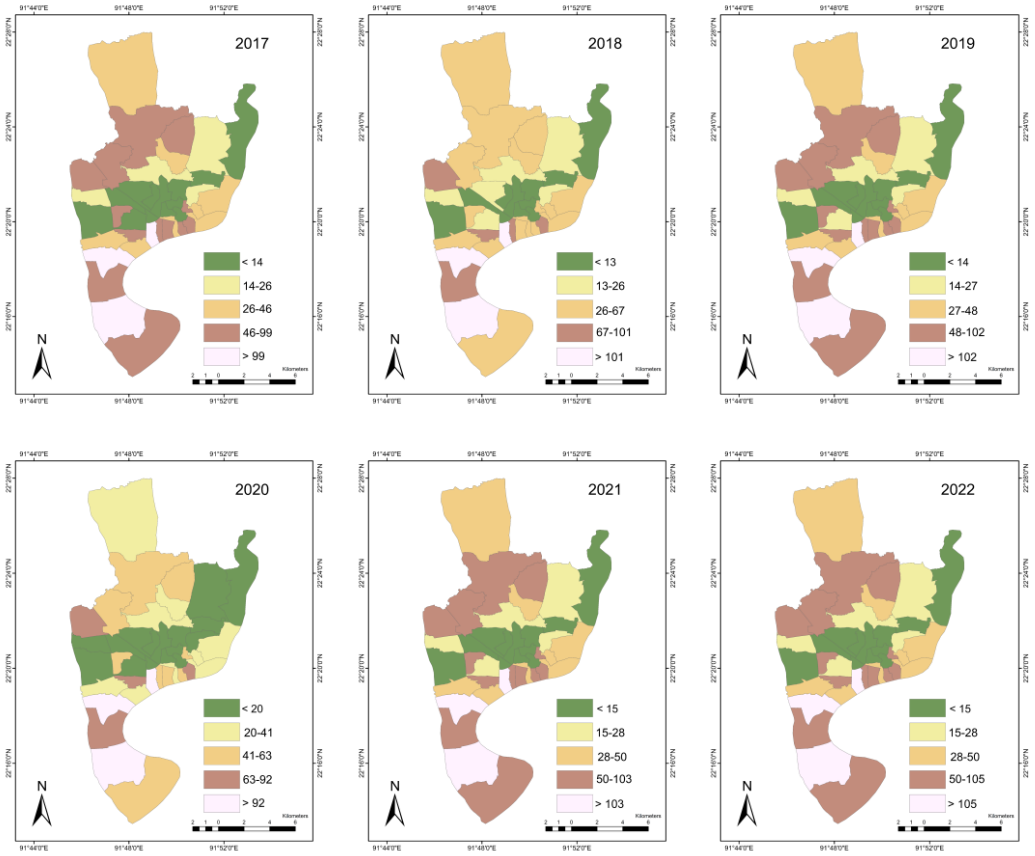

Fig. 4.35 Spatial pattern of the premature incidences due to asthma

Based on the incidence rate of lower respiratory symptoms, it's evident that the occurrence rate is greater than that of asthma. Consequently, the incidences in each ward are significantly higher than those related to asthma outcomes. This dynamic contributes to certain wards having a higher number of preventable cases, causing disparities in geographical distribution patterns. Also, relative risk of the two health outcomes is different which caused a variation in the spatial distribution. A spatial representation of premature health incidences due to lower respiratory infections is provided in Fig. 4.36.

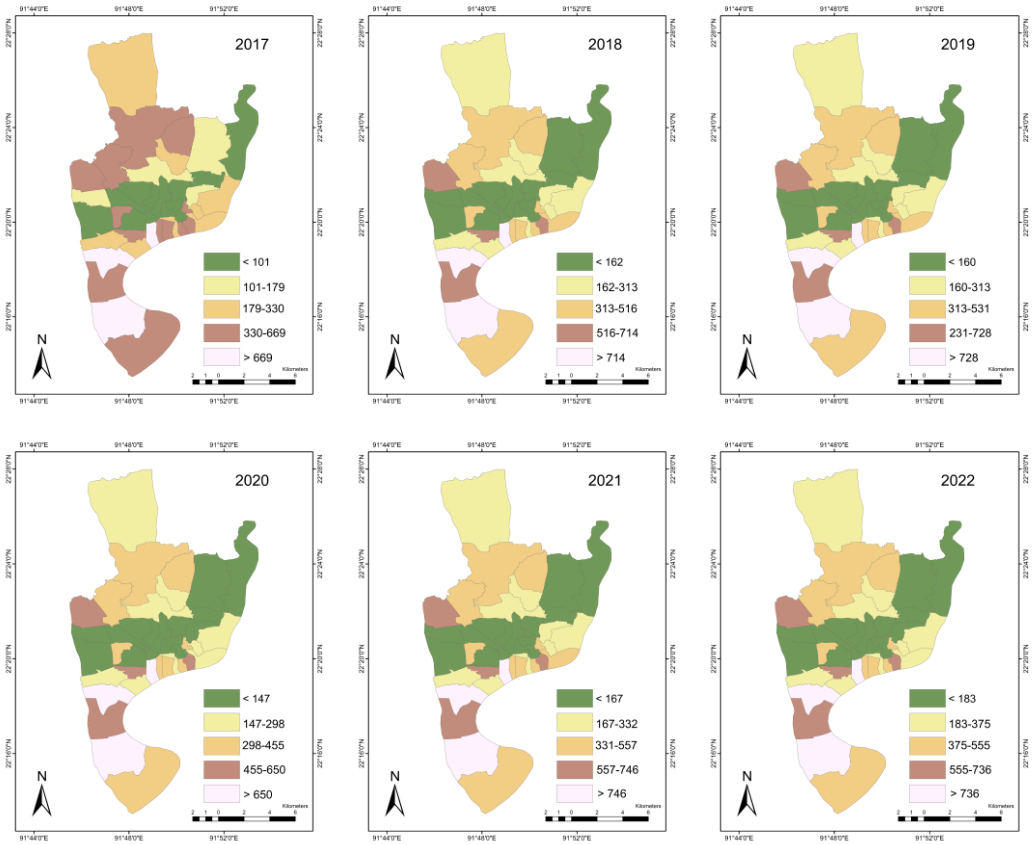

Fig. 4.36 Spatial pattern of the premature incidences due to LRI

4.6 Particulate Matter reported death and Contribution to GDP

Air pollution results in escalated expenses for environmental remediation, diminished consumer expenditure, and early death. Furthermore, it can have adverse effects on educational achievement and long-term earnings (Barker, 1995; Currie and Vogl, 2013). According to a study carried out in India, reducing air pollution to safe levels has the potential to reduce health costs by 10% (Gupta, 2008). In developing countries, a 20% improvement in air quality may result in a 1.3-hour increase in working hours (Hanna and Oliva, 2016).

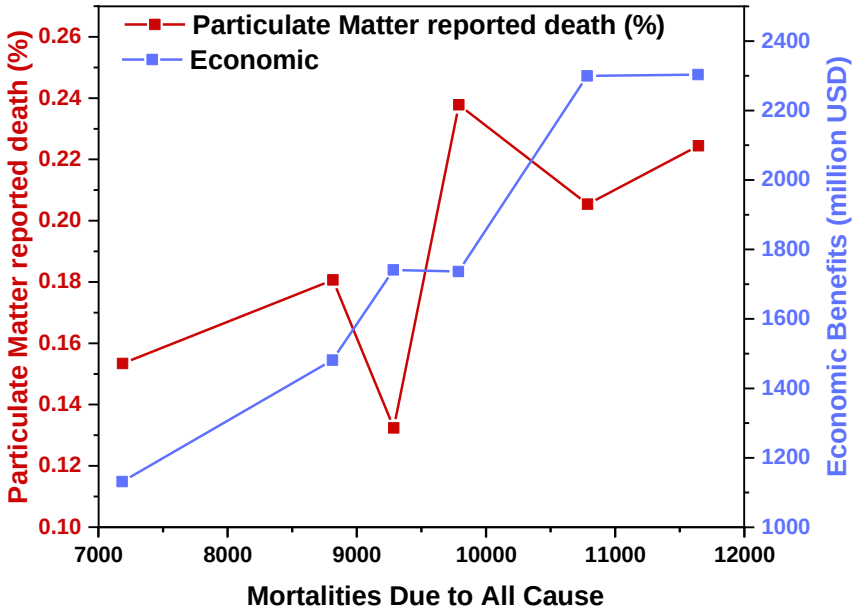

Fig. 4.37 Particulate Matter Reported Death due to all cause and economic benefits

N.B. (Left Y axis-represents Particulate Matter reported death and Right Y axis represents Economic Benefits in million USD)

The Fig. 4.37 displays the particulate matter reported death as well as the associated economic benefit. Notably, based on information from the Central Intelligence Agency (CIA), Bangladesh's GDP for 2023 was estimated at 460.2 billion US dollars (PPP-adjusted) (*The World Bank*, 2023). The Particulate matter reported death was estimated to be between 13% to 22%. For 197651 premature mortalities the particulate matter reported death was 22 % with an economic cost of 2300 million USD. Again for 157408 mortalities the PM reported death was 13 % with an economic cost of 1131 million USD. So, the cost is aligned with the reported death. The more the reported death the more cost a country needs to bear which is a burden to GDP. In 2016, the average $PM_{2.5}$ related mortality rate in the 74 cities of China were 32% after the reduction in particulate matter (Fang et al., 2016). The mortality rates vary with $PM_{2.5}$ concentration. In a study in USA,

$PM_{2.5}$ related mortality of about 5.92% from three specific causes in 2010 (Apte et al., 2015). A combined mortality of 13% was estimated China due to the reduction in particulate matter (Cheng et al 2013). A mortality of about 13 to 20 percentages were also estimated in China in another study (G. Yang et al., 2013). The cumulative cost of all mortalities and morbidities is presented in the Table 4.4. The highest cumulative cost is almost 0.82% of Bangladesh GDP obtained for the year 2021 (465 Billion USD). The study in China accounted for 0.64 % of GDP, 0.40 %, 1.2%, 2.1, 1.6% which is close to ours result (Cheng et al 2013; G. Yang et al., 2013; Nasari et al., 2016; Wu et al., 2021).

Table 4.4. Summary of Economic Benefits and in relation to GDP

Mortalityand Morbidity effects	2017	2018	2019	2020	2021	2022
Economic Benefits (USD)						
All Cause	1.13E+09	1.48E+09	1.73E+09	1.74E+09	2.3E+09	2.3E+09
Hospital Admission	653756.5	1026312	1319023	1284642	2012651	1893174
Minor Restricted Activity Days	89850.73	135054.7	160897.5	162759.6	219885.4	227066
Work loss days	17526.66	27185.49	32800.71	17379.5	46603.43	47066.32
LRI	48851	64295	72420	64685	89312	97449
Asthma	9075	11316	12542	9975	15279	16553
Total	1.88E+09	2.40E+09	2.87E+09	2.83E+09	3.80E+09	3.83E+09
As a ratio of GDP (%)	0.40	0.52	0.62	0.61	0.82	0.82

Comparing GDP is a complex endeavour due to the utilisation of several valuation methodologies, including willingness-to-pay (WTP), human capital (HC), and cost-of-illness (COI) approaches. Furthermore, the assessment of health points is an important criterion. In this study, comparative analysis has been conducted between the Gross Domestic Product (GDP) and various health indicators, including all-cause mortality, hospital admissions, work loss days

(WLD), medically restricted activity days (MRAD), asthma, and lower respiratory infections (LRI).

4.7 Comparison of BenMAP-CE simulation between WHO and BNAAQS threshold value simulation

The threshold value of WHO is 10 μg/m^3 and 20 μg/m^3 for and $PM_{2.5}$ and PM_{10} respectively whereas the standard value of BNAAQS is 15μg/m^3 and 50 μg/m^3 for $PM_{2.5}$ and PM_{10} respectively. The variations in these threshold values clearly illustrate that, between the two control exposure standards, WHO is more stringent than BNAAQS. These variations are depicted in Fig. 4.38 and 4.39 showing only the point estimates. These variations are consistent with other studies (Bayat, Planning, et al., 2019; Manojkumar and Srimuruganandam, 2021; Nasari et al., 2016; Wu et al., 2021).

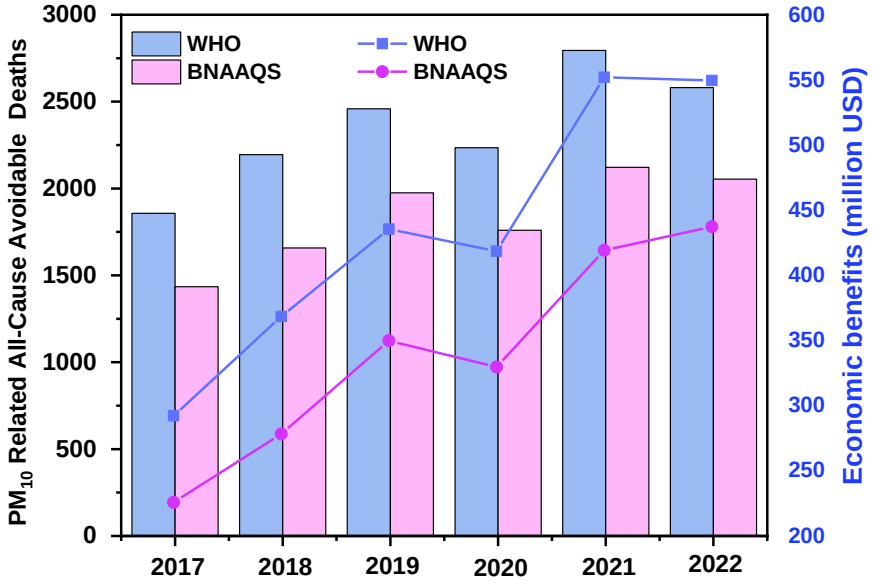

Fig. 4.38 Comparison of PM_{10} related premature deaths and economic benefits as per WHO and NAAQS simulations

N.B. (Box plot represents PM_{10} reported death-Left Y axis and Line Graph represents Economic Benefits in million USD-Right Y axis)

As depicted in Fig. 4.38, there are more premature incidents in the case of WHO simulations compared to BNAAQS simulations. This is primarily due to the more stringent threshold values set by WHO. Given the higher number of premature incidents in the WHO scenario, the economic benefits are also greater in this case. The same trend can be observed in Fig. 4.39. Furthermore, the number of premature health incidents is higher in the BNAAQS simulation for the year 2021, similar to the trend observed in other health endpoints in the WHO simulation. It's worth noting that the year 2020 saw a decline in premature health incidents, attributed to the pandemic situation and the resulting improvement in air quality.

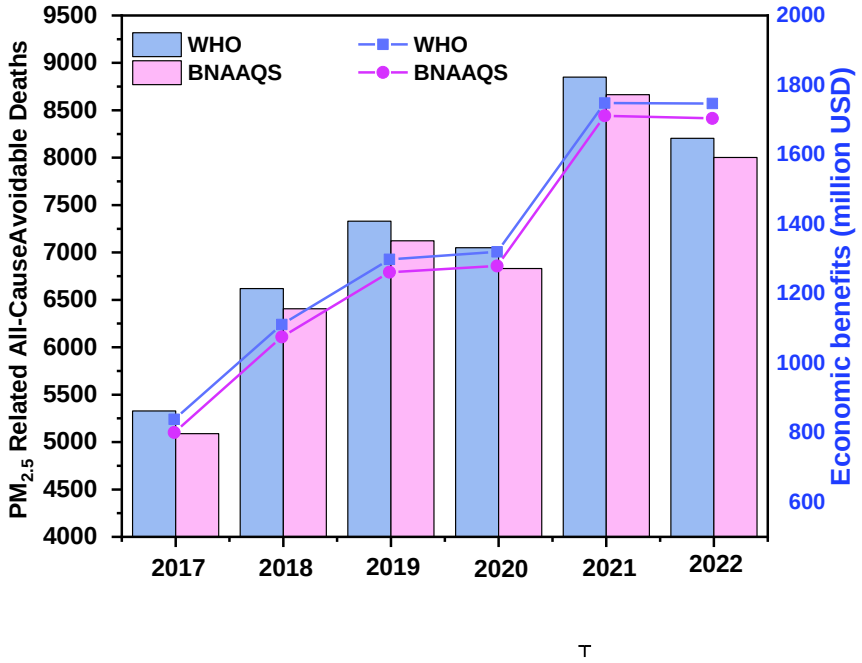

Fig. 4.39 40 Comparison of $PM_{2.5}$ related premature deaths and economic benefits as per WHO and NAAQS simulations

N.B. (Box plot represents PM_{10} reported death-Left Y axis and Line Graph represents Economic Benefits in million USD-Right Y axis)

The comparison between Fig. 4.38 and 4.39 highlights a substantial and noticeable difference, particularly in the case of PM_{10}, where the WHO threshold

value is 2.5 times higher than the BNAAQS value. This variation results in a more evident difference in economic benefits between the two simulations, as shown in Fig. 4.38. However, for $PM_{2.5}$, the WHO threshold value being only 1.5 times that of BNAAQS brings the results between the two simulations closer. Therefore, to portray the scenario with the highest premature incidents and economic benefits, the WHO simulation was utilized for all the analyses.

4.8 Summary of the results

In the bustling landscape of Chattogram City Corporation (CCC), persistent combat against air pollution is taking place, uncovering significant revelations through a comprehensive study utilizing the BenMAP-CE tool This meticulous examination explores diverse scenarios recommended by both the World Health Organization (WHO) and NAAQS, homing in on the impact of particulate matter and heavy metals, weaving a nuanced narrative of their environmental repercussions. The utilization of Landsat-8 imaging emerges as a pivotal element, contributing significantly to the accurate prediction of $PM_{2.5}$ and PM_{10} concentrations, showcasing an impressive R^2 value of 0.654 and 0.516, respectively. Across the city, ambient particulate matter concentrations exhibit a broad spectrum, with specific zones surpassing health guidelines during the dry season. PM concentrations soar to alarming levels, exceeding BNAAQS and WHO threshold values, indicating a hazardous situation linked to health risks. Notably, heavy metals, while not directly correlated with particulate matter, concentrate in zones marked by industrial and commercial pollution, posing a considerable health threat. Average concentrations of heavy metals like Cu, Ni, Cr, Zn, and Fe are striking, underscoring the gravity of the situation. The association between particulate matter and an estimated 7,185 premature fatalities in 2017 reveals a concerning trend, with numerical fluctuations tied to prevailing circumstances. The economic impact of averting deaths ranges from

1.131 billion to 2.297 billion US dollars within CCC, with cardiovascular deaths surpassing respiratory deaths by 0.15 to 0.17 times. Contributions of Cardiovascular and Respiratory diseases to all-cause mortality unveil crucial insights, contributing 0.07% and 0.2% to GDP, respectively. Ratios of death contributions and non-accidental health endpoints provide a nuanced perspective, with GEMM estimates surpassing LL models. Cause-specific death analysis for $PM_{2.5}$ indicates a hierarchy with IHD> Stroke>COPD>LRI>LC. Morbidity costs, avoidable hospital admissions, and economic benefits add depth to the study, emphasizing the multifaceted impact on cardiac and respiratory outcomes. In essence, this study, within the broader context of Bangladesh's GDP, encapsulates a holistic understanding of environmental challenges and their intricate interplay with health and economy in CCC, providing a compelling call to action.

Chapter 5. CONCLUSIONS and RECOMMENDATIONS

5.1 General

The intent of this study was to assess the execution of a policy that is in conformity with the standards set by the Bangladesh National Ambient Air Quality Standard (BNAAQS) and World Health Organisation (WHO), using the BenMAP-CE tool. The primary focus of the study revolved around utilising air quality modelling to estimate levels of particulate matter in Chattogram City Corporation. Additionally, an evaluation was conducted to determine the health effects related with airborne particulate matter. The research also aimed to evaluate the health implications of heavy metal pollution in particulate matter. Chapter 4 provides a comprehensive analysis of the primary outcomes and deductions derived from the study. This section offers a succinct summary of the notable results, acknowledges the diverse constraints encountered during the study, and finishes by proposing suggestions for prospective directions of future research.

5.2 Conclusions

The present study has yielded significant findings pertaining to the impact on air quality and human health, achieved through a comprehensive analysis that involved the comparison policy scenarios recommended by WHO and NAAQS. The focus of analysis encompassed two pollutants, particulate matter, and their examination incorporated various metrics, including concentration levels, excess premature mortality, economic co-benefits, and policy cost offset. Additionally, the study also took into account the presence of heavy metals and its related carcinogenic and non-carcinogenic effect in its assessment. Data included in the tool were model and monitor data of Particulate matter, Gridded Population data

from Worldpop data, mortality and morbidity rates from IHME, relative risk from epidemiological studies, and economic value of each health endpoint from World Bank and other relevant literature. The major conclusions from the study are as follows:

- The temporal trend of particulate matter concentrations demonstrated a significant rise between 2017 and 2019, succeeded by a reduction in 2020, a zenith in 2021, and a marginal decline in 2022. The trend exhibited a high degree of conformity with the spatial variability that was observed throughout the corresponding time frame. Nevertheless, certain discrepancies were observed at particular locations, potentially ascribed to variables such as unanticipated urbanisation initiatives or insufficient public knowledge.
- The analysis revealed that selected trace metals, including Zn, Fe, Cu, Cr, Mn, and Ni, present in particulate matter or air pollutants, exceeded the desirable values, indicating elevated concentrations. Additionally, their degree of contamination ranged from moderate to considerable. While these metals on their own may not pose immediate health risks, their presence at these levels, especially in conjunction with particulate matter, has the potential to exacerbate health issues associated with particulate pollution.
- The BenMAP-CE tool demonstrated substantial health and economic benefits from air quality improvement policies in CCC. The study estimated the prevention of 7185 to 11643 premature deaths due to all cause health outcome, resulting in an economic benefit ranging from 1.131 billion US dollars to 2.297 billion US dollars, contributing 0.45% to 0.82% to the GDP. Cardiovascular diseases accounted for more premature deaths than respiratory diseases, and 5-causes of death were ranked as IHD>Stroke>COPD>LRI>LC. Additionally, the age group 5 to 17 exhibited premature morbidity effects related to asthma

and lower respiratory infections. As the incidence rate of LRI was higher than asthma so the premature incidences were higher in case of LRI for child group. Apart from it BenMAP-CE showed an premature case of 22603 to 34573 minor restricted activity days, 3123 to 7327 work loss days and 2894 to 4932 of premature hospital admission due to both cardiac and respiratory outcomes. The observed rise in PM levels couldn't be attributed solely to population growth and was influenced by various factors, including differences in air quality and relative risk. This conclusion is supported by the findings of numerous relative risk models.

5.3 Limitations

Assessing the study's result uncertainty rigorously is challenging due to the lack of pertinent data. Nevertheless, it is valuable to pinpoint and discuss the primary sources of uncertainty, as this not only aids in a better understanding of the findings but also contributes to improving future investigation. The limitations of the study are stated here.

- This study tried to assume the toxicity of particulate matter along with chemical composition. However, it could not consider all the chemical composition due to unavailability of the reagent. Hence only six heavy metal risks were assessed.
- Epidemiological Studies relating to particulate matter with various health endpoints are not available in our country and thus there is a need for conducting such studies.
- Due to inaccessibility of city specific baseline rate this study assumed the rate to be same among all the cities in the study while there may be substantial disparities due to social economics, environments and health services.

- Also, the population in a city exposed by the same average particulate matter concentration although the personal exposure in a city indicated high space time variation (Jyoti et al.,2017)
- Also, the valuation method, choice of health impact value, inflation and discount rate adjustment may overestimate or underestimate the monetary cost.

5.4 Implications of the study

The Health Impact Assessment (HIA) analysis by BenMAP-CE revealed that air pollution has a significant impact on public health in areas characterized by high concentrations of polluted air and substantial populations. This finding suggests that the public health consequences of air quality in metropolitan areas with lower to moderate exposure levels should not be overlooked. From a public health perspective, the study's estimates indicate that merely reducing particulate matter (PM) concentrations in the Chattogram City Corporation (CCC) area to meet World Health Organization threshold values and BNAAQS is insufficient. More robust measures are required to safeguard public health. Furthermore, HIA-AQ, or the Health Impact Assessment of Air Quality, is a useful tool for assessing the impact of various pollutants on human health. Data on other air pollutants, such as ozone, sulfur dioxide, carbon monoxide, and polycyclic aromatic hydrocarbons (PAHs), should also be considered for future research, with a focus on fine PM and its component parts. The present study surely provides a hands-on cause-affect-benefits mapping to be used by a variety of stakeholders, including policy makers, public health professionals, environmental scientists, and community groups for understanding the health and economic impacts of air pollution and for developing strategies to improve air quality. This study provides an important synergy for quantifying health and economic benefits derived from urban air quality improvement. This gist of

analysis is always helpful for decision makers to adopt policy making into the environmental accounting and auditing perspectives.

5.5 Recommendations for future study

This study represents the inaugural effort in this country to examine the potential discrepancies resulting from different exposure windows, such as the GEMM model and LL model, when estimating the mortality burden and economic costs attributed to particulate matter in CCC area from 2017 to 2022. It also illuminates the distribution patterns of mortality burden within two distinct age groups: children and adults. Furthermore, this research aims to establish a link between the airborne dust particle, particularly heavy metals, and its health risk assessment. Notably, the study adopted the WHO standard, most stringent scenario in this study, as the Bangladesh National Ambient Air Quality Standard is relatively less stringent compared to the standards set by the WHO. In this subject, there exist ample prospects for comprehensive study and development. The following suggestions are made for upcoming studies in this field.

- In future modeling studies, it is essential to move beyond considering overall emissions and focus on the source apportionment of emissions. This entails examining emissions from specific sources such as roadside dust, industries such as cement factories, power plants, brick kilns, traffic, open burning, and other relevant contributors. By delving into source-specific emissions, this study can gain a more detailed and nuanced understanding of the sources and their respective impacts on air quality and public health.
- A comparison of the study's findings could be conducted using alternative health effect assessment models.

REFERENCES

Abd Elnabi, M. K., Elkaliny, N. E., Elyazied, M. M., Azab, S. H., Elkhalifa, S. A., Elmasry, S., Mouhamed, M. S., Shalamesh, E. M., Alhorieny, N. A., Abd Elaty, A. E., Elgendy, I. M., Etman, A. E., Saad, K. E., Tsigkou, K., Ali, S. S., Kornaros, M., and Mahmoud, Y. A.-G. (2023). Toxicity of Heavy Metals and Recent Advances in Their Removal: A Review. *Toxics*, *11*(7), 580. https://doi.org/10.3390/toxics11070580

Abel, D. W., Holloway, T., Harkey, M., Meier, P., Ahl, D., Limaye, V. S., and Patz, J. A. (2018). Air-quality-related health impacts from climate change and from adaptation of cooling demand for buildings in the eastern United States: An interdisciplinary modeling study. *PLOS Medicine*, *15*(7), e1002599. https://doi.org/10.1371/journal.pmed.1002599

Abelsohn, A., Stieb, D., Sanborn, M. D., and Weir, E. (2002). Identifying and managing adverse environmental health effects: 2. Outdoor air pollution. *Canadian Medical Association Journal*, *166*(9), 1161. http://www.cmaj.ca/content/166/9/1161.abstract

ADB and CAI Asia. (2006). *A CAI-Asia Program Sustainable Urban Transport in Asia Making the Vision a Reality*.

Ahmed, F., Bibi, M. H., and Ishiga, H. (2007). Environmental assessment of Dhaka City (Bangladesh) based on trace metal contents in road dusts. *Environmental Geology*, *51*(6), 975–985. https://doi.org/10.1007/s00254-006-0367-1

Ahmed, M., Guo, X., and Zhao, X.-M. (2016). Determination and analysis of trace metals and surfactant in air particulate matter during biomass burning haze episode in Malaysia. *Atmospheric Environment*, *141*, 219–229. https://doi.org/10.1016/j.atmosenv.2016.06.066

AIR CLEANERS FOR PARTICULATE CONTAMINANTS. (2020).

Air Pollution and Climate Change. (2002). https://www.rifs-potsdam.de/en/output/dossiers/air-pollution-and-climate-change

Alamgir, M., Islam, M., Hossain, N., Kibria, M., and Rahman, M. (2015). Assessment of Heavy Metal Contamination in Urban Soils of Chittagong City, Bangladesh. *International Journal of Plant and Soil Science*, *7*(6), 362–372. https://doi.org/10.9734/ijpss/2015/18424

Aldegunde, J. A. Á., Bolaños, E. Q., Fernández-Sánchez, A., Saba, M., and Caraballo, L. (2023). Environmental and Health Benefits Assessment of Reducing PM2.5 Concentrations in Urban Areas in Developing Countries: Case Study Cartagena de Indias. *Environments*, *10*(3), 42. https://doi.org/10.3390/environments10030042

Alfaro, M. R., Montero, A., Ugarte, O. M., do Nascimento, C. W. A., de Aguiar Accioly, A. M., Biondi, C. M., and da Silva, Y. J. A. B. (2015). Background concentrations and reference values for heavy metals in soils of Cuba. *Environmental Monitoring and Assessment*, *187*(1), 4198. https://doi.org/10.1007/s10661-014-4198-3

Alvarez-Mendoza, C. I., Teodoro, A. C., Torres, N., and Vivanco, V. (2019). Assessment of Remote Sensing Data to Model PM10 Estimation in Cities with a Low Number of Air Quality Stations: A Case of Study in Quito, Ecuador. *Environments*, *6*(7), 85. https://doi.org/10.3390/environments6070085

American Cancer Society. (2022). https://www.cancer.org/cancer/risk-prevention/understanding-cancer-risk/known-and-probable-human-carcinogens.html

Ametepey, S. T., Cobbina, S. J., Akpabey, F. J., Duwiejuah, A. B., and Abuntori, Z. N. (2018). Health risk assessment and heavy metal contamination levels in vegetables from Tamale Metropolis, Ghana. *International Journal of Food Contamination*, *5*(1), 5. https://doi.org/10.1186/s40550-018-0067-0

Amsalu, E., Wang, T., Li, H., Liu, Y., Wang, A., Liu, X., Tao, L., Luo, Y., Zhang, F., Yang, X., Li, X., Wang, W., and Guo, X. (2019). Acute effects of fine particulate matter (PM2.5) on hospital admissions for cardiovascular disease in Beijing, China: a time-series study. *Environmental Health*, *18*(1), 70. https://doi.org/10.1186/s12940-019-0506-2

Anenberg, S. C., Belova, A., Brandt, J., Fann, N., Greco, S., Guttikunda, S., Heroux, M.-E., Hurley, F., Krzyzanowski, M., Medina, S., Miller, B., Pandey, K., Roos, J., and Van Dingenen, R. (2016a). Survey of Ambient Air Pollution Health Risk Assessment Tools. *Risk Analysis*, *36*(9), 1718–1736. https://doi.org/10.1111/risa.12540

Anenberg, S. C., Belova, A., Brandt, J., Fann, N., Greco, S., Guttikunda, S., Heroux, M.-E., Hurley, F., Krzyzanowski, M., Medina, S., Miller, B., Pandey, K., Roos, J., and Van Dingenen, R. (2016b). Survey of Ambient Air Pollution Health Risk Assessment Tools. *Risk Analysis*, *36*(9), 1718–1736. https://doi.org/10.1111/risa.12540

Apte, J. S., Marshall, J. D., Cohen, A. J., and Brauer, M. (2015). Addressing Global Mortality from Ambient PM $_{2.5}$. *Environmental Science and Technology*, *49*(13), 8057–8066. https://doi.org/10.1021/acs.est.5b01236

Assi, M. A., Hezmee, M. N. M., Haron, A. W., Sabri, M. Y., and Rajion, M. A. (2016). The detrimental effects of lead on human and animal health. *Veterinary World*, *9*(6), 660–671. https://doi.org/10.14202/vetworld.2016.660-671

Azeh Engwa, G., Udoka Ferdinand, P., Nweke Nwalo, F., and N. Unachukwu, M. (2019). Mechanism and Health Effects of Heavy Metal Toxicity in Humans. In

Poisoning in the Modern World - New Tricks for an Old Dog? IntechOpen. https://doi.org/10.5772/intechopen.82511

Badaloni, C., Cesaroni, G., Cerza, F., Davoli, M., Brunekreef, B., and Forastiere, F. (2017). Effects of long-term exposure to particulate matter and metal components on mortality in the Rome longitudinal study. *Environment International*, *109*, 146–154. https://doi.org/10.1016/j.envint.2017.09.005

Balali-Mood, M., Naseri, K., Tahergorabi, Z., Khazdair, M. R., and Sadeghi, M. (2021). Toxic Mechanisms of Five Heavy Metals: Mercury, Lead, Chromium, Cadmium, and Arsenic. *Frontiers in Pharmacology*, *12*. https://doi.org/10.3389/fphar.2021.643972

Balmes, J. R., Fine, J. M., and Sheppard, D. (1987). Symptomatic Bronchoconstriction after Short-Term Inhalation of Sulfur Dioxide. *American Review of Respiratory Disease*, *136*(5), 1117–1121. https://doi.org/10.1164/ajrccm/136.5.1117

Baltas, H., Sirin, M., Gökbayrak, E., and Ozcelik, A. E. (2020). A case study on pollution and a human health risk assessment of heavy metals in agricultural soils around Sinop province, Turkey. *Chemosphere*, *241*, 125015. https://doi.org/10.1016/j.chemosphere.2019.125015

Bangladesh. Parisaṃkhyāna Byuro. Statistics and Informatics Division. (2011). *Bangladesh population and housing census, 2011. National report.*

Bayat, R., Ashrafi, K., Shafiepour Motlagh, M., Hassanvand, M. S., Daroudi, R., Fink, G., and Künzli, N. (2019). Health impact and related cost of ambient air pollution in Tehran. *Environmental Research*, *176*, 108547. https://doi.org/10.1016/j.envres.2019.108547

Bayat, R., Planning, T. U., Ashrafi, K., and Daroudi, R. (2019). *Estimation of Tehran's PM2.5 health effects, using BenMAP-CE*. *February 2020*.

BBS. (2002). http://203.112.218.65:8008/WebTestApplication/userfiles/Image/PopMonographs/Volume-12_UM.pdf

Begum, B. A., Biswas, S. K., and Hopke, P. K. (2011). Key issues in controlling air pollutants in Dhaka, Bangladesh. *Atmospheric Environment*, *45*(40), 7705–7713. https://doi.org/10.1016/j.atmosenv.2010.10.022

Begum, B. A., Biswas, S. K., Markwitz, A., and Hopke, P. K. (2010). Identification of Sources of Fine and Coarse Particulate Matter in Dhaka, Bangladesh. *Aerosol and Air Quality Research*, *10*(4), 345–353. https://doi.org/10.4209/aaqr.2009.12.0082

Begum, B. A., Hopke, P. K., and Markwitz, A. (2013a). Air pollution by fine particulate matter in Bangladesh. *Atmospheric Pollution Research*, *4*(1), 75–86. https://doi.org/10.5094/APR.2013.008

Begum, B. A., Hopke, P. K., and Markwitz, A. (2013b). Air pollution by fine particulate matter in Bangladesh. *Atmospheric Pollution Research*, *4*(1), 75–86. https://doi.org/10.5094/APR.2013.008

Bhasin, G., Kauser, H., and Athar, M. (2002). Iron augments stage-I and stage-II tumor promotion in murine skin. *Cancer Letters*, *183*(2), 113–122. https://doi.org/10.1016/S0304-3835(02)00116-7

Bhattacharya, S., Cropper, M., and Alberini, A. (2007). The Value of Mortality Risk Reductions in Delhi, India. *Journal of Risk and Uncertainty*, *34*, 21–47.

Biswas, S. K. (2019). *Clean Air and Sustainable Environment Project View project Particulate Matter and Black Carbon Monitoring at Urban Environment in Bangladesh View project Masud Rana Clean Air and Sustainable Environment Project 7 PUBLICATIONS 103 CITATIONS SEE PROFILE*. https://doi.org/10.13140/RG.2.2.14741.17128

Block, G. T., and Yeung, M. (1982). Asthma induced by nickel. *JAMA*, *247*(11), 1600–1602.

Bollati, V., Marinelli, B., Apostoli, P., Bonzini, M., Nordio, F., Hoxha, M., Pegoraro, V., Motta, V., Tarantini, L., Cantone, L., Schwartz, J., Bertazzi, P. A., and Baccarelli, A. (2010). Exposure to Metal-Rich Particulate Matter Modifies the Expression of Candidate MicroRNAs in Peripheral Blood Leukocytes. *Environmental Health Perspectives*, *118*(6), 763–768. https://doi.org/10.1289/ehp.0901300

Boningari, T., and Smirniotis, P. G. (2016). Impact of nitrogen oxides on the environment and human health: Mn-based materials for the NO x abatement. *Current Opinion in Chemical Engineering*, *13*, 133–141. https://doi.org/10.1016/j.coche.2016.09.004

Briffa, J., Sinagra, E., and Blundell, R. (2020a). Heavy metal pollution in the environment and their toxicological effects on humans. *Heliyon*, *6*(9), e04691. https://doi.org/10.1016/j.heliyon.2020.e04691

Briffa, J., Sinagra, E., and Blundell, R. (2020b). Heavy metal pollution in the environment and their toxicological effects on humans. *Heliyon*, *6*(9), e04691. https://doi.org/10.1016/j.heliyon.2020.e04691

Brunekreef, B., and Sunyer, J. (2003). Asthma, rhinitis and air pollution: is traffic to blame? *European Respiratory Journal*, *21*(6), 913–915. https://doi.org/10.1183/09031936.03.00014903

Burnett, R., Chen, H., Szyszkowicz, M., Fann, N., Hubbell, B., Pope, C. A., Apte, J. S., Brauer, M., Cohen, A., Weichenthal, S., Coggins, J., Di, Q., Brunekreef, B., Frostad, J., Lim, S. S., Kan, H., Walker, K. D., Thurston, G. D., Hayes, R. B., … Spadaro, J. V. (2018a). Global estimates of mortality associated with long-term exposure to

outdoor fine particulate matter. *Proceedings of the National Academy of Sciences*, *115*(38), 9592–9597. https://doi.org/10.1073/pnas.1803222115

Burnett, R., Chen, H., Szyszkowicz, M., Fann, N., Hubbell, B., Pope, C. A., Apte, J. S., Brauer, M., Cohen, A., Weichenthal, S., Coggins, J., Di, Q., Brunekreef, B., Frostad, J., Lim, S. S., Kan, H., Walker, K. D., Thurston, G. D., Hayes, R. B., … Spadaro, J. V. (2018b). Global estimates of mortality associated with longterm exposure to outdoor fine particulate matter. *Proceedings of the National Academy of Sciences of the United States of America*, *115*(38), 9592–9597. https://doi.org/10.1073/pnas.1803222115

Cai, J., Peng, C., Yu, S., Pei, Y., Liu, N., Wu, Y., Fu, Y., and Cheng, J. (2019). Association between PM2.5 Exposure and All-Cause, Non-Accidental, Accidental, Different Respiratory Diseases, Sex and Age Mortality in Shenzhen, China. *International Journal of Environmental Research and Public Health*, *16*(3), 401. https://doi.org/10.3390/ijerph16030401

Cesaroni, G., Badaloni, C., Gariazzo, C., Stafoggia, M., Sozzi, R., Davoli, M., and Forastiere, F. (2013). Long-term exposure to urban air pollution and mortality in a cohort of more than a million adults in Rome. *Environmental Health Perspectives*, *121*(3), 324–331. https://doi.org/10.1289/ehp.1205862

Chen, B., Hong, C., and Kan, H. (2004). Exposures and health outcomes from outdoor air pollutants in China. *Toxicology*, *198*(1–3), 291–300. https://doi.org/10.1016/j.tox.2004.02.005

Chen, L., and Bai, Z. (2017). Response to comment on "Assessment of population exposure to PM2.5 for mortality in China and its public health benefit based on BenMAP". *Environmental Pollution*, *231*, 1212. https://doi.org/10.1016/j.envpol.2017.06.003

Chen, L., Bai, Z., Kong, S., Han, B., You, Y., Ding, X., Du, S., and Liu, A. (2010). A land use regression for predicting NO2 and PM10 concentrations in different seasons in Tianjin region, China. *Journal of Environmental Sciences*, *22*(9). https://doi.org/10.1016/S1001-0742(09)60263-1

Chen, L., Shi, M., Gao, S., Li, S., Mao, J., Zhang, H., Sun, Y., Bai, Z., and Wang, Z. (2017). Assessment of population exposure to PM2.5 for mortality in China and its public health benefit based on BenMAP. *Environmental Pollution*, *221*, 311–317. https://doi.org/10.1016/j.envpol.2016.11.080

Chen, L., Shi, M., Li, S., Bai, Z., and Wang, Z. (2017). Combined use of land use regression and BenMAP for estimating public health benefits of reducing PM2.5 in Tianjin, China. *Atmospheric Environment*, *152*, 16–23. https://doi.org/10.1016/j.atmosenv.2016.12.023

Chen, L., Shi, M., Li, S., Gao, S., Zhang, H., Sun, Y., Mao, J., Bai, Z., Wang, Z., and Zhou, J. (2017). Quantifying public health benefits of environmental strategy of PM2.5 air quality management in Beijing–Tianjin–Hebei region, China. *Journal of Environmental Sciences (China)*, *57*, 33–40. https://doi.org/10.1016/j.jes.2016.11.014

Chen, X., Ward, T. J., Sarkar, C., Ho, K.-F., and Webster, C. (2022). Health risks of adults in Hong Kong related to inhalation of particle-bound heavy metal(loid)s. *Air Quality, Atmosphere and Health*, *15*(4), 691–706. https://doi.org/10.1007/s11869-021-01115-6

Choe, S.-Y., Kim, S.-J., Kim, H.-G., Lee, J. H., Choi, Y., Lee, H., and Kim, Y. (2003). Evaluation of estrogenicity of major heavy metals. *Science of The Total Environment*, *312*(1–3), 15–21. https://doi.org/10.1016/S0048-9697(03)00190-6

Chonokhuu, S., Batbold, C., Chuluunpurev, B., Battsengel, E., Dorjsuren, B., and Byambaa, B. (2019). Contamination and Health Risk Assessment of Heavy Metals in the Soil of Major Cities in Mongolia. *International Journal of Environmental Research and Public Health*, *16*(14), 2552. https://doi.org/10.3390/ijerph16142552

Climate Change and Food Security. (2010). NRC.

Computers in Earth and Environmental Sciences. (2022). Elsevier. https://doi.org/10.1016/C2020-0-03210-X

Cone, J. E. (1987). Occupational lung cancer. *Occupational Medicine (Philadelphia, Pa.)*, *2*(2), 273–295.

Conte, M., Gaioli, F., Perone, E., Sörensson, A., Svensson, T., and Tarela, P. (2002). *Valuation of Local Human Health Effects of GHG Mitigation Mariana Conte Grand (Universidad del CEMA) Impacts of Greenhouse and Local Gases Mitigation Options on Air Pollution in the Buenos Aires Metropolitan Area: Valuation of Human Health Effects* *.

Cowie, C. (2012). *Health Risk Assessment-Preliminary Work to Identify Concentration-Response Functions for Selected Ambient Air Pollutants Report prepared for EPA Victoria Bin Jalaludin*.

D. N. Moriasi, J. G. Arnold, M. W. Van Liew, R. L. Bingner, R. D. Harmel, and T. L. Veith. (2007). Model Evaluation Guidelines for Systematic Quantification of Accuracy in Watershed Simulations. *Transactions of the ASABE*, *50*(3), 885–900. https://doi.org/10.13031/2013.23153

Dalton, T. P., Kerzee, J. K., Wang, B., Miller, M., Dieter, M. Z., Lorenz, J. N., Shertzer, H. G., Nebert, D. W., and Puga, A. (2001). Dioxin Exposure Is an Environmental Risk Factor for Ischemic Heart Disease. *Cardiovascular Toxicology*, *1*(4), 285–298. https://doi.org/10.1385/CT:1:4:285

Davidson, K., Hallberg, A., Mccubbin, D., and Hubbell, B. (2007). *ANALYSIS OF PM 2.5 USING BENMAP 203 ANALYSIS OF PM 2.5 USING THE ENVIRONMENTAL BENEFITS MAPPING AND ANALYSIS PROGRAM (BENMAP)*. http://www.camx.com;

DEFRA. (2008). *An Economic Analysis to inform the Air Quality Strategy*. www.defra.gov.uk

Deletic, A., and Orr, D. W. (2005). Pollution Buildup on Road Surfaces. *Journal of Environmental Engineering*, *131*(1), 49–59. https://doi.org/10.1061/(ASCE)0733-9372(2005)131:1(49)

Dhaka Tribune. (2023). *Dhaka Tribune*. https://www.dhakatribune.com/bangladesh/262762/study-dhaka-sees-7%25-rise-in-air-pollution-in-2021

Dihan, M. R., Abu Nayeem, S. M., Roy, H., Islam, Md. S., Islam, A., Alsukaibi, A. K. D., and Awual, Md. R. (2023). Healthcare waste in Bangladesh: Current status, the impact of Covid-19 and sustainable management with life cycle and circular economy framework. *Science of The Total Environment*, *871*, 162083. https://doi.org/10.1016/j.scitotenv.2023.162083

Ding, D., Xing, J., Wang, S., Liu, K., and Hao, J. (2019a). Estimated contributions of emissions controls, meteorological factors, population growth, and changes in baseline mortality to reductions in ambient pm2:5 and pm2:5-related mortality in china, 2013–2017. *Environmental Health Perspectives*, *127*(6). https://doi.org/10.1289/EHP4157

Ding, D., Xing, J., Wang, S., Liu, K., and Hao, J. (2019b). Estimated contributions of emissions controls, meteorological factors, population growth, and changes in baseline mortality to reductions in ambient pm2:5 and pm2:5-related mortality in china, 2013–2017. *Environmental Health Perspectives*, *127*(6). https://doi.org/10.1289/EHP4157

Ding, D., Xing, J., Wang, S., Liu, K., and Hao, J. (2019c). Estimated contributions of emissions controls, meteorological factors, population growth, and changes in baseline mortality to reductions in ambient pm2:5 and pm2:5-related mortality in china, 2013–2017. *Environmental Health Perspectives*, *127*(6), 1–12. https://doi.org/10.1289/EHP4157

Ding, D., Zhu, Y., Jang, C., Lin, C. J., Wang, S., Fu, J., Gao, J., Deng, S., Xie, J., and Qiu, X. (2016). Evaluation of health benefit using BenMAP-CE with an integrated scheme of model and monitor data during Guangzhou Asian Games. *Journal of Environmental Sciences (China)*, *42*, 9–18. https://doi.org/10.1016/j.jes.2015.06.003

Dockery, D. W., and Pope III, C. A. (1994). ACUTE RESPIRATORY EFFECTS OF PARTICULATE AIR POLLUTION. In *Annu. Rev. Public Health* (Vol. 15). www.annualreviews.org

Dockery et al. (1993). *NEJM199312093292401*.

DoE. (2012). *"Air Pollution Reduction Strategy for Bangladesh Final Report."* https://www.semanticscholar.org/paper/Air-Pollution-Reduction-Strategy-for-Bangladesh/a162734badbb64d530d55708226e4eacb4d12a39

Duong, T. T. T., and Lee, B.-K. (2011). Determining contamination level of heavy metals in road dust from busy traffic areas with different characteristics. *Journal of Environmental Management*, *92*(3), 554–562. https://doi.org/10.1016/j.jenvman.2010.09.010

Ebrahimi, M., Khalili, N., Razi, S., Keshavarz-Fathi, M., Khalili, N., and Rezaei, N. (2020). Effects of lead and cadmium on the immune system and cancer progression. *Journal of Environmental Health Science and Engineering*, *18*(1), 335–343. https://doi.org/10.1007/s40201-020-00455-2

Faiz, Y., Siddique, N., and Tufail, M. (2012). Pollution level and health risk assessment of road dust from an expressway. *Journal of Environmental Science and Health - Part A Toxic/Hazardous Substances and Environmental Engineering*, *47*(6), 818–829. https://doi.org/10.1080/10934529.2012.664994

Fang, D., Wang, Q., Li, H., Yu, Y., Lu, Y., and Qian, X. (2016a). Mortality effects assessment of ambient PM2.5 pollution in the 74 leading cities of China. *Science of the Total Environment*, *569–570*, 1545–1552. https://doi.org/10.1016/j.scitotenv.2016.06.248

Fang, D., Wang, Q., Li, H., Yu, Y., Lu, Y., and Qian, X. (2016b). Mortality effects assessment of ambient PM2.5 pollution in the 74 leading cities of China. *Science of The Total Environment*, *569–570*, 1545–1552. https://doi.org/10.1016/j.scitotenv.2016.06.248

Fann, N., Fulcher, C. M., and Hubbell, B. J. (2009). The influence of location, source, and emission type in estimates of the human health benefits of reducing a ton of air pollution. *Air Quality, Atmosphere and Health*, *2*(3), 169–176. https://doi.org/10.1007/s11869-009-0044-0

Fann, N. L., Nolte, C. G., Sarofim, M. C., Martinich, J., and Nassikas, N. J. (2021). Associations Between Simulated Future Changes in Climate, Air Quality, and Human Health. *JAMA Network Open*, *4*(1), e2032064. https://doi.org/10.1001/jamanetworkopen.2020.32064

Fauser, Patrik., and Forsogsanlag Riso. (1999). *Particulate air pollution with emphasis on traffic generated aerosols*. Riso National Laboratory.

Fernández-Pacheco, V. M., López-Sánchez, C. A., Álvarez-Álvarez, E., López, M. J. S., García-Expósito, L., Yudego, E. A., and Carús-Candás, J. L. (2018). Estimation of PM10 Distribution using Landsat5 and Landsat8 Remote Sensing. *The 2nd International Research Conference on Sustainable Energy, Engineering, Materials and Environment*, 1430. https://doi.org/10.3390/proceedings2231430

Fishbein, L., Infante, P., Landrigan, P., William Lloyd, J., Mason, T. J., Mastrofnatteo, E., Norseth, T., Pershagen, G., Saffiotti, U., and Saracci, R. (1981). Problems of Epidemiological Evidence*. In *Environmental Health Perspectives* (Vol. 40).

Fomba, K. W., van Pinxteren, D., Müller, K., Spindler, G., and Herrmann, H. (2018). Assessment of trace metal levels in size-resolved particulate matter in the area of Leipzig. *Atmospheric Environment*, *176*, 60–70. https://doi.org/10.1016/j.atmosenv.2017.12.024

Fonseca-Nunes, A., Jakszyn, P., and Agudo, A. (2014). Iron and Cancer Risk—A Systematic Review and Meta-analysis of the Epidemiological Evidence. *Cancer Epidemiology, Biomarkers and Prevention*, *23*(1), 12–31. https://doi.org/10.1158/1055-9965.EPI-13-0733

Fowler, B. A., National Research Council (U.S.). Committee on Measuring Lead in Critical Populations., National Research Council (U.S.). Board on Environmental Studies and Toxicology., and National Research Council (U.S.). Commission on Life Sciences. (1993). *Measuring lead exposure in infants, children, and other sensitive populations*. National Academy Press.

Friedrich, R., and Droste-Franke, B. (2013). *ExternE Externalities of Energy Methodology Energy Infrastructure Attack Database (EIAD) View project COGNAC study View project*. https://www.researchgate.net/publication/232075838

Galvão, E. S., Santos, J. M., Lima, A. T., Reis, N. C., Orlando, M. T. D., and Stuetz, R. M. (2018). Trends in analytical techniques applied to particulate matter characterization: A critical review of fundaments and applications. *Chemosphere*, *199*, 546–568. https://doi.org/10.1016/j.chemosphere.2018.02.034

Gao, P., Guo, H., Zhang, Z., Ou, C., Hang, J., Fan, Q., He, C., Wu, B., Feng, Y., and Xing, B. (2018). Bioaccessibility and exposure assessment of trace metals from urban airborne particulate matter (PM10 and PM2.5) in simulated digestive fluid. *Environmental Pollution*, *242*, 1669–1677. https://doi.org/10.1016/j.envpol.2018.07.109

Gao, Z.-F., Long, H.-M., Dai, B., and Gao, X.-P. (2019). Investigation of reducing particulate matter (PM) and heavy metals pollutions by adding a novel additive from metallurgical dust (MD) during coal combustion. *Journal of Hazardous Materials*, *373*, 335–346. https://doi.org/10.1016/j.jhazmat.2019.03.057

Garg, B. D., Cadle, S. H., Mulawa, P. A., Groblicki, P. J., Laroo, C., and Parr, G. A. (2000). Brake Wear Particulate Matter Emissions. *Environmental Science and Technology*, *34*(21), 4463–4469. https://doi.org/10.1021/es001108h

Gbadamosi, M. R., Afolabi, T. A., Ogunneye, A. L., Ogunbanjo, O. O., Omotola, E. O., Kadiri, T. M., Akinsipo, O. B., and Jegede, D. O. (2018). Distribution of radionuclides and heavy metals in the bituminous sand deposit in Ogun State, Nigeria – A multi-dimensional pollution, health and radiological risk assessment. *Journal of Geochemical Exploration*, *190*, 187–199. https://doi.org/10.1016/j.gexplo.2018.03.006

GISGEOGRAPHY. (2023).

Goldsmith, J. R., and Landaw, S. A. (1968). Carbon Monoxide and Human Health. *Science*, *162*(3860), 1352–1359. https://doi.org/10.1126/science.162.3860.1352

Goonetilleke, A., Egodawatta, P., and Kitchen, B. (2009). Evaluation of pollutant build-up and wash-off from selected land uses at the Port of Brisbane, Australia. *Marine Pollution Bulletin*, *58*(2), 213–221. https://doi.org/10.1016/j.marpolbul.2008.09.025

Grottker, M. (1987). Runoff quality from a street with medium traffic loading. *Science of The Total Environment*, *59*, 457–466. https://doi.org/10.1016/0048-9697(87)90469-4

Grzetic, I., and Ghariani, A. (2008). Potential health risk assessment for soil heavy metal contamination in the central zone of Belgrade (Serbia). *Journal of the Serbian Chemical Society*, *73*(8–9), 923–934. https://doi.org/10.2298/JSC0809923G

Gujre, N., Rangan, L., and Mitra, S. (2021). Occurrence, geochemical fraction, ecological and health risk assessment of cadmium, copper and nickel in soils contaminated with municipal solid wastes. *Chemosphere*, *271*, 129573. https://doi.org/10.1016/j.chemosphere.2021.129573

Guo, G., Zhang, D., and Wang, Y. (2021). Characteristics of heavy metals in size-fractionated atmospheric particulate matters and associated health risk assessment based on the respiratory deposition. *Environmental Geochemistry and Health*, *43*(1), 285–299. https://doi.org/10.1007/s10653-020-00706-z

Gurung, A., Son, J.-Y., and Bell, M. L. (2017). Particulate Matter and Risk of Hospital Admission in the Kathmandu Valley, Nepal: A Case-Crossover Study. *American Journal of Epidemiology*, *186*(5), 573–580. https://doi.org/10.1093/aje/kwx135

Guttikunda, S. (2006). *Impact Analysis of Brick Kilns on the Air Quality in Dhaka, Bangladesh*.

Hakanson, L. (1980). An ecological risk index for aquatic pollution control.a sedimentological approach. *Water Research*, *14*(8), 975–1001. https://doi.org/10.1016/0043-1354(80)90143-8

Halim, C. E., Short, S. A., Scott, J. A., Amal, R., and Low, G. (2005). Modelling the leaching of Pb, Cd, As, and Cr from cementitious waste using PHREEQC. *Journal of Hazardous Materials*, *125*(1–3), 45–61. https://doi.org/10.1016/j.jhazmat.2005.05.046

Hammitt, J. K., and Robinson, L. A. (2011). The Income Elasticity of the Value per Statistical Life: Transferring Estimates between High and Low Income Populations. *Journal of Benefit-Cost Analysis*, *2*(1), 1–29. https://doi.org/10.2202/2152-2812.1009

Han, X., Lu, X., Qinggeletu, and Wu, Y. (2017). Health Risks and Contamination Levels of Heavy Metals in Dusts from Parks and Squares of an Industrial City in Semi-Arid Area of China. *International Journal of Environmental Research and Public Health*, *14*(8), 886. https://doi.org/10.3390/ijerph14080886

Handbook of Air Pollution From Internal Combustion Engines. (1998). Elsevier. https://doi.org/10.1016/B978-0-12-639855-7.X5038-8

Hannah Ritchie, F. S. and M. R. (2018). *Causes of death*. https://ourworldindata.org/causes-of-death#citation

Hassan, A., Ilyas, S. Z., Agathopoulos, S., Hussain, S. M., Jalil, A., Ahmed, S., and Baqir, Y. (2021). Evaluation of adverse effects of particulate matter on human life. *Heliyon*, *7*(2). https://doi.org/10.1016/j.heliyon.2021.e05968

Health Effect Institute. (2019). *A SPECIAL REPORT ON GLOBAL EXPOSURE TO AIR POLLUTION AND ITS DISEASE BURDEN*.

Health Effects Institute. (1990). *A SPECIAL REPORT ON GLOBAL EXPOSURE TO AIR POLLUTION AND ITS DISEASE BURDEN*.

Healthy People 2030. (2020). Environmental Conditions. https://health.gov/healthypeople/priority-areas/social-determinants-health/literature-summaries/environmental-conditions

Herngren, L., Goonetilleke, A., and Ayoko, G. A. (2005). Understanding heavy metal and suspended solids relationships in urban stormwater using simulated rainfall. *Journal of Environmental Management*, *76*(2), 149–158. https://doi.org/10.1016/j.jenvman.2005.01.013

Hien, N. L. H., and Kor, A.-L. (2022). Analysis and Prediction Model of Fuel Consumption and Carbon Dioxide Emissions of Light-Duty Vehicles. *Applied Sciences*, *12*(2), 803. https://doi.org/10.3390/app12020803

Ho, T. H., Van Dang, C., Pham, T. T. B., and Wangwongwatana, S. (2023). Assessment of health and economic benefits of reducing fine particulate matter (PM2.5) concentration in Ho Chi Minh City, Vietnam. *Hygiene and Environmental Health Advances*, *6*, 100045. https://doi.org/10.1016/j.heha.2023.100045

Hoffmann, C., Maglakelidze, M., von Schneidemesser, E., Witt, C., Hoffmann, P., and Butler, T. (2022). Asthma and COPD exacerbation in relation to outdoor air pollution in the metropolitan area of Berlin, Germany. *Respiratory Research*, *23*(1), 64. https://doi.org/10.1186/s12931-022-01983-1

Hong, Y., and LaBresh, K. A. (2006). Overview of the American Heart Association "Get With the Guidelines" Programs. *Critical Pathways in Cardiology: A Journal of Evidence-Based Medicine*, *5*(4), 179–186. https://doi.org/10.1097/01.hpc.0000243588.00012.79

Hoque, M. Md. M., Khan, Md. M., Sarker, Md. E., Hossain, Md. N., Islam, Md. S., Khan, Md. M. H., Shil, M., and Sarker, Md. N. I. (2022a). Assessment of Seasonal Variations of Air Quality and AQI Status: Evidence from Chittagong, Bangladesh. *Indonesian Journal of Environmental Management and Sustainability*, *6*(3), 88–97. https://doi.org/10.26554/ijems.2022.6.3.88-97

Hoque, M. Md. M., Khan, Md. M., Sarker, Md. E., Hossain, Md. N., Islam, Md. S., Khan, Md. M. H., Shil, M., and Sarker, Md. N. I. (2022b). Assessment of Seasonal Variations of Air Quality and AQI Status: Evidence from Chittagong, Bangladesh. *Indonesian Journal of Environmental Management and Sustainability*, *6*(3), 88–97. https://doi.org/10.26554/ijems.2022.6.3.88-97

Hossain, B., Ryakitimbo, C. M., and Sohel, Md. S. (2020). Climate Change Induced Human Displacement in Bangladesh: A Case Study of Flood in 2017 in Char in Gaibandha District. *Asian Research Journal of Arts and Social Sciences*, 47–60. https://doi.org/10.9734/arjass/2020/v10i130140

Hossen, M. A., Pal, S. K., and Hoque, A. (2018). Assessment of Air Quality for Selected Locations in Chittagong City Corporation Area, Bangladesh. *International Journal of Innovative Research in Engineering and Management*, *5*(4), 121–128. https://doi.org/10.21276/ijirem.2018.5.4.1

Hu, M., Wang, Y., Wang, S., Jiao, M., Huang, G., and Xia, B. (2021). Spatial-temporal heterogeneity of air pollution and its relationship with meteorological factors in the Pearl River Delta, China. *Atmospheric Environment*, *254*, 118415. https://doi.org/10.1016/j.atmosenv.2021.118415

Hu, Y., Qi, S., Wu, C., Ke, Y., Chen, J., Chen, W., and Gong, X. (2012). Preliminary assessment of heavy metal contamination in surface water and sediments from Honghu Lake, East Central China. *Frontiers of Earth Science*, *6*(1), 39–47. https://doi.org/10.1007/s11707-012-0309-z

Huang, D., Xu, J., and Zhang, S. (2012). Valuing the health risks of particulate air pollution in the Pearl River Delta, China. *Environmental Science and Policy*, *15*(1), 38–47. https://doi.org/10.1016/j.envsci.2011.09.007

Huang, Y.-C., and Ghio, A. (2006). Vascular Effects of Ambient Pollutant Particles and Metals. *Current Vascular Pharmacology*, *4*(3), 199–203. https://doi.org/10.2174/157016106777698351

Hubbell, B. J., Hallberg, A., McCubbin, D. R., and Post, E. (2005). Health-Related Benefits of Attaining the 8-Hr Ozone Standard. *Environmental Health Perspectives*, *113*(1), 73–82. https://doi.org/10.1289/ehp.7186

IARC Monographs on the evaluation of Carcinogenic Risks to Humans. (1996). IARC Monographs on the evaluation of Carcinogenic Risks to Humans

Idris, A. M., Said, T. O., Brima, E. I., Sahlabji, T., Alghamdi, M. M., El-Zahhar, A. A., Arshad, M., and El Nemr, A. M. (2020). *ASSESSMENT OF CONTENTS OF SELECTED HEAVY METALS IN STREET DUST FROM KHAMEES-MUSHAIT CITY, SAUDI ARABIA, USING MULTIVARIATE STATISTICAL ANALYSIS, GIS MAPPING, GEOCHEMICAL INDICES AND HEALTH RISK*.

IHME. (2019). Global Burden of DIsease (GBD). Retrieved 1 July 2023, from https://www.healthdata.org/gbd

IQAir. (2022). AIR QUALITY ANALYSIS AND STATISTICS FOR BANGLADESH. https://www.iqair.com/bangladesh

Ite, A. E., Udousoro, I. I., and Ibok, U. J. (2014). Distribution of Some Atmospheric Heavy Metals in Lichen and Moss Samples Collected from Eket and Ibeno Local Government Areas of Akwa Ibom State, Nigeria. *American Journal of Environmental Protection*, *2*(1), 22–31. https://doi.org/10.12691/env-2-1-5

Jadaa, W., and Mohammed, H. (2023). Heavy Metals – Definition, Natural and Anthropogenic Sources of Releasing into Ecosystems, Toxicity, and Removal Methods – An Overview Study. *Journal of Ecological Engineering*, *24*(6), 249–271. https://doi.org/10.12911/22998993/162955

Jaishankar, M., Tseten, T., Anbalagan, N., Mathew, B. B., and Beeregowda, K. N. (2014a). Toxicity, mechanism and health effects of some heavy metals. *Interdisciplinary Toxicology*, *7*(2), 60–72. https://doi.org/10.2478/intox-2014-0009

Jaishankar, M., Tseten, T., Anbalagan, N., Mathew, B. B., and Beeregowda, K. N. (2014b). Toxicity, mechanism and health effects of some heavy metals. *Interdisciplinary Toxicology*, *7*(2), 60–72. https://doi.org/10.2478/intox-2014-0009

Jan, A., Azam, M., Siddiqui, K., Ali, A., Choi, I., and Haq, Q. (2015). Heavy Metals and Human Health: Mechanistic Insight into Toxicity and Counter Defense System

of Antioxidants. *International Journal of Molecular Sciences*, *16*(12), 29592–29630. https://doi.org/10.3390/ijms161226183

Ji, W., Zhou, B., and Zhao, B. (2019). Potential reductions in premature mortality attributable to PM2.5 by reducing indoor pollution: A model analysis for Beijing-Tianjin-Hebei of China. In *Environmental Pollution* (Vol. 245). Elsevier Ltd. https://doi.org/10.1016/j.envpol.2018.10.082

John H. Seinfeld, S. N. P. (1985). *Atmospheric Chemistry and Physics: From Air Pollution to Climate Change, 3rd Edition*. https://www.wiley.com/en-us/Atmospheric+Chemistry+and+Physics%3A+From+Air+Pollution+to+Climate+Change%2C+3rd+Edition-p-9781118947401

Johnbull, O., Abbassi, B., and Zytner, R. G. (2018). Risk assessment of heavy metals in soil based on the geographic information system-Kriging technique in Anka, Nigeria. *Environmental Engineering Research*, *24*(1), 150–158. https://doi.org/10.4491/eer.2018.130

Kabir, M. H., Rashid, M. H., Wang, Q., Wang, W., Lu, S., and Yonemochi, S. (2021a). Determination of Heavy Metal Contamination and Pollution Indices of Roadside Dust in Dhaka City, Bangladesh. *Processes*, *9*(10), 1732. https://doi.org/10.3390/pr9101732

Kabir, M. H., Rashid, M. H., Wang, Q., Wang, W., Lu, S., and Yonemochi, S. (2021b). Determination of Heavy Metal Contamination and Pollution Indices of Roadside Dust in Dhaka City, Bangladesh. *Processes*, *9*(10), 1732. https://doi.org/10.3390/pr9101732

Kacholi, D. S., and Sahu, M. (2018). Levels and Health Risk Assessment of Heavy Metals in Soil, Water, and Vegetables of Dar es Salaam, Tanzania. *Journal of Chemistry*, *2018*, 1–9. https://doi.org/10.1155/2018/1402674

Kader Newaz, K., Kumar Pal, S., Hossain, S., and Kabir, A. (2020). Evaluation of heavy metal pollution risk associated with road sediment. *Environmental Engineering Research*. https://doi.org/10.4491/eer.2020.239

Kagawa, J. (1985). Evaluation of biological significance of nitrogen oxides exposure. *The Tokai Journal of Experimental and Clinical Medicine*, *10*(4), 348–353.

Kamani, H., Mahvi, A. H., Seyedsalehi, M., Jaafari, J., Hoseini, M., Safari, G. H., Dalvand, A., Aslani, H., Mirzaei, N., and Ashrafi, S. D. (2017). Contamination and ecological risk assessment of heavy metals in street dust of Tehran, Iran. *International Journal of Environmental Science and Technology*, *14*(12), 2675–2682. https://doi.org/10.1007/s13762-017-1327-x

Kampa, M., and Castanas, E. (2008a). Human health effects of air pollution. *Environmental Pollution*, *151*(2), 362–367. https://doi.org/10.1016/j.envpol.2007.06.012

Kampa, M., and Castanas, E. (2008b). Human health effects of air pollution. *Environmental Pollution*, *151*(2), 362–367. https://doi.org/10.1016/j.envpol.2007.06.012

Kamran, S., Shafaqat, A., Samra, H., Sana, A., Samar, F., Muhammad, B. S., Saima, A. B., and Hafiz, M. T. (2013). Heavy Metals Contamination and what are the Impacts on Living Organisms. *Greener Journal of Environmental Management and Public Safety*, *2*(4), 172–179. https://doi.org/10.15580/GJEMPS.2013.4.060413652

Kan, H., London, S. J., Chen, G., Zhang, Y., Song, G., Zhao, N., Jiang, L., and Chen, B. (2007). Differentiating the effects of fine and coarse particles on daily mortality in Shanghai, China. *Environment International*, *33*(3), 376–384. https://doi.org/10.1016/j.envint.2006.12.001

Kastury, F., Smith, E., Karna, R. R., Scheckel, K. G., and Juhasz, A. L. (2018). An inhalation-ingestion bioaccessibility assay (IIBA) for the assessment of exposure to metal(loid)s in PM10. *Science of The Total Environment*, *631–632*, 92–104. https://doi.org/10.1016/j.scitotenv.2018.02.337

Keen, S., and Altieri, K. (2016). The health benefits of attaining and strengthening air quality standards in Cape Town. *Clean Air Journal*, *26*(2), 22–27. https://doi.org/10.17159/2410-972x/2016/v26n2a9

Khalaf, E. M., Mohammadi, M. J., Sulistiyani, S., Ramírez-Coronel, A. A., Kiani, F., Jalil, A. T., Almulla, A. F., Asban, P., Farhadi, M., and Derikondi, M. (2022a). Effects of sulfur dioxide inhalation on human health: a review. *Reviews on Environmental Health*, *0*(0). https://doi.org/10.1515/reveh-2022-0237

Khalaf, E. M., Mohammadi, M. J., Sulistiyani, S., Ramírez-Coronel, A. A., Kiani, F., Jalil, A. T., Almulla, A. F., Asban, P., Farhadi, M., and Derikondi, M. (2022b). Effects of sulfur dioxide inhalation on human health: a review. *Reviews on Environmental Health*, *0*(0). https://doi.org/10.1515/reveh-2022-0237

Khatun Syed Yusuf Saadat Kashfia Ashraf, F. (2023). *Evidence Paper Air Pollution in Bangladesh Drivers, Impacts and Solutions*. www.cpd.org.bd

Kim, C.-H., Meng, F., Kajino, M., Lim, J., Tang, W., Lee, J.-J., Kiriyama, Y., Woo, J.-H., Sato, K., Kitada, T., Minoura, H., Kim, J., Lee, K.-B., Roh, S., Jo, H.-Y., and Jo, Y.-J. (2021). Comparative Numerical Study of PM2.5 in Exit-and-Entrance Areas Associated with Transboundary Transport over China, Japan, and Korea. *Atmosphere*, *12*(4), 469. https://doi.org/10.3390/atmos12040469

Kim, D., Kim, J., Jeong, J., and Choi, M. (2019). Estimation of health benefits from air quality improvement using the MODIS AOD dataset in Seoul, Korea. *Environmental Research*, *173*, 452–461. https://doi.org/10.1016/j.envres.2019.03.042

Kim, S.-Y., Kim, E., and Kim, W. J. (2020). Health Effects of Ozone on Respiratory Diseases. *Tuberculosis and Respiratory Diseases*, *83*(Supple 1), S6–S11. https://doi.org/10.4046/trd.2020.0154

Krupnick, J. L., Sotsky, S. M., Elkin, I., Simmens, S., Moyer, J., Watkins, J., and Pilkonis, P. A. (2006). The Role of the Therapeutic Alliance in Psychotherapy and Pharmacotherapy Outcome: Findings in the National Institute of Mental Health Treatment of Depression Collaborative Research Program. *FOCUS*, *4*(2), 269–277. https://doi.org/10.1176/foc.4.2.269

Kumar, S. (2012). *On Heavy Metal Pollution from a Suburban Road Network*.

Laden, F., Schwartz, J., Speizer, F. E., and Dockery, D. W. (2006). Reduction in fine particulate air pollution and mortality: Extended follow-up of the Harvard Six Cities Study. *American Journal of Respiratory and Critical Care Medicine*, *173*(6), 667–672. https://doi.org/10.1164/rccm.200503-443OC

Li, D., Lu, Q., Cai, L., Chen, L., and Wang, H. (2023). Characteristics of Soil Heavy Metal Pollution and Health Risk Assessment in Urban Parks at a Megacity of Central China. *Toxics*, *11*(3), 257. https://doi.org/10.3390/toxics11030257

Li, N., Friedrich, R., and Schieberle, C. (2022). Exposure of Individuals in Europe to Air Pollution and Related Health Effects. *Frontiers in Public Health*, *10*. https://doi.org/10.3389/fpubh.2022.871144

Liu, M., Saari, R. K., Zhou, G., Li, J., Han, L., and Liu, X. (2021). Recent trends in premature mortality and health disparities attributable to ambient PM2.5 exposure in China: 2005–2017. *Environmental Pollution*, *279*, 116882. https://doi.org/10.1016/j.envpol.2021.116882

Loughner, C. P., Follette-Cook, M. B., Duncan, B. N., Hains, J., Pickering, K. E., Moy, J., and Tzortziou, M. (2020). The benefits of lower ozone due to air pollution emission reductions (2002–2011) in the Eastern United States during extreme heat. *Journal of the Air and Waste Management Association*, *70*(2), 193–205. https://doi.org/10.1080/10962247.2019.1694089

Lu, F., Xu, D., Cheng, Y., Dong, S., Guo, C., Jiang, X., and Zheng, X. (2015). Systematic review and meta-analysis of the adverse health effects of ambient PM2.5 and PM10 pollution in the Chinese population. *Environmental Research*, *136*, 196–204. https://doi.org/10.1016/j.envres.2014.06.029

Lu, X., Wang, L., Lei, K., Huang, J., and Zhai, Y. (2009). Contamination assessment of copper, lead, zinc, manganese and nickel in street dust of Baoji, NW China. *Journal of Hazardous Materials*, *161*(2–3), 1058–1062. https://doi.org/10.1016/j.jhazmat.2008.04.052

Luo, G., Zhang, L., Hu, X., and Qiu, R. (2020). Quantifying public health benefits of PM2.5 reduction and spatial distribution analysis in China. *Science of the Total Environment*, *719*. https://doi.org/10.1016/j.scitotenv.2020.137445

Luo, X.-S., Xue, Y., Wang, Y.-L., Cang, L., Xu, B., and Ding, J. (2015). Source identification and apportionment of heavy metals in urban soil profiles. *Chemosphere*, *127*, 152–157. https://doi.org/10.1016/j.chemosphere.2015.01.048

Ma, L., Yang, Z., Li, L., and Wang, L. (2016). Source identification and risk assessment of heavy metal contaminations in urban soils of Changsha, a mine-impacted city in Southern China. *Environmental Science and Pollution Research*, *23*(17), 17058–17066. https://doi.org/10.1007/s11356-016-6890-z

Maclure, M. (1991). The Case-Crossover Design: A Method for Studying Transient Effects on the Risk of Acute Events. *American Journal of Epidemiology*, *133*(2), 144–153. https://doi.org/10.1093/oxfordjournals.aje.a115853

Mahmood, A., Hu, Y., Nasreen, S., and Hopke, P. K. (2019). Airborne Particulate Pollution Measured in Bangladesh from 2014 to 2017. *Aerosol and Air Quality Research*, *19*(2), 272–281. https://doi.org/10.4209/aaqr.2018.08.0284

Mahmud, M. (2009). On the contingent valuation of mortality risk reduction in developing countries. *Applied Economics*, *41*(2), 171–181. https://doi.org/10.1080/00036840600994252

Maji, K. J. (2020). Substantial changes in PM2.5 pollution and corresponding premature deaths across China during 2015–2019: A model prospective. *Science of The Total Environment*, *729*, 138838. https://doi.org/10.1016/j.scitotenv.2020.138838

Maji, K. J., Arora, M., and Dikshit, A. K. (2018). Premature mortality attributable to PM2.5 exposure and future policy roadmap for 'airpocalypse' affected Asian megacities. *Process Safety and Environmental Protection*, *118*, 371–383. https://doi.org/10.1016/j.psep.2018.07.009

Maji, K. J., Dikshit, A. K., Arora, M., and Deshpande, A. (2018). Estimating premature mortality attributable to PM2.5 exposure and benefit of air pollution control policies in China for 2020. *Science of The Total Environment*, *612*, 683–693. https://doi.org/10.1016/j.scitotenv.2017.08.254

Maji, K. J., Ye, W.-F., Arora, M., and Shiva Nagendra, S. M. (2018). PM2.5-related health and economic loss assessment for 338 Chinese cities. *Environment International*, *121*, 392–403. https://doi.org/10.1016/j.envint.2018.09.024

Majumder, A. K., Nayeem, A. Al, Patoary, M. N. A., and Carter, W. S. (2020). Temporal variation of ambient particulate matter in Chattogram City, Bangladesh. *Journal of Air Pollution and Health*. https://doi.org/10.18502/japh.v5i1.2857

Majumder, A., Madheswaran, S., and Institute for Social and Economic Change. (2014). *Value of statistical life : a meta-analysis with mixed effects regression model*.

MALO, J., CARTIER, A., DOEPNER, M., NIEBOER, E., EVANS, S., and DOLOVICH, J. (1982). Occupational asthma caused by nickel sulfate. *Journal of Allergy and Clinical Immunology*, *69*(1), 55–59. https://doi.org/10.1016/0091-6749(82)90088-4

Manojkumar, N., and Srimuruganandam, B. (2021). Health benefits of achieving fine particulate matter standards in India – A nationwide assessment. *Science of the Total Environment*, *763*. https://doi.org/10.1016/j.scitotenv.2020.142999

Maria Trimarchi and Ann Meeker. (2001, January 2). *Health | HowStuffWorks*.

Masindi, V., and Muedi, K. L. (2018). Environmental Contamination by Heavy Metals. In *Heavy Metals*. InTech. https://doi.org/10.5772/intechopen.76082

Massey, D. D., Kulshrestha, A., and Taneja, A. (2013). Particulate matter concentrations and their related metal toxicity in rural residential environment of semi-arid region of India. *Atmospheric Environment*, *67*, 278–286. https://doi.org/10.1016/j.atmosenv.2012.11.002

Masters. (2004a). *Introduction to Environmental Engineering and Science , Second Edition, Prentice Hall of India Private Limited, New Delhi, India,*. https://books.google.com/books/about/Introduction_To_Environmental_Engineerin.html?id=JFUSkgEACAAJ

Masters. (2004b). *Introduction to Environmental Engineering and Science, Second Edition, Prentice Hall of India Private Limited, New Delhi, India, 2004.*

Masum, M. H., and Pal, S. K. (2020). Statistical evaluation of selected air quality parameters influenced by COVID-19 lockdown. *Global Journal of Environmental Science and Management*, *6*, 85–94. https://doi.org/10.22034/GJESM.2019.06.SI.08

Matsumoto, S. T., Mantovani, M. S., Malaguttii, M. I. A., Dias, A. L., Fonseca, I. C., and Marin-Morales, M. A. (2006). Genotoxicity and mutagenicity of water contaminated with tannery effluents, as evaluated by the micronucleus test and comet assay using the fish Oreochromis niloticus and chromosome aberrations in onion root-tips. *Genetics and Molecular Biology*, *29*(1), 148–158. https://doi.org/10.1590/S1415-47572006000100028

Mayr, F. B., Spiel, A., Leitner, J., Marsik, C., Germann, P., Ullrich, R., Wagner, O., and Jilma, B. (2005). Effects of Carbon Monoxide Inhalation during Experimental Endotoxemia in Humans. *American Journal of Respiratory and Critical Care Medicine*, *171*(4), 354–360. https://doi.org/10.1164/rccm.200404-446OC

Mccubbin, D. (2009). *Health Impacts of Diesel, Based on Data from the NationalScale Air Toxics Assessment (NATA)*.

Mccubbin, D. (2011). *Health Benefits of Alternative PM 2.5 Standards*.

Men, C., Liu, R., Xu, F., Wang, Q., Guo, L., and Shen, Z. (2018). Pollution characteristics, risk assessment, and source apportionment of heavy metals in road dust in Beijing, China. *Science of The Total Environment*, *612*, 138–147. https://doi.org/10.1016/j.scitotenv.2017.08.123

Men, C., Wang, Y., Liu, R., Wang, Q., Miao, Y., Jiao, L., Shoaib, M., and Shen, Z. (2021). Temporal variations of levels and sources of health risk associated with heavy metals in road dust in Beijing from May 2016 to April 2018. *Chemosphere*, *270*, 129434. https://doi.org/10.1016/j.chemosphere.2020.129434

Meng, C., Liu, J., Li, Y., Han, J., and Xu, D. (2019). [Application of BenMAP-CE software in health risk assessment of air pollution in China]. *Wei sheng yan jiu = Journal of hygiene research*, *48*(4), 659–663. http://europepmc.org/abstract/MED/31601355

Miguel, E. de, Llamas, J. F., Chacón, E., Berg, T., Larssen, S., Røyset, O., and Vadset, M. (1997). Origin and patterns of distribution of trace elements in street dust: Unleaded petrol and urban lead. *Atmospheric Environment*, *31*(17), 2733–2740. https://doi.org/10.1016/S1352-2310(97)00101-5

Miller. (2000). *Variations of VSL between countries*. https://www.researchgate.net/publication/238369152

Mishra, R. K., Agarwal, A., and Shukla, A. (2021). Predicting Ground Level PM $_{2.5}$ Concentration Over Delhi Using Landsat 8 Satellite Data. *International Journal of Remote Sensing*, *42*(3), 827–838. https://doi.org/10.1080/2150704X.2020.1832279

Mitra, S., Chakraborty, A. J., Tareq, A. M., Emran, T. Bin, Nainu, F., Khusro, A., Idris, A. M., Khandaker, M. U., Osman, H., Alhumaydhi, F. A., and Simal-Gandara, J. (2022). Impact of heavy metals on the environment and human health: Novel therapeutic insights to counter the toxicity. *Journal of King Saud University - Science*, *34*(3), 101865. https://doi.org/10.1016/j.jksus.2022.101865

MOLLER, D., BROOKS, S., BERNSTEIN, D., CASSEDY, K., ENRIONE, M., and BERNSTEIN, I. (1986). Delayed anaphylactoid reaction in a worker exposed to chromium. *Journal of Allergy and Clinical Immunology*, *77*(3), 451–456. https://doi.org/10.1016/0091-6749(86)90179-X

Moryani, H. T., Kong, S., Du, J., and Bao, J. (2020). Health Risk Assessment of Heavy Metals Accumulated on PM2.5 Fractioned Road Dust from Two Cities of Pakistan. *International Journal of Environmental Research and Public Health*, *17*(19), 7124. https://doi.org/10.3390/ijerph17197124

Narain, U., and Sall, C. (2016). *Methodology for Valuing the Health Impacts of Air Pollution*. World Bank, Washington, DC. https://doi.org/10.1596/24440

Nargis, A., Habib, A., Islam, M. N., Chen, K., Sarker, M. S. I., Al-Razee, A. N. M., Liu, W., Liu, G., and Cai, M. (2022). Source identification, contamination status and

health risk assessment of heavy metals from road dusts in Dhaka, Bangladesh. *Journal of Environmental Sciences*, *121*, 159–174. https://doi.org/10.1016/j.jes.2021.09.011

Nasari, M. M., Szyszkowicz, M., Chen, H., Crouse, D., Turner, M. C., Jerrett, M., Pope, C. A., Hubbell, B., Fann, N., Cohen, A., Gapstur, S. M., Diver, W. R., Stieb, D., Forouzanfar, M. H., Kim, S.-Y., Olives, C., Krewski, D., and Burnett, R. T. (2016). A class of non-linear exposure-response models suitable for health impact assessment applicable to large cohort studies of ambient air pollution. *Air Quality, Atmosphere and Health*, *9*(8), 961–972. https://doi.org/10.1007/s11869-016-0398-z

National Heart Foundation of Bangladesh. (2023).

Neumann, J. E., Amend, M., Anenberg, S., Kinney, P. L., Sarofim, M., Martinich, J., Lukens, J., Xu, J.-W., and Roman, H. (2021). Estimating PM2.5-related premature mortality and morbidity associated with future wildfire emissions in the western US. *Environmental Research Letters*, *16*(3), 035019. https://doi.org/10.1088/1748-9326/abe82b

Newaz, K. K., Pal, S. K., Hossain, S., and Karim, A. (2021). Evaluation of heavy metal pollution risk associated with road sediment. *Environmental Engineering Research*, *26*(3). https://doi.org/10.4491/eer.2020.239

Nirmalkar, J., Haswani, D., Singh, A., Kumar, S., and Sunder Raman, R. (2021). Concentrations, transport characteristics, and health risks of PM2.5-bound trace elements over a national park in central India. *Journal of Environmental Management*, *293*, 112904. https://doi.org/10.1016/j.jenvman.2021.112904

Nishikawa, H., Ng, C. F. S., Madaniyazi, L., Seposo, X. T., Dhoubhadel, B. G., Pokhrel, D., Pokhrel, A. K., Verma, S. C., Shrestha, D., Raya, G. B., and Hashizume, M. (2021). Ambient PM2.5 and Daily Hospital Admissions for Acute Respiratory Infections: Effect Modification by Weight Status of Child. *Atmosphere*, *12*(8), 1009. https://doi.org/10.3390/atmos12081009

Niu, Z., Liu, F., Yu, H., Wu, S., and Xiang, H. (2021). Association between exposure to ambient air pollution and hospital admission, incidence, and mortality of stroke: an updated systematic review and meta-analysis of more than 23 million participants. *Environmental Health and Preventive Medicine*, *26*(1), 15. https://doi.org/10.1186/s12199-021-00937-1

NOVEY, H., HABIB, M., and WELLS, I. (1983). Asthma and IgE antibodies induced by chromium and nickel salts. *Journal of Allergy and Clinical Immunology*, *72*(4), 407–412. https://doi.org/10.1016/0091-6749(83)90507-9

O'Brien, T., Xu, J., and Patierno, S. R. (2001). Effects of glutathione on chromium-induced DNA crosslinking and DNA polymerase arrest: Molecular mechanisms

of metal Toxicity and carcinogenesis. *Molecular and Cellular Biochemistry*, *222*(1/2), 173–182. https://doi.org/10.1023/A:1017918330073

Ogundele, L. T., Owoade, O. K., Hopke, P. K., and Olise, F. S. (2017). Heavy metals in industrially emitted particulate matter in Ile-Ife, Nigeria. *Environmental Research*, *156*, 320–325. https://doi.org/10.1016/j.envres.2017.03.051

Ommi, A., Emami, F., Zíková, N., Hopke, P. K., and Begum, B. A. (2017). Trajectory-Based Models and Remote Sensing for Biomass Burning Assessment in Bangladesh. *Aerosol and Air Quality Research*, *17*(2), 465–475. https://doi.org/10.4209/aaqr.2016.07.0304

Ostro, B. D., and Rothschild, S. (1989). Air pollution and acute respiratory morbidity: An observational study of multiple pollutants. *Environmental Research*, *50*(2), 238–247. https://doi.org/10.1016/S0013-9351(89)80004-0

Pal, S. K., and Roy, R. (2021). Evaluating heavy metals emission' pattern on road influenced by urban road layout. *Transportation Research Interdisciplinary Perspectives*, *10*, 100362. https://doi.org/10.1016/j.trip.2021.100362

Pastuszka, J. S., Rogula-Kozłowska, W., and Zajusz-Zubek, E. (2010). Characterization of PM10 and PM2.5 and associated heavy metals at the crossroads and urban background site in Zabrze, Upper Silesia, Poland, during the smog episodes. *Environmental Monitoring and Assessment*, *168*(1–4), 613–627. https://doi.org/10.1007/s10661-009-1138-8

Peled, R. (2011). Air pollution exposure: Who is at high risk? *Atmospheric Environment*, *45*(10), 1781–1785. https://doi.org/10.1016/j.atmosenv.2011.01.001

Peng, X., XiaoYun, L., ZhaoRong, L., TianTian, L., and YuHua, B. (2009a). Exposure-response functions for health effects of ambient participate matter pollution applicable for China. *China Environmental Science*, *29*(10), 1034–1040.

Peng, X., XiaoYun, L., ZhaoRong, L., TianTian, L., and YuHua, B. (2009b). Exposure-response functions for health effects of ambient participate matter pollution applicable for China. *China Environmental Science*, *29*(10), 1034–1040.

Petavratzi, E., Kingman, S., and Lowndes, I. (2005). Particulates from mining operations: A review of sources, effects and regulations. *Minerals Engineering*, *18*(12), 1183–1199. https://doi.org/10.1016/j.mineng.2005.06.017

Pfeiffer, R. L. (2005). *Sampling For PM10 and PM2.5 Particulates Sampling For PM10 and PM2.5 Particulates 11 Sampling For PM10 and PM2.5 Particulates*. https://digitalcommons.unl.edu/usdaarsfacpub/1393

Pope, C. A., and Dockery, D. W. (2006a). Health Effects of Fine Particulate Air Pollution: Lines that Connect. *Journal of the Air and Waste Management Association*, *56*(6), 709–742. https://doi.org/10.1080/10473289.2006.10464485

Pope, C. A., and Dockery, D. W. (2006b). Health effects of fine particulate air pollution: Lines that connect. *Journal of the Air and Waste Management Association*, *56*(6), 709–742. https://doi.org/10.1080/10473289.2006.10464485

Pope III, C. A. (2002). Lung Cancer, Cardiopulmonary Mortality, and Long-term Exposure to Fine Particulate Air Pollution. *JAMA*, *287*(9), 1132. https://doi.org/10.1001/jama.287.9.1132

Proshad, R., Dey, H. C., Ritu, S. A., Baroi, A., Khan, M. S. U., Islam, M., and Idris, A. M. (2023). A review on toxic metal pollution and source-oriented risk apportionment in road dust of a highly polluted megacity in Bangladesh. *Environmental Geochemistry and Health*, *45*(6), 2729–2762. https://doi.org/10.1007/s10653-022-01434-2

Pyatha, S., Kim, H., Lee, D., and Kim, K. (2022). Association between Heavy Metal Exposure and Parkinson's Disease: A Review of the Mechanisms Related to Oxidative Stress. *Antioxidants*, *11*(12), 2467. https://doi.org/10.3390/antiox11122467

Quigley, R. J., and Taylor, L. C. (2004). Evaluating health impact assessment. *Public Health*, *118*(8), 544–552. https://doi.org/10.1016/j.puhe.2003.10.012

Rahman, M. M., Nahar, K., Begum, B. A., Hopke, P. K., and Thurston, G. D. (2022). Respiratory Emergency Department Visit Associations with Exposures to Fine Particulate Matter Mass, Constituents, and Sources in Dhaka, Bangladesh Air Pollution. *Annals of the American Thoracic Society*, *19*(1), 28–38. https://doi.org/10.1513/AnnalsATS.202103-252OC

Rajaram, B. S., Suryawanshi, P. V., Bhanarkar, A. D., and Rao, C. V. C. (2014). Heavy metals contamination in road dust in Delhi city, India. *Environmental Earth Sciences*, *72*(10), 3929–3938. https://doi.org/10.1007/s12665-014-3281-y

Rall, D. P. (1974). Review of the Health Effects of Sulfur Oxides. *Environmental Health Perspectives*, *8*, 97–121. https://doi.org/10.1289/ehp.74897

Ramírez, O., da Boit, K., Blanco, E., and Silva, L. F. O. (2020). Hazardous thoracic and ultrafine particles from road dust in a Caribbean industrial city. *Urban Climate*, *33*, 100655. https://doi.org/10.1016/j.uclim.2020.100655

Rastegari Mehr, M., Keshavarzi, B., Moore, F., Sharifi, R., Lahijanzadeh, A., and Kermani, M. (2017). Distribution, source identification and health risk assessment of soil heavy metals in urban areas of Isfahan province, Iran. *Journal of African Earth Sciences*, *132*, 16–26. https://doi.org/10.1016/j.jafrearsci.2017.04.026

Robinson, L. A., Hammitt, J. K., and O'Keeffe, L. (2019). Valuing Mortality Risk Reductions in Global Benefit-Cost Analysis. *Journal of Benefit-Cost Analysis*, *10*(S1), 15–50. https://doi.org/10.1017/bca.2018.26

Robiul Hussain, M., Paul, A., Robiul Hussain, M. I., Paul, A. I., and Md Zahedul Islam III I, A. Z. (2016). *Research Article International Journal of Advancement in Remote Sensing, GIS and Geography Bangladesh Space Research and Remote Sensing Organization (SPARRSO)* (Vol. 4, Issue 2). https://www.researchgate.net/publication/312200013

Rouf. (2011). *6668*.

Rouf, M. A., Nasiruddin, M., Hossain, A. M. S., and Islam, M. S. (2012a). Trend of ambient air quality in Chittagong City. In *Bangladesh J. Sci. Ind. Res* (Vol. 47, Issue 3). www.banglajol.info

Rouf, M. A., Nasiruddin, M., Hossain, A. M. S., and Islam, M. S. (2012b). Trend of ambient air quality in Chittagong City. In *Bangladesh J. Sci. Ind. Res* (Vol. 47, Issue 3). www.banglajol.info

Roy, S., Zaman, S. U., Joy, K. S., Jeba, F., Kumar, P., and Salam, A. (2023). Impact of fine particulate matter and toxic gases on the health of school children in Dhaka, Bangladesh. *Environmental Research Communications*, *5*(2), 025004. https://doi.org/10.1088/2515-7620/acb90d

Ryan, T. P., and Aust, S. D. (1992). The Role of Iron in Oxygen-Mediated Toxicities. *Critical Reviews in Toxicology*, *22*(2), 119–141. https://doi.org/10.3109/10408449209146308

Safari, Z., Fouladi-Fard, R., Vahedian, M., Mahmoudian, M. H., Rahbar, A., and Fiore, M. (2022). Health impact assessment and evaluation of economic costs attributed to PM2.5 air pollution using BenMAP-CE. *International Journal of Biometeorology*, *66*(9), 1891–1902. https://doi.org/10.1007/s00484-022-02330-1

Schwartz, J., and Dockery, D. W. (1992a). Increased Mortality in Philadelphia Associated with Daily Air Pollution Concentrations. *American Review of Respiratory Disease*, *145*(3), 600–604. https://doi.org/10.1164/ajrccm/145.3.600

Schwartz, J., and Dockery, D. W. (1992b). Particulate Air Pollution and Daily Mortality in Steubenville, Ohio. *American Journal of Epidemiology*, *135*(1), 12–19. https://doi.org/10.1093/oxfordjournals.aje.a116195

Shang, Y., Sun, Z., Cao, J., Wang, X., Zhong, L., Bi, X., Li, H., Liu, W., Zhu, T., and Huang, W. (2013). Systematic review of Chinese studies of short-term exposure to air pollution and daily mortality. *Environment International*, *54*, 100–111. https://doi.org/10.1016/j.envint.2013.01.010

SHANMUGAM, K. R. (2001). Self Selection Bias in the Estimates of Compensating Differentials for Job Risks in India. *Journal of Risk and Uncertainty*, *22*(3), 263–275. http://www.jstor.org/stable/41761031

Sherris, A. R., Begum, B. A., Baiocchi, M., Goswami, D., Hopke, P. K., Brooks, W. A., and Luby, S. P. (2021). Associations between ambient fine particulate matter and child respiratory infection: The role of particulate matter source composition in Dhaka, Bangladesh. *Environmental Pollution*, *290*, 118073. https://doi.org/10.1016/j.envpol.2021.118073

Simon, N., Cropper, M., Alberini, A., and Arora, S. (1999). *Valuing mortality reductions in India: a study of compensating wage differentials* (Policy Research Working Paper Series, Issue 2078). The World Bank. https://EconPapers.repec.org/RePEc:wbk:wbrwps:2078

Slezakova, K., da Conceição Alvim-Ferraz, M., and do Carmo Pereira, M. (2012). Elemental Characterization Of Indoor Breathable Particles at a Portuguese Urban Hospital. *Journal of Toxicology and Environmental Health, Part A*, *75*(13–15), 909–919. https://doi.org/10.1080/15287394.2012.690707

Sojobi, A. O. (2016). Evaluation of groundwater quality in a rural community in North Central of Nigeria. *Environmental Monitoring and Assessment*, *188*(3), 192. https://doi.org/10.1007/s10661-016-5149-y

Soleimani, M., Amini, N., Sadeghian, B., Wang, D., and Fang, L. (2018). Heavy metals and their source identification in particulate matter (PM2.5) in Isfahan City, Iran. *Journal of Environmental Sciences*, *72*, 166–175. https://doi.org/10.1016/j.jes.2018.01.002

Song, B., Guo, G., Lei, M., and Wang, Y. (2018). Assessments of contamination and human health risks of heavy metals in the road dust from a mining county in Guangxi, China. *Human and Ecological Risk Assessment: An International Journal*, *24*(6), 1606–1622. https://doi.org/10.1080/10807039.2017.1419815

Song, C., He, J., Wu, L., Jin, T., Chen, X., Li, R., Ren, P., Zhang, L., and Mao, H. (2017). Health burden attributable to ambient PM2.5 in China. *Environmental Pollution*, *223*, 575–586. https://doi.org/10.1016/j.envpol.2017.01.060

South, A. (2006). *Bangladesh Country Environmental Analysis (In Two Volumes) Volume II: Technical Annex: Health Impacts of Air and Water Pollution in Bangladesh*.

Stewart, D. R., Saunders, E., Perea, R. A., Fitzgerald, R., Campbell, D. E., and Stockwell, W. R. (2017). Linking Air Quality and Human Health Effects Models: An Application to the Los Angeles Air Basin. *Environmental Health Insights*, *11*. https://doi.org/10.1177/1178630217737551

Suryawanshi, P. V, Rajaram, B. S., Bhanarkar, A. D., and Chalapati Rao, C. V. (2016a). Determining heavy metal contamination of road dust in Delhi, India. *Atmósfera*. https://doi.org/10.20937/ATM.2016.29.03.04

Suryawanshi, P. V, Rajaram, B. S., Bhanarkar, A. D., and Chalapati Rao, C. V. (2016b). Determining heavy metal contamination of road dust in Delhi, India. *Atmósfera*. https://doi.org/10.20937/ATM.2016.29.03.04

Tan, S. Y., Praveena, S. M., Abidin, E. Z., and Cheema, M. S. (2016). A review of heavy metals in indoor dust and its human health-risk implications. *Reviews on Environmental Health*, *31*(4), 447–456. https://doi.org/10.1515/reveh-2016-0026

Tchounwou, P. B., Yedjou, C. G., Patlolla, A. K., and Sutton, D. J. (2012a). *Heavy Metal Toxicity and the Environment* (pp. 133–164). https://doi.org/10.1007/978-3-7643-8340-4_6

Tchounwou, P. B., Yedjou, C. G., Patlolla, A. K., and Sutton, D. J. (2012b). *Heavy Metal Toxicity and the Environment* (pp. 133–164). https://doi.org/10.1007/978-3-7643-8340-4_6

The World Bank. (2023). Bangladesh Needs Urgent Actions to Curb Air Pollution.

Tian, Y., Liu, H., Wu, Y., Si, Y., Li, M., Wu, Y., Wang, X., Wang, M., Chen, L., Wei, C., Wu, T., Gao, P., and Hu, Y. (2019). Ambient particulate matter pollution and adult hospital admissions for pneumonia in urban China: A national time series analysis for 2014 through 2017. *PLOS Medicine*, *16*(12), e1003010. https://doi.org/10.1371/journal.pmed.1003010

Torres, E. B. , S. R. D. , G. J. L. , S. J. N. , V. J. T. , V. R. J. N. , R. B. M. and Q. L. L. (2008). *Completion Report Philippines: Metro Manila Air Quality Improvement Sector Development Program*.

Trujillo-González, J. M., Torres-Mora, M. A., Keesstra, S., Brevik, E. C., and Jiménez-Ballesta, R. (2016). Heavy metal accumulation related to population density in road dust samples taken from urban sites under different land uses. *Science of The Total Environment*, *553*, 636–642. https://doi.org/10.1016/j.scitotenv.2016.02.101

TUREKIAN, K. K., and WEDEPOHL, K. H. (1961). Distribution of the Elements in Some Major Units of the Earth's Crust. *GSA Bulletin*, *72*(2), 175–192. https://doi.org/10.1130/0016-7606(1961)72[175:DOTEIS]2.0.CO;2

US EPA. (2007.-a). *Air Quality Criteria for Particulate Matter*.

US EPA. (2007-b). *sepupdatedpolicy15 (1)*.

US EPA. (1994). National Air Quality and Emissions Trend. https://www.epa.gov/air-trends/air-quality-national-summary

US EPA. (2001). *Air Quality Criteria for Particulate Matter*.

US EPA. (2011).

US EPA. (2018). *2014 National Emissions Inventory, version 2 Technical Support Document*.

US EPA. (2022, November 2). *Human Health Risk Models and Tools*. https://www.epa.gov/risk/human-health-risk-models-and-tools

US EPA, and Factors Program, E. (2011). *Exposure Factors Handbook: 2011 Edition*. www.epa.gov

USDOE. (2011). *The Risk Assessment Information System (RAIS). U.S. Department of Energy's Oak Ridge Operations Office (ORO)*.

USEPA. (2013).

USEPA. (2015). *U.S. Environmental Protection Agency (EPA) International Decontamination Research and Development Conference*.

USGS. (2021). Landsat 8.

Van Munster, K. (2018). *Modeling Health Effects of Particulate Matter Emissions From Modeling Health Effects of Particulate Matter Emissions From Heavy Duty Diesel Trucks Involved in High Volume Hydraulic Heavy Duty Diesel Trucks Involved in High Volume Hydraulic Fracturing with BenMAP-CE Fracturing with BenMAP-CE*. https://scholarworks.rit.edu/theses

Voorhees, A. S., Wang, J., Wang, C., Zhao, B., Wang, S., and Kan, H. (2014a). Public health benefits of reducing air pollution in Shanghai: A proof-of-concept methodology with application to BenMAP. *Science of the Total Environment*, *485–486*(1), 396–405. https://doi.org/10.1016/j.scitotenv.2014.03.113

Voorhees, A. S., Wang, J., Wang, C., Zhao, B., Wang, S., and Kan, H. (2014b). Public health benefits of reducing air pollution in Shanghai: A proof-of-concept methodology with application to BenMAP. *Science of the Total Environment*, *485–486*(1), 396–405. https://doi.org/10.1016/j.scitotenv.2014.03.113

Wadud, Z., and Khan, T. (2013). Air Quality and Climate Impacts Due to CNG Conversion of Motor Vehicles in Dhaka, Bangladesh. *Environmental Science and Technology*, *47*(24), 13907–13916. https://doi.org/10.1021/es402338b

Wahab, M. I. A., Razak, W. M. A. A., Sahani, M., and Khan, M. F. (2020). Characteristics and health effect of heavy metals on non-exhaust road dusts in Kuala Lumpur. *Science of The Total Environment*, *703*, 135535. https://doi.org/10.1016/j.scitotenv.2019.135535

Wang, F., Qiu, X., Cao, J., Peng, L., Zhang, N., Yan, Y., and Li, R. (2021). Policy-driven changes in the health risk of PM2.5 and O3 exposure in China during 2013–2018. *Science of The Total Environment*, *757*, 143775. https://doi.org/10.1016/j.scitotenv.2020.143775

WHO. (1999). https://apps.who.int/iris/handle/10665/42167

WHO. (2022). World Health Statistics 2022. https://www.who.int/news/item/20-05-2022-world-health-statistics-2022

Winther, M.; S. E. (2011). *HEAVY METAL EMISSIONS fOR DANISH ROAD TRANSpORT*.

Wiseman, C. L. S., Levesque, C., and Rasmussen, P. E. (2021). Characterizing the sources, concentrations and resuspension potential of metals and metalloids in the thoracic fraction of urban road dust. *Science of The Total Environment*, *786*, 147467. https://doi.org/10.1016/j.scitotenv.2021.147467

Witkowska, D., Słowik, J., and Chilicka, K. (2021). Heavy Metals and Human Health: Possible Exposure Pathways and the Competition for Protein Binding Sites. *Molecules*, *26*(19), 6060. https://doi.org/10.3390/molecules26196060

Woodruff, T. J., Parker, J. D., and Schoendorf, K. C. (2006). Fine Particulate Matter ($PM_{2.5}$) Air Pollution and Selected Causes of Postneonatal Infant Mortality in California. *Environmental Health Perspectives*, *114*(5), 786–790. https://doi.org/10.1289/ehp.8484

World Bank. (2006). *World Development Report 2007*. The World Bank. https://doi.org/10.1596/978-0-8213-6541-0

World Health Organization. (1999). *The world health report 1999 : making a difference.* World Health Organization.

WorldPop. (2023). https://www.worldpop.org/datacatalog/

Wu, W., Yao, M., Yang, X., Hopke, P. K., Choi, H., Qiao, X., Zhao, X., and Zhang, J. (2021). Mortality burden attributable to long-term ambient PM2.5 exposure in China: using novel exposure-response functions with multiple exposure windows. *Atmospheric Environment*, *246*, 118098. https://doi.org/10.1016/j.atmosenv.2020.118098

Xie, S., Zhang, Y., Qi, L., and Tang, X. (2003). Spatial distribution of traffic-related pollutant concentrations in street canyons. *Atmospheric Environment*, *37*(23), 3213–3224. https://doi.org/10.1016/S1352-2310(03)00321-2

Xie, Y., Dai, H., Zhang, Y., Wu, Y., Hanaoka, T., and Masui, T. (2019). Comparison of health and economic impacts of PM2.5 and ozone pollution in China. *Environment International*, *130*, 104881. https://doi.org/10.1016/j.envint.2019.05.075

Xu, J., Yao, M., Wu, W., Qiao, X., Zhang, H., Wang, P., Yang, X., Zhao, X., and Zhang, J. (2021). Estimation of ambient PM2.5-related mortality burden in China by 2030 under climate and population change scenarios: A modeling study. *Environment International*, *156*, 106733. https://doi.org/10.1016/j.envint.2021.106733

Xu, X., Cao, X., and Zhao, L. (2013). Comparison of rice husk- and dairy manure-derived biochars for simultaneously removing heavy metals from aqueous

solutions: Role of mineral components in biochars. *Chemosphere*, *92*(8), 955–961. https://doi.org/10.1016/j.chemosphere.2013.03.009

Yang, A., Lo, K., Zheng, T., Yang, J., Bai, Y., Feng, Y., Cheng, N., and Liu, S. (2020). Environmental heavy metals and cardiovascular diseases: Status and future direction. *Chronic Diseases and Translational Medicine*, *6*(4), 251–259. https://doi.org/10.1016/j.cdtm.2020.02.005

Yang, G., Wang, Y., Zeng, Y., Gao, G. F., Liang, X., Zhou, M., Wan, X., Yu, S., Jiang, Y., Naghavi, M., Vos, T., Wang, H., Lopez, A. D., and Murray, C. J. (2013). Rapid health transition in China, 1990–2010: findings from the Global Burden of Disease Study 2010. *The Lancet*, *381*(9882), 1987–2015. https://doi.org/10.1016/S0140-6736(13)61097-1

Yang, L. (2020). A novel approach of Landsat 8 imagery to predict PM $_{2.5}$ concentrations in a south-eastern coastal city of China. *IOP Conference Series: Earth and Environmental Science*, *619*(1), 012046. https://doi.org/10.1088/1755-1315/619/1/012046

Yang, P., Zhang, Y., Wang, K., Doraiswamy, P., and Cho, S.-H. (2019). Health impacts and cost-benefit analyses of surface O3 and PM2.5 over the U.S. under future climate and emission scenarios. *Environmental Research*, *178*, 108687. https://doi.org/10.1016/j.envres.2019.108687

Yin, P., Brauer, M., Cohen, A., Burnett, R. T., Liu, J., Liu, Y., Liang, R., Wang, W., Qi, J., Wang, L., and Zhou, M. (2017). Long-term fine particulate matter exposure and nonaccidental and cause-specific mortality in a large national cohort of Chinese men. *Environmental Health Perspectives*, *125*(11), 117002-1-117002–117011. https://doi.org/10.1289/EHP1673

Yuan, W., Yang, N., and Li, X. (2016). Advances in Understanding How Heavy Metal Pollution Triggers Gastric Cancer. *BioMed Research International*, *2016*, 1–10. https://doi.org/10.1155/2016/7825432

Žero, S., Huremović, J., Memić, M., and Muhić-Šarac, T. (2017). Determination of total and bioaccessible metals in airborne particulate matter from an urban and a rural area at Sarajevo. *Toxicological and Environmental Chemistry*, *99*(4), 641–651. https://doi.org/10.1080/02772248.2016.1207173

Zhang, W., Lin, S., Hopke, P. K., Thurston, S. W., van Wijngaarden, E., Croft, D., Squizzato, S., Masiol, M., and Rich, D. Q. (2018). Triggering of cardiovascular hospital admissions by fine particle concentrations in New York state: Before, during, and after implementation of multiple environmental policies and a recession. *Environmental Pollution*, *242*, 1404–1416. https://doi.org/10.1016/j.envpol.2018.08.030

Zhao, C., Wang, Y., Yang, Q., Fu, R., Cunnold, D., and Choi, Y. (2010). Impact of East Asian summer monsoon on the air quality over China: View from space. *Journal of Geophysical Research*, *115*(D9), D09301. https://doi.org/10.1029/2009JD012745

Zheng, X., Xu, X., Yekeen, T. A., Zhang, Y., Chen, A., Kim, S. S., Dietrich, K. N., Ho, S.-M., Lee, S.-A., Reponen, T., and Huo, X. (2016). Ambient Air Heavy Metals in PM2.5 and Potential Human Health Risk Assessment in an Informal Electronic-Waste Recycling Site of China. *Aerosol and Air Quality Research*, *16*(2), 388–397. https://doi.org/10.4209/aaqr.2014.11.0292

Zhou, C., Li, S., and Wang, S. (2018). Examining the impacts of urban form on air pollution in developing countries: A case study of China's megacities. *International Journal of Environmental Research and Public Health*, *15*(8). https://doi.org/10.3390/ijerph15081565

Zhu, X., Yu, W., Li, F., Liu, C., Ma, J., Yan, J., Wang, Y., and Tian, R. (2021). Spatio-temporal distribution and source identification of heavy metals in particle size fractions of road dust from a typical industrial district. *Science of The Total Environment*, *780*, 146357. https://doi.org/10.1016/j.scitotenv.2021.146357

ANNEXURE

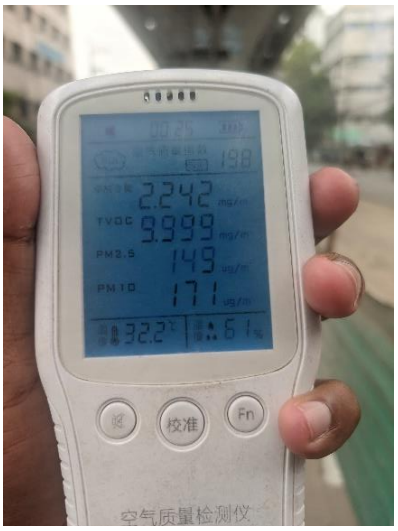

Fig. A.1 Measuring Instrument for particulate matter concentration

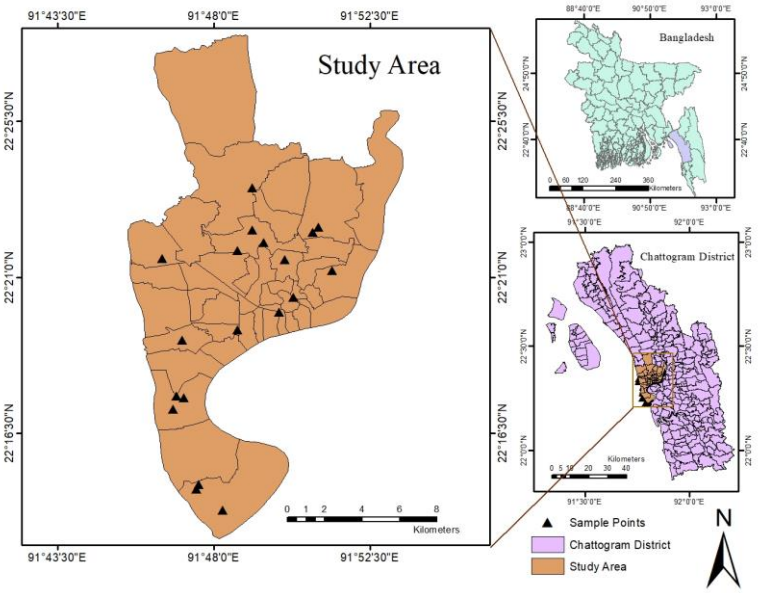

Fig. A.2 Monitoring Sites of Heavy Metal Samples

Table A.1 Symbology of the investigated hazardous element for HRA

Variables	Value	References
IngR (mg/d): Dust ingestion rate for receptor	Resident, 200 for children and 100 for adult	USDOE 2011; USEPA 1997
EF (d/yr): Exposure frequency	75 for residents	USDOE 2011
ED (yr): Exposure duration	30 for adult resident and 6 for children	USDOE 2011
BW (kg): Average body weight	15 for child and 60 for adult resident	FAO 2006; Man et al. 2010
AT_{nc} (d): Averaging time for non-carcinogenic effects	ED × 365 for residents	USDOE 2011
AT_{ca} (d): Averaging time for carcinogenic effects	LT × 365 for residents	USDOE 2011; USEPA 1997
LT (yr): Lifetime	70 for adult residents	WHO 2014
ET (h/d): Exposure time	1 for residents for the site specific	USDOE 2011
CF (kg/mg): Conversion factor	1×10^{-6}	Man et al. 2010, 2013
SA (cm^2): Skin surface that are available for exposure	Resident, 2800 for child and 3300 for adult	USDOE 2011
AF (mg/cm^2): Dust to skin adherence factor	Resident, 0.2 for child and 0.007 for adult	USDOE 2011
ABS_d (unitless): Dermal absorption factor	0.03 for As and 0.001 for other metals	USEPA 2011
InhR (m^3/d): Inhalation rate	20 for both adult and child	USEPA 1997
PEF (m^3/kg): Particle emission factor	1.36×10^9	USDOE 2011; USEPA 2011
C (mg/kg)	Concentration of metal in dust;	
ABS_{GI}	Gastrointestinal absorption factor;	
CDI_{ing}, CDI_{inh}, and CDI_{dermal}	Chronic daily intake or dose contacted through oral ingestion (mg/kg/d), inhalation of (mg/m^3 for non-cancer and $\mu g/m^3$ for cancer), and dermal contact (mg/kg/d) with dust particles, respectively;	
$CSF_{ing}(mg/kg/d)^{-1}$	Chronic oral slope factor;	
CSF_{dermal}	Chronic dermal slope factor, = CSF_{ing}/ABS_{GI}	
IUR $(\mu g/m^3)^{-1}$	Chronic inhalation unit risk;	
RfD_{ing}(mg/kg/d)	Chronic oral reference dose;	
RfC_{inh} (mg/m^3)	Chronic inhalation reference concentration;	
RfD_{dermal}	Chronic dermal reference dose, =$RfD_{ing}\times ABS_{GI}$	

Table A.2 Value of the investigated hazardous element for HRA

Metals	$RfD_{ingestion}$	ABS_{GI}	$RfD_{inhalation}$	$CSF_{ingestion}$ (mg/kg/day)$^{-1}$	IUR $(\mu g/m^3)^{-1}$	RfD_{dermal}
Cr	0.003[a]	0.013	2.86E-05	0.5	0.025	0.0006
Mn	0.14	0.04	5.00E-05			0.0018
Fe	300	45	0.7			13500
Zn	0.3	1	0.3			0.06
Cu						0.012
Ni	0.02		0.026			
References	USDOE 2011	USEPA 2011	USDOE 2011	USDOE 2011	USDOE 2011	

Table A.2.1

Table A.3. Health Risk Assessment for Carcinogenic and Non-Carcinogenic Risk

Carcinogenic Risk and Hazard Quotient	Comments
Carcinogenic Risk $<10^{-6}$	Insignificant
Carcinogenic Risk 10^{-6}-10^{-4}	Considerable
Carcinogenic Risk $>10^{-4}$	Unacceptable
Non-Carcinogenic CDI < $\boldsymbol{R_fD}$ and HQ≤1	no adverse health effect
Non-Carcinogenic CDI < $\boldsymbol{R_fD}$ and HQ≤1	adverse health effect

Table A.4. Cost Breakup for Hospital Admissions, Cardiac Outcome

Direct Cost (BDT)	
Pathology Charges	12460
X-ray/Ultasono	2000-5000
Medicine	500
Registration	100
Transport	700
Informal Payment	300
Minimum Cardiac operation	1,70000
Cabin	4000 (per day)
Emergency	10000
ICU	6500
Heart Failure Unit	2500
Oxygen, Dialyses, ABG, BI, CI CAP	9100
In Direct Cost	
Length of stay	4 days
Per day income	500
Total Cost	232160

Table A.5. Cost Breakup for Hospital Admissions, Respiratory Diseases

Direct Cost (BDT)	
Ventilation Charge	6000
ICU	12000
Cabin	4000
Infusion Charge	3000
Diagonistic Charges	5000
Medicine	500-800
Transport	700
Informal Payment	300
In Direct Cost (BDT)	
Length of stay	3
Per day income	500
Total Cost	66000

NB The medicine cost was based on the literature review and web sources

Table A.6. Developed Regression Model for predicting Particulate Matter concentration

$PM_{2.5}$ model:

Model Summary				
Model	R	R Square	Adjusted R Square	Std. Error of the Estimate
1	.809[a]	.654	.585	55.01662
a. Predictors: (Constant), b1, b4, b2				

Coefficients						
Model		Unstandardized Coefficients		Standardized Coefficients	t	Sig.
		B	Std. Error	Beta		
1	(Constant)	-326.280	155.287		-2.101	.053
	b2	11.722	3.929	14.078	2.984	.009
	b4	-5.408	1.617	-4.330	-3.345	.004
	b1	-6.794	2.509	-9.770	-2.690	.017
a. Dependent Variable: $PM_{2.5}$						

So, the defined model is

$$PM_{2.5} = -326.280 + (-6.794 \times b1) + (11.722 \times b2) + (-5.408 \times b4) \quad \text{A.1}$$

PM_{10}

Model Summary				
Model	R	R Square	Adjusted R Square	Std. Error of the Estimate
1	.718[a]	.516	.419	147.53794

a. Predictors: (Constant), b3, b1, b2

Coefficients						
Model		Unstandardized Coefficients		Standardized Coefficients	t	Sig.
		B	Std. Error	Beta		
1	(Constant)	-453.886	416.908		-1.089	.293
	b1	-11.445	5.219	-7.312	-2.193	.045
	b2	23.184	9.115	12.326	2.551	.022
	b3	-13.488	4.556	-4.986	-2.959	.010

a. Dependent Variable: PM_10

So, the defined model is

$$PM_{10} = -453.886 + (-11.445 \times b1) + (23.184 \times b2) + (-13.49 \times b3) \quad \text{A.2}$$

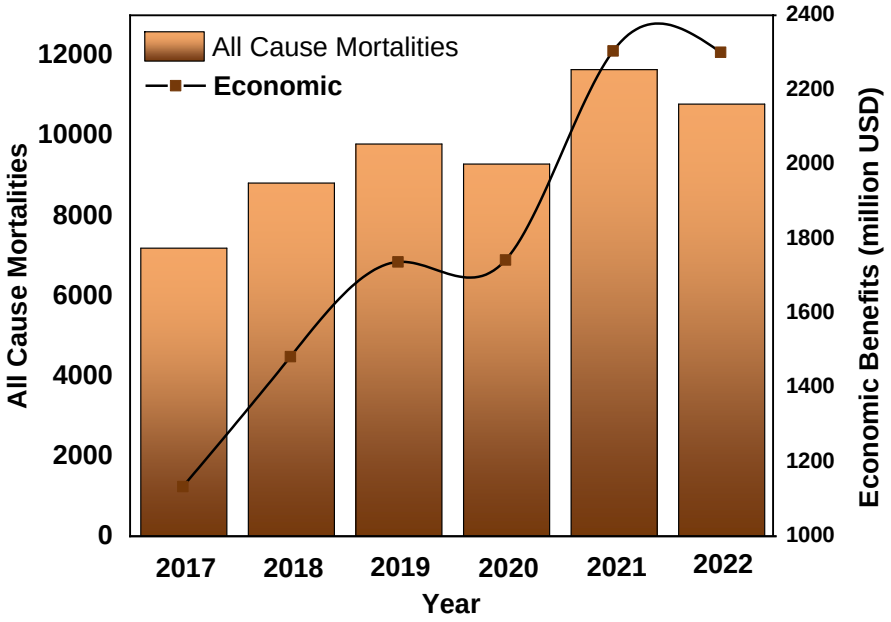

Figure A.3 Health Benefit Due to All Cause Mortality

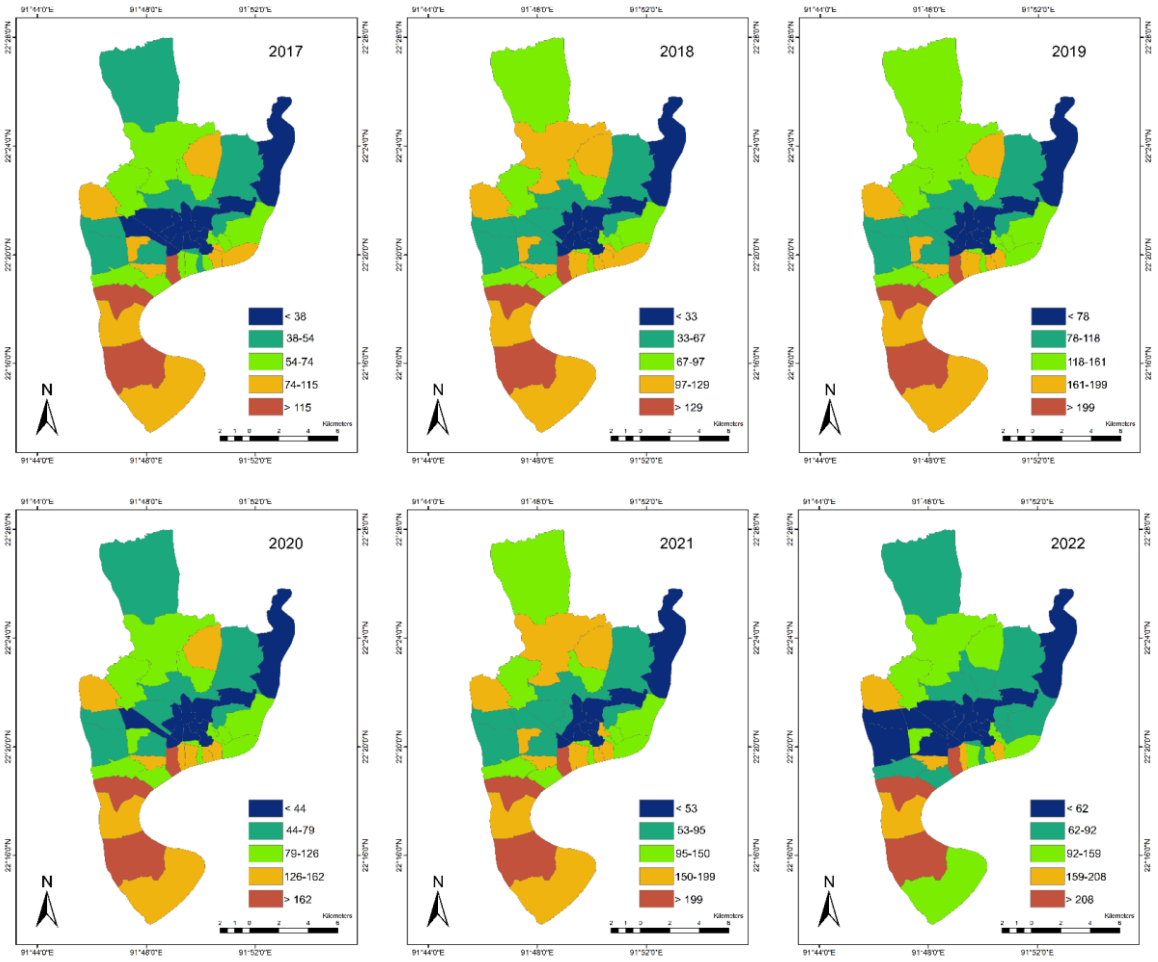

Fig. A.4 $PM_{2.5}$ related premature deaths due to cardiac outcome

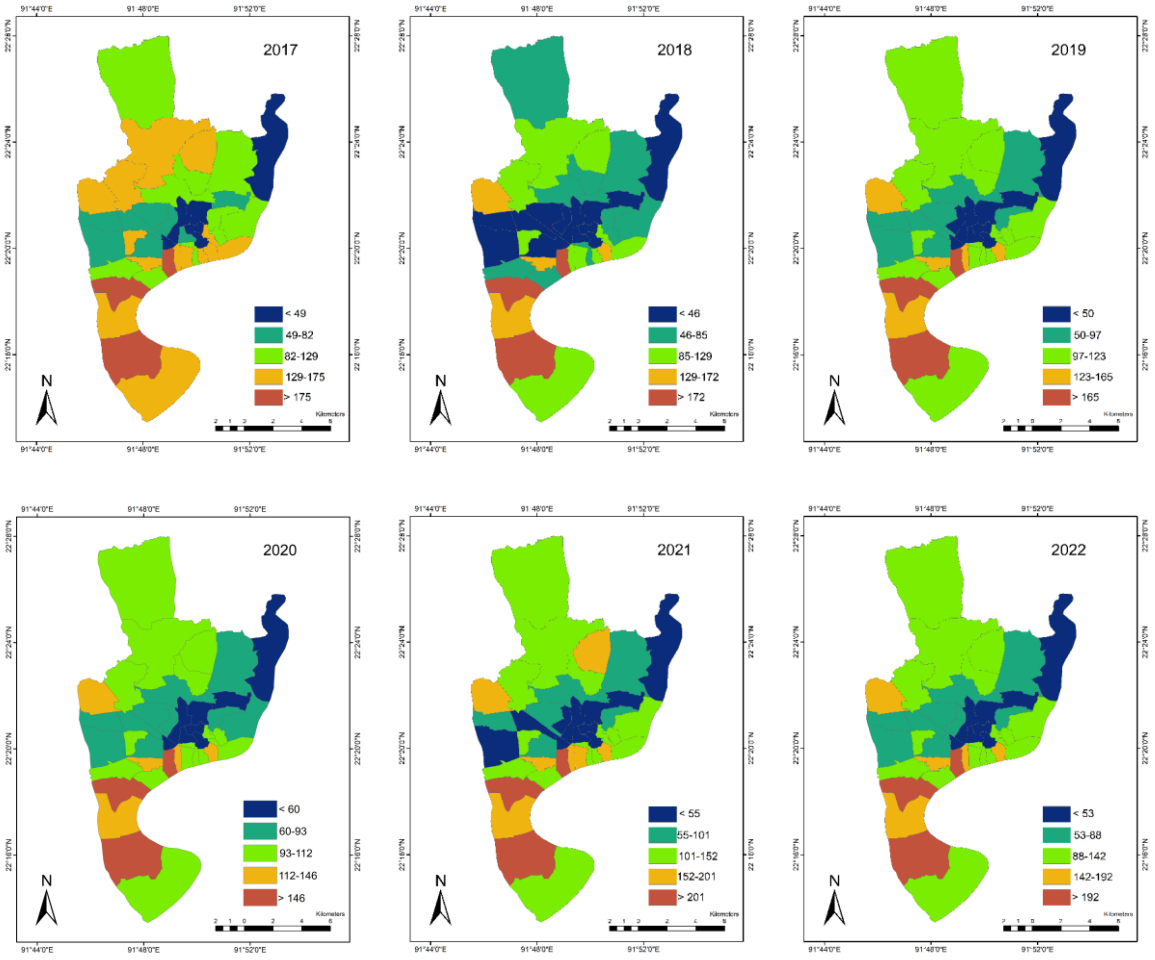

Fig. A.5 $PM_{2.5}$ related premature deaths due to respiratory deaths

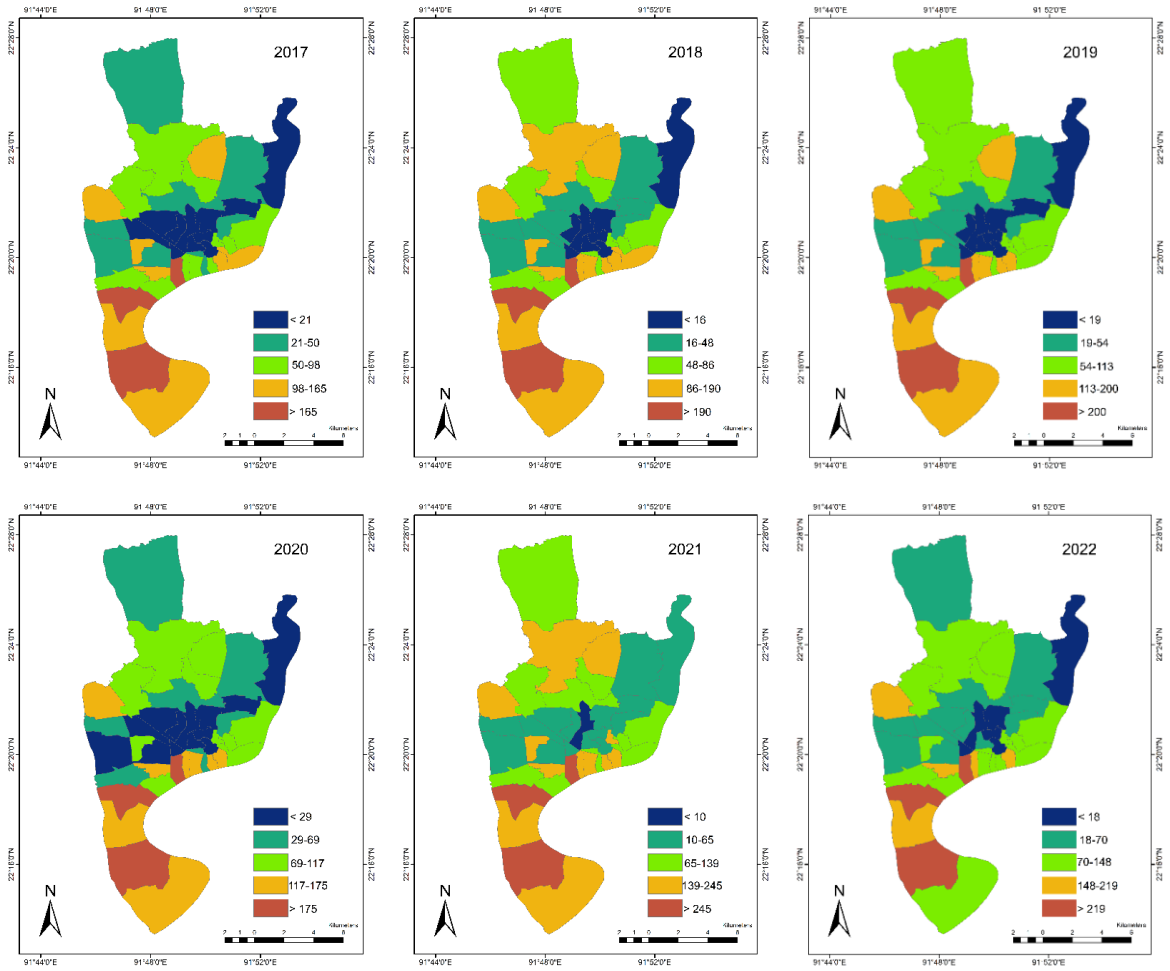

Fig. A.6 PM_{10} related premature deaths due to cardiac outcome

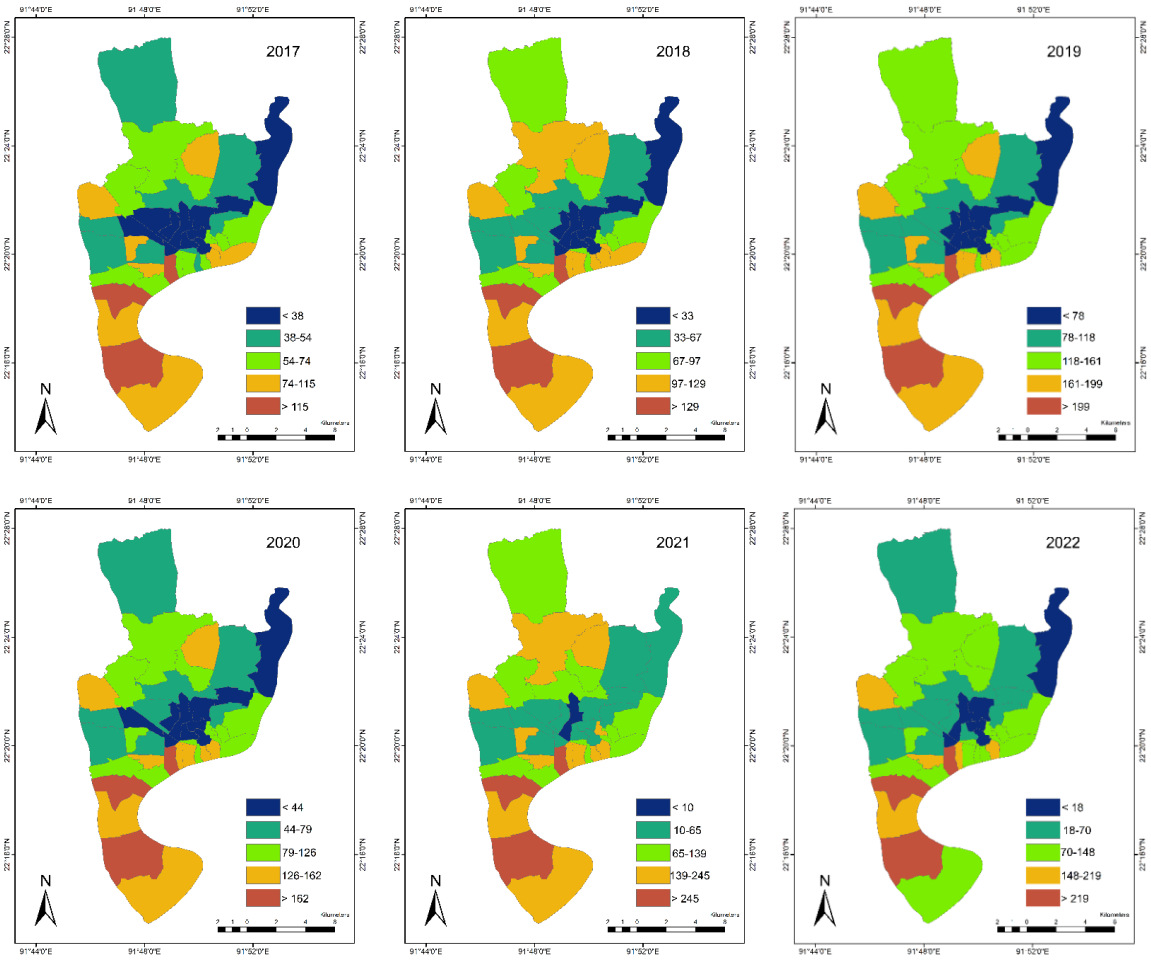

Fig. A.7 PM_{10} related premature deaths due respiratory outcome

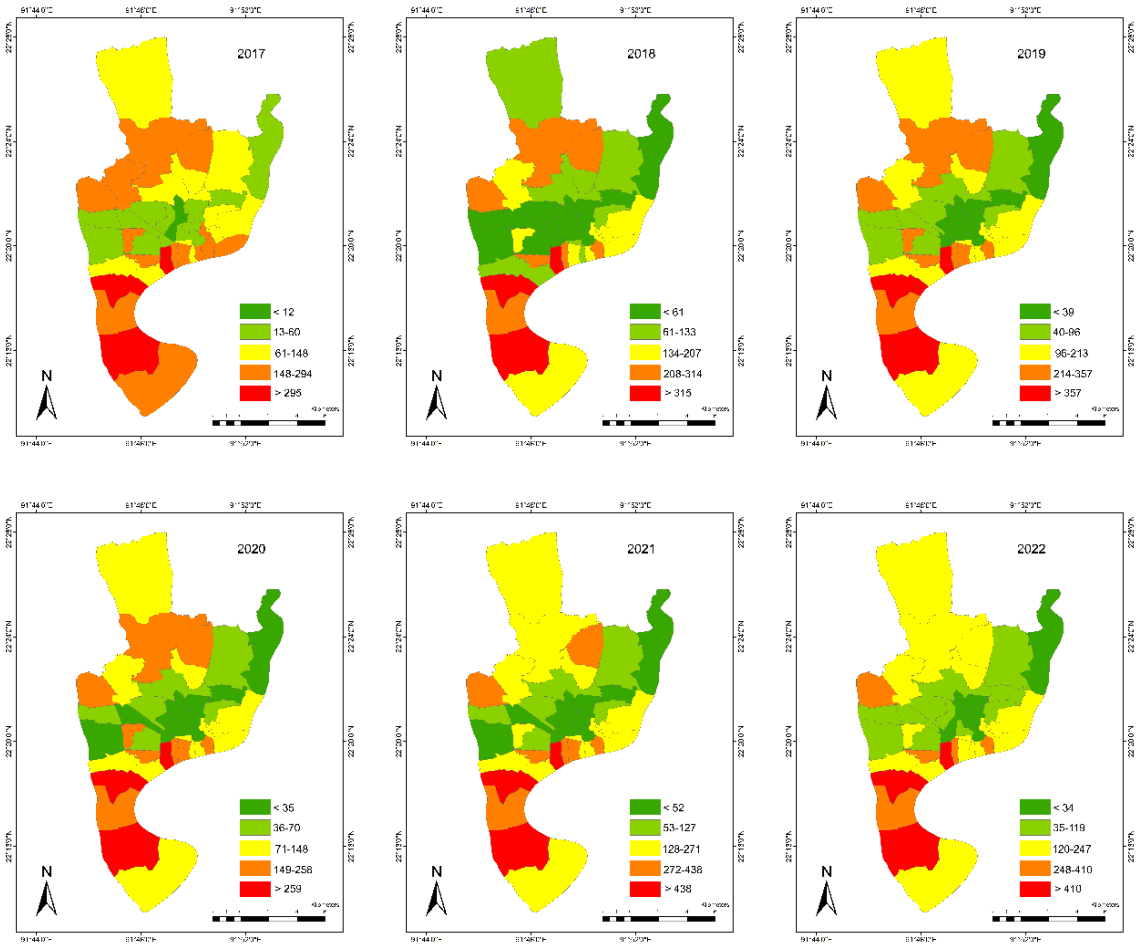

Fig. A.8 Premature deaths due to NCD+LRI by GEMM model

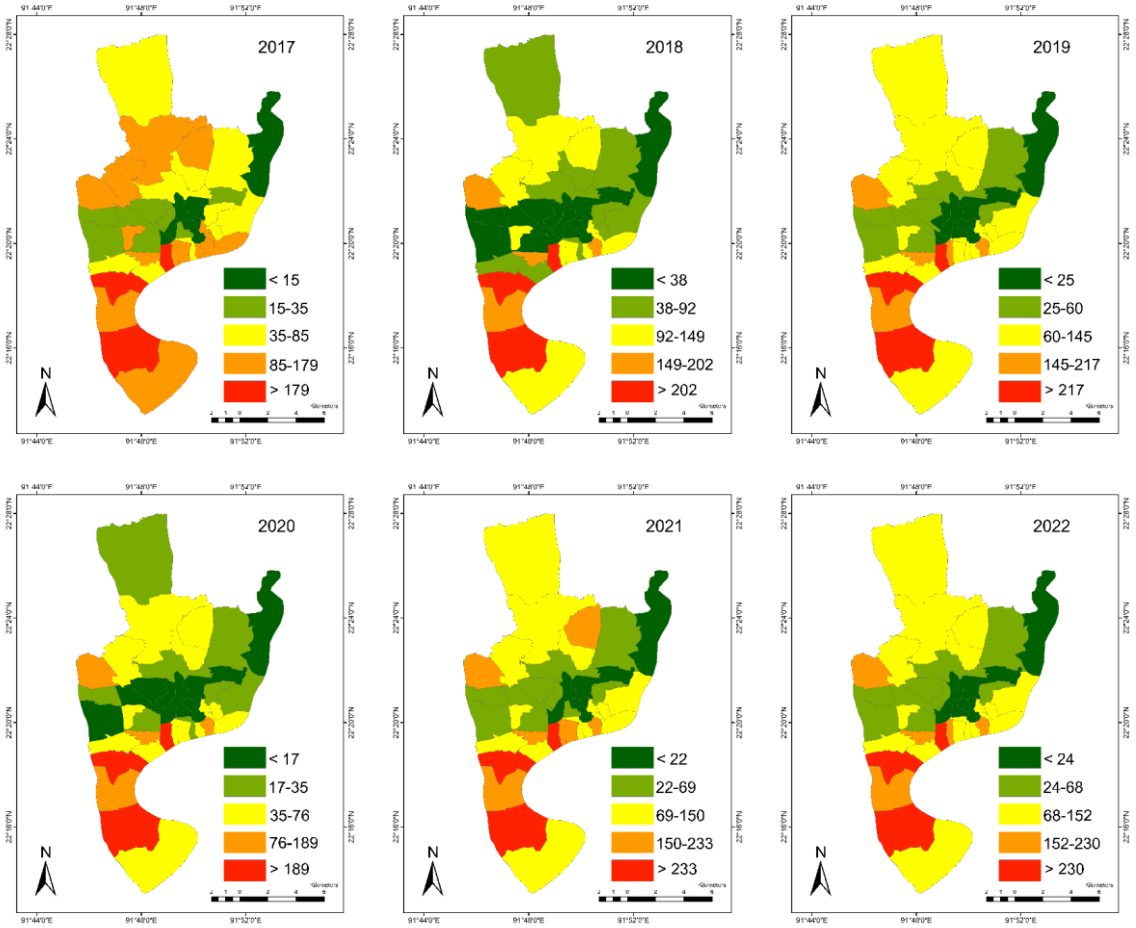

Fig. A.9 Premature deaths due to NCD+LRI by LL model

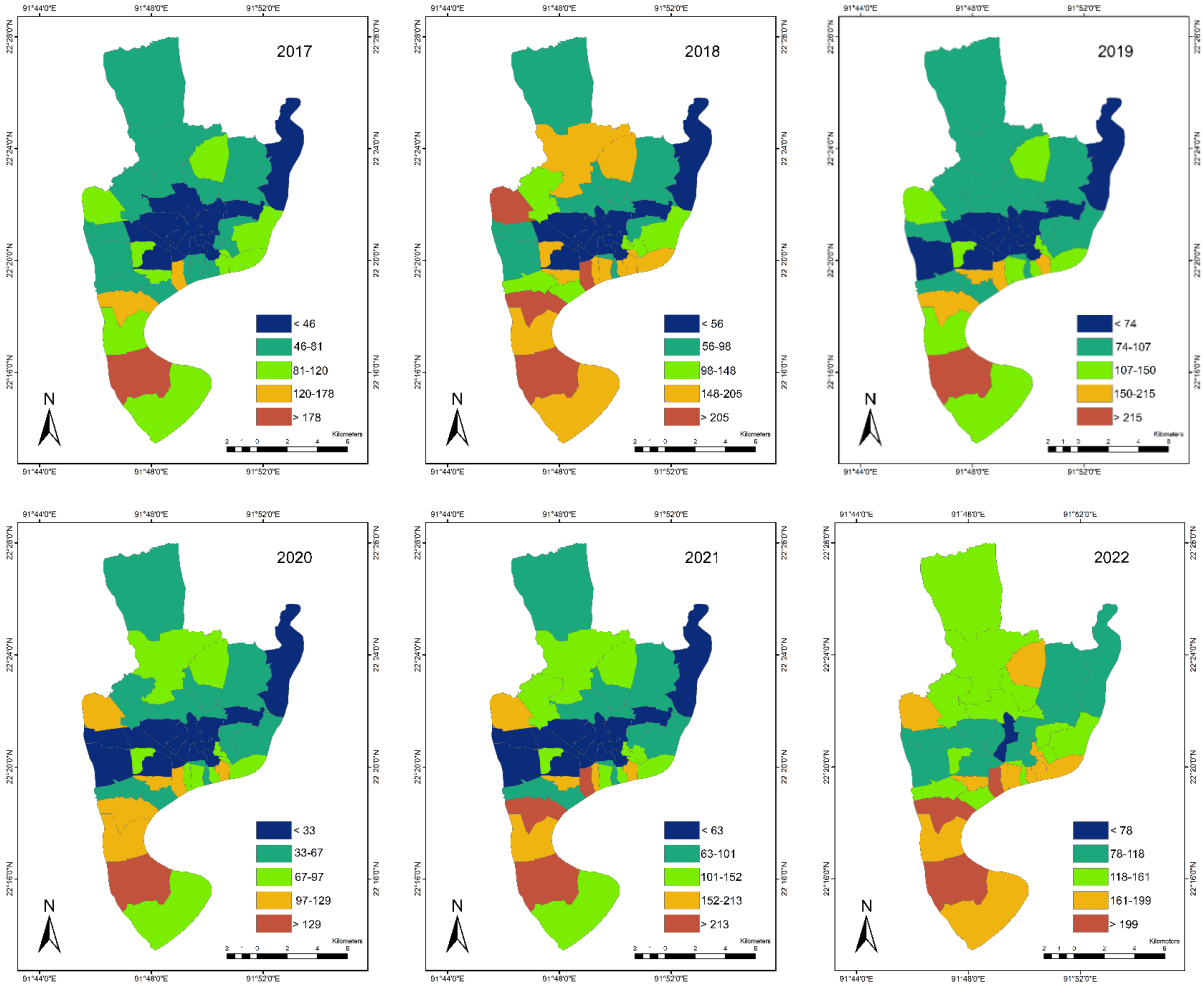

Fig. A.10 PM_{10} related hospital admission of cardiac outcome

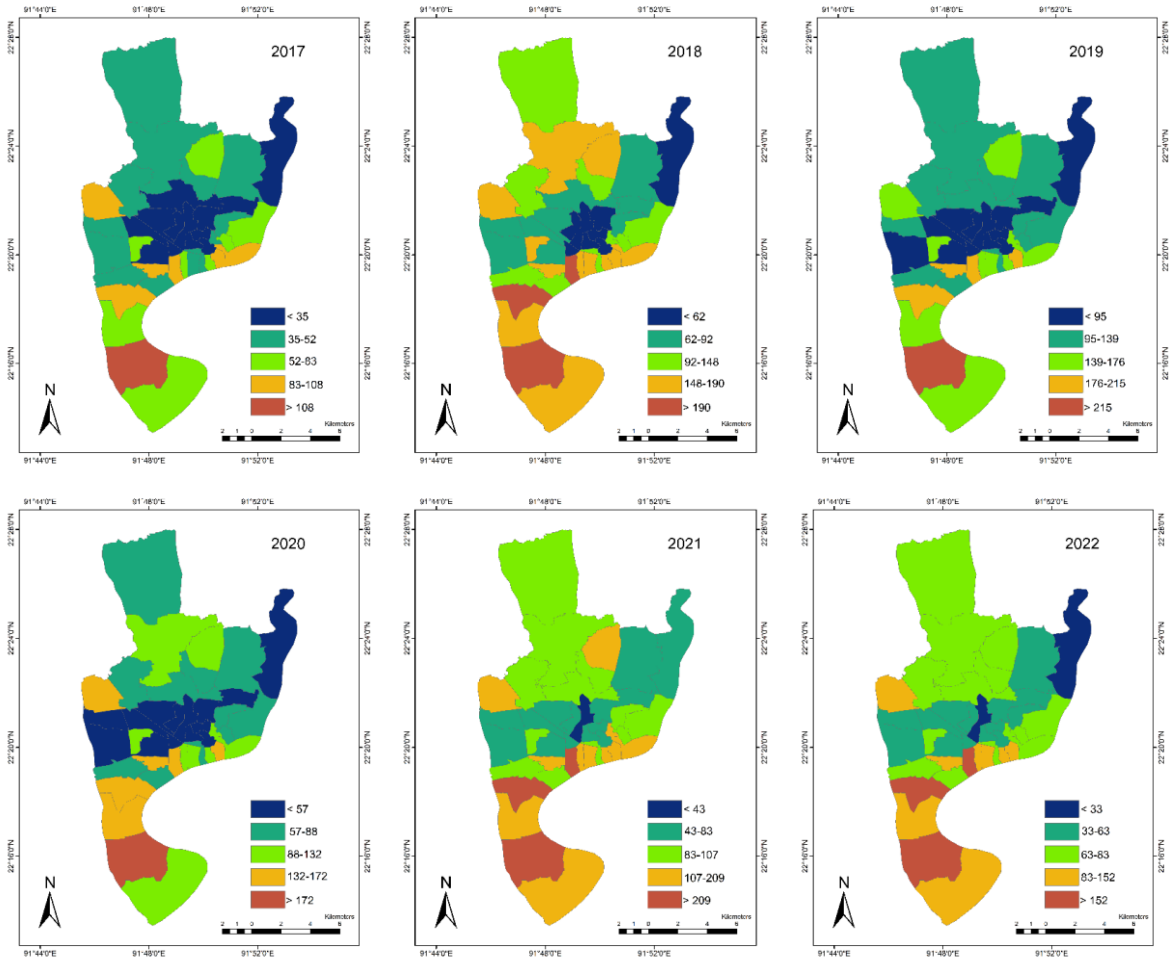

Fig. A.11 PM_{10} related hospital admission of respiratory outcome

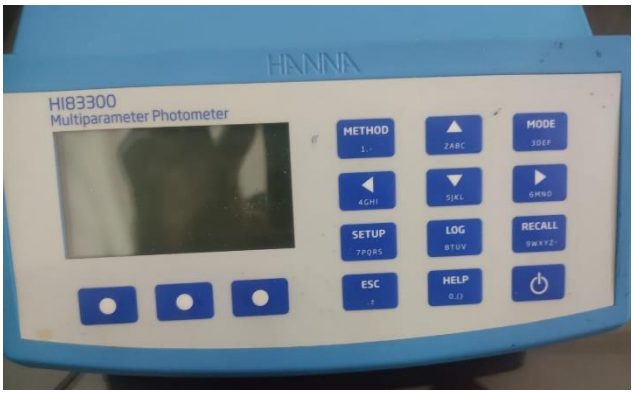

Fig. A.12 PM_{10} related hospital admission of respiratory outcome

Table A.7. Monetary Cost due to all cause, respiratory and cardiac deaths

	2.5 percentile			97.5 Percentile		
	Monetary Cost (US $)					
Year	All Cause	Respiratory	Cardiac	All Cause	Respiratory	Cardiac
2017	5.70E+08	1.14E+08	2.32E+08	1.43E+09	2.86E+08	6.84E+08
2018	7.87E+08	1.57E+08	3.42E+08	1.81E+09	3.62E+08	8.47E+08
2019	1.06E+09	2.12E+08	4.20E+08	2.08E+09	4.15E+08	9.70E+08
2020	9.76E+08	1.95E+08	4.12E+08	2.14E+09	4.28E+08	1.01E+09
2021	1.31E+09	2.61E+08	6.43E+08	2.64E+09	5.28E+08	1.18E+09
2022	1.28E+09	2.56E+08	5.96E+08	2.73E+09	5.45E+08	1.25E+09

Table A.8. Monetary Cost due to GEMM-COD andNCD+LRI

	2.5 percentile		97.5 Percentile	
	Monetary Cost (US $)			
Year	GEMM 5-Causes of Death	GEMM (NCD+LRI)	GEMM 5-Causes of Death	GEMM (NCD+LRI)
2017	3.72E+08	8.33E+08	6.22E+08	1.08E+09
2018	4.87E+08	9.61E+08	7.85E+08	1.24E+09
2019	5.66E+08	1.11E+09	8.98E+08	1.43E+09
2020	6.41E+08	1.16E+09	1.04E+09	1.41E+09
2021	7.28E+08	1.46E+09	1.08E+09	1.83E+09
2022	7.55E+08	1.47E+09	1.15E+09	1.88E+09

Table A.9. Monetary Cost due to LL-COD andNCD+LRI

	2.5 percentile		97.5 Percentile	
	Monetary Cost (US $)			
Year	5-Causes of Death	NCD+LRI	5-Causes of Death	NCD+LRI
2017	2.91E+08	4.59E+08	4.94E+08	7.13E+08
2018	3.65E+08	5.66E+08	6.04E+08	8.65E+08
2019	4.17E+08	6.48E+08	6.85E+08	9.86E+08
2020	4.28E+08	5.63E+08	7.09E+08	8.84E+08
2021	5.04E+08	7.88E+08	8.15E+08	1.19E+09
2022	5.35E+08	8.34E+08	8.71E+08	1.26E+09

Table A.10. Monetary cost due to $PM_{2.5}$ related Hospital Admission

	2.5 percentile		97.5 Percentile	
	$PM_{2.5}$ related Hospital Admission Monetary Cost (US $)			
Year	Respiratory	Cardiac	Respiratory	Cardiac
2017	3.62E+04	8.68E+04	1.94E+05	5.21E+05
2018	5.42E+04	1.45E+05	3.12E+05	6.87E+05
2019	6.61E+04	1.87E+05	3.93E+05	9.35E+05
2020	5.25E+04	1.83E+05	3.88E+05	8.23E+05
2021	9.62E+04	2.97E+05	5.95E+05	1.37E+06
2022	8.87E+04	2.81E+05	5.79E+05	1.33E+06

Table A.11. Monetary cost due to PM_{10} related Hospital Admission

	2.5 percentile		97.5 Percentile	
	PM_{10} related Hospital Admission Monetary Cost (US $)			
Year	Respiratory	Cardiac	Respiratory	Cardiac
2017	3.36E+04	6.72E+04	1.94E+05	3.97E+05
2018	4.64E+04	8.52E+04	2.76E+05	6.96E+05
2019	6.29E+04	1.18E+05	3.26E+05	7.93E+05
2020	3.65E+04	1.02E+05	4.02E+05	7.97E+05
2021	9.73E+04	2.10E+05	5.48E+05	1.14E+06
2022	8.85E+04	1.75E+05	5.23E+05	1.12E+06

Table A.12. Monetary cost due to WLD and MRAD

	2.5 percentile		97.5 Percentile	
	Monetary Cost (US $)			
Year	WLD	MRAD	WLD	MRAD
2017	1.92E+06	9.72E+06	2.46E+06	1.26E+07
2018	2.45E+06	1.21E+07	3.09E+06	1.53E+07
2019	2.70E+06	1.32E+07	3.38E+06	1.65E+07
2020	3.27E+06	1.55E+07	4.00E+06	1.87E+07
2021	3.02E+06	1.46E+07	3.75E+06	1.80E+07
2022	1.92E+06	9.72E+06	2.46E+06	1.26E+07

Table A.13 Monetary cost due to Asthma and LRI (child)

	2.5 percentile		97.5 Percentile	
	Monetary Cost (US $)			
Year	Asthma	LRI	Asthma	LRI
2017	3.50E+07	9.18E+07	3.52E+07	2.08E+08
2018	3.67E+07	9.47E+07	3.67E+07	1.79E+08
2019	3.81E+07	1.06E+08	3.82E+07	1.87E+08
2020	4.13E+07	1.35E+08	4.14E+07	2.09E+08
2021	4.28E+07	1.95E+08	4.28E+07	3.25E+08
2022	3.50E+07	9.18E+07	3.52E+07	2.08E+08